Bendix Technical Journal

VOL. 4 NO. 2 SUMMER/AUTUMN 1971

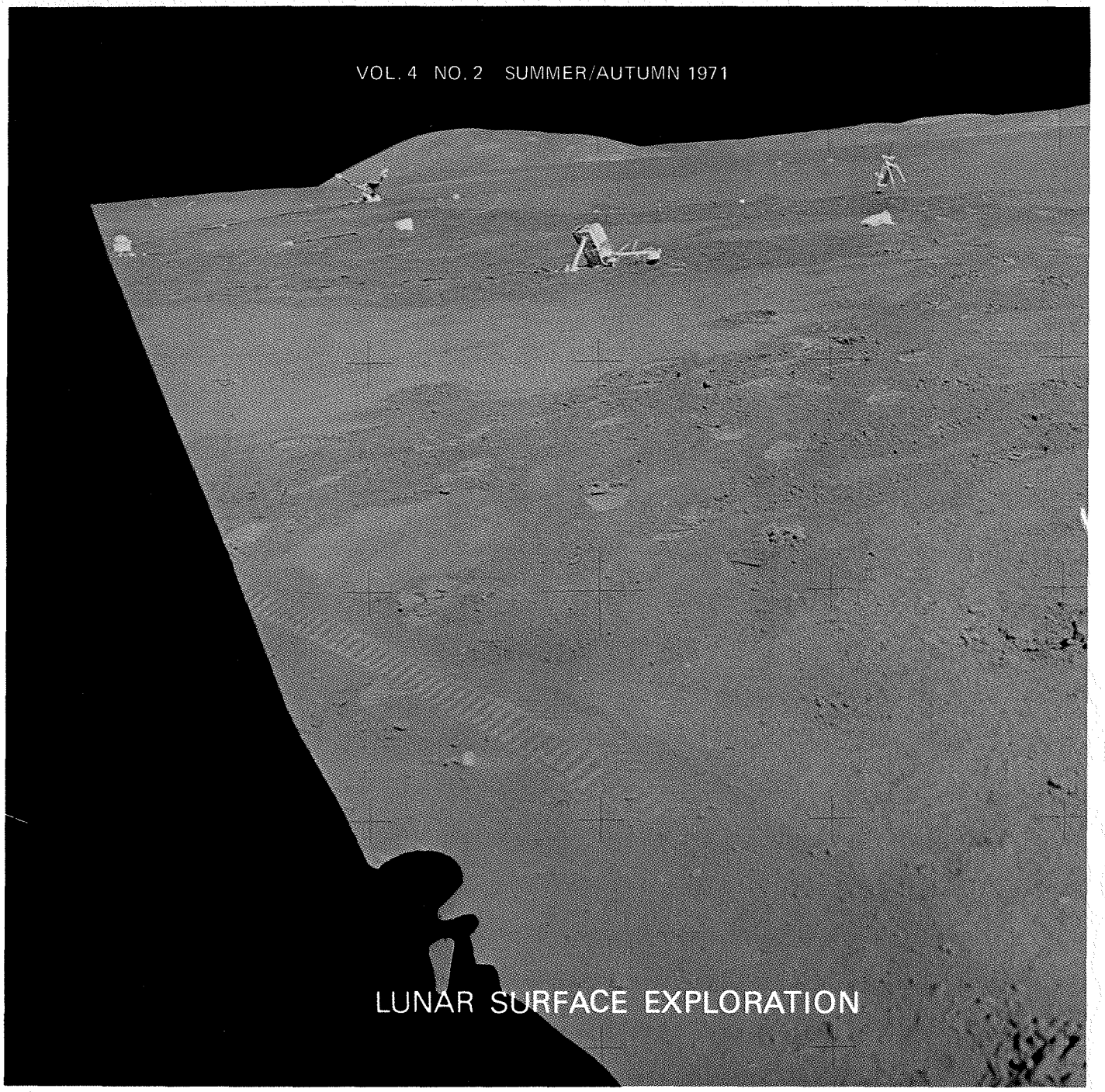

LUNAR SURFACE EXPLORATION

Bendix

LAUDERDALE

The Bendix Technical Journal publishes noteworthy results of scientific and engineering work accomplished by the people of The Bendix Corporation.

TECHNICAL CONSULTANTS for this Issue

B. J. Rusky, *Issue Coordinator*
Aerospace Systems Division

P. S. Curry
Aerospace Systems Division

E. S. Van Valkenburg
Aerospace Systems Division

The cover photograph of the Apollo 15 Lunar Surface Experiments Package was made by Astronauts David Scott and Jim Irwin prior to lift-off from the lunar surface.

Published three times a year by The Bendix Corporation. A. P. Fontaine, Chairman and Chief Executive Officer; W. M. Blumenthal, President and Chief Operating Officer. Subscriptions: $5.00 per year; individual copies: $2.00. Address all correspondence to: The Editor, *Bendix Technical Journal*, The Bendix Corporation Executive Offices, Bendix Center, Southfield, Michigan 48076.

Microfilmed by University Microfilms, Inc., 301 North Zeeb Road, Ann Arbor, Michigan 48106.

BENDIX TECHNICAL JOURNAL
LUNAR SURFACE EXPLORATION

CONTENTS

Volume 4 Number 2 Summer/Autumn 1971

Future Issues: Pollution Detection and Control
Image Data Processing
Automation

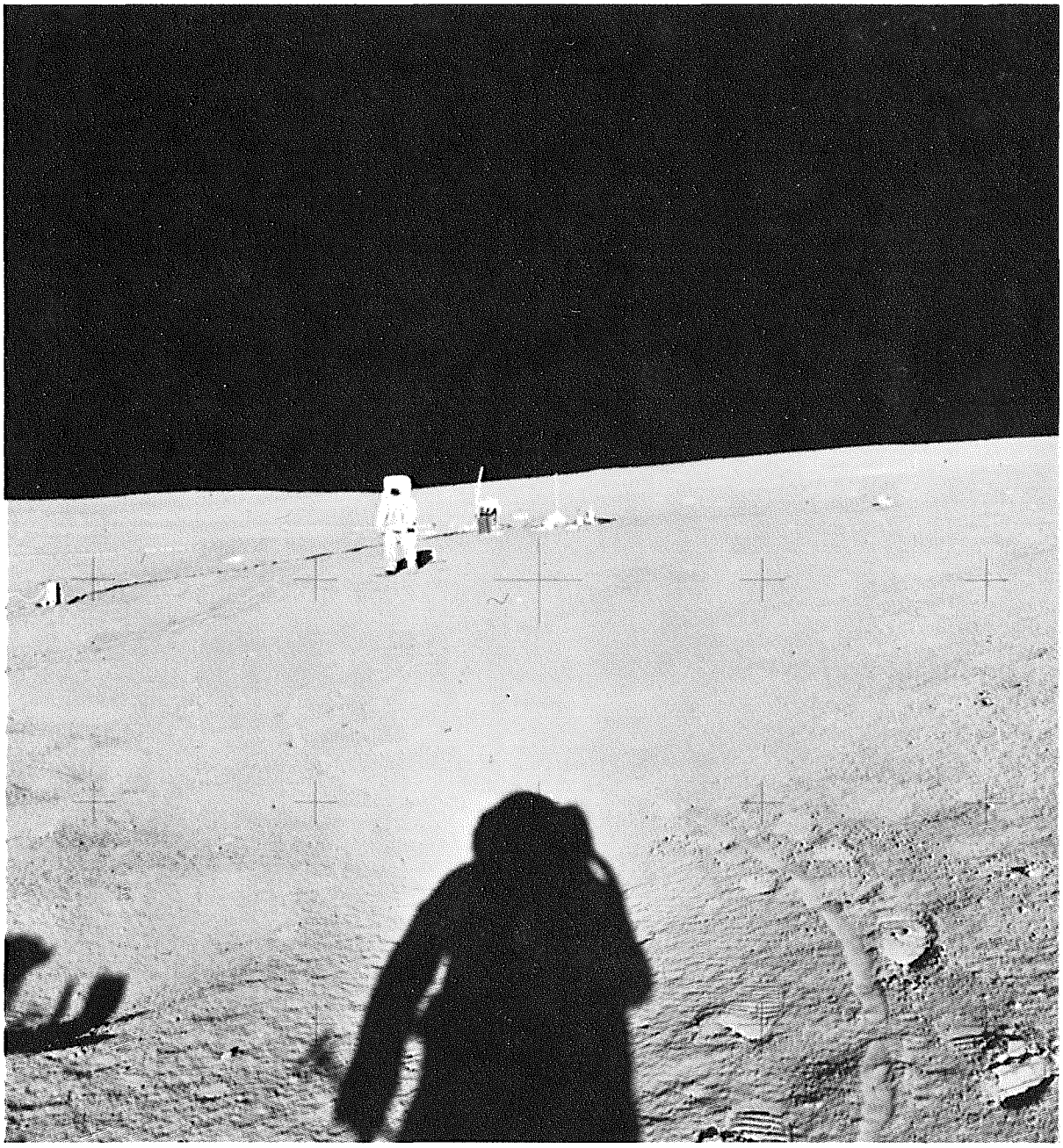

GUEST EDITORIAL

James A. McDivitt
Colonel, United States Air Force
Manager, Apollo Spacecraft Program Office
NASA Manned Spacecraft Center

The Apollo program, which has taken man further in his exploration of his surroundings than any previous endeavor in history, began with a spark of imagination in 1959. It was obvious that this spark would ignite an expansive family of technical and engineering innovations required to accomplish such a feat. Much has been discussed and published regarding the extraordinary nature of the Apollo vehicle and booster programs, the related operations facilities, and the associated philosophical and social issues. There is one area in particular, however, that very clearly and distinctively underlines the basic intent of the Apollo program, that demonstrates the inventiveness sparked by the program, and that is even now providing a wealth of knowledge, the impact of which will extend far into the history of man. This area is the scientific exploration of the lunar surface implemented by the Apollo Lunar Surface Experiments Package, commonly referred to as ALSEP.

At the outset of the Apollo program, it was quickly recognized that – in addition to the attention that would necessarily be focused on transportation systems – attention should be given to the development of methods and equipment for detailed lunar exploration and evaluation. The major goal was a completely self-contained science station to be deployed and activated by the Apollo astronauts and left to operate on the lunar surface for some time after astronaut departure. During the initial years of the program, many concepts were reviewed and many potential instruments evaluated. These actions resulted in the basic definition of the ALSEP.

It is easy to imagine the variety of issues that required recognition, the problems that had to be solved, and the inventiveness that was required to provide and operate an ALSEP. How, for example, was a complex system of experiments to be contained and located in the Apollo vehicles for transportation? How could instruments be constructed to operate for extensive periods on the lunar surface in the face of extreme temperature variations and limited size and power? How could these same instruments be made easily deployable by the astronauts? How was electric power to be generated to permit the system to operate for years? These and many other questions have been successfully answered by combining the wealth of experience gained in past development programs with new techniques developed specifically for the ALSEP program.

The ALSEP has now been completed and demonstrated. The system was conceived, designed, developed, fabricated, and put into operation on the moon's surface within very little more than three years after the actual start of hardware development. Although the original experiments package was intentionally limited in size and complexity to be consistent with the objectives of the Apollo 11 mission, it provided history-making insight into the lunar environment and structure. The full-sized packages emplaced on the Apollo 12, 14, and 15 missions have since provided an absolutely unprecedented amount of information concerning lunar atmosphere, magnetic fields, particle and plasma impingement, physical structure, and meteorite impacts. These ALSEP systems have also verified that such equipment can be produced to operate over very long periods of time in extremely severe environments. Although the Apollo 11 system was required to operate for only one lunar day, it did in fact continue to operate for four and one-half months. The Apollo 12 system, designed to operate for up to one year, is still providing data. The Apollo 14 and Apollo 15 systems are also performing with no operational problems.

With the additional ALSEP systems planned for the Apollo 16 and 17 flights, it should be possible to develop a relatively complete picture of the moon, its surroundings, and its relationships to the earth and the sun. This network of instruments, emplaced in various locations on the front face of the moon, will once again demonstrate man's capability to implement his most imaginative ideas and to continue to expand his knowledge of the universe.

ALSEP: The Scientific Voice of the Moon

L. R. LEWIS

A network of scientific stations is today continuously relaying long-term science data to earth from the lunar surface. The data are transmitted from scientific experiments deployed on the moon as a part of Apollo missions 12, 14, and 15. Similar packages are to be deployed on Apollo missions 16 and 17. This paper presents an overview of Apollo Lunar Surface Experiments Package (ALSEP) design and development, with particular emphasis on constraints imposed on the system and on those aspects of ALSEP design that are unique to this system among space systems. The status of experiments deployed on Apollo missions 12 and 14 is discussed briefly. The individual experiments are described in detail in subsequent papers.

INTRODUCTION

The objectives of lunar surface exploration as it was to be carried out as a part of the Apollo program were defined by the National Academy of Sciences Space Science Board and by National Aeronautics and Space Administration Lunar Exploration and Science Conferences during the time period 1963 to 1965. The activity assigned highest priority for early Apollo landings was the collection of the greatest feasible number and variety of lunar samples. Second in priority was the emplacement of lunar surface observatories for long-term scientific investigation. The basic science data to be obtained by the observatories were to define

- the internal structure and composition of the moon;
- heat flow from the lunar interior;
- tectonic processes and meteorite impacts, with an assessment of their importance in the genesis of surface features;
- near-surface geologic structure;
- the existence and nature of the moon's magnetic field;
- the interaction of the solar plasma with the moon's magnetic field;
- the nature of and variations in the lunar gravitational field;
- characteristics of particulate solar radiation reaching the lunar surface;
- the nature of the earth's magnetospheric tail;
- the nature of the tenuous lunar atmosphere and the composition of gases released by tectonic and impact processes; and
- the precise orbit and libration pattern of the moon.

Beginning in August 1965, preliminary design tasks were performed in parallel by three contractors* to define the lunar surface science support systems. In March 1966, we at this facility were selected by the NASA Manned Spacecraft Center as prime contractor for the design, integration, test, and systems management of the scientific exploration system known as the Apollo Lunar Surface Experiments Package (ALSEP). ALSEP instruments are carried to the moon on the Apollo spacecraft and set up on the lunar surface by the Apollo crew. Using a self-contained power supply and communications equipment, each ALSEP collects and transmits to earth scientific and engineering data for extended periods of time following astronaut departure. The system has flown on Apollo 12 and all subsequent missions.

A variation of the ALSEP, known as the Early Apollo Scientific Experiments Package (EASEP), was flown on Apollo 11, the first flight to land on the moon. Deployment of this package, an abbreviated version of the ALSEP, is shown in Figure 1; it differs from the ALSEP in that solar panels were used in place of a radioisotope thermoelectric generator (RTG) to generate electric power, and simplified experiments were incorporated to reduce the extra-vehicular-activity (EVA) time of the astronaut.

Because of power and weight limitations, no single flight can carry all the experiments. Table I details the seven different experiment arrays assigned to the individual Apollo flights. Each ALSEP incorporates between four and seven of the total of fifteen experiments that have been developed.†

*Aerospace Systems Division of The Bendix Corporation, Ann Arbor, Michigan; Space-General Corporation, El Monte, California; and TRW, Incorporated, Los Angeles, California.

†Four of these experiments – the Lunar Surface Magnetometer (LSM), the Solar Wind Spectrometer (SWS), the Suprathermal Ion Detector Experiment (SIDE), and the Cold-Cathode Ion Gage Experiment (CCGE) – are Government-furnished equipment; the other eleven are provided by The Bendix Corporation on either a build in-house or a subcontract basis.

Table I Experiment Mission Assignments

Experiment	Principal Investigator[a]	Mission, Array, Deployment Date, and Landing Site						
		Apollo 11 EASEP 20 July 1969 Mare Tranquillitatis (23.5°E, 0.6°N)	Apollo 12 ALSEP A 19 November 1969 Oceanus Procellarum (23.4°W, 3.2°S)	Apollo 13 ALSEP B (Mission Aborted)	Apollo 14 ALSEP C 5 February 1971 Fra Mauro (17.5°W, 3.7°S)	Apollo 15 ALSEP A-2 31 July 1971 Hadley Rille (3.6°E, 26.1°N)	Apollo 16 ALSEP D April 1972 Descartes[b] (15.5°E, 8.9°S)	Apollo 17 ALSEP E January 1973 Alphonsus[b] (4.1°W, 13.9°S)
Passive Seismic Experiment (PSE)	Gary Latham Lamont-Doherty Geological Observatory, Columbia Univ.	●	●	●	●	●	●	
Laser-Ranging Retroreflector (LRRR) · 100 Corner	J. E. Faller Wesleyan University	●			●			
· 300 Corner						●		
Lunar Surface Magnetometer (LSM)	Palmer Dyal Ames Research Center		●			●	●	
Solar Wind Spectrometer (SWS)	Conway W. Snyder Jet Propulsion Laboratory		●			●		
Suprathermal Ion Detector Experiment (SIDE)	John Freeman Rice University		●		●	●		
Heat Flow Experiment (HFE)	Mark Langseth Lamont-Doherty Geological Observatory, Columbia Univ.			●		●	●	●
Charged-Particle Lunar Environment Experiment (CPLEE)	B. O'Brien/D. Reasoner Rice University			●	●			
Cold-Cathode Ion Gage Experiment (CCGE)	Francis Johnson University of Texas			●				
Active Seismic Experiment (ASE)	Robert Kovach Stanford University				●		●	
Lunar Seismic Profiling Experiment (LSP)	Robert Kovach Stanford University							●
Lunar Surface Gravimeter (LSG)	Joseph Weber University of Maryland							●
Lunar Mass Spectrometer (LMS)	John H. Hoffman University of Texas							●
Lunar Ejecta Meteoroid Experiment (LEAM)	Otto Berg Goddard Space Flight Center							●
Dust Detector (DD)	James Bates Manned Spacecraft Center	●	●	●	●	●		

[a] For most experiments, a team of co-investigators is responsible for definition of experiment requirements and interpretation of science data; only the principal investigator is listed here.

[b] Tentative location.

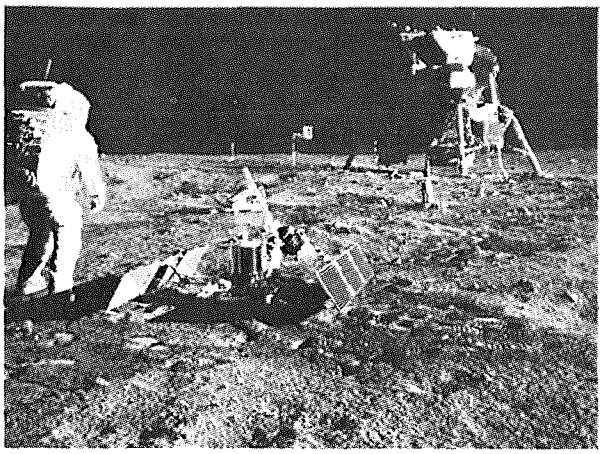

Figure 1 Apollo 11 Early Apollo Scientific Experiments Package (EASEP)

DESIGN GUIDELINES AND CONSTRAINTS

Design of the ALSEP systems for Apollo missions 12 through 16 was governed by the following guidelines and constraints:

- Operating lifetime of one year.
- Deployability of experiments and supporting subsystems within astronaut capabilities and safety constraints.
- Capability of withstanding the natural and induced mission environments (launch, boost, and descent vibration and shock; lunar surface temperature variations between +250° F and -300° F; lunar surface dust; vacuum).
- Capability of full operation during both lunar day and lunar night.
- Operating capability with Manned Space Flight Network telemetry ground stations, with a downlink bit error rate of 10^{-4} or less and an uplink bit error rate of 10^{-9} or less.
- Compatibility with Lunar Module interfaces (internal volume of 15 cubic feet, system weight constraints of about 300 pounds, and stowed center-of-gravity constraints).
- Capability of deployment at lunar longitudes of ±45 degrees and latitudes of ±25 degrees.
- Deployability at sun angles of 7 to 25 degrees.
- Maintainability of system thermal control when all exposed surfaces are degraded by dust or ultraviolet radiation.
- Capability of withstanding extended ground testing without damage.

The ALSEP for Apollo 17 was redesigned with reliability improvements that provide an operational lifetime of two years. Mechanical and electrical interface flexibility has been increased to accommodate a new array of experiments and landing sites with longitudes up to ±60 degrees and latitudes of ±45 degrees.

ALSEP CONFIGURATION

The ALSEP is transported to the moon in the descent stage of the Lunar Module (LM). In its stowed configuration, shown in Figure 2, the ALSEP consists of two subpackages and a fuel cask assembly.* The two subpackages mount within the LM scientific equipment (SEQ) bay; each package is approximately 24x27x21 inches in size, and their combined volume is about 15 cubic feet. A four-point LM interface, two bullet pins on the rear and two latch bars on the front, is provided for locking the ALSEP subpackages in place. The astronaut releases each package from the LM and lowers it to the lunar surface by pulling on a single lanyard. He transports them "bar-bell" style, connected at their bases with a carry bar, to the ALSEP deployment site. Both packages also have a handle and can be carried in the more difficult suitcase style in a contingency situation.

Subpackage 1

Subpackage 1 is shown in its stowed and deployed configurations in Figure 3. The lower portion of the package is a primary structure within which are housed the central electronics, which include the data

*The Apollo 11, 14, and 15 ALSEP systems contain in addition a Laser-Ranging Retroreflector (LRRR) Experiment, which is described in detail in a subsequent paper.

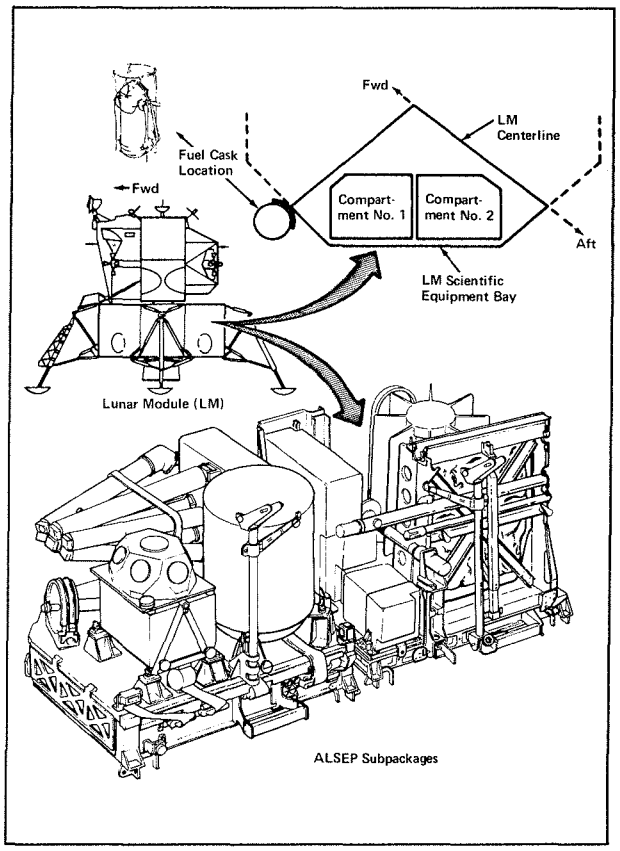

Figure 2 Location of the ALSEP within the Lunar Module

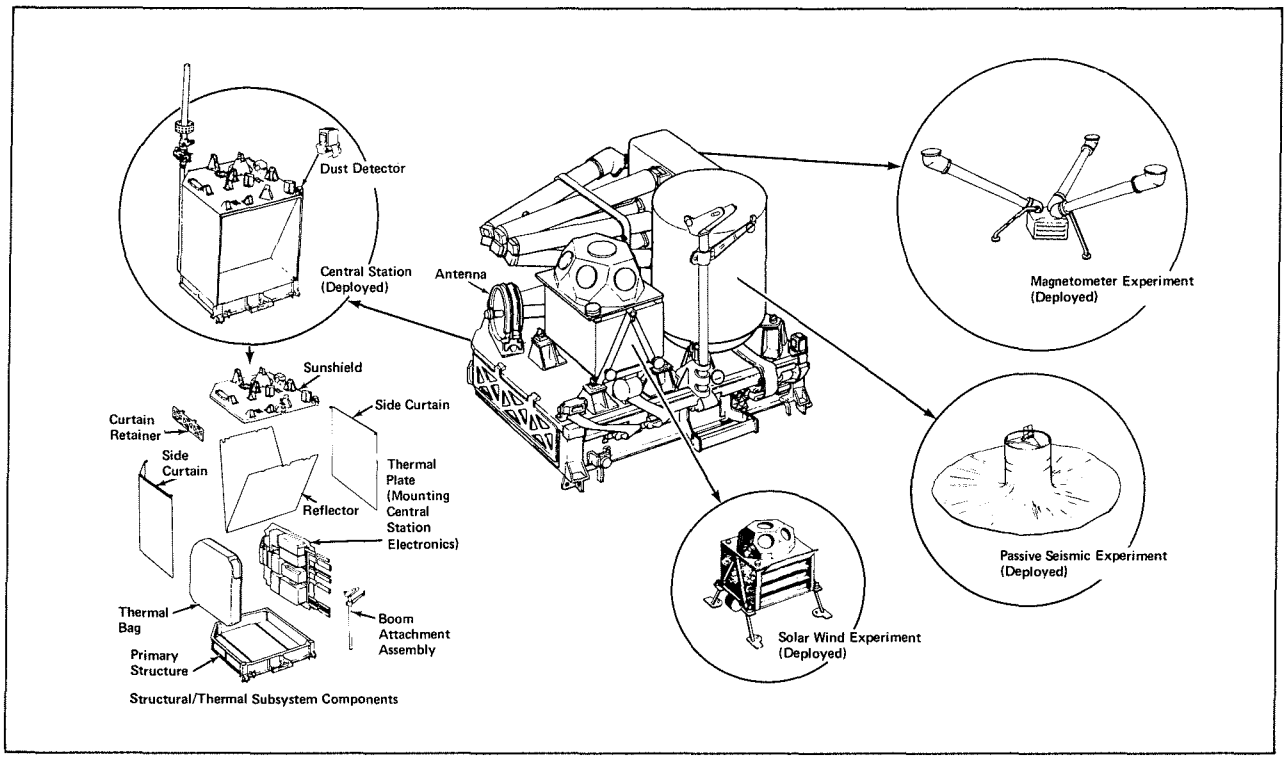

Figure 3 ALSEP Subpackage 1 (Apollo 12 and 15 Configuration)

handling, r.f. uplink, r.f. downlink, and power distribution subsystems. These subsystems are mounted on a thermal radiating plate, surrounded on five sides by a multilayered superinsulation thermal bag. Immediately above the primary structure is a rigid structural honeycomb plate which is used as an experiment-mounting structure during lunar transit and as a sunshield for the thermal radiating plate after experiment deployment. In the stowed configuration, the sunshield is attached to the primary structure and the experiments are attached to the sunshield with quick-release quarter-turn fasteners* capable of providing a preload during the induced-environments portion of the missions. When the experiments are removed, the sunshield is released and self-erects to a height of 27 inches above the thermal plate with the aid of four tubular extension springs. Multilayer aluminized-Mylar and Kapton superinsulation side curtains automatically unfold as the sunshield rises and cover the east and west sides of the package. These side curtains prevent sunlight from falling directly on the thermal radiating plate. On missions at lunar latitudes greater than 5 degrees, a third side curtain is added to the side of the package facing the lunar equator.

In the erected configuration, shown in Figure 4, the electronic and thermal portions of subpackage 1 are referred to as the Central Station. Flat conductor cables are used to connect the experiments to the Central Station. Kapton-covered cable was selected because of its excellent electrical and mechanical properties and its low weight. Cable lengths for the various experiments vary from 10 to 70 feet, in accord with scientific requirements for avoiding mutual interference. The cable is stowed in cable reels mounted either under or beside each experiment.

*A special Boyd-bolt fastener was developed by The Bendix Corporation for this application.

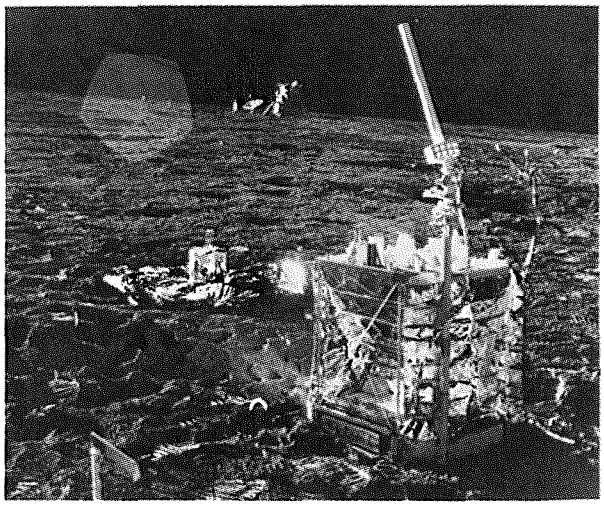

Figure 4 Apollo 12 ALSEP Central Station Deployed on the Moon

A helical S-band antenna is also carried on subpackage 1. The antenna is attached to an aiming mechanism and an antenna mast, which in turn is locked into the primary structure. The aiming mechanism provides for leveling of the antenna platform, alignment to the sunline, and positioning in azimuth and elevation to yield an overall antenna-pointing-accuracy capability of ±1 degree.

Subpackage 2

Subpackage 2 is shown in its stowed and deployed configurations in Figure 5. It consists of a rigid structural pallet on which are mounted one or two experiments, together with the SNAP-27 radioisotope thermoelectric generator (RTG) assembly, the antenna-aiming mechanism, special ALSEP deployment tools, and – on two Apollo flights – an astronaut geologic-hand-tool carrier. The generator assembly is permanently attached to the aluminum pallet; all other equipment is attached to subpallets and removed from the pallet early in deployment. This arrangement minimizes astronaut activity near the generator assembly during its warm-up cycle. The removable equipment is tied down with quick-release fasteners similar to those used on subpackage 1. The special tools carried include the universal handling tool used for releasing fasteners and for carrying experiments and other equipment, the special fuel cask tools discussed below, and a dual-purpose carry bar and antenna mast.

Fuel Cask Assembly

The fuel cask assembly is a translunar-flight stowage system for the plutonium-238 radioisotope fuel source used to power the ALSEP radioisotope thermoelectric generator. The assembly is mounted external to the Lunar Module and to the left of the LM scientific equipment bays.

SPECIAL DESIGN CONSIDERATIONS

Development of the Apollo Lunar Surface Experiments Package presented several unique challenges with respect to design, as compared with other space experiment systems. The most significant of these challenges are discussed in the sections that follow.

Environment Severity

The environments to which the ALSEP system is exposed include the vibration, acceleration, and shock associated with Saturn V and Lunar Module

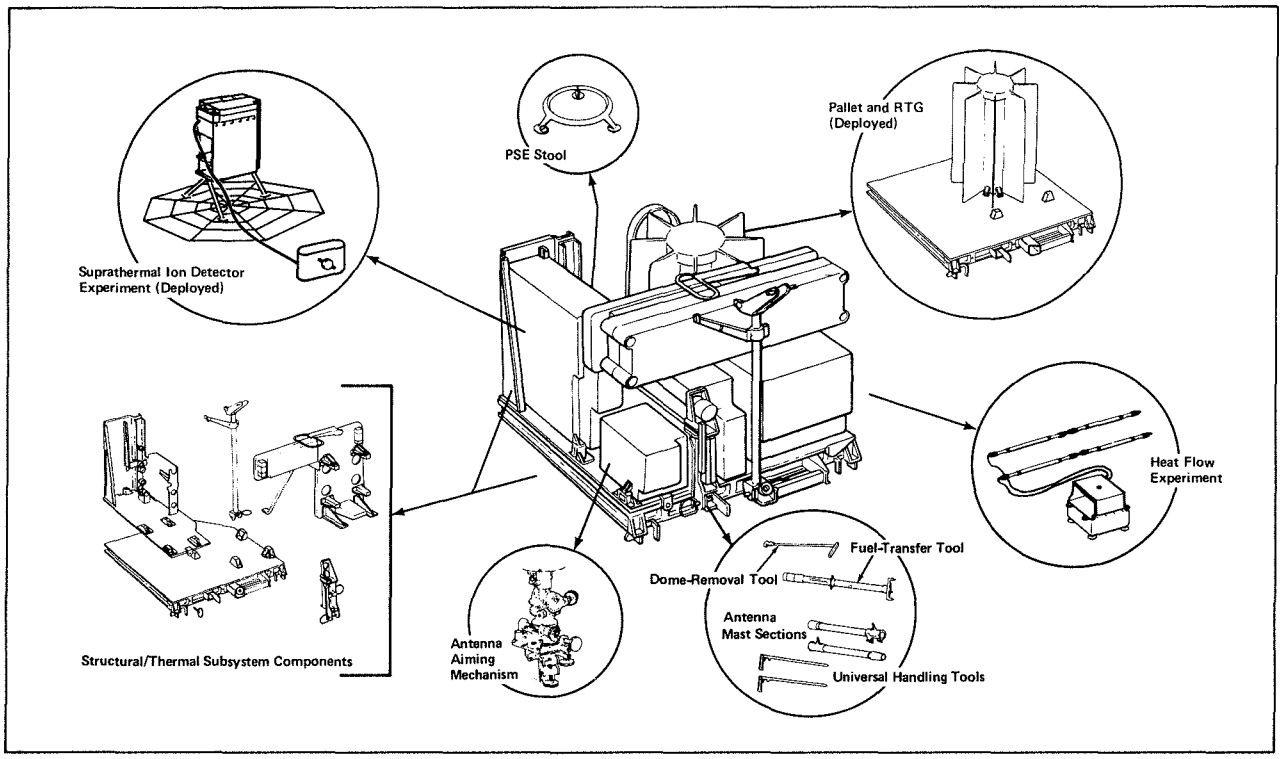

Figure 5 ALSEP Subpackage 2 (Apollo 15 Configuration)

launch, boost, and lunar descent; zero gravity during translunar flight; vacuums ranging from 10^{-4} Torr in Lunar Module storage down to 10^{-12} Torr on the lunar surface; lunar surface micrometeoroid and space radiation; transportation compartment and lunar surface temperatures; and lunar surface dust conditions. Of these, the last two pose the most severe design constraints.

Lunar surface temperatures vary slowly over the 28-earth-day lunar-day/lunar-night cycle from a daytime high of +250°F to a nighttime low of -300°F. Coupled with this, the lunar surface is covered with a deep layer of a fine-grain sticky dust very similar to powdered cement. It must be assumed, therefore, that all uncovered surfaces may become dust covered and thermally degraded as a consequence of astronaut handling and deployment and ultraviolet exposure. The biggest technical problem that had to be solved was how to provide a reliable thermal control system for the ALSEP under these lunar surface temperature and dust conditions.

Because active systems such as louvers, thermal switches, and heat pipes had to be ruled out for reasons of reliability, a variety of passive thermal systems were developed to provide acceptable Central Station and experiment-electronics operating temperatures. The approach used for the Central Station and for several of the experiments incorporates a sunshield/specular-reflector/side-curtain arrangement that prevents solar radiation from falling directly on thermal radiating surfaces. Most of the thermal radiation from the lunar surface is reflected from the specular reflector so that it does not impinge on thermal radiation areas. The remainder of the experiment or Central Station is surrounded by a superinsulating thermal bag made up of multiple layers of aluminized Mylar, which thermally isolates the electronics from the external temperatures. Temperature gradients between equipment external surfaces and equipment electronics of up to 340 Fahrenheit degrees have been maintained over gaps of less than 0.25 inch.

In some experiments, dust covers close over instrument apertures and/or thermal radiating surfaces; these are removed by the astronaut following deployment or by remote command following Lunar Module ascent. The thermal radiating surfaces in such cases are assumed to be dust free. On Apollo 14 and subsequent flights, the Central Station and most of the experiments are protected by dust covers to reduce dust accumulation during astronaut deployment activities.

A thermal blanket approach is employed in the Passive Seismic Experiment, which has a thermal-control design goal of 125±2°F. A superinsulation shroud 5 feet in diameter covers the top of the experiment and is laid on the lunar surface surrounding the experiment. This blanket, in combination

with the poor thermal conductivity of the lunar surface, tends to isolate the experiment from the large lunar surface temperature variations.

ALSEP packages are deployed at distances from the Lunar Module ranging from 300 to 1000 feet. The 300-foot minimum was selected to ensure that the experiments are not damaged by LM-ascent dust and debris or by plume heating effects. The astronauts can carry the packages no more than 1000 feet without excessive fatigue.

Reliability Constraints

The reliability required for continuous operation over periods of one and two years was obtained by

- keeping designs simple and eliminating unknowns. The ALSEP is necessarily a state-of-the-art system;
- designing electronics that utilize existing, proven-reliable piece parts (acceptable parts and materials lists);
- performing extensive tests to verify the reliability of the piece parts used when proven parts were unavailable;
- derating all parts significantly with respect to applied thermal and electrical stresses to reduce the probability of stress failures;
- providing redundancy for critical functions and components;
- eliminating single-point failure modes in design; and
- conducting an analysis of each failure noted in the test program to determine whether it was random in nature or indicative of a design deficiency requiring design improvement.

It was possible to make the ALSEP simpler and much more reliable than unmanned science systems of the same type by using the astronaut to perform complex Central Station and experiment-setup operations. At the same time, all designs were kept as simple as possible with respect to astronaut interfaces and activity requirements.

Numerical reliability analyses played only a small part in the program and were used mainly to determine which of several design approaches was the better from the standpoint of reliability. System-reliability design requirements of 0.90 were established for the Apollo 12 through 16 systems for one-year operation; a requirement of 0.90 for two-year operation was established for the Apollo 17 system. In addition, a five-year-operation design goal was targeted for the Apollo 17 system. To provide a tangible guideline for enforcing a strong reliability approach, a reliability/design integration team allocated a design goal to each subsystem and component. The design integration engineer was then able to exercise reliability-oriented trade-offs to obtain the best system possible within such system constraints as weight, volume, power, and number of experiments to be carried.

Although the reliability approach required the reeducation of a number of engineers and added to system design and development costs, its validity is attested to by the fact that the Apollo 12 ALSEP has been operating without a significant failure for 22 months as of the date of this writing.

Astronaut Interface Constraints

A number of severe human-factors constraints were imposed on ALSEP design, among them the spacesuit constraints, the 1/6-*g* environment, the extreme lunar lighting conditions, the weird lunar surface photometric function, and a variety of astronaut psychological factors. Like the reliability constraints, these constraints were met by keeping design mechanically simple and by making astronaut operations few and uncomplicated.

Extensive study and testing early in the program defined astronaut requirements with respect to reach heights, knob sizes, dial readability, force- and torque-applying limitations, and activity limitations imposed by astronaut fatigue factors. To validate astronaut capabilities, equipment functions, and task times, full-scale models were built and entire deployment sequences were enacted by spacesuited subjects on simulated lunar surfaces. Many of the test sequences involved 1/6-*g*-weight ALSEP subpackages carried by suited subjects in a 1/6-*g* simulation rig. Parts that could not be reduced to 1/6-*g* weight and still maintain a training model identical in size, fit, or function were evaluated with 1-*g* models in a KC-135 aircraft, where parabolic trajectories provide periods of 1/6 *g* lasting from 25 to 30 seconds. The crew usually undergoes approximately 125 minutes of KC-135 1/6-*g* simulation in its training sequence.

Power Source Constraints

The ALSEP prime power source must operate continuously for one year or more, during both lunar day and lunar night. It must have a power output of at least 63 watts, and thermal input rates must be consistent with LM vehicle constraints. It must require only simple and safe astronaut tasks, must operate reliably, and must be capable of withstanding the environments described above. Its weight and volume must be consistent with total system weights.

The requirements for day and night operation, along with the reliability and weight constraints, can only be met by a radioisotope thermoelectric generator (RTG) system. In the SNAP-27, which was designed and developed especially for the ALSEP, the heat source is separated from the thermoelectric converter, permitting their separate shipment to the moon. The generator can thus be integrated with the experiments package and the Lunar Module during transit without concern over thermal and electrical considerations; the LM/ALSEP interfaces are in turn greatly simplified, and astronaut safety is upgraded. The radioisotope-fuel-capsule heat source is located in a graphite cask external to the LM thermal enclosure for most efficient heat rejection.

FUEL CASK ASSEMBLY

The fuel cask assembly,* shown in Figure 6, has five major components: a graphite fuel cask, a cask band assembly, the mounting structure, a heat shield, and an astronaut guard.

The graphite cask is constructed primarily of graphite and beryllium and is designed to withstand and to radiate heat from the fuel capsule throughout the period from shortly before launch to lunar deployment. The cask has the form of an earth-atmospheric reentry body, and, like the fuel capsule, is capable of withstanding the high-impact shock load of reentry and hard landings intact. A breech-lock cover or dome provides loading and deployment capability for the fuel capsule with minimum effort and maximum safety.

The cask is rigidly held by a band assembly consisting of one longitudinal and two circumferential titanium bands. Should an abort occur, the titanium bands melt at the point that the LM descent stage reenters the earth's atmosphere, releasing the fuel cask to reenter separately. The validity of the design was demonstrated in the unfortunate termination of the Apollo 13 mission; although the Lunar Module broke up and disintegrated, a body having the aerodynamic characteristics of the graphite fuel cask was tracked all the way to impact in one of the deeper areas of the Pacific Ocean.

The band assembly is held at upper and lower trunnion points. A tilting-gear-box mechanism attached to the lower trunnion permits the astronaut to rotate the fuel cask from the vertical position to about 15 degrees below the horizontal for dome removal, as shown in Figure 7. The upper trunnion is firmly held during flight but is released prior to tilting via an astronaut-actuated shear-pin-cutter arrangement.

The heat shield is mounted directly behind the fuel cask to minimize the heat input to the Lunar Module. The shield consists of layers of gold-plated and aluminum-plated insulating material.

A tubular astronaut guard pivots with the fuel cask to prevent the astronaut from inadvertently approaching too closely or touching the hot cask.

RADIOISOTOPE THERMOELECTRIC GENERATOR

The SNAP-27 radioisotope thermoelectric generator (RTG) system* was developed specifically to accommodate the ALSEP mission.† The generator

*The fuel cask and generator assemblies are discussed in detail here since they are not described in subsequent papers.

†The system was developed by the General Electric Company for the U.S. Atomic Energy Commission, which provided it to the National Aeronautics and Space Administration.

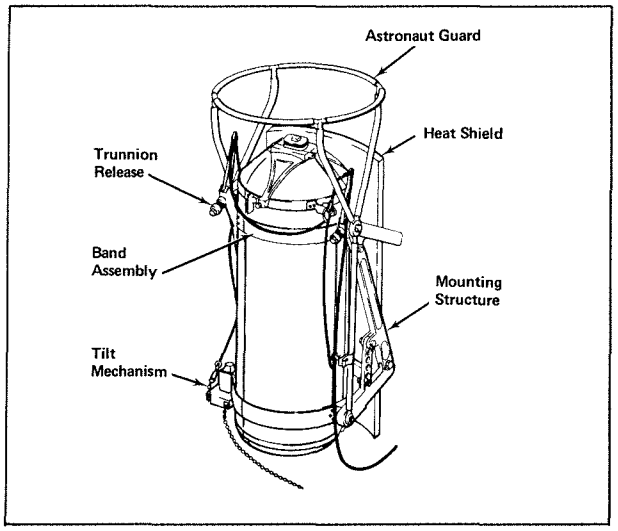

Figure 6 Fuel Cask Assembly

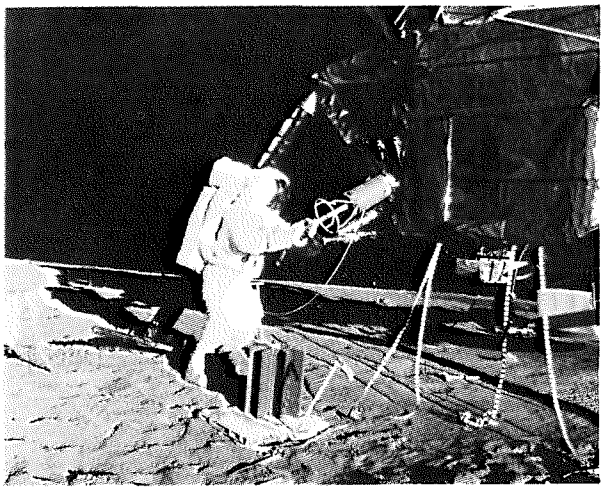

Figure 7 Apollo 12 Astronaut Tilting Fuel Cask and Removing Fuel Capsule

assembly, with the fuel capsule installed, is shown in the isometric cutaway in Figure 8. The system was designed to produce not less than 63.5 watts after a full year of lunar operation, assuming up to two years of earth storage for each fuel capsule. Heat from the $^{238}PuO_2$-fueled unit, with its nominal power of 1480 watts, is transmitted to the beryllium hot frame of the generator by radiation coupling. During normal operation on the lunar surface, the temperature of the capsule is 1350°F and that of the generator hot frame is 1100°F. Heat flow through the 442 thermoelectric couples in the system is such that the cold-side thermoelectric temperature is maintained at 525°F in the lunar-environment normal operating mode. Heat loss due to leakage between couples is kept to a minimum by the high-density packing of powdered Min-K insulation.

The thermoelectric material used in the SNAP-27 couple design is lead telluride. Each element forming the couple is integrally assembled such that the hot-side interface is free and the cold side is soldered to spherical caps. Electrically, two series strings of couples are connected in parallel, with each couple electrically laddered to prevent string loss in the event of a couple failing open-circuit.

The prime structural member of the generator is the outer beryllium case. Eight fins are brazed onto the cold frame to increase the radiating area and to reduce cold-frame temperatures.

The power outputs of the radioisotope thermoelectric generators deployed on Apollo missions 12, 14, and 15 have been greater than anticipated. Initial power was 73.6 watts for the Apollo 12 generator, 72.5 watts for the Apollo 14 generator, and 74.7 watts for the Apollo 15 generator.

ALSEP STATUS REPORT

The nature and importance of the science data being obtained by the various ALSEP systems are reflected in the Apollo Lunar Surface Experiments Package Status Report dated 4 March 1971. The following information is abstracted from that report.

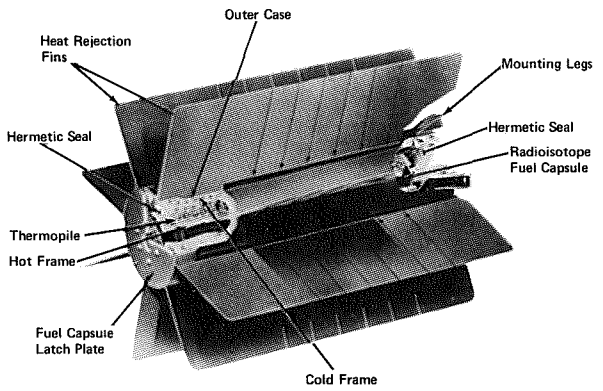

Figure 8 SNAP-27 Generator Assembly

Gary Latham, Principal Investigator for the Passive Seismic Experiment, reports that as the moon, in its monthly orbit, neared the time of closest approach to the earth at perigee on 25 February, seismic signals and clouds of gas were detected by the seismic, atmospheric-pressure, and particle detectors of the two geophysical stations then in operation on the lunar surface. Sixteen seismic events were recorded during a six-day interval beginning three days before perigee and ending three days after perigee. It is during such periods, when the pull of earth's gravity on the moon is greatest, that moonquakes have occurred most frequently in the past. Four of the seismic signals were recorded by both geophysical stations; twelve were recorded only at the Apollo 14 station. The signals were so small that scientists analyzing the data have been frustrated thus far in their attempts to locate the source. The fact that the greater number of signals has been recorded at the Apollo 14 station and that vibrations are much more rapid there implies, however, that the active region is much closer to the Apollo 14 station than to the Apollo 12 station. Indeed, it may be located in the crater Fra Mauro – a suggestion already made by the seismic team on the basis of data analyzed earlier. The exact source will probably not be determined until readings have been recorded through several perigee crossings in the course of the next few months.

Two events of particular interest to lunar scientists have been recorded by the cold-cathode-gage portion of the Suprathermal Ion Detector Experiment, which can measure pressures lower than the best vacuum achievable in earth laboratories. The first event began at 8:47 p.m. CST on 21 February 1971 and lasted for one hour. The second event began at 10:38 a.m. CST on 22 February and continued for over nine hours. The pressure at the Apollo 14 station increased tenfold during the first event, accompanied by an increase in the local concentration of gaseous ions. Both events appear to have been large clouds of gas moving rapidly over the lunar surface. It is impossible to determine at present whether these clouds escaped from the lunar interior as hot volcanic emissions or whether they have some other source; they will be studied with intense interest as possible clues to the present state of the lunar interior. Some astronomers have long thought gas clouds of this type to be the cause of the strange white and colored flashes observed periodically on the lunar surface by scientists studying the moon through telescopes. According to Gary Latham, the appearance of the

second gas cloud coincided with a moonquake, suggesting that the gas may escape through fissures or cracks in the surface that open when the surface is shaken by quakes.

John Freeman, Principal Investigator for the Suprathermal Ion Detector Experiment (SIDE), reports that gas ion clouds near the lunar surface have been detected almost simultaneously by the Apollo 12 and 14 stations. Freeman finds the ion clouds interesting because they have higher energy, as evidenced by their speed, than one would expect of ions heated solely by the moon's surface. By correlating data already obtained with additional data from subsequent measurements, he hopes to determine whether the gas clouds originate naturally on the moon or form from residual gases from the Lunar Module. If they originate naturally, it will be important to determine by what mechanism they are heated.

David Reasoner, Principal Investigator for the Charged-Particle Lunar Environment Experiment (CPLEE), reports that in less than a month of operation, the experiment has returned some ten million measurements of the charged-particle flows bombarding the lunar surface. The environment monitored by the CPLEE includes the long comet-like magnetic tail of earth, the so-called transition region or boundary of the tail, and the solar wind (particles streaming out from the sun in interplanetary space). Unique and fascinating data have been received from each of these regions. Within the tail, particles have been found that are quite similar to the particles that cause the aurora on earth. Along the boundary of the tail, streams of electrons have been detected – electrons presumably generated near the earth that have flowed to the vicinity of the moon. According to Reasoner, the transition region is literally full of particles of all types, and data from this region may help to explain exactly how the solar wind affects the magnetic tail of earth. Very surprisingly, measurements of solar particles striking the surface show that the strength of the solar wind varies rapidly, much like that of winds on earth on a gusty day. Reasoner points out that the charged-particle experiment can detect from the moon certain processes occurring near the earth that affect radio communications, the aurora being one such effect. He also indicates that information on the interaction between magnetic fields and charged particles is fundamental to plasma physics and bears directly on efforts to develop nuclear-fusion power sources.

As of 1 October 1971, the Apollo 12 ALSEP, the Apollo 14 ALSEP, and the Apollo 15 ALSEP have operated successfully for 680, 237, and 61 earth-days, respectively. The electrical and thermal control systems of all Central Stations have performed faultlessly. The Apollo 12 ALSEP has executed about 10,700 commands, the Apollo 14 about 3700 commands, and the Apollo 15 about 2300 commands. The Apollo 12 and 14 RTG power sources still provide an output of about 72.0 watts. The output of the Apollo 12 generator, which was as high as 74 watts at the beginning of the mission, is slowly decreasing as anticipated.

All the Apollo 12 ALSEP experiments are still operating and providing excellent science data. The Solar Wind Spectrometer is operating nominally; the operations of the Suprathermal Ion Detector, the Lunar Surface Magnetometer, and the Passive Seismic Experiment are slightly degraded.

At the Apollo 14 station, the Passive Seismic Experiment, the Active Seismic Experiment, and the Lunar Surface Magnetometer continue to operate and provide good data. The Charged-Particle Lunar Environment Experiment operated successfully until it experienced a partial failure of a high-voltage supply on 5 June 1971; very limited data have been obtained from it since that time.

All Apollo 15 experiments and the Central Station are providing excellent data.

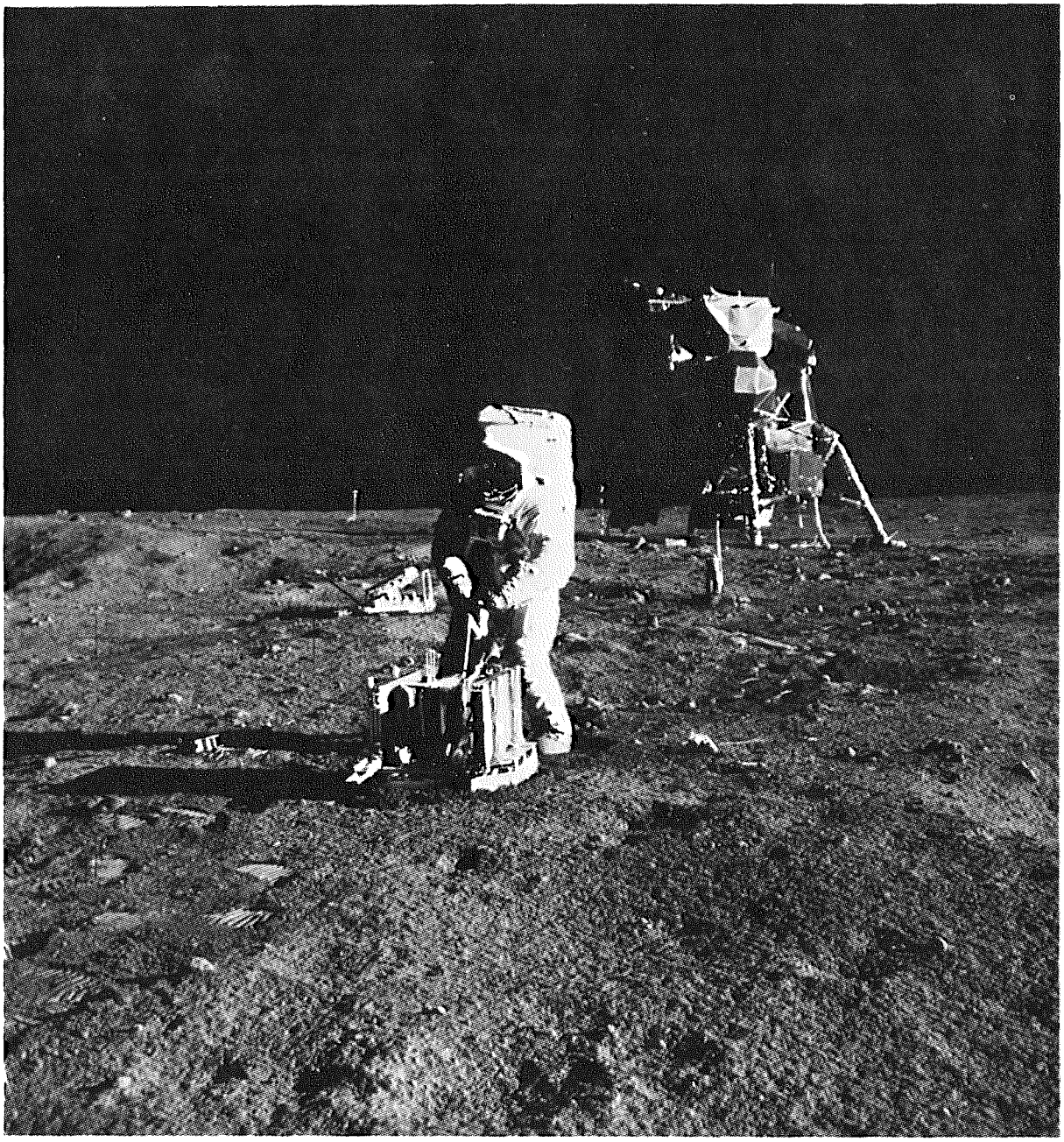

Some Aspects of ALSEP Structural/Thermal Design

J. L. McNAUGHTON

Design of the Apollo Lunar Surface Experiments Package (ALSEP) presented a considerable challenge in that it had to accommodate the structural and thermal requirements of the experiments themselves; weight and volume limitations imposed by the nature of the mission; launch, flight, and landing environments; crew interface and deployment constraints on the lunar surface; and long-term operation in the lunar environment. Package hardware had to be capable of withstanding launch vibrations of up to 20 g's at science compartment temperatures ranging between 0°F and 160°F. Structural and thermal design had to afford post-deployment passive thermal protection to the ALSEP electronics and power system under exposure to the vacuum of space at an effective temperature of absolute zero (-460°F), as well as to direct solar radiation and lunar surface temperatures ranging from -300°F to +250°F. Also to be considered was the material degradation that would result from exposure to lunar dust, ultraviolet radiation, and charged particles. This paper describes how these structural/thermal design requirements were met, and presents telemetered data which indicate satisfactory structural/thermal system performance throughout all phases of Apollo missions 12, 14, and 15.

INTRODUCTION

The Apollo Lunar Surface Experiments Package (ALSEP) is a system of scientific experiments carried to the moon on each Apollo mission and deployed on the lunar surface by the Apollo crew. Apollo 11 carried the Early Apollo Scientific Experiments Package (EASEP), which consisted of a passive seismometer and a laser-ranging retroreflector. Other experiments have since been developed, and these have been assigned, four to six per flight, for deployment during Apollo missions 12 through 17. Along with the experiments, each ALSEP contains a nuclear power generator and data processing and transmission equipment.

Because the experiments had to be interchangeable from one flight array to the next, flexibility in mechanical and electrical design became a major requirement. This paper describes some of the technical trade-offs that were conducted with respect to system weight, power, volume, mounting area, crew constraints, and thermal performance in arriving at the basic configuration. Such key design aspects as mechanical packaging, fastener systems, support structures, and thermal control are discussed in detail. Data are presented that demonstrate the structural/thermal design functionality of the Apollo 12, 14, and 15 ALSEP data systems and the satisfactory thermal performance of the electronics equipment during both lunar day and lunar night.

ALSEP OPERATION AND DESIGN CONSTRAINTS

In the stowed configuration, the ALSEP is made up of two subpackages. Subpackage 1 consists of the data subsystem, the antenna, and three experiments. Subpackage 2 contains one or two experiments, depending on the flight array, as well as the SNAP-27 radioisotope thermoelectric generator (RTG), crew tools, and the aiming mechanism. On the lunar surface, the astronauts unload the two subpackages, fuel the thermoelectric generator with a radioisotope fuel capsule (stored on the exterior of the Lunar Module in the fuel cask assembly), and transport the subpackages more than 300 feet to the mission deployment site. Here the experiments are removed and deployed at predetermined distances from the main data subsystem, as indicated in Figure 1. By the time deployment is complete, the RTG has generated a sufficient level of electric power to operate the data subsystem and the experiments, and data begin to be collected and transmitted back to the Manned Space Flight Network on earth.

Challenging constraints were imposed on ALSEP system design by structural/thermal and deployment requirements and by the nature of the lunar environment. Temperature limits specified for the data-subsystem mounting plates were 0°F to 125°F under

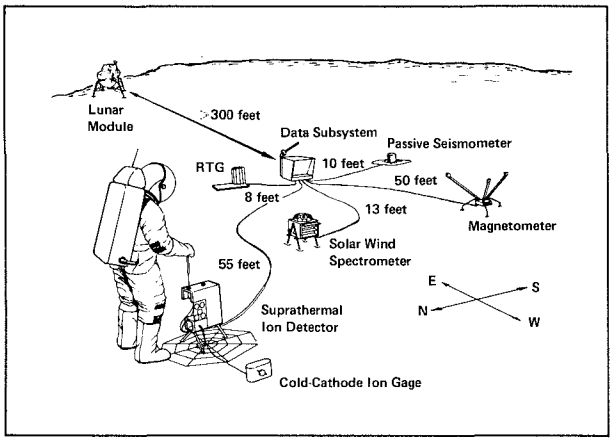

Figure 1 ALSEP Deployment Schematic

operating conditions and 0°F to 160°F in the nonoperating mode; the corresponding limits specified for the electronic components were -22°F to 158°F and -65°F to 160°F, respectively. The data-subsystem thermal control system was to maintain temperatures within these ranges even under conditions in which all horizontal heat-rejection surfaces exposed to solar radiation were totally covered with a layer of lunar dust. This requirement ruled out conventional thermal control concepts which directly reject heat to space, since their use would result in noonday temperatures in excess of 250°F. The thermal constraint imposed on the thin films and superinsulation materials used in system design was a capability of withstanding exhaust-plume heating of 2 BTU per square foot during Lunar Module ascent from the lunar surface.

The total system weight allocated to the ALSEP for stowage on the Lunar Module was typically 285 pounds per array. The two subpackages were to occupy a volume of no more than 15 cubic feet, and the maximum weight per compartment subpack was to be 155 pounds. System components were to be capable of withstanding the vibration levels detailed in Table I.

A major overall design requirement was high reliability over a 1-year operating period, with redundant modes of operation provided to meet contingency situations during ALSEP deployment. Deployment was to require a minimum of astronaut participation, and the physical capabilities of the crew imposed major constraints on equipment-removal and deployment design. The package was to be deployable at latitudes and longitudes within ±45 degrees of the equator to encompass all potential Apollo landing sites and was to have a minimum deployment distance from the Lunar Module of 300 feet to preclude damage from Lunar-Module-ascent debris and dust effects. Thermal-control and data-return considerations required that both the Central Station and the experiments be capable of alignment both vertically and in the east/west direction.

The environmental parameters that affected overall thermal design and material selection are listed in Table II. Lunar surface temperature as a function of time during the 29.5-day lunation cycle is illustrated graphically in Figure 2.

Table II Lunar Environment Parameters

Parameter	Value
Lunar Surface Temperature Range	-300°F to +250°F
Space Temperature	-460°F
Incident Solar Energy Level	130 watts per square foot
Lunar Albedo (average)	0.07
Lunar Surface Emittance (average)	0.93
Pressure	10^{-12} Torr

Table I ALSEP Vibration-Tolerance Requirements

Vibration Type	Vibration Magnitude, *g*'s		Vibration Frequency, cycles per second
	Subpackage 1 (rms)	Subpackage 2 (rms)	
Launch and Boost			
X Axis	5.8	6.4	20 – 2000
Y Axis	5.0	5.0	20 – 2000
Z Axis	5.9	5.3	20 – 2000
Lunar Descent			
X, *Y*, and *Z* Axes	3.2	3.2	20 – 2000
Sine			
X, *Y*, and *Z* Axes	0.2 in double amplitude		5 – 12
	1.5		12 – 100
Acceleration	14		60
Shock	15 (sawtooth pulse for 11 msec)		

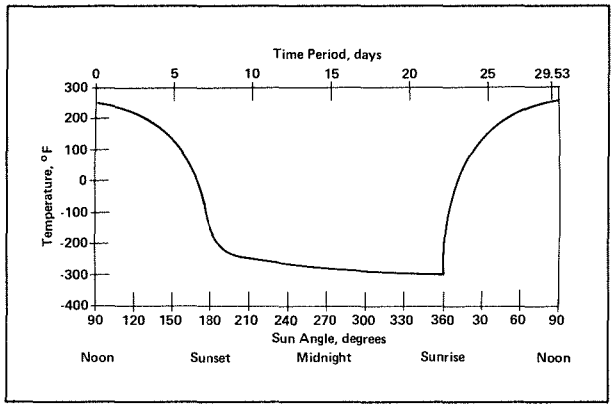

Figure 2 Lunar Surface Temperature as a Function of Time

PACKAGE CONFIGURATION

The ALSEP structural/thermal subsystem includes the basic structural assembly of subpackages 1 and 2, the fuel cask structure, the experiment subpallets, crew tools and carry bar, and the antenna and its aiming mechanism.

Subpackage 1

As shown in Figure 3, the structural/thermal portion of subpackage 1 consists of the primary structure, thermal plate, sunshield, side and rear curtains and reflector, thermal bag, boom assembly, experiment connectors, and astronaut switches.

The primary structure provides tie-down points for installing the subpackage in the scientific equipment (SEQ) bay of the Lunar Module. It also houses the data-subsystem electronics which are mounted on the thermal plate, isolating them from the wide fluctuations in the lunar temperature environment. The heat generated by the central electronics is dissipated to space by radiation from the thermal plate, the temperature of which remains within the range 0°F to 125°F.

The sunshield provides mechanical attachment points for mounting the experiments, the antenna, and the boom attachment by which the subpackage is lowered from the Lunar Module. Through modifications in the interface bracketry and the release fasteners by which the experiments are mounted, the sunshield implements array-design flexibility and experiment interchangeability. The fasteners are located at critical load points within the sunshield structure and are so arranged that load paths are brought directly to the Lunar Module interface points. The sunshield is raised during lunar deployment by the Apollo crew and thereafter, along with side and rear curtains and reflector, provides thermal protection for the electronics.

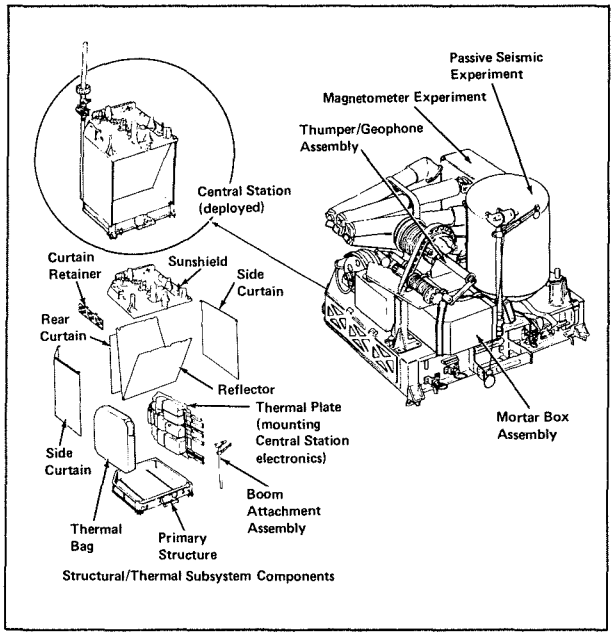

Figure 3 Structural/Thermal Components of ALSEP Subpackage 1

Subpackage 2

The structural/thermal portion of subpackage 2, shown in Figure 4, consists of the main equipment pallet, one or two experiment-mounting subpallets, the crew tools and tool carrier used on the lunar surface, a boom assembly similar to that on subpackage 1, and the antenna gimbal. Following removal of the subpackage 2 hardware at the deployment site, the radioisotope thermoelectric generator is mounted to the pallet, which then serves as its structural base and thermal radiator throughout mission operation.

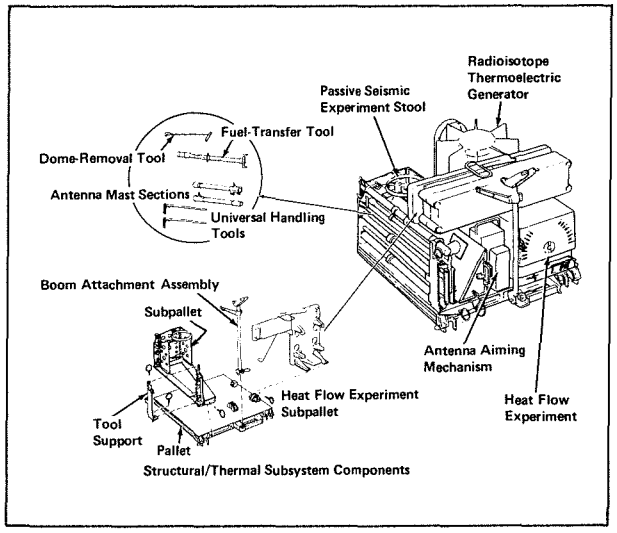

Figure 4 Structural/Thermal Components of ALSEP Subpackage 2

Tools available to the crew to implement ALSEP deployment include a dome-removal tool (DRT), a fuel-transfer tool (FTT), and two universal handling tools (UHT). The dome-removal tool implements dome removal and handling by engaging, locking in, and unlocking a nut on the dome of the fuel cask; rotation of the nut releases the dome. The fuel-transfer tool – three movable fingers that engage the fuel capsule and lock in place when the knurled section of the handle is rotated – is used to transfer the capsule from the fuel cask to the thermoelectric generator; release is accomplished by rotating the handle in the opposite direction. The universal handling tools are used to release tie-down fasteners, to transport experiment subsystems, and to emplace and manipulate the experiments on the lunar surface. The Allen Wrench tool tip engages the socket-head Boyd-bolt fasteners to rotate and release the bolts. A ball-type locking device provides a rigid interface between the tool and each subsystem receptacle. The tool is operated by a trigger-like lever near the handle.

Fuel Cask Assembly

The basic structure, thermal shield, cask bands, and cask guard make up the fuel cask assembly. The structure, which provides tie points for attaching the fuel cask to the exterior of the Lunar Module, is equipped with a thermal shield that reflects fuel-capsule thermal radiation away from the Lunar Module. The cask bands, clamped onto the cask, provide tie points for its attachment to the structure. The lower band incorporates a mechanism for tilting the fuel cask to gain access to the fuel capsule. The guard prevents astronaut contact with the 800°F cask during deployment.

Two temperature transducers monitor thermal-shield temperatures, and, in turn, assembly temperatures, during prelaunch and flight for transmittal through the LM telemetry system.

Antenna Mast

The antenna mast is made up of two sections that lock together and then lock onto the two ALSEP subpackages. On the lunar surface, the mast serves as a handle for carrying the subpackages "bar-bell" style to the deployment site. It is then attached to subpackage 1 to support the aiming mechanism and antenna.

KEY DESIGN FEATURES

Design of the ALSEP differed from that of previous space probes and scientific instruments in that a human interface was introduced, imposing mobility and dexterity limitations and visual and safety requirements. Several conflicting packaging configurations were suggested by area and volume constraints in the Lunar Module, in combination with requirements for survivability in the flight environment, operability in the lunar environment, and deployability with a minimum of crew participation. Moreover, redundancy had to be incorporated in all aspects of structural/thermal design to eliminate the possibility of single-point failures leading to partial or total

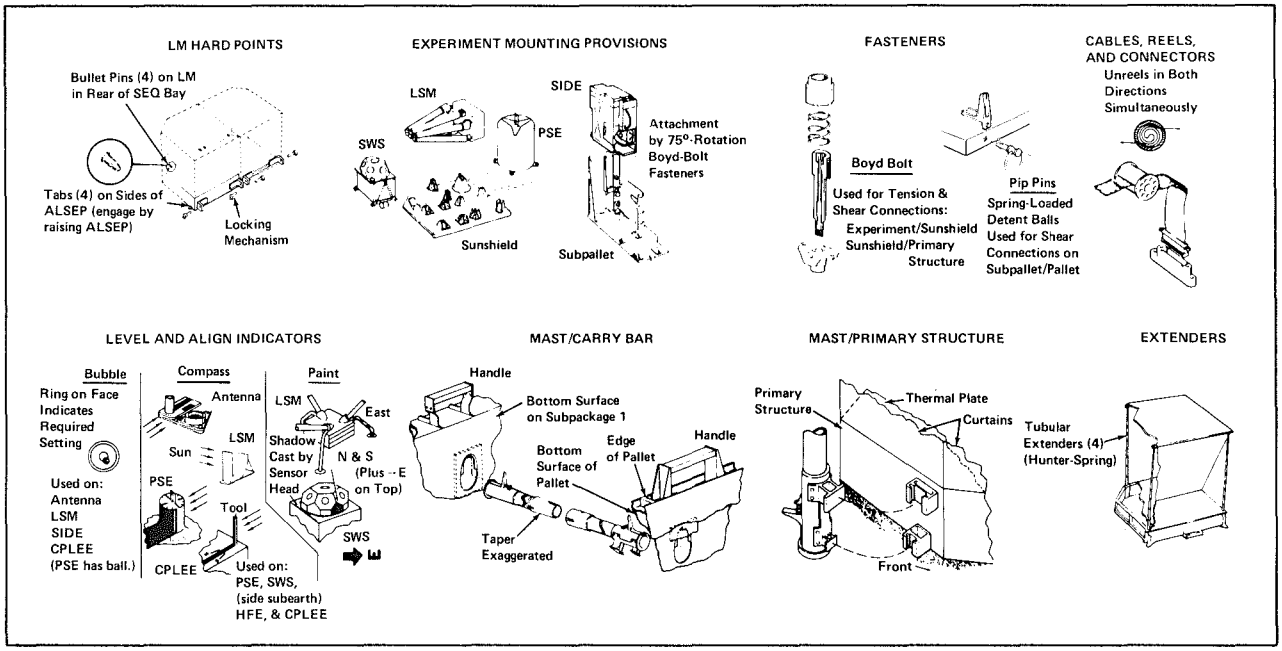

Figure 5 Major Mechanical Design Features

system failure. Final design form and material selection was therefore based on trade-offs conducted with respect to weight, volume, form, strength, and functional and environmental considerations. The major mechanical features that resulted are detailed in Figure 5. Table III lists the most important system components and the materials chosen for their fabrication, along with the key characteristics or functions that governed the choice.

Two key concepts – those for fastener release and thermal control – were developed specifically to accommodate the configuration selected and the materials used in final ALSEP design. These concepts are discussed in detail in the sections that follow.

Fastener Release

The ALSEP package, which in the stowed configuration can occupy no more than 15 cubic feet of space, must be capable of being manually removed from the Lunar Module and put into operation by spacesuited astronauts on the lunar surface. Achievement of a highly compact yet lightweight packaging design, that would demand of the Apollo crew no undue physical exertion, required that a new type of fastener-release system be developed. To this end, a major study was conducted to determine what existing hardware and system technology might be applicable to a fastener system consistent with ALSEP

Table III Key Features of and Materials Selected for Major Subpackage Components

Component	Material	Key Features and Characteristics
Primary Structure	aluminum (forged)	Has unique high-strength precision design. Houses electronics and is main support structure for equipment and experiments.
Thermal Plate	aluminum	Has high strength and flatness requirements. Supports electronics and provides flatness very critical to thermal-control heat transfer and electrical grounding.
Sunshield	aluminum (honeycomb)	Unique double-function structure that supports experiments in the stowed configuration and forms the top of the thermal enclosure in the deployed configuration.
Thermal Curtains and Masks	Mylar/fabric (alternating layers) Kapton (outer layer)	Form three sides of five-sided thermal enclosure above thermal plate.
Cable Reels • Flat • Radio-Frequency	 • Teflon • magnesium	Implement compact cable stowage and simple pull-out deployment. House permanent electrical connections.
Astromate	aluminum	Provides manual electrical-connection capability at deployment site.
Carry Bar	aluminum	Dual-function tool that forms dumbbell-mode structural interconnections for carrying equipment, then serves as mast for the S-band antenna system.
Tools • UHT • DRT • FTT	aluminum with CRES[a] interface fittings	 • Multipurpose handling tool used in ALSEP deployment. • Tool for fuel-cask dome removal. • Tool for transferring fuel from fuel cask to RTG.
Boyd-Bolt Fasteners	CRES[a]	Mechanical fasteners used on all ALSEP equipment.
Sockets	aluminum/CRES[a]	Implement UHT mating to all ALSEP components.
Release Systems • Velcro • Pull Rings • Lanyards • Latching Mechanisms • Clips • Pins	 • nylon • CRES[a] • Tufbraid • aluminum/CRES[a] • aluminum/CRES[a] • CRES[a]	Devices keyed to require minimal astronaut exertion. • Provides simple positive attachment. • Simple-release handles. • Provide access to remote release points. • Have positive-locking features. • Simple, quick-release locking devices. • Simple, quick-release locking devices.
Boom Assembly	titanium/aluminum	Implements remote release of the ALSEP from the LM.
Aiming Mechanism	magnesium/Vespel	Semiequatorial pointing device for aiming the S-band antenna toward a mean subearth point. Preset for prime landing site.
Leveling and Alignment Devices	aluminum/paints/films	Provided for all experiments, the antenna, and the Central Station.

[a]Corrosion-resistant eutectic steel.

structural design requirements and crew deployment considerations.

System Requirements

There are approximately 50 individual tie-down attachments on the two subpackages of a typical ALSEP array, all of which must be released during deployment. On subpackage 1, 20 fasteners hold the primary structure to the sunshield and thermal plate, 12 attach the experiments to the sunshield, and 2 mount the antenna to the sunshield. On subpackage 2, 11 interface points exist between the experiments and the pallet and subpallets, 3 between the RTG cable reel and the pallet, and 2 between the aiming mechanism and the pallet.

To develop the new design, it was necessary that the functional, structural, and environmental constraints to be imposed on the system be established. With respect to astronaut activity it was stipulated that, assuming the use of a crew interface tool, the fastener-release system was to require torques not exceeding 20 inch pounds for rotation of the fastener, vertical push forces not exceeding 20 pounds, vertical pull forces not exceeding 5 pounds, and rotation not exceeding 75 degrees for fastener engagement or release. Design was to implement positive visual release, with no danger of reengagement, galling, or cold welding. The fastener was to be capable of repeated usage without degradation or decreased reliability, and engagement and release were to require less than 10 seconds total time.

Structurally, the fastener was to have a maximum diameter of 0.25 inch and a grip length of 0.1 inch to 1.4 inches. The limits established for load-carrying capability were 300 to 500 pounds for preload, 900 pounds tension and 1730 pounds shear for rated load, and 1200 pounds tension and 2500 pounds shear for ultimate load.

Once these requirements had been established, an extensive survey was conducted to assess all existing mechanical, pneumatic, deflagration, and electrical fastener-release systems. System components were evaluated in terms of weight, development time and cost, reliability, crew deployment requirements, and crew safety. Results of the study indicated the need for a quick-release, manually operated fastener capable of high-bolt-tension preloading (>1200 pounds) and simultaneous release at low torques (<20 inches per pound) during deployment. Since these requirements were met by no existing fastener system, a development program was initiated which resulted in the Boyd-bolt fastener, the principal characteristics of which are substantial strength in shear and tension; small-rotation release requirements, with a positive stop indication; low-torque release requirements under pretension loads; adjustable grip; and high dynamic-load capability.

System Description and Operation

Figure 6 illustrates the construction of the Boyd-bolt fastener. A floating receptacle is attached to a base structure with two rivets or screws. This receptacle contains in its upper cylindrical section two locking splines and two release splines. Beneath the section containing these splines is a threaded section containing a four-lead thread. The thread is removed in the opposing 90-degree segments to provide for a breach-type engagement with the bolt.

The end of the bolt that mates with the floating receptacle also contains a four-lead thread with flats on opposing sides, leaving approximately 90 degrees of thread in opposing segments. Immediately above the threads are two locking balls whose action is controlled by the position of the central spindle. In the raised position, the spindle prevents the balls from moving toward the center of the bolt and thus provides for positive engagement of the balls with either the locking or the release splines. The spindle is maintained in its free position by a spring. At the top of the bolt is a double-hex socket, which is used in conjunction with a six-pointed stud on the end of the release tool. A pretension nut is threaded to the upper end of the bolt. A release spring, captive under the pretension nut, is compressed against the top surface of the upper assembly being joined; this spring provides an upward release force to disengage the bolt from the floating receptacle.

To assemble the fastener, a six-pointed tool is inserted into the bolt socket, causing the spindle to be depressed and, in turn, releasing the locking balls. The bolt is then inserted into the receptacle, with the locking balls oriented in line with the spline, and rotated clockwise 75 degrees until the locking balls hit

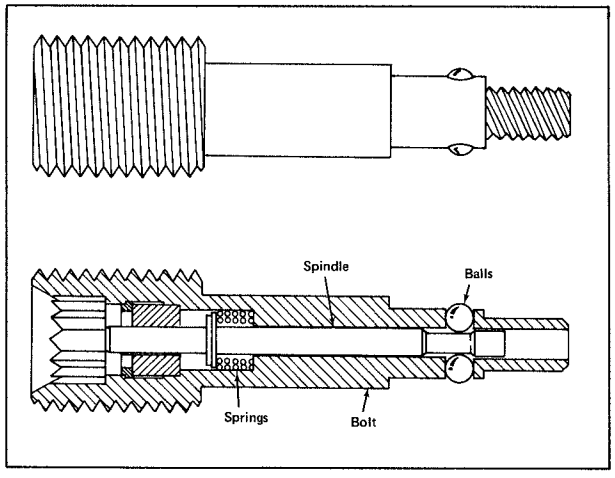

Figure 6 The Boyd-Bolt Fastener

the edge of the spline and the bolt can no longer turn. The hex tool is withdrawn from the bolt and the spindle moves upward, locking the balls in the locking splines. This prevents rotation and hence disengagement of the threads under vibration conditions. The pretension nut is then tightened to provide the necessary preload – in the case of the ALSEP, 500 pounds – between the parts being joined.

To release the fastener, the hex tool is inserted into the bolt socket, automatically unlocking the balls. A counterclockwise rotation of approximately 75 degrees disengages the bolt threads from the receptacle threads, and the release spring drives the bolt and pretension nut assembly out of the receptacle. The positive-stop characteristic of the fastener is implemented by a spiral pin, pressed into the receptacle to dead-end the threads; the bolt threads hit this pin and can turn no further than 75 degrees. When the tool is removed from the bolt, the balls again lock, preventing reengagement of the threads.

Thermal Control

Design Constraints

The requirement that all thermal control surfaces exposed to solar radiation in the ALSEP Central Station be capable of sustaining 100 percent dust coverage without degradation in system performance necessitated the development of a new structural/thermal design concept. This requirement cannot be met by previously developed systems that use direct radiators in conjunction with low-solar-absorptance/high-emittance thermal control coatings because solar energy normal to any radiating surface on the moon produces peak temperatures of approximately 250°F if the surface is dust covered. In the case of a radiating surface such as the ALSEP data-subsystem thermal plate, the heat being dissipated from the internal electronics would increase this temperature by several hundred degrees if the dust layer were only 1/16 inch thick.

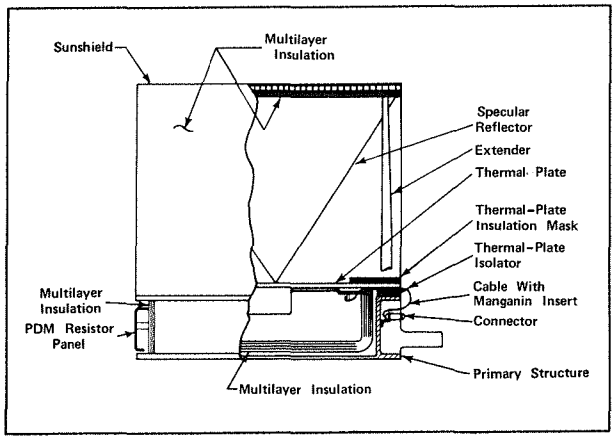

Figure 7 ALSEP Central Station Thermal Control

In developing the new thermal control concept, several other factors had to be considered. The thermal plate had to be kept in shadow for all solar angles between 0 and 180 degrees – that is, from sunrise to sunset. Solar heating angles and alignment requirements were complicated by the constraint that the ALSEP be deployable at any potential landing site within ±45 degrees of the equator. Finally, although heat dissipations from the electronics of the various flight arrays would differ widely, the system had to maintain a fixed passive operating-temperature range for each array.

Design Description

The concept selected for thermal control of the ALSEP data subsystem* is passive in operation, and the design is such that the electronic components are isolated from the effects of the widely varying lunar thermal environment. The thermal dissipation from the electronics is radiated to space from a thermal plate, which maintains a 0-to-125°F heat sink. Although spectrally selective thermal coatings are utilized, the system will function satisfactorily even if the coatings exposed to solar radiation are degraded by dust or other phenomena.

The general configuration of the Central Station thermal-control subsystem in the deployed mode is detailed in Figure 7. A multilayer reflective-insulation compartment houses the primary ALSEP electronic components and the mounting plate for these components. The mounting plate serves to radiate the internally generated heat directly to space. The effective radiating area of the plate determines its temperature level for given surface optical properties and given rates of internal heat dissipation and hence is an important design parameter.

The radiator surface is protected from direct solar radiation throughout lunar day by an insulated sunshield, which is deployed by the astronaut at the lunar deployment site. Since this protection must not interfere with direct radiative coupling between the radiator and space, package alignment must be a part of the deployment procedure. The two vertical side panels of the sunshield (referred to as side curtains) must be oriented to face approximately in an east/west direction, the exact orientation depending upon the location of the landing site. A specularly reflecting surface is positioned between the sunshield and the plate to minimize radiative interchange between

*H. E. Collicott and J. L. McNaughton, "Thermal Control in a Lunar Environment," *Bendix Technical Journal* 3 (No. 1), 1-15 (Spring 1970).

the plate and the lunar surface via reflection from the bottom of the sunshield structure and the side curtains. This reflector, which is a thin film of a polyester (Mylar) coated with aluminum to provide the specular reflective surface, is folded and stowed under the sunshield and is automatically deployed with the sunshield.

Two multilayer-insulation masks cover the top outer seven inches along the front and rear edges of the thermal plate. The masks limit the energy leaving the plate and also prevent direct solar heating in cases of off-equator deployment and/or package misalignment. Conductive isolation of the thermal plate from the lunar surface is accomplished by stand-offs and low-thermal-conductivity cable inserts. The stand-offs provide a high resistance between the radiator and the thermally exposed primary structure to which it is mounted. The cable inserts minimize heat leakage through the wires and cabling that penetrate the electronics compartment and are exposed to the lunar surface and to space. Isolation of the electronics compartment from radiation is accomplished by a thermal bag, by multilayer insulation between the structure and the thermal plate, by reflective coatings on structure and thermal-plate interior surfaces, and by reflective surface coatings on the subsystem electronics.

The power-dissipation-module (PDM) resistor panel functions as a heat sink for excess RTG power output and therefore minimizes thermal dissipation within the electronics compartment. Although the data-subsystem thermal control concept is passive in design, the PDM panel provides various commandable backup modes for controlling the distribution of power dissipation. Upon command, some of the power dissipated by the power control unit can be dumped on the PDM panel; on the other hand, power can be diverted from the panel and into heaters fastened to the thermal plate. These command capabilities provide the additional thermal control that the data subsystem may require in the extreme temperature environments of lunar noon and lunar night.

MATERIAL SELECTION

Translation of ALSEP structural/thermal requirements into a final system configuration required the application of a number of new materials and processes, with emphasis on thermal control coatings and insulation films. The materials included solar reflectors, such as white paints, used to achieve low daytime surface temperatures; infrared reflectors, used to reflect infrared energy away from critical thermal surfaces; and high- and low-temperature films and multilayer blankets, used to insulate the electronics and other thermally critical equipment.

Some specific materials, their thermal properties, and their uses are listed in Table IV.

LUNAR SURFACE THERMAL PERFORMANCE

As of September 1971, three Apollo missions have successfully deployed Apollo Lunar Surface Experiments Packages on the moon. Apollo 12 landed in the Ocean of Storms at 23.4 degrees west longitude and 3.2 degrees south latitude on 19 November 1969 and has been operating for 22 months. The Apollo 14 ALSEP was deployed nearby at Fra Mauro (17.5 degrees west longitude and 3.7 degrees south latitude) on 5 February 1971 and has operated for 7 months. The Apollo 15 flight, the first off-equatorial landing mission, deployed its ALSEP on 31 July 1971 at Hadley Rille, which is situated 3.6 degrees east and 26.1 degrees north of the equator.

Table IV Special ALSEP Surface Materials

Material/Finish	Solar Absorptance α	Infrared Emittance ϵ	α/ϵ	Use	Temperature Limit, °F
S-13G White Paint	0.20	0.9	0.22	solar reflector	350
Z-93 White Paint	0.18	0.95	0.19	solar reflector	500
Vacuum-Deposited Aluminum	0.10	0.02	5.0	infrared reflector	300
Gold Plating	0.25	0.04	6.2	infrared reflector	600
Aluminized Mylar	0.10	0.02	5.0	internal insulation layer and reflector	300
SiO_2 Deposited on Aluminized Mylar	0.15	0.60	0.25	external insulation coating	300
Aluminized Kapton	0.47	0.80	0.59	external insulation layer	750
Aluminized Teflon (Type A)	0.17	0.70	0.24	external shroud material	400

Prelaunch performance of the nuclear-fuel-capsule loading and cooling system and in-flight temperatures measured at various ALSEP locations have been well within expected limits for all flights. Deployment of the structural/thermal portions of all three packages has gone without incident. Successful operation of the structural/thermal system is reflected in the three plots of first-lunation thermal performance shown in Figure 8. Average electronics-plate temperatures indicate that the flexibility in structural packaging required to accommodate different experiment combinations and different landing-site latitudes and topographies was achieved without sacrificing the goals specified for system performance.

The maximum daytime temperatures attained by the Apollo 12, 14, and 15 systems – 97°F, 124°F, and 115°F, respectively – are well within the 125°F design requirement. Their respective nighttime minima of 0°F, 16°F, and 1°F also meet the specification minimum of 0°F. Because excess power proved to be available in all three systems, electric heaters were activated, which raised the nighttime minima to 23°F, 40°F, and 3°F, respectively; the same improvement did not result in each case because the power available for heating the electronics varied.

Initial turn-on temperatures at the time of deployment depend on temperatures in the scientific equipment bay of the Lunar Module, which differ markedly from flight to flight. A lunar eclipse that occurred during the first earth day of Apollo 14 and Apollo 15 ALSEP operation resulted in thermal-plate temperature losses of 35 to 40 Fahrenheit degrees. During the approximately 4.5-hour duration of such an eclipse, the solar heat input to the moon drops from 130 watts per square foot to a negligible level and then rises again, the drop resulting in a rapid loss of heat from the lunar surface; since the Central Station undergoes direct heat interchange with the lunar surface, the sudden drop in lunar surface temperature is indirectly reflected in the ALSEP data. The temperature of the sunshield, which is directly exposed to the sun, drops approximately 300 Fahrenheit degrees during the same period.

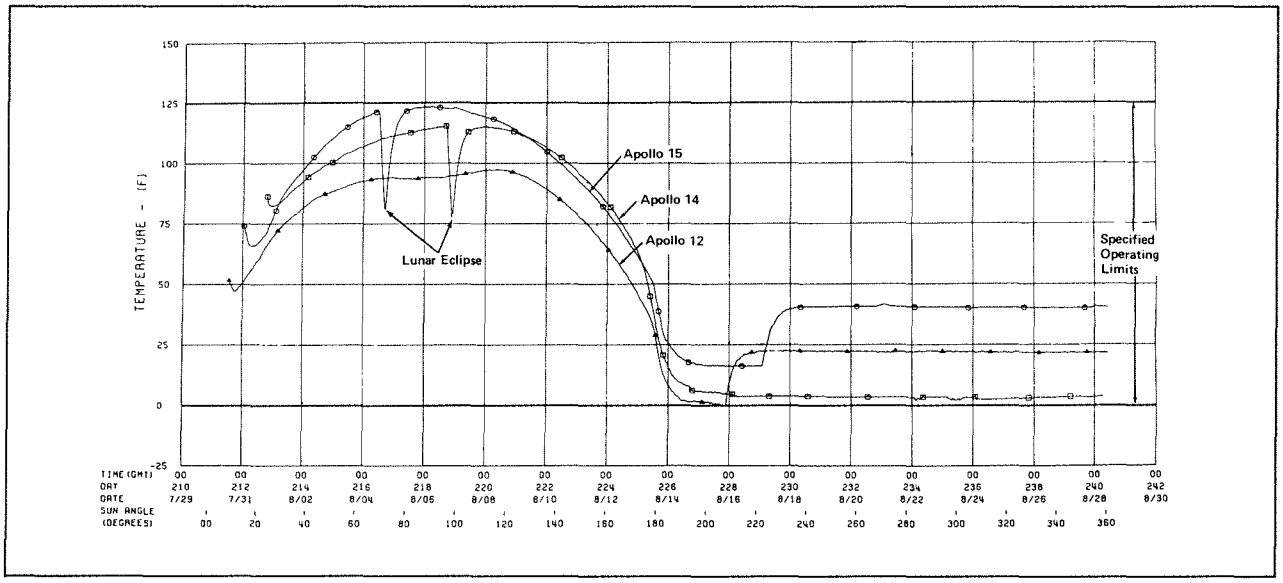

Figure 8 Thermal Performance of Apollo 12, 14, and 15 ALSEP Systems

The ALSEP Central Station Data Subsystem

W. M. TOSH

The data subsystem, around which the ALSEP Central Station is designed, implements address recognition, decoding, and routing for 100 usable commands transmitted by the Manned Space Flight Network to control the operation of the ALSEP experiments. It also collects and formats scientific data from the experiments, as well as engineering data for monitoring the performance of the experiments and supporting subsystems, and transmits these to earth as pulse-code modulation on an S-band telemetry signal. Its design incorporates extensive redundancy to ensure long-term reliability in the environmental extremes of the lunar surface. This paper discusses the data subsystem in detail and touches on the functions of such other Central Station components as the power conditioning unit and the electric power subsystem. The dust detector, which is mounted on the sunshield of the Central Station, is also described briefly.

THE DATA SUBSYSTEM

The data subsystem (DSS) is the focal point for control of the ALSEP experiments and for the collection, processing, and transmission to the Manned Space Flight Network (MSFN) of scientific and engineering-status data. The subsystem consists of a series of integrated units, interconnected as shown in Figure 1, which function to receive and decode uplink (earth-to-moon) commands, to time and control experiment subsystems, and to collect and transmit the downlink (moon-to-earth) data. The antenna receives the uplink command signals and routes them through the diplexer to the command receiver and then to the command decoder for address recognition, decoding, and command execution. Downlink data transmission is accomplished via the data processor, the transmitter, the diplexer, and the antenna. The DSS is

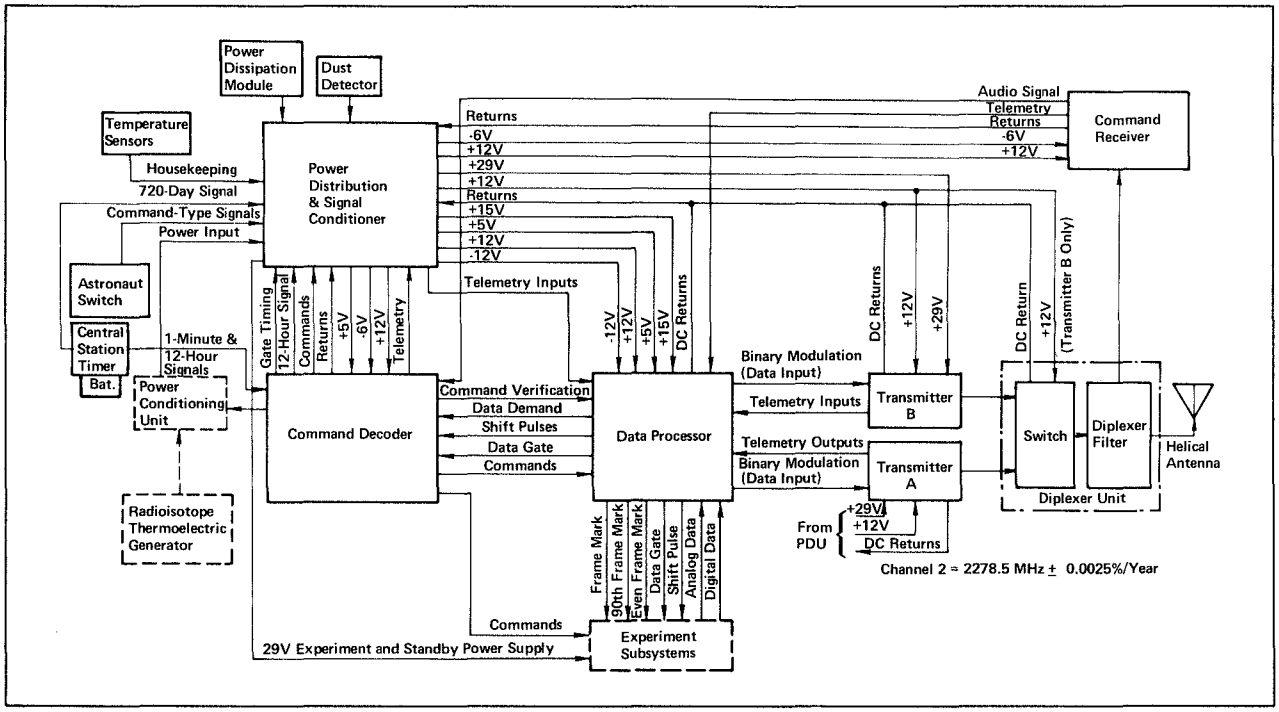

Figure 1 ALSEP Data Subsystem

designed with sufficient flexibility to interface with and to collect and process data from up to five of nine different experiment subsystems for each mission.

The components of the data subsystem are mounted on a thermal plate 23.25 inches by 20 inches in size, as shown in Figure 2. The plate is large enough to accommodate in addition the central electronics for two experiments. The components are linked electrically by a preformed harness through connectors having multiple pins (up to 244). Coaxial cables link the command receiver and transmitters to the diplexer switch and filter and thence to the antenna. The entire assembly is thermally insulated to maintain a temperature range of 0 to 135°F throughout the lunar day/night cycle.

The Central Station – the name assigned to the data subsystem and associated units – also incorporates temperature sensors, manual control switches, and thermal plate heaters. The manual control switches permit the astronaut to start system operation in the event that the uplink cannot be established.

Earth-to-Moon Command Transmission

ALSEP system control is exercised through commands transmitted by the Manned Space Flight Network (MSFN); these commands are checked for proper address and for command bit error, then decoded and routed to the proper experiment subsystem. The components that form the command link are designed to achieve a bit error probability of 10^{-9} ($P_e \leq 10^{-9}$) in recognizing and decoding command messages.

Command Signal Processing

The command data are transmitted by the MSFN at a frequency of 2119 megahertz. The carrier, modulated with a 2-kilohertz subcarrier and a 1-kilohertz synchronizing subcarrier, is received by the DSS antenna, routed through the diplexer, demodulated by the command receiver, decoded by the command decoder, and applied to the appropriate experiment and support subsystems as discrete commands. These commands control the operation of the experiment and its subsystems and initiate command verification functions.

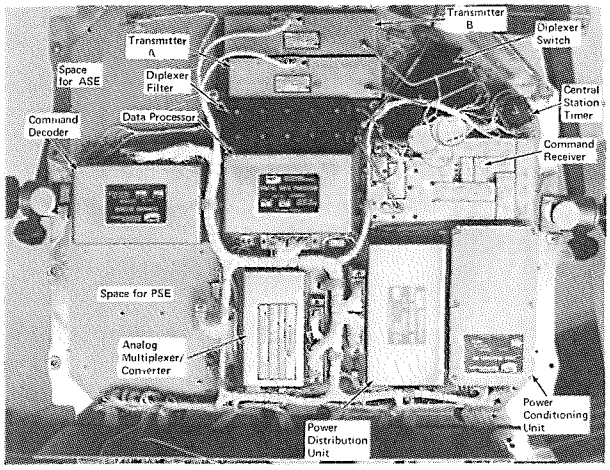

Figure 2 ALSEP Central Station Configuration

The antenna is a modified axial helix, designed to receive and transmit a circularly polarized S-band signal with an approximate gain of +15 decibels and a 3-decibel bandwidth of approximately 30 degrees. The antenna is mounted on a gear-driven gimbal platform that enables the astronaut to aim the antenna pattern toward the center of the earth's libration pattern. A diplexer filter connects the antenna through a low-loss path to the command receiver and simultaneously isolates the receiver from the transmitter output.

The receiver is a single-conversion device having a noise figure sufficient to meet the system P_e specification and to provide a margin of 6 to 8 decibels, with nominal performance of all parts of the link. Two local-oscillator/driver-amplifier circuits (designated A and B) provide operational redundancy. A level-sensor and local-oscillator switch circuit determines which local oscillator supplies the mixing signal; the level sensor monitors the local-oscillator signal and automatically switches to the redundant oscillator when signal level drops below a preset value. The receiver output, a 2-kilohertz command-data subcarrier modulated with a 1-kilohertz synchronization signal, is applied to the command decoder. Selected receiver parameters, including temperature, local-oscillator signal level, received signal level, circuit-A local-oscillator level, circuit-B local-oscillator level, and 1-kilohertz output are monitored in the downlink.

Command Signal Decoding

The command decoder receives the combined 2-kilohertz command-data subcarrier and 1-kilohertz synchronization signal from the command receiver, demodulates the subcarrier to provide digital timing and command data, and searches for proper address; upon address recognition, it decodes the command data and applies discrete commands to the appropriate experiment or subsystem. Figure 3 is a functional block diagram of the command decoder.*

Reliability is enhanced by redundant subsections that provide alternate paths (A and B) for decoding a command message. The two subsections function

*This diagram does not include the demodulator section.

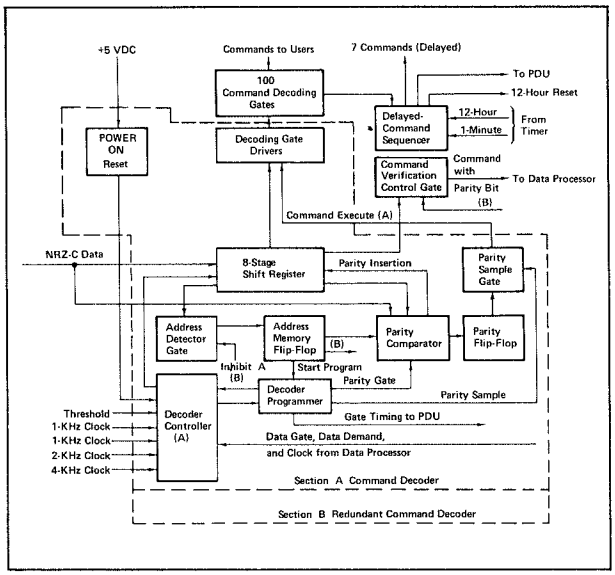

Figure 3 Digital Command Decoder

identically, but their address gates respond to different address information, and the MSFN operator may select either to decode and process a command. Reliability is further enhanced by a delayed-command sequencer that provides an automatic means for the local generation of commands in the event of uplink failure.

Since up to five ALSEP systems may eventually operate on the moon simultaneously, and since a single frequency (2119 megahertz) is used to transmit all command data, each system is assigned a unique address, with a separate address for each of the two sections of the command decoder. A command message consists of a 20-bit (1-kilobit-per-second) preamble, the 7-bit decoder command address, the command complement (7 bits), the 7-bit command, and a final 20 bits for timing the command-execution period. The 20-bit preamble provides time for the demodulator to acquire phase lock, enable the NRZ-C bit stream to the decoder shift register, and activate the threshold to start address search. Following reception of a valid address, the 7-bit command complement is shifted into the register. While this is happening, during the next 7-bit period, a bit-by-bit comparison is made between the command complement and the command. If the comparison is true, a ONE is inserted into one stage of the register and an EXECUTE signal activates decoding and execution of the command over the next 20 milliseconds. This technique ensures that only valid commands are executed. Following its execution, the command is held in the register until a data demand is received from the data processor, whereupon the 7-bit command and the ONE are inserted in the telemetry signal for transmission to earth. By checking this command verification word (CVW), the operator can verify that a valid command was received by the system and can identify the command that was decoded.

Of the 128 combinations available from the 7-bit command, 100 are used to control the system. Undesirable patterns such as all ONE's, all ZERO's, or single ONE's and ZERO's are not used. Each of the 100 commands is provided to the user through its own line driver.

The electronics, which are packaged on multilayer printed-circuit boards (up to twelve layers thick), have a weight of 2.7 pounds and occupy a 69-cubic-inch volume. Their operating power is 1.3 watts.

The reliability of command signal decoding has been effectively demonstrated by the Apollo 12, Apollo 14, and Apollo 15 ALSEP systems. As of September 1971, nearly 16,000 commands had been decoded and properly executed at the three lunar laboratories.

Moon-to-Earth Telemetry

The telemetry signal is biphase-modulated with the science and engineering data. The components associated with data collection, organization, and transmission are identified in Figures 1 and 2, previously presented.

The Data Processor

The data processor generates ALSEP timing and control signals, collects and formats both analog and digital data, and provides pulse-coded (PCM) data to modulate the downlink transmission. The processor consists of a digital data processor and an analog multiplexer/converter, the latter for engineering-status data. As can be seen in Figure 2, the two sections are contained in separate packages.

Functionally, either of two redundant data-processing channels (processor X and processor Y in Figure 4) may be selected to perform the data processing function. Both process analog as well as digital data. The digital data are applied directly to the processor channels. The analog (engineering) data are applied to a 90-channel analog multiplexer, where each of 90 data sources is sampled once every 54 seconds, the data being then digitized and transmitted to earth. The analog-to-digital converters use a ramp-generation technique to encode the analog signal into an 8-bit digital word. A single 8-bit conversion is made for each telemetry frame.

The data processor operates at one of three bit rates: a normal rate of 1060 bits per second, a rate of 10,600 bits per second in conjunction with the Active Seismic Experiment, and a contingency rate of 530

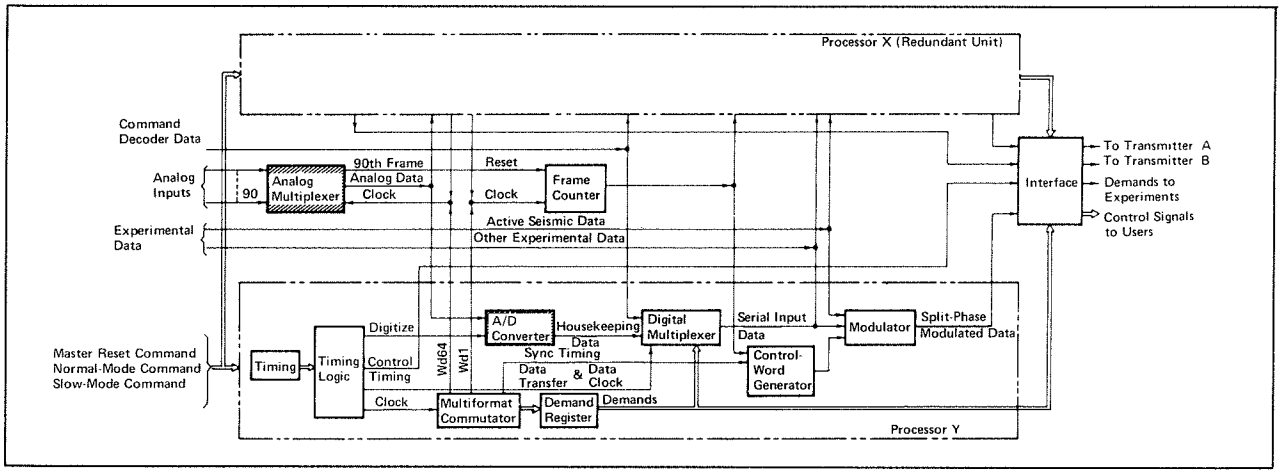

Figure 4 Data Processor

bits per second for improvement in bit error rate with degraded telemetry signal. The bit error probability acceptable for moon-to-earth telemetry is 10^{-4}, a requirement that is more than met by system performance.

In the normal mode, the demand signals to the data sources (the experiments) are one word in length and approximately 9.45 milliseconds in duration. The data processor formats the data collected from the experiments into the telemetry format shown in Figure 5. The frame rate in the normal mode is $1\frac{21}{32}$ frames per second or 0.6 second per complete data frame. Each frame contains 64 words of 10 bits each or a total of 640 bits. The first three 10-bit words (30 bits) are used for control, a single 10-bit word is used for command verification, and another 10-bit word is subcommutated with housekeeping data; the other words are assigned to the experiments. Format flexibility is such that word assignments can be changed to meet the science requirements of the individual experiments.

Within the 30-bit control, 22 bits – an 11-bit Barker code followed by the same code complemented – are used to attain synchronization at the MSFN ground stations. The next seven bits identify frames 1 through 90 for correlation of the 90 channels of analog multiplexer data. The final control bit provides normal- or slow-mode information during the first two frames of the 90-frame sequence, and identifies the data-processor serial number during the third through the fifth frames of the sequence.

To ensure synchronous operation, the data processor supplies a system clock to all experiments. In addition, a frame mark, an even frame mark, a 90th frame mark, and data gate signals can be made available where they are required by experiment design. Each output signal from the data processor is routed through its own line driver, and any failure affects one signal only.

1 x	2 x	3 x	4 x	5 0	6 x	7 s	8 x
9 _	10 x	11 _	12 x	13 _	14 x	15 I	16 x
17 0	18 x	19 0	20 0	21 0	22 x	23 s	24 x
25 _	26 x	27 _	28 x	29 _	30 x	31 I	32 x
33 H	34 x	35 o	36 x	37 o	38 x	39 s	40 x
41 _	42 x	43 _	44 x	45 _	46 CV	47 I	48 x
49 0	50 x	51 0	52 x	53 0	54 x	55 s	56 I
57 _	58 x	59 _	60 x	61 _	62 x	63 I	64 x

1 Frame = 64 Ten-Bit Words = 640 Bits

Word Key

Legend	Number per Frame	Assignment
x	3	Control
X	29	Passive Seismic (short-period)
–	12	Passive Seismic (long-period seismic)
o	2	Passive Seismic (long-period tidal and temperature)
0	7	Magnetometer
S	4	Solar Wind
I	5	Suprathermal Ion Detector/CCGE
CV	1	Command Verification (all zeros if no command)
H	1	Housekeeping

Figure 5 Format for Telemetry Data

The Transmitter

As Figures 1 and 2 indicate, each data subsystem is equipped with two identical transmitters that provide standby operational redundancy; either can be selected to transmit the downlink data. Each transmitter generates an S-band frequency carrier, which is biphase-modulated by the coded binary bit stream from the data processor. The transmitter operates at a preselected frequency in the 2275- to 2279-megahertz range, with a stability of 0.0025 percent per year. A minimum r.f. output power of 1 watt is required to meet the downlink error-probability constraint of 10^{-4} or less.

The transmitter is made up of a crystal-controlled oscillator operating at approximately 142 megahertz,

followed by a buffer and a phase modulator. The digital data from the data processor are applied to the modulator for carrier modulation. Amplifiers and two 2X multipliers increase the carrier frequency to 568 megahertz. A 4X varactor multiplier provides the S-band output to a stripline filter, which reduces spurious harmonics to 30 decibels below the carrier. Additional rejection of unwanted signals in the diplexer filter and circulator switch (see Figure 1) ensures that spurious signals are within electromagnetic-interference (EMI) specifications. To keep the output power relatively constant over the operating temperature range, an automatic-gain-control (AGC) circuit continuously samples the output and uses this level to control the gain of an amplifier at the input to the multiplier chain.

Input current, automatic gain control, and two temperature points are monitored from moon-to-earth telemetry data.

Power Distribution

The power distribution unit (PDU) distributes power to experiment and Central Station components (see Figures 1 and 2) and provides circuit-overload protection and power switching. The unit also conditions selected telemetry signals prior to their input to the multiplexer. A block diagram of the PDU is shown in Figure 6. All circuits are packaged on five printed-circuit boards. A "mother board" interconnects these boards to a rectangular, screw-lock, 244-pin connector, through which the electrical inputs are made.

Since the power available to the ALSEP system has a fixed upper limit that must not be exceeded by system power demand, a POWER OFF sequencer is incorporated in the power distribution unit to provide for automatic load adjustment. Reserve power – the difference between the power available and the power in demand at any given time – is continuously monitored in the PDU and referenced to the input voltage. Should this reserve drop below a preset level (nominally 700 milliwatts), a level detector is activated and the power-off (ripple-off) sequence begins. A delay network of 135±15 milliseconds prevents response to momentary transient conditions. If the reserve power remains below the threshold level for a period longer than the delay time, the POWER-OFF-sequencer input logic gate is enabled, starting a five-stage binary counter whose input is a 1-kilohertz clock. The output of this counter is decoded to generate three EXPERIMENT STANDBY SELECT commands, separated by 8 milliseconds. If at any point in the counting sequence the reserve-power threshold level is reestablished, the counter is reset to prevent further experiment power switching.

Control of and power switching for the individual experiments is accomplished by magnetic latching relays, four transistor relay drivers and one magnetic latching relay that acts as an overload sensor or circuit breaker.* The interconnections for one of the five experiment-control circuits are shown in Figure 7. Each circuit has three command inputs: OPERATION-POWER ON, STANDBY, and POWER OFF. A manually operated switch on the exterior of the Central Station makes it possible for an astronaut to command the operational POWER ON mode for all experiments in case the uplink cannot be established. Resettable breakers in the operational power line of each experiment, adjusted to trip at 500±50 milliamperes, provide system protection in case an experiment failure should produce an excessive power demand. When currents in excess of 500±50 milliamperes are sensed, the circuit breaker generates the TRIP signal, which is applied to the STANDBY SELECT driver. This transfers the +29 volts d.c. in relay 1 from the circuit breaker to relay 2 and simultaneously ensures that relay 2 is connected to the experiment standby power line. Relay 2 in turn now applies power to the experiment standby or survival line, to a summing network for status telemetry, and

*U.S. Patent 3,579,041, which covers this unique power-switching design, was granted to H. Reinhold and W. Reynolds on 18 May 1971.

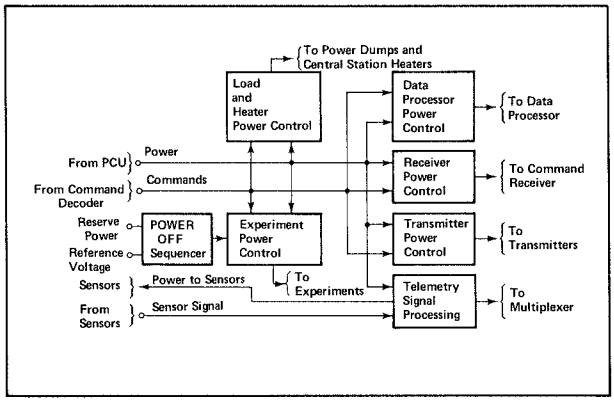

Figure 6 Power Distribution Unit

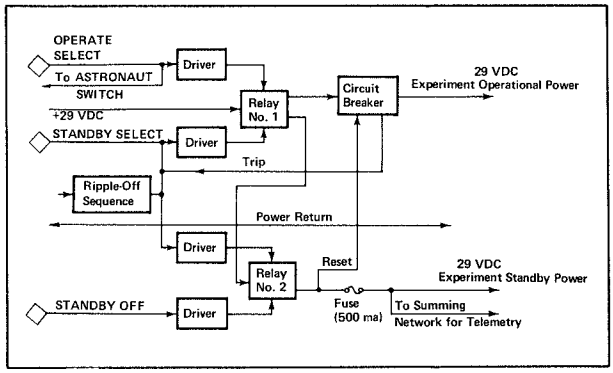

Figure 7 Experiment Power Control Circuit

to the circuit-breaker reset coil. An OPERATE SELECT or ASTRONAUT SWITCH command will restore the experiment to its operational mode; a STANDBY OFF command will remove all experiment power.

On ALSEP missions that carry only four experiments, the power control circuit normally assigned to the fifth experiment is used to augment thermal control features of the Central Station. Two networks of resistors, mounted on the thermal plate, are connected to this circuit. One, sized to dissipate 10 watts with 29 volts applied, is connected to the operational POWER ON line; the other, sized to dissipate 5 watts with 29 volts applied, is connected to the standby POWER ON line. With this arrangement, discrete amounts of available reserve power can be used to limit the minimum Central Station temperature during lunar night.

Transmitter power control circuits provide for the selection of either transmitter A or transmitter B ON or OFF and for automatic transfer to the alternate unit should an overload be sensed on either the 12-volt or the 29-volt d.c. input power line. Other power controls implement the selection of redundant sections, heaters, power dumps, and the like.

Power to the command receiver is supplied through a circuit breaker at a +12-volt d.c. level. Locally generated reset pulses are automatically applied to this circuit breaker at 12-hour or 18-hour intervals.

Conditioning of the telemetry signals to provide a 0- to 5-volt d.c. level is accomplished with divider resistors for thermistor and nickel-wire temperature sensors and voltage monitors. Operational amplifiers are used for the low-level temperature signals from the power system.

THE ELECTRIC POWER SYSTEM

The electric power subsystem (EPS), which consists of a radioisotope thermoelectric generator assembly, a fuel capsule assembly, a fuel cask, and a power conditioning unit, provides conditioned electric power for ALSEP lunar operation. Thermal energy is supplied by a radioisotope source and is converted by a thermoelectric couple assembly (thermopile) into electrical energy through thermoelectric action caused by the temperature difference between the hot frame and the cold frame. Excess heat from the thermopile is conducted through the cold frame (outer case) to a thermal radiator (heat rejection fins) for dissipation into the lunar environment; thus the cold frame is kept at a lower temperature than the hot frame and the thermoelectric action is maintained. The energy produced provides a minimum of 63 watts at 16 volts to the power conditioning unit, where it is converted, regulated, and filtered to yield six operating voltages for the data subsystem, the experiments, and the support subsystems. Temperatures are monitored at three cold-frame and three hot-frame locations to provide six temperature signals to the data subsystem.

The Apollo 12 radioisotope thermoelectric generator (RTG), placed on the moon in November 1969, initially produced approximately 73 watts of power; after 19 months of operation, the output was down to a level of 72 watts and has remained constant at that level. The Apollo 14 RTG has a power output of about 72 watts and the Apollo 15 RTG an output of about 74 watts.

The power conditioning subsystem, shown diagrammatically in Figure 8, is responsible for

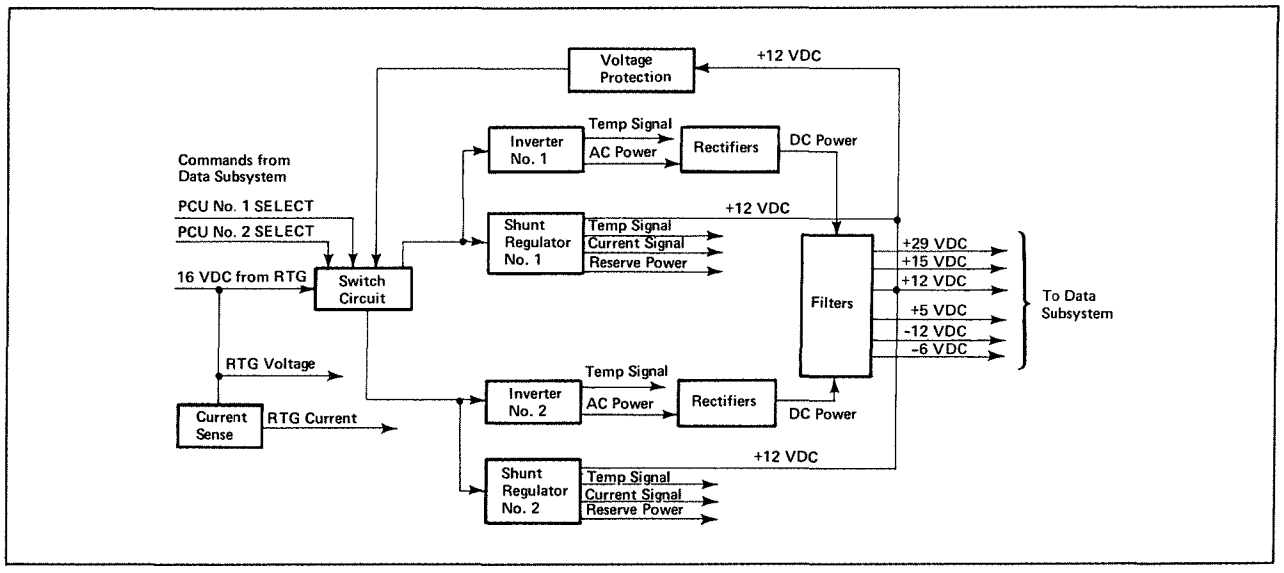

Figure 8 Power Conditioning Subsystem

voltage conversion and regulation and also provides a constant load for protection of the radioisotope thermoelectric generator. Each ALSEP system is equipped with two redundant power conditioners, made up of a d.c./d.c. power converter (inverter and rectifiers), which converts the 16-volt RTG output into the six voltages required for system operation, and a shunt voltage regulator, which maintains the output voltages within approximately ±1 percent. The filters and switches are common to both units, either of which may be selected by command. The +12-volt level is monitored to switch from unit 1 to unit 2 should the level drop to about 11 volts, indicating a failure.

THE CENTRAL STATION TIMER

The Central Station timer for the EASEP system deployed on the Apollo 11 mission and for the three ALSEP systems assigned to Apollo missions 12, 13, and 14, respectively, is a switching mechanism which is driven by an Accutron clock powered by a long-life mercury cell battery. The timer is housed in a black anodized-aluminum case approximately 2.6 inches long and 1.3 inches in diameter. The unit weighs 0.25 pound.

Timing pulses start when the RTG cable is mated to the Central Station. A 360-hertz oscillator drives a gear train which closes the timing switch at 1-minute, 12-hour, and 720-day intervals. The 1-minute and 12-hour closures are continuously repetitive and are applied to the delayed-command sequencer in the command decoder; the 720-day closure occurs only once and initiates a permanent OFF command to the ALSEP transmitter.

The ALSEP systems designed for Apollo missions 15 and 16 carry a resettable solid-state timer. This timer generates its own reset signal upon initial application of +12-volt d.c. power from the power conditioning unit, beginning its count at zero. It will retain its count during approximately 30 seconds of power loss. It outputs 1-minute, 18-hour, and 1.5-month timing and telemetry signals and a 97±5-day TRANSMITTER OFF signal. A TIMER RESET command is periodically transmitted from earth to return the timer to its initial state. The design is such that the transmitter will be turned off after a maximum of 97 days should system control be lost as a result of command-link failure.

All electronics for the solid-state timer are mounted on three circuit boards, housed in an aluminum case approximately 2.8 inches high, 1.4 inches wide, and 2.2 inches long. Electrical connections are made through a 37-pin connector. Maximum weight of the unit is 7.3 ounces.

THE DUST DETECTOR

Although not an integral part of the data subsystem, the dust-detector sensor is mounted on the Central Station sunshield, and its signal-processing electronics are contained in the power distribution unit.

The dust detector carried on the Apollo 12 mission was designed to collect data for the assessment of dust accretion and the measurement of thermal-surface degradation. The detector has two components: a sensor package with three photocells orientated on three sides to face the ecliptic path of the sun, and a printed-circuit board for processing circuits. Each cell has an active area 2 centimeters by 2 centimeters in size, which is protected by a blue filter to cut off ultraviolet wavelengths below 0.4 micron and by a cover slide to prevent radiation damage. A thermistor is attached to the rear of each cell to monitor cell temperature. The sensor package is connected through an H-film cable to the printed-circuit board, which is located in the power distribution unit.The outputs of the three cells are applied to three amplifiers, which condition the signals and apply them, along with the thermistor outputs, to analog-data channels of the data subsystem. Dust accumulation on the cell surfaces reduces the solar illumination which they detect.

The EASEP dust detector and those flown on Apollo missions 14 and 15 are modified Dust, Thermal, and Radiation Engineering Measurements (DTREM) packages designed to obtain data for assessing dust accretion, lunar radiation, and lunar surface brightness temperature. The DTREM sensor package, which mounts on the Central Station sunshield, contains three solar cells 1 centimeter by 2 centimeters in size, located on the top horizontal surface. A temperature sensor is attached to the underside of the center solar cell, and two others are attached to the inside and outside, respectively, of the side of the package (surface 3). The sensor package is connected through an H-film cable to a printed-circuit board located in the power distribution unit.

Analysis of the radiation environment is accomplished by comparing the output-voltage reductions exhibited by the three solar cells when exposed to radiation degradation. Two of the cells are protected by 6-mil fused-silica filter cover glasses to reduce the amount of solar radiation reaching them; the third cell has no radiation protection. One of the protected cells has been irradiated to reduce its sensitivity to the radiation environment, and its output is used as a base in the measurement analysis. By virtue of the differences in their sensitivity and protection, the three cells form a simple spectrometer, which measures proton dose in two energy intervals. The

thermistor attached to the underside of the center cell provides a measure of solar-cell temperature.

Because the resistive temperature sensor on the outside of surface 3 is insulated from the DTREM structure, the temperature it measures is primarily the result of thermal radiative exchange with the lunar surface and deep space. The resistive temperature sensor on the inside of surface 3 provides the DTREM-structure temperature data required to quantitatively define the heat leaks to the outside temperature sensor. These data, together with ALSEP sunshield and electronics temperature measurements, are used to derive the lunar surface brightness temperature.

The solar cell outputs are applied to three amplifiers, which condition the signals and apply them, along with the temperature signals, to three subcommutated analog-data channels of the data subsystem.

The Passive Seismic Experiment

D. K. BRESEKE
J. LEWKO, JR.

The ALSEP Passive Seismic Experiment (PSE) is designed to detect and measure lunar tectonic activity, free oscillations, and tidal deformations to extend man's knowledge of the lunar interior. The PSE was deployed on each of Apollo missions 11, 12, 14, and 15, and is scheduled for deployment on Apollo 16, the goal being a seismic network similar to though smaller than seismic networks used in geophysical exploration on earth. This paper describes experiment design, with emphasis on factors unique to the Apollo mission, and discusses instrument operation and performance parameters. Experiment results obtained to date are summarized briefly.

INTRODUCTION

Seismic exploration has proved to be one of the most powerful geophysical tools for establishing the internal structure and composition of the earth. Active seismic exploration involves the measurement of ground motions produced by explosive charges, the position, magnitude, and timing of which are controlled; passive seismic exploration involves the measurement of ground motions associated with natural events. The detection of ground motion by a seismometer is based on the principle that a mass, finely suspended by a system of springs and hinges, will retain its position in the presence of ground motion, whereas the frame to which it is mounted will follow the motion of the ground. A comparison of the relative positions of mass and frame thus defines the motion or seismic wave. High requirements with respect to instrument sensitivity and recorded-spectrum fidelity account for the complexity of state-of-the-art seismometers.

The Passive Seismic Experiment (PSE) developed for the Apollo Lunar Surface Experiments Package (ALSEP) is designed to measure lunar surface vibrations produced by natural and artificial sources of seismic energy. Such measurements will contribute significantly to our knowledge of the internal structure and composition of the moon, the nature of the forces that cause moonquakes and moon deformations, and the numbers and masses of meteorites striking the lunar surface.

Moonquakes are a manifestation of internal strain accumulation and energy release within the moon. Analysis of the velocity, frequency, amplitude, and attenuation of the lunar-surface wave motions involved should reveal much concerning lunar internal structure and the physical properties of the subsurface materials. With three seismometers now operating simultaneously on the moon, triangulation measurement techniques can be used to determine quake epicenters and depths. Relating these data to existing surface features – faulting, volcanism, meteorite impact, and the like – should lead to a better understanding of how such features develop. To determine the elastic properties of the moon as a whole, measurements are also made of the free oscillations that result from large seismic events, and of variations in surface tilt due to tidal effects.

EXPERIMENT DESCRIPTION

The ALSEP Passive Seismic Experiment, the components of which are seen in Figure 1, is made up of a sensor assembly, the Central Station electronics, a thermal shroud, and a leveling stool.

The sensor assembly consists of four seismometers: a short-period seismometer to detect vertical motion of the lunar surface over a frequency range of 0.05 to 20 hertz, and three long-period seismometers, mounted orthogonally, to detect wave motion in both vertical and horizontal planes at frequencies of 0.004 to 2.0 hertz. The stillness of the lunar environment – that is, the absence of noise due to winds, ocean tides, machinery, and human activity – permits these instruments to be designed with far greater sensitivity than earth-based seismometers. The lunar-seismometer minimum detectable signal results from ground motion of 0.3 millimicron and is recorded on earth magnified by a factor of 10 million. Measurements of lunar-surface tidal motion and variations in

Gary V. Latham of the Lamont-Doherty Geological Observatory at Columbia University is Principal Investigator for the Passive Seismic Experiment. Instrument design incorporates seismometers previously developed by the Observatory.

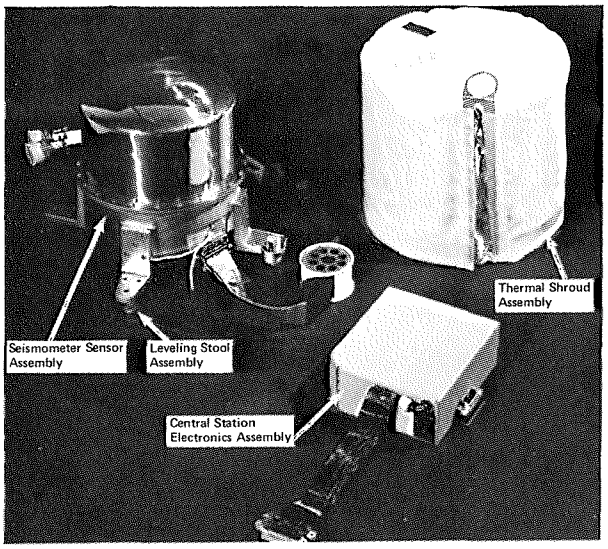

Figure 1 Passive Seismic Experiment Components

gravity are derived from the triaxial long-period seismometer system by signal filtering. These seven science signals – four seismic and three tidal – plus an eighth for sensor temperature are transmitted to the PSE Central Station electronics through a pair of 10-foot 27-conductor flat Kapton-coated tape cables.

Although mounted within the ALSEP Central Station, the PSE central electronics are functionally and electrically a part of the Passive Seismic Experiment. The electronics provide power conditioning, thermal control, command logic for controlling experiment functions, and data handling for the sensor assembly. The PSE science data are formated in the Central Station along with ALSEP engineering data and science data from the other ALSEP experiments. These data are transmitted to earth at a data rate of 1060 bits per second. The Central Station also receives commands from earth and routes them to the experiments for which they are intended. Power for the Central Station is supplied by the radioisotope thermoelectric generator.

In the deployed configuration, the sensor assembly rests on a leveling stool at a distance of about 10 feet from the ALSEP Central Station, covered by a thermal shroud as shown in Figure 2. The leveling stool simultaneously couples the seismometers with lunar surface motion and isolates them thermally and electrically from the lunar surface. The shroud, a multilayered blanket of highly reflective surfaces, extends over a lunar surface area 5 feet in diameter and insulates the sensor from the temperature extremes of lunar day and night to provide the controlled thermal environment required for proper operation.

The physical parameters of the Passive Seismic Experiment are listed in Table I. The power requirements are listed in Table II.

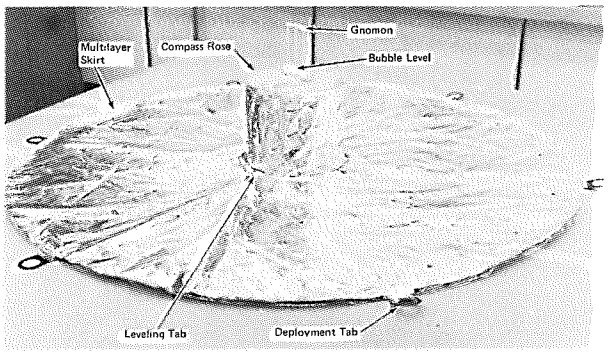

Figure 2 Deployed Thermal Shroud

Table I Physical Parameters for the Passive Seismic Experiment

Component	Parameter	
	Weight, pounds	Dimensions, inches
Sensor	18.0	11.1 x 9.1(diameter)
Shroud	3.6	15 x 11(diameter)
Central Station Electronics	4.2	7.25 x 6.50 x 2.75
Leveling Stool	0.4	2.3 x 11(diameter)

Table II Power Requirements for the Passive Seismic Experiment

Functional Mode	Power, watts
Standby	3.5
Basic Operation	4.2
Thermal Control	5.0 (maximum)
Leveling	3.0 (per axis)

GENERAL DESIGN CONSTRAINTS

The nature of the Apollo mission imposed unique constraints on the design, manufacture, and test of the seismometer system for the Passive Seismic Experiment. Volume and weight were naturally the initial major problems, conventional seismic instruments being prohibitively large for lunar application. A typical long-period single-axis seismometer weighs approximately 65 pounds and occupies 5000 cubic inches; the entire lunar sensor assembly, including the four seismometers, weighs 18 pounds and occupies a volume of 700 cubic inches. The weight and volume reductions were achieved in a number of ways, notable among them the use of beryllium throughout the sensor, both as a structural member and as a seismometer element.

Other design constraints were imposed by the remoteness of seismometer operation. The delicate suspension system of a seismometer is normally adjusted intermittently following installation to maintain the degree of tuning desired. All PSE seismometers must be adjusted either prior to launch or by command from earth following deployment. A total of fifteen commands can be transmitted to the experiment for purposes of calibrating the seismometers, altering amplifier gain, driving the leveling platform on which the long-period seismometers are mounted, raising and lowering the point from which the long-period vertical seismometer is suspended, altering the operating mode of the sensor-assembly thermal control heater, and uncaging or freeing the seismometers for operation.

The requirement that the experiment be deployable by a spacesuited astronaut within a 5- to 6-minute time period imposed further constraints on system design. The astronaut carries the stool and the sensor/shroud assembly with the aid of the universal handling tool, which locks into sockets provided on this and all other ALSEP assemblies; deployment is completed in a normal standing position, using only the release trigger on the tool. To deploy the shroud, the tool is used to pull a release pin and tug at deployment tabs that implement unfolding. Leveling is accomplished by pressing on leveling tabs until a level condition is indicated by a bubble level. Alignment readings are obtained by reading the angle of a gnomon shadow line.

The severe launch and lunar-temperature environments also imposed unique constraints. To protect these delicate, finely adjusted instruments during launch, the four seismometers and their suspension systems are caged by pneumatic bellows assemblies, which, locked together, can be released by a command from earth. Once on the moon, the long-period seismometers, which are highly sensitive to temperature variations, require a degree of thermal control well beyond the capabilities of standard space thermal-control systems for proper operation in a lunar-temperature environment ranging from −300°F to +250°F. To meet the design goal of control to within ±0.38°F, provision was made for a 5-watt proportional heater and a large thermal insulating shroud, capable of being stowed in a small volume.

Prior to deployment of the Apollo 11 Passive Seismic Experiment, nothing was known about the seismicity of the moon. Speculation with regard to seismic activity represented two opposing points of view: that the moon was very quiet, a cold dead body, and that the moon was very noisy by reason of impacts and fractures resulting from thermal variations. System design therefore had to incorporate a variable amplifier gain, including one extreme that could not be tested in the seismic background of the earth.

The lower gravitation force on the lunar surface posed a final design and testing problem. The necessity for functional testing on earth and operability on the moon required that seismometer mass, an extremely critical parameter, be adjustable. The adjustment was made by removing 0.625 kilogram of mass for earth testing.

LEVELING STOOL

The Passive Seismic Experiment leveling stool provides the base for the deployed sensor and couples the instrument to the lunar surface. The frame of the stool is a circular ring 7 inches in diameter, which serves as a bull's-eye for astronaut placement of the sensor. The hemispherical base of the sensor interfaces with the three isolators mounted on the upper portion of the stool ring; beneath the ring, three leg/footpad supports rest on the lunar surface. By adjusting the orientation of the sensor base on the three-point interface, it is possible to compensate for a ±15-degree off-level stool position.

The minimum-weight requirement, as well as the science requirement for a ground-motion transmissibility of unity ±10 percent over the frequency range d.c. to 26.5 hertz, was met by forming the stool ring and legs as a single beryllium structure. Glass epoxy isolators bonded in the stool ring as a three-point interface meet thermal control constraints and provide electrical isolation of the sensor base from the lunar surface. To reduce the thermal radiation between the sensor base and the leveling stool, and, in turn, the heat flow between the sensor and the moon, the stool was gold-plated to have an emissivity of the order of 0.05.

The leg/footpad combinations were sized to support the static load of the seismometer without sinking into the lunar surface. Based on the lunar surface characteristics encountered in the Apollo 12 mission, however, the stool/footpad area was increased so that the static load was reduced from 0.61 pound per square inch for the Apollo 12 instrument to 0.30 pound per square inch for subsequent instruments.

THERMAL SHROUD

The thermal control system for the Passive Seismic Experiment sensor contains both active and passive elements. The active element is a proportional heater within the sensor. The passive elements are the thermal shroud and the surface finishes that cover the sensor. The system is designed to maintain a nominal operating temperature of 126±18°F; the design goal, which must be approached if the tidal science data are to be fully utilized, is a control range of ±0.38°F.

Thermal shroud design is based on the principle of radiation shielding by multilayer construction. The only structural member of the shroud is an internal aluminum cylinder that fits over and attaches to the PSE sensor in both stowed and deployed configurations. Upon this cylinder are stacked ten layers of 0.25-mil two-sided aluminized Mylar, with nylon spacers between the layers. The skirt of the shroud, which is 5 feet in diameter, contains twenty layers of aluminized Mylar. In addition, a single layer of 2-mil aluminized Teflon covers the entire shroud; Teflon was selected for this outer layer because of its low absorptivity/emissivity ratio (0.15/0.70) and because of the protection it affords against solar radiation.

In the stowed configuration, the folded skirt of the shroud is contained within a girdle and occupies a small volume around and on top of the sensor. The constraint on this volume played a major role in shroud design. At the time of deployment, the astronaut pulls a release pin and removes and discards the girdle. The shroud skirt is then unfolded and positioned as shown in Figure 2.

In the deployed configuration, the thermal shroud tends to isolate the sensor from the temperature extremes seen on the lunar surface – from the heat load of direct solar radiation during lunar day and from the heat sink of deep space during lunar night. The sensor base is exposed to the lunar surface directly beneath it to provide for minimal heat exchange as the limited effects of the external environment are experienced. The shroud implements temperature control at this point of exposure by isolating a surface area 5 feet in diameter around the sensor, through which the day and night extremes must be conducted.

The top of the thermal shroud serves as a platform for the instrumentation used by the astronauts in initial experiment orientation. A 5-degree bubble level mounted near the center of the shroud provides a 1-degree leveling capability. A central spring-mounted gnomon and a 360-degree compass rose, designed to accommodate a variety of potential deployment sun angles, are mounted on the top periphery of the shroud and enable the astronaut to read the sun-shadow line to within ±1 degree. Leveling-status and sun-shadow data are required to establish the orientation of the seismometers within the sensor with respect to lunar coordinates, so that variations in signals received by the horizontal seismometers can be properly compared and analyzed.

SENSOR ASSEMBLY

The makeup of the passive seismometer sensor is shown in Figure 3. The long-period triaxial seismometers are mounted within the gimbal ring that is seen

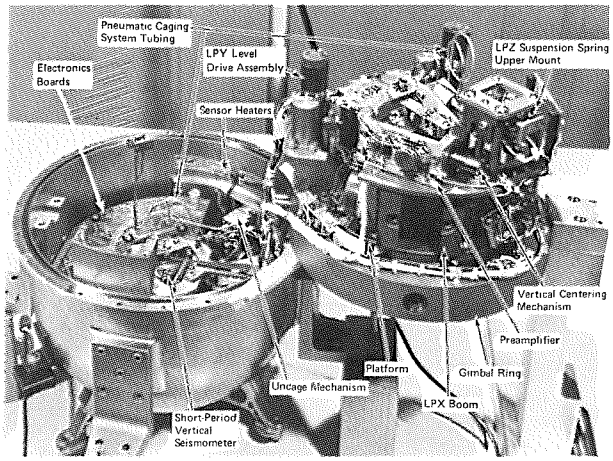

Figure 3 Passive Seismic Sensor Assembly

swung out of the sensor base.

The gimbal ring containing the gimballed platform is mounted in the sensor base by two flexural pivots that extend outward from the ring to the base. Mounting points for the platform itself are provided by a second pair of flexural pivots, displaced by 90 degrees, that extend inward from the ring. These flexural pivots play two vital roles: they serve as mechanical interface points for the gimbal ring, which must transmit seismic signals, and they are capable of the axial rotation that is necessary for leveling the seismometers.

Leveling of the horizontal-axis (X- and Y-axis) seismometers is accomplished by means of two leveling drive assemblies. One permits adjustment of gimbal ring position relative to the base; the other permits adjustment of platform position relative to the gimbal ring.

The sensor base provides a mounting surface for the short-period seismometer, four individual electronics boards, the sensor heaters and sensistors, and the uncage mechanism assembly. The lower hemisphere of the base is round to permit uniform rotation within the leveling stool. Four legs attached to the base serve to secure the instrument to the ALSEP pallet, to secure the thermal shroud assembly to the sensor, and to interconnect with the universal handling tool, permitting the astronaut to carry the instrument to the leveling stool during lunar deployment. The sensor base and the majority of the mechanical parts of the sensor are made of beryllium, which was selected for its special mechanical, thermal, and weight characteristics.

Long-Period Seismometers

The PSE sensor incorporates two swinging-gate-type horizontal seismometers in the configuration

shown in Figure 4. Each of these long-period seismometers (LPX and LPY) has a lunar mass of 0.75 kilogram, a lunar natural period of 15 seconds, a capacitive transducer for signal pick-off, and a coil for feedback control and calibration.

The natural period is established in the following way. A component of the gravitational force acting on the 0.75-kilogram mass provides a torque opposite to the restoring torque that is provided by the flexural pivots. The small gravitational component is developed when the boom mass is suspended from a point above its pivot in such a way that the entire mass is free to rotate about a slightly tilted axis; rotation raises the mass and boom against gravity, and a small restoring force is produced. The long-period instrument is adjusted to have a lunar natural period of 15 seconds by removing five-sixths of its inertial mass and adjusting its period to $15/6^{1/2}$ or 6.2 seconds. This method of adjustment has two advantages: The tension on the suspension system during adjustment is the same as that under lunar conditions with full lunar inertial mass, and the lunar operating period can be accurately predicted independent of the ratio K/α, where K is the total restoring constant and α is the tilt angle between vertical and the flexure block assembly. For final adjustment, the tilt angle α is varied by driving the entire platform with the X and Y leveling drive motors. The maximum off-level condition of the platform is established at ±0.25 degree.

The configuration of the long-period vertical seismometer (LPZ), that of a modified LaCoste suspension, is also shown in Figure 4. The capacitive transducer is mounted on the top of the mass, and the coil is mounted below. A pair of flat hinges suspend the boom end from the sensor framework. The mass is

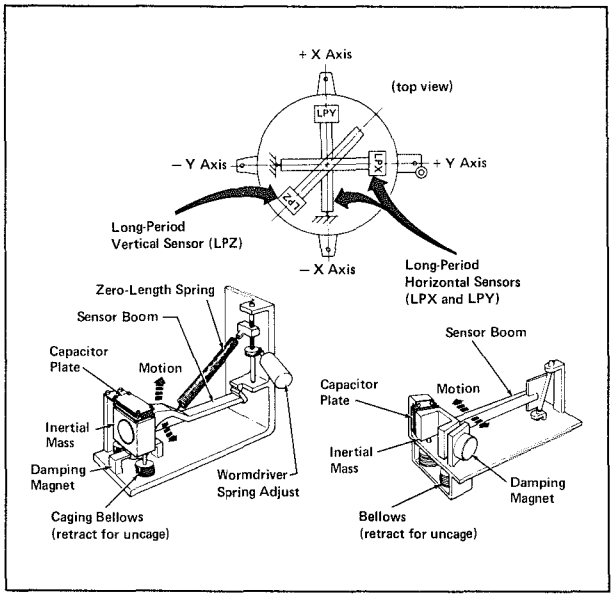

Figure 4 Long-Period-Seismometer Configuration

suspended by a zero-length isoelastic spring, which is used because of its minimal thermoelastic modulus. A technique has been devised for compensating for the effects of temperature variations on both the period and the position of the boom in the basic structure. In this thermal compensation technique, the relative differential expansion between an Invar compensator bar and the beryllium structural members of the seismometer is measured, and the results are converted to a length value for the compensator bar, which is trimmed to compensate for drift and period changes attributable to suspension-spring changes and differential expansion of structural members. The vertical-seismometer capacitive transducer is centered, after the X and Y seismometers are leveled, using a drive motor that sets the position of the upper hinge point of the suspension spring.

The three long-period seismometers are placed on the gimbal platform assembly, which is in the gimbal ring, as shown in Figure 4. The seismometer transducers are electrically interconnected to the electronics preamplifiers via litz wires, which physically and electrically attach the back end of each boom to the fixed portion of the flexure holding structure. The effect of the litz wires on the period is negligible.

Each seismometer employs a coil/magnet combination for seismometer damping and for applying feedback current and calibration signals. With the full lunar mass, the nominal damping is 0.85 critical; for earth operation without lunar mass, the nominal damping is 2.09 critical. The required damping is achieved by shunting the coil with a circuit resistance nominally equal to the coil resistance. The generator constant required under this condition is 7.1 newtons per ampere.

Full-scale seismic output for all three long-period seismometers is 10 microns (0.0004 inch) peak-to-peak. Full-scale tidal output is 10 seconds of arc for the horizontals and 8 milligals for the vertical. Seismometer mechanical travel is limited to ±0.021 inch for the horizontals and to ±0.030 inch for the vertical.

Short-Period Seismometer

A cross section of the short-period seismometer (SPZ) is shown in Figure 5. The seismic mass of approximately 0.54 kilogram is a magnet assembly, supported by a cantilever tapered suspension spring and held in place by a 0.005 suspension wire and six delta-wire suspension rods.

The short-period seismometer is designed to sense vertical motion and has a natural frequency of 1.0 hertz. The sensing coil assembly is fixed within the seismometer-frame housing in such a way that motion of the magnet assembly caused by ground motion

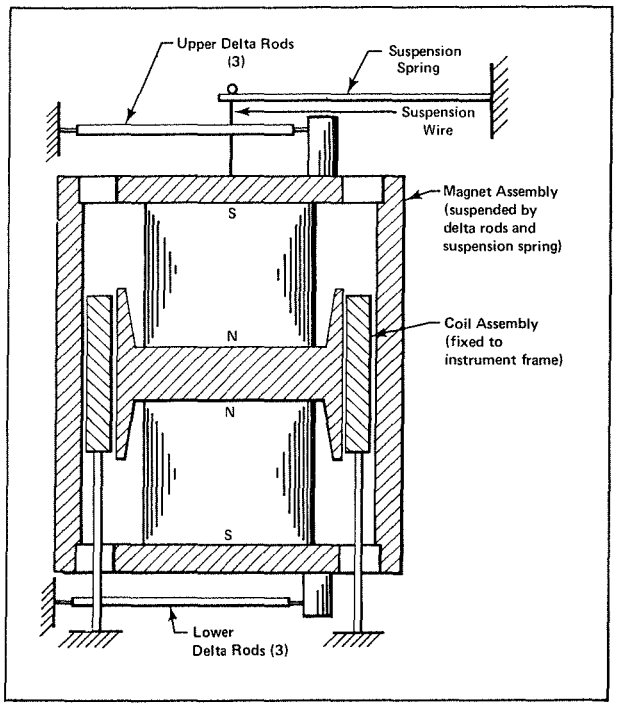

Figure 5 Short-Period-Seismometer Configuration

generates a voltage proportional to motion velocity. The magnetic-circuit/coil combination was patterned after that used in the short-period seismometer developed for the Lunar Surveyor system.

Since the mass of the short-period seismometer cannot be modified to remove five-sixths of its weight, the lunar spring is replaced in SPZ tests on earth by a spring capable of supporting a load six times as great.

Pneumatic Caging Mechanism

A mass-caging system is used to protect the delicate suspension systems of the seismometers and to ensure system calibration during all phases of handling, launch from earth, descent to the lunar surface, and deployment. The system includes mass-caging bellows for the triaxial long-period sensors and the short-period sensor, a clamp mechanism and bellows for the LPZ suspension spring, and an uncage mechanism assembly.

The mass-caging bellows assembly, shown in Figure 6, consists of six bellows units, interconnected in series to a tube manifold. Each bellows has a drive pin on top, which engages the three triaxial seismometer masses, causing them to raise away from the gimbal platform. Figure 7 is an end view of the mass-caging bellows for the LPZ seismometer. As the pins move through the platform and the mass leaves the gimbal ring, a caging screw mounted in the mass accomplishes mechanical locking by seating in a conical

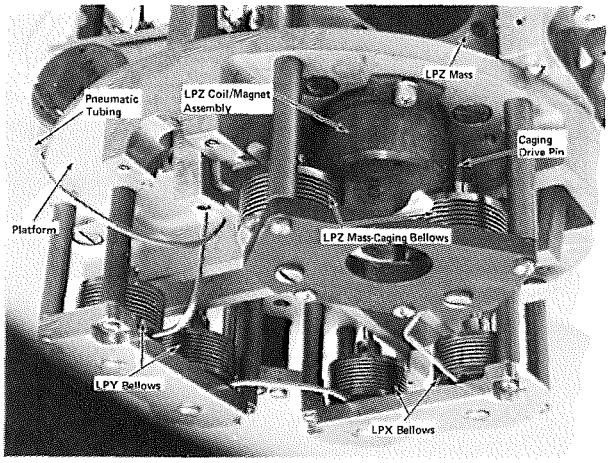

Figure 6 Mass-Caging Bellows Assembly

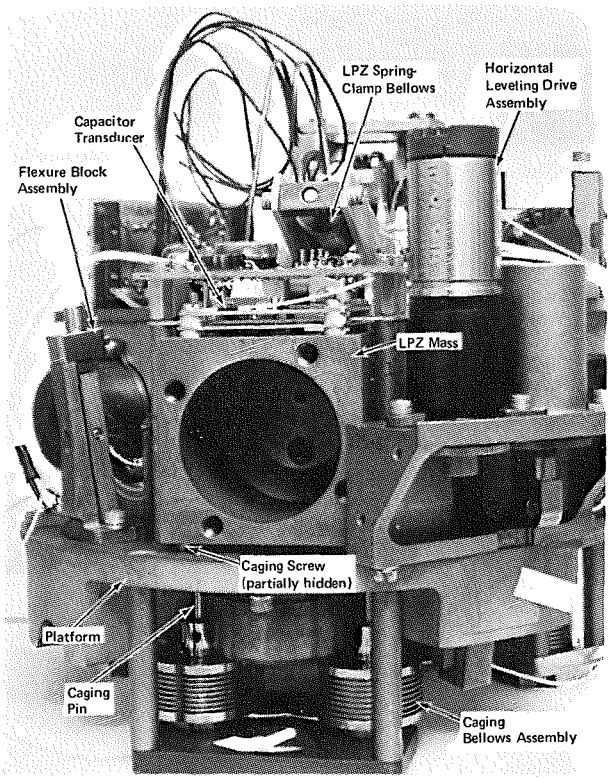

Figure 7 Mass-Caging Bellows for Long-Period Vertical Seismometer

shoulder of the platform. When the caging pressure is released, the caging pins retract, and the masses are lowered on their respective suspension systems.

The clamp mechanism that retains the LPZ suspension spring is shown in Figure 8. This clamp is closed by expansion of the clamp bellows. When clamped, the suspension spring cannot vibrate or create stress on the spring suspension wires.

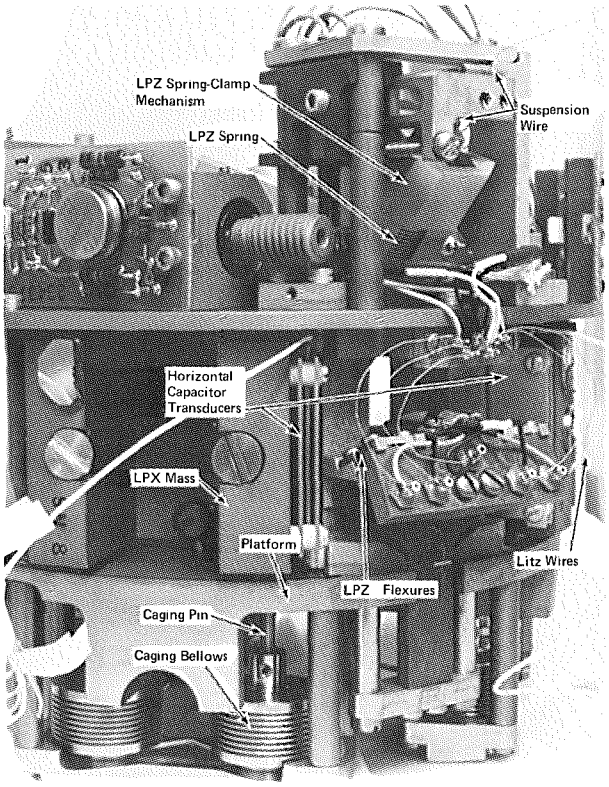

Figure 8 Spring Clamp Mechanism for Long-Period Vertical Seismometer

Protection of the short-period seismometer is provided by a bellows assembly that forces the magnet mass to rise against fixed stops within the top plate of the instrument. When this occurs, the tension is removed from the suspension wire and the entire SPZ seismometer is locked to itself.

The design of the uncage mechanism assembly is detailed in Figure 9. The pressure transducer indicates the caging pressure of the caging system, nominally 343±10 pounds per square inch absolute. The caging-system pressurization line, used to pressurize the system, is crimped shut and solder sealed after completion of the last pressurization cycle. The two pyrotechnic piston actuators are activated by earth command after the instrument has been deployed and leveled. Upon firing, the piston actuators contact the break-off valve, cracking the valve, and the caging gas is exhausted to space.

Sensor Electronics

Passive Seismic Experiment electronics are contained in both the Central Station and the sensor. Included in the sensor electronics are circuits for the long- and short-period seismometers, the leveling control, the uncage function, and thermal control.

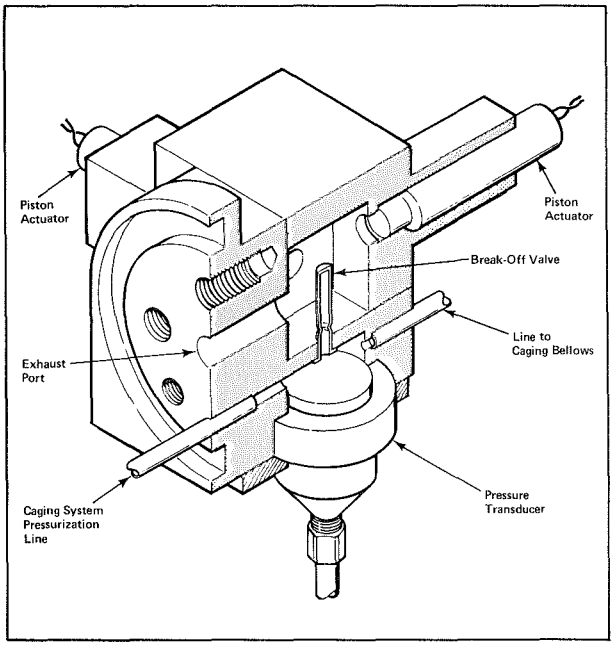

Figure 9 Uncaging-Mechanism Configuration

Long-Period Electronics

The system parameters that determine the characteristics of the long-period electronic circuits are capacitive transducer sensitivity, overall system amplitude sensitivity and dynamic range, and system frequency response. The theoretical sensitivity of the transducer is 25 millivolts per micron of displacement, based on a capacitance of 20 picofarads and a 22-volt peak-to-peak voltage across the capacitor plates. As shown in Figure 10, the circuits consist of a long-period preamplifier, a demodulator, and a feedback filter. A 3-kilohertz oscillator furnishes the carrier for the capacitive transducer and demodulator reference.

The long-period preamplifier provides a high-impedance input to permit minimum loading of the capacitive transducer; it also provides sufficient gain to obtain a good signal-to-noise ratio and minimum signal levels before demodulation. The demodulator converts the amplifier a.c. voltage from the preamplifier to a d.c. level having an amplitude proportional to the offset from the null point of the capacitive transducer and a polarity that shows the direction of offset. The feedback filter circuit provides the low-pass filter required to obtain the desired system response. The output of the filter includes tidal data from the vertical seismometer and tilt data from the horizontal seismometers. The filter is switched out during leveling operations to obtain direct feedback, shortening the response period of the seismometer and permitting more rapid leveling.

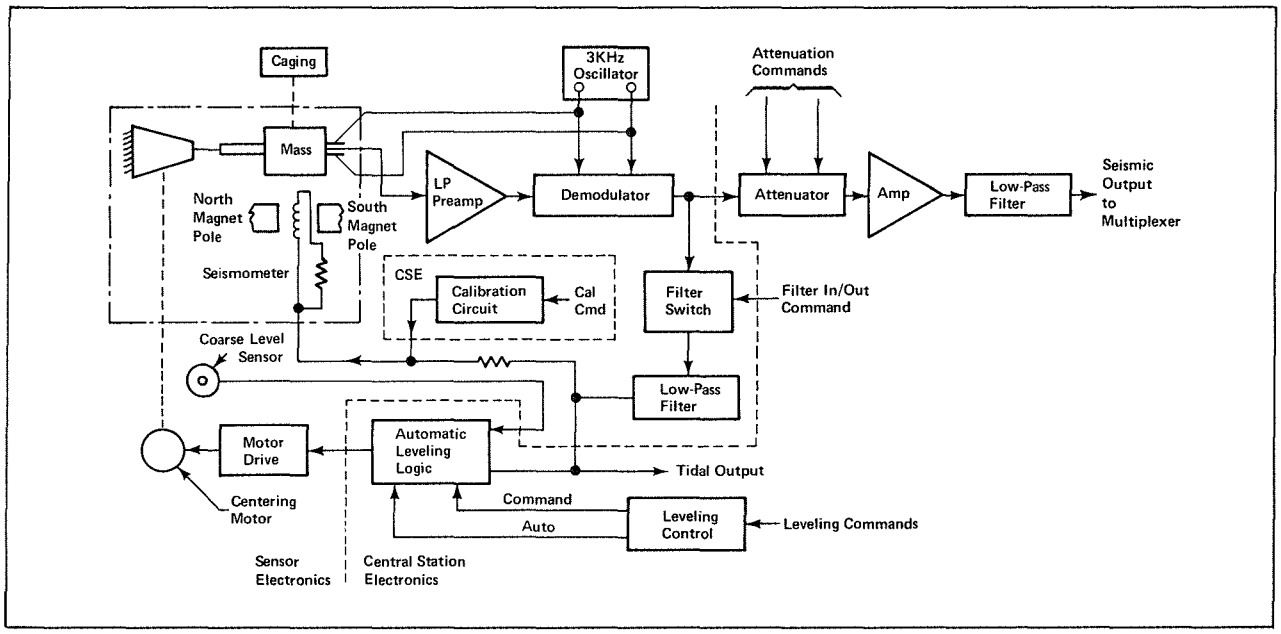

Figure 10 Long-Period-Seismometer Electronics

The basic output of the long-period seismometers is proportional to the amplitude of ground motion above the natural frequency. The upper limit of the seismometer frequency response is set by the instrument multiplexing rate. Four or five samples per cycle of the highest frequency of interest are needed to reproduce the input waveform with reasonable accuracy; at a five-sample-per-second rate, the maximum frequency for the long-period seismometer becomes 1 hertz. Consideration of the theory of modulation also imposes an absolute upper frequency limit equal to half the multiplex repetition rate.

Frequency response curves for both long- and short-period seismometers are plotted in Figure 11. The long-period response is shaped by filters superimposed on the basic servo system response. A simple spring/mass system without feedback, at a natural period of 15 seconds, has a flat displacement response to approximately 15 seconds and drops off at a rate of -12 decibels per octave at longer periods. Since system stiffness is proportional to the amount of feedback, the natural period will fall to 2.25 seconds if a portion of the output is fed back degeneratively, without a filter in the feedback loop. With a simple resistance/capacitance low-pass filter included in the loop, however, seismometer response for periods much shorter than the filter corner will follow the -12-decibel-per-octave rolloff of the simple system. Beyond the filter corner, the response also follows the -12-decibel-per-octave rolloff, though it is lower than the response of the simple system by the feedback factor. Between these points, response drops off at a rate of -18 decibels per octave -- the sum of the original 12 decibels per octave and the filter rolloff of 6 decibels per octave. The filter thus improves the long-term sensitivity (drift) of the seismometer without seriously affecting its performance near its natural period.

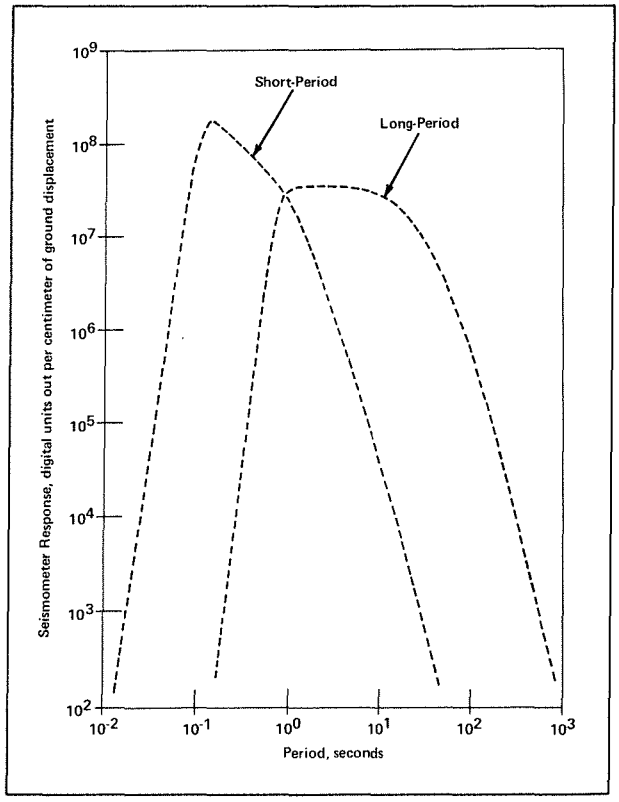

Figure 11 Seismometer Frequency-Response Curves

The choice of feedback factor and corner frequency depends on the application. In general, the tighter the feedback, the longer the corner frequency must be if the system is to remain stable. In the PSE system, a corner frequency of 6300 seconds and a feedback factor of 33 decibels result in a seismometer that will act as a simple spring/mass system (without feedback) up to about 140 seconds.

Short-Period Electronics

The short-period preamplifier consists of four differential amplifier stages and a dual field-effect-transistor emitter/follower output stage. Low-noise dual transistors are used throughout the amplifier. A negative feedback from the output to the input provides proper damping impedance for the seismometer. The use of feedback damping improves the theoretical signal-to-noise ratio of the seismometer/amplifier system by 3 decibels over the use of an external damping resistor and a high-impedance amplifier. The gain and noise requirements of the amplifier are determined by the minimum ground motion to be measured, the generator constant of the seismometer, and the dynamic range of the system. The PSE amplifier has an input noise of 0.25 volt peak-to-peak over a bandwidth of 0.05 to 10 hertz, a nominal gain of 750, and an output voltage of 10 volts peak-to-peak minimum clipping. The amplifier is a.c.-coupled to the field-effect-transistor emitter/follower output with a low-frequency cutoff of 0.05 hertz to eliminate amplification of any d.c. drift.

The output of the short-period seismometer is proportional to ground velocity above its natural period. As in the case of the long-period channels, the upper limit of short-period frequency response is determined by the multiplexing rate. The frequency response curve is shown in Figure 11.

Sensor Leveling

To operate properly, the LPX and LPY seismometers must be leveled from the ±5-degree orientation established by the astronaut to within a few seconds of arc. Automatic or manual leveling can be elected by earth command. In the automatic mode, the driving is controlled either by the coarse sensor, a mercury switch, or by the tidal output of the long-period seismometers. The coarse sensor is usually used for initial leveling following deployment, and the tidal signal is used throughout the remainder of the mission. The mercury switch opens when the platform is within 8 arc-minutes of horizontal. The tidal signal, operating through a differential amplifier, levels the platform to within better than 1 second of arc. In the manual mode, direction and speed of the motor drive are selected by command. Power to each leveling motor is individually controlled by earth command, whether in the automatic or the manual leveling mode.

The mass of the vertical long-period seismometer is centered by adjusting the position of the upper end of the suspension spring. In the automatic mode, the tidal signal is used to control the operation of the Z-axis centering motor, and the position of the mass can be adjusted to within 1 micron of center. There is no Z-axis coarse sensor. Operation of the centering motor can also be commanded in the manual mode.

Sensor Caging

The uncaging mechanism is made up of a capacitive-discharge circuit, a piston, and a break-off valve in the bellows pressurization system. Two commands are required to complete the uncaging cycle. The first causes the charging of the 1600-microfarad capacitor in the capacitive-discharge circuit. The second, transmitted after a minimum of 30 seconds, causes the charged capacitor to be discharged through the piston-actuator bridgewire. This bridgewire initiates the piston actuator, breaking the break-off valve and depressurizing the caging bellows.

Thermal Control

Control and measurement of sensor temperature are critical to PSE operation and data interpretation. Because the relative positions of the long-period sensors vary with temperature, it is necessary to level and center them frequently if temperature is not finely controlled. More important, any temperature-induced position variations are superimposed on tilt and gravitational measurements, increasing the complexity of data interpretation.

The sensor-temperature monitoring circuit is made up of a temperature-sensing bridge circuit and a differential amplifier. A 3-kilohertz signal from the 3-kilohertz oscillator in the long-period channels is applied to the input of the bridge circuit, which is balanced at 126°F. Two platinum sensistors in the bridge arms, mounted on the base of the sensor assembly, sense changes in assembly temperature. Changes of as little as 0.02°F unbalance the bridge enough to develop a temperature output signal from the differential amplifier, which is proportional to the direction and amount of the change. This signal controls the sensor heater circuits and is also applied to the multiplexer as the eighth PSE science channel.

The thermal control circuits include a logic circuit, a heater-power relay, a bypass relay, a multivibrator, a heater-power switch, and the heater. Operating power is applied to the heater-power relay from the

PSE power distribution circuits. This relay and the bypass relay control the operating mode of the heater. Three modes of operation – automatic, thermostat bypass (manual on), and power off – are provided for. The heater-power switch is turned on and off at a 3-kilohertz rate by the multivibrator. When the heater-power switch is on and the heater-power relay is closed, operating power is connected to the heater. The multivibrator controls the length of time that power is supplied to the heater-power switch on the basis of the temperature signal received from the temperature-monitoring circuits. The period lengthens when the temperature falls and shortens when the temperature rises.

CENTRAL STATION ELECTRONICS (CSE)

The PSE Central Station electronics assembly is mounted to the ALSEP Central Station thermal plate and connected directly to the Central Station harness. Two 10-foot PSE sensor cables are mated to two CSE cables on the Central Station bulkhead. Manganin is used in the CSE cables to minimize heat loss from the ALSEP Central Station.

The CSE assembly consists of long- and short-period-seismometer signal conditioning circuits, calibration circuits, a d.c./d.c. power converter, command and engineering-status circuits, timing-control and multiplexer circuits, and an analog-to-digital converter. These electronics are contained on eleven printed-circuit boards. Discrete components are mounted in conventional form on ten of the boards; the digital assembly on the eleventh board has the form of three welded micropackage modules. The analog-to-digital converter is also packaged in modular form and mounted in the CSE assembly.

Long-Period Electronics

The long-period portion of the PSE Central Station electronics includes the attenuator, the postamplifier, and the low-pass filter circuits. These circuits amplify the seismic signal to obtain the system sensitivity required, adjust system sensitivity in 10-decibel steps as commanded from the ALSEP data subsystem, and filter the output to obtain the proper response to limit aliasing, which occurs at frequencies greater than half the sampling rate. The long-period attenuator is a ladder network with two field-effect transistors that switch in their respective shunt resistors on command from the ALSEP data subsystem. The attenuator output is coupled to the amplifier through a resistance/capacitance network, which removes the d.c. tidal component from the seismic signal. The cutoff frequency of this filter is 0.01 hertz. The low-pass filter consists of four active 12-decibel-per-octave sections for a total of 48 decibels per octave. A conventional emitter/follower provides a low-output impedance to the multiplexer.

Short-Period Electronics

The Central Station short-period electronics are essentially the same as the long-period electronics except that, since the short-period preamplifier output is differential, the short-period attenuator and amplifier are differential. The low-pass-filter cutoff frequency is 10 hertz, with variations due to component tolerances having the same effect as in the long-period circuits. All the short-period electronics are d.c.-coupled, since the preamplifier d.c. isolation is accomplished in the sensor.

The short-period printed-circuit board also contains a ±2.5-volt reference regulator for the analog-to-digital converter. Because the same reference is used for the calibration circuits, drifts due to changes in the reference tend to cancel.

Calibration Circuits

The calibration circuits provide a direct current to the calibration coil of the short-period seismometer and to the feedback coil of the long-period seismometer. This calibration current is applied and removed on command from the ALSEP data subsystem at a level that provides about one-fourth full-scale output.

The calibration attenuators use the +2.5-volt reference supply as the calibration voltage source. This voltage is switched on by command, and the amplitude is set using the same basic circuitry as that used for the signal attenuators in the long- and short-period boards. The fact that the calibration voltage is maximum when the signal gain is minimum permits the system output from the calibration pulse to be the same for all attenuator settings. The exact calibration current is adjusted during initial setup and test of the seismometers to establish a known system output level to calibration commands.

Power Converter

The Passive Seismic Experiment operates from two 29-volt d.c. lines provided by the ALSEP power distribution unit. The survival power line supplies power to the survival heaters only; all circuits operate from the functional power line. During normal operation, the 29-volt d.c. functional power is applied to the leveling circuits, the sensor heater, and the power converter. The power converter, in turn, provides +12, +5, and -12 volts direct current to the analog and digital circuits.

Incoming functional power is routed through a passive input filter and returned through a current limiter. A voltage-controlled multivibrator operates a transistor switch, which controls the power to a standard transistor inverter circuit. Use of a high-frequency inverter and filtering of all voltage lines minimize noise susceptibility and radiation. The inverter provides full-wave rectified power at +12, +5, and - 12 volts direct current.

Digital Circuits

The digital circuits include the signal processing system and the command electronics for the Passive Seismic Experiment. The signal processing system multiplexes the eight analog inputs and converts them to digital form at the proper time in response to control pulses from the ALSEP data subsystem. Digital seismic and temperature data are shifted out in serial form in response to shift pulses from the same source. The command electronics receive command pulses from the ALSEP data subsystem and convert these to the logic levels required by the PSE circuits.

Signal Processing

Multiplexing is accomplished by means of a word position counter, select decode logic, and field-effect-transistor (FET) gates. The word position counter counts words after the even frame mark. Between successive even-frame-mark pulses, 128 word positions are counted, each frame consisting of 64 words, with two words alternately switched each frame as required by the ALSEP format. The select decode logic selects the appropriate word-times from the binary counter and switches on the appropriate FET multiplexer switch.

Analog-to-digital conversion is accomplished by means of a 10-bit analog-to-digital converter. The parallel output of the converter is transferred to an output shift register and shifted out serially upon command from the data processor.

System timing is controlled by inputs from the ALSEP electronics.

Command Functions

A total of fifteen commands from earth can be transmitted to the Passive Seismic Experiment to control signal calibration and gain in the four seismic data channels; filtering in the long-period feedback circuits; leveling mode, speed, direction, and leveling-motor power for each axis during leveling of the long-period sensors; operating mode for the sensor-assembly heater; and arming and uncaging of the seismometers. The commands are channeled over fifteen separate command lines connecting the ALSEP command decoder to the PSE Central Station electronics, which route the commands over separate lines to the sensor assembly.

All fifteen command logic circuits are composed of one or more flip-flops. Four of these circuits are made up of 2-bit serially connected counters which provide four stable output states. Three of these counters control switches that select sections of step-attenuators in the signal paths and in the calibration circuits of the four seismic data channels. The fourth counter controls switching relays in the sensor-assembly heater control circuits. The other eleven flip-flops control switches that apply power to associated circuits.

The preset logic circuit has the form of a one-shot multivibrator, which generates the preset pulse to the other logic circuits when triggered by the application of ALSEP operating power.

EXPERIMENT PERFORMANCE

To date, four Passive Seismic Experiments have been deployed on the lunar surface, and each successive instrument has functioned to provide additional exploration data of significance.

The instrument carried as a part of the Early Apollo Scientific Experiments Package (EASEP) on Apollo 11 was not deployed independently but remained on the Central Station with minimal thermal control. This instrument measured a large number of seismic events, both short-period and long-period, over a thermal range of +40°F to +200°F (as compared with the design specification of 126±18°F). At the time the EASEP seismometer was turned off by internal electronics, it was still functioning as designed.

The Apollo 12 and Apollo 14 instruments – deployed in November 1969 and February 1970, respectively – have recorded a number of seismic events and continue to function. All measurements made to date indicate the lunar seismic background to be extremely low as compared with that on earth, the difference being a factor of 10^2 to 10^4. Between events, the seismic output is below the minimum detectable 0.3-millimicron signal, a detection level that exceeds the design goal. The electric noise level is less than the least significant bit of ALSEP data. Since seismic-event magnitude is also low, the instruments are operated at maximum gain, a gain at which the seismometers cannot be tested in the earth environment.

With the thermal control modifications incorporated in the Apollo 14 experiment, the internal temperature of the instrument is maintained at 124.2°F during lunar night and rises to a maximum

of 132.5°F during lunar day. This performance exceeds the design requirements and limits the thermal effects seen in the tidal data.

Principal Investigator Gary Latham has analyzed the data obtained from the first three missions[1, 2, 3] and has formulated tentative lunar models based on the results. Such events have been recorded as crew activity prior to lift-off from the lunar surface, venting of gasses and thermal popping from the Lunar Module descent stage left on the moon, artificial impacts of the S-IVB booster stage and the Lunar Module on the lunar surface, meteoroid impacts, and internal lunar tectonic events.

Analysis indicates that the thermal energy of the moon is very low and that its structure is unlike that seen anywhere on earth. The moonquakes recorded thus far are few in number, small in magnitude, and centered at several specific locations. All have occurred at perigee, when the earth's gravitational forces are at a maximum, presumably resulting in release of internal strain in the lunar interior.

All the seismic wave trains recorded on the moon are similar to one another but very different from wave trains observed on earth. The impact of the Apollo 14 Lunar Module produced a wave approximately 1 hour in duration; the same event on earth would be expected to produce a wave having a duration of only a few minutes. This difference suggests a heterogeneous lunar surface layer in which there is a high degree of scattering and/or dispersion, with an underlayer of extremely low seismic attenuation.

The deployment of the Apollo 15 Passive Seismic Experiment on 31 July 1971 completed the three-instrument network that is required to definitively establish the locations of lunar seismic activity and the properties of the lunar interior. Numerous events have been recorded on all three instruments. Analysis of the data is still in progress.

REFERENCES

1. G. V. Latham, et al., "Passive Seismic Experiment," *Apollo 11 Preliminary Science Report*, NASA SP-214, Section 6 (1969).
2. G. V. Latham, et al., "Passive Seismic Experiment," *Apollo 12 Preliminary Science Report*, NASA SP-235, Section 3 (1970).
3. G. V. Latham, et al., "Passive Seismic Experiment," *Apollo 14 Preliminary Science Report*, NASA SP-272, Section 6 (1971).

The Active Seismic Experiment

J. R. McDOWELL

Determining the existence or nonexistence of a lunar crust, the origins and internal structures of the lunar maria and the lunar highlands, and the origin of the lunar soil is fundamental to an understanding of the origin and evolution of the moon, the earth, and the terrestrial planets. As a step in this direction, a seismic refraction system has been developed for use on manned lunar landings to provide information concerning the lunar-subsurface geologic structure to depths of 75 to 500 feet. The system, known as the Active Seismic Experiment (ASE), is a part of the Apollo Lunar Surface Experiments Package (ALSEP); it has been deployed on Apollo 14 and is scheduled for deployment again on Apollo 16. The experiment involves the generation and monitoring of artificial seismic waves ranging in frequency from 3 to 250 hertz in the lunar surface and near-subsurface. The seismic waves are artificially produced by two different explosive devices and are detected by miniature seismometers or geophones. The data that result are telemetered to earth for study and interpretation.

INTRODUCTION

The scientific objective of the Active Seismic Experiment (ASE) is to determine the physical properties of lunar near-surface materials. Seismic energy is artificially produced by two different explosive devices, transmitted through the lunar surface materials, and detected by miniature seismometers (geophones); the resulting wave trains (in the 3- to 250-hertz range) are telemetered to earth for interpretation. The ASE is also used, for short periods of time, to monitor natural lunar seismic waves in the same frequency range. Penetration of seismic energy to varying depths (down to approximately 500 feet) is achieved, and wave velocities through several layers of near-surface materials are investigated, by varying the explosion-to-detector distance and the size of the explosive charge. The velocities of the compressional seismic waves, their frequency spectra, and their attenuations are all functions of the physical constants of the lunar near-surface rocks. Interpretation of these data permits rock type and character, as well as degree of induration and lunar-material bearing strength, to be inferred.

EXPERIMENT DESCRIPTION

During a lunar mission on which the Active Seismic Experiment is carried, the astronauts deploy a line of geophones at intervals of 10, 160, and 310 feet from the ALSEP Central Station. These three geophones are used to detect seismic waves induced in the lunar subsurface both while the astronauts are on the moon and after their departure.

In the first instance, the astronaut walks back along the deployed geophone line, using a "thumping" device to induce seismic energy into the lunar soil. The thumper contains 21 Apollo standard initiators (ASI's), which are fired by the astronaut at 15-foot intervals marked along the 300 feet of geophone cable. Since the thumper is used to stow and deploy the geophones and cabling, the assembly is referred to as the thumper/geophone assembly.

In the second instance, the seismic energy is produced by a launching device, capable of launching four rocket-propelled, explosive grenades to lunar ranges of 500, 1000, 3000, and 5000 feet. The grenades contain 0.1, 0.3, 0.6, and 1.0 pound of high explosive, respectively. The device, known as the mortar package assembly, is emplaced by the astronaut so that its firing line is aligned to be 180 degrees from the deployed geophone line. The grenades are launched by earth command after the departure of the astronauts, for a period of up to one year following lunar deployment.

If the distance between the geophones and the energy source is known, the velocity of the seismic waves can be determined by analysis of the time interval between the energy (explosion) instant and the detection of the seismic-wave arrivals. In the thumper mode, the range determination is based on a

---

The basic scientific requirements for the Active Seismic Experiment were developed under the direction of Principal Investigator R. L. Kovach (Department of Geophysics, Stanford University) and Co-Principal Investigator J. Watkins (Department of Geology, University of North Carolina).

knowledge of the marked interval on the geophone cable at which the astronaut fires the ASI. The instant of ASI initiation is detected by a pressure switch and telemetered as a real-time event (RTE). In the grenade mode, the range determination is based on the parameters of a ballistic trajectory assumed to be ideal. The launch angle of the grenade is determined from measurements made of the pitch and roll angles of the mortar package prior to each launch. Initial velocity data are provided by range-line breakwire circuits, which are broken at the beginning and at the end of a 25-foot interval of line deployed at launch, the breaks being telemetered as real-time events. Time of flight is furnished by a transmitter in each grenade which is activated at launch and destroyed upon explosive impact; loss of the transmitter signal occurs at the instant of explosion and is also telemetered as a real-time event. Using these parameters (launch angle, velocity, and time of flight), grenade range can be determined to within ±5 percent. The time of thumper ASI initiation and the time of grenade detonation are known to within ±0.1 millisecond.

The seismic detectors are three identical geophones—electromagnetic transducers that translate high-frequency seismic energy into electric signals. The outputs of the three geophones are applied to separate logarithmic compression amplifiers to obtain maximum dynamic range and maximum sensitivity.

The Active Seismic Experiment uses seven commands transmitted from the Manned Space Flight Network to arm and fire the grenades and to effect geophone calibration. Other commands are used to effect power distribution to the ASE from the ALSEP data subsystem and to place the data subsystem in the active seismic mode. The three channels of seismic data generated by the ASE, along with 13 channels of engineering data, are converted to digital form within the experiment for transmission to earth. A 20-bit digital word format and a 10,600-bit-per-second data rate are used in the ASE to ensure accurate encoding and transmission of critical real-time-event data and to provide a relatively high frequency seismic-data-handling capability. The higher bit rate and the longer word length are incompatible with the normal ALSEP format and preclude the usual data collection from other experiments during the time the ASE is activated. Five significant measurements from the ALSEP electric power subsystem are included in the ASE telemetry format as engineering data. The experiment formats the seismic and engineering data and applies them to the data-subsystem modulator for modulation and downlink transmission.

EXPERIMENT DESIGN

The Active Seismic Experiment, the components of which are shown in Figure 1, is made up of three major subsystems: the thumper/geophone assembly, the mortar package assembly, and the Central Station electronics. The experiment weighs 34.66 pounds. Size and weight data for each of the subsystems are presented in Table I; system power requirements are listed in Table II.

Thumper/Geophone Assembly

The thumper/geophone assembly is constructed almost entirely of magnesium alloy and is so designed that it folds into three sections for stowage. It is electrically connected to the ALSEP Central Station by 318 feet of flat, four-conductor, H-film cable, which is stowed on a split spool on the upper end of the thumper handle and unwound by the astronaut during deployment. Also stowed on the thumper until deployment are the three geophones, the geophone cabling, and an aluminum-alloy geophone flag. The geophone cabling is wound on a reel at the lower end of the thumper. The geophones are mounted in individual stowage sockets in the reel assembly and held in by removable clips. The geophone flag is similarly stowed in a socket in the reel assembly and is deployed at the second geophone emplacement to aid the astronaut in the visual alignment of the geophones. The thumper is held horizontally during

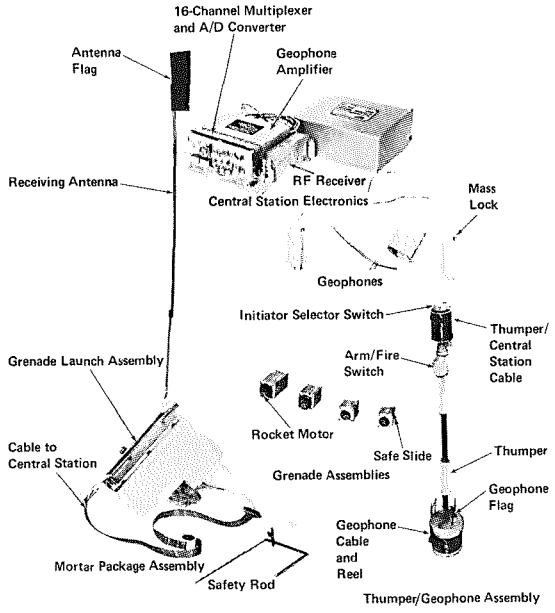

Figure 1 The Active Seismic Experiment

Table I Active Seismic Experiment Subsystem Parameters

Subsystem or Component	Parameter	Value
Thumper/Geophone Assembly	Length (folded)	14.5 inches
	Weight	7.59 pounds
• Thumper	Length (deployed)	44.5 inches
	Weight (including cables and initiators)	4.64 pounds
• Geophones	Height (including spike)	4.80 inches
	Diameter	1.66 inches
	Weight (three geophones with cables)	2.95 pounds
Mortar Package	Envelope Height	11.5 inches
	Envelope Width	6.0 inches
	Envelope Length	15.25 inches
	Weight	17.00 pounds
• Mortar Box Assembly	Height	11.5 inches
	Width	6.0 inches
	Length	15.25 inches
	Weight (including antenna and cables)	6.39 pounds
• Grenade Launch Assembly	Width	9.0 inches
	Length	13.7 inches
	Depth	6.23 inches
	Weight (including grenades)	10.88 pounds
• Grenades	Cross Section	2.7 inches
	Length	4-6 inches
	Weight[a]	8.08 pounds
Central-Electronics Assembly	Height	2.75 inches
	Width	6.18 inches
	Length	6.77 inches
	Weight	3.22 pounds
Mortar-Package Pallet Assembly	Width	24.0 inches
	Length	26.0 inches
	Weight	6.85 pounds

[a]Grenades 1, 2, 3, and 4 weigh 2.67, 2.19, 1.70, and 1.52 pounds, respectively.

Table II System Power Requirements

Type	Amount
Voltage	
ASE-Activated	+29, +15, −12, and +5 volts d.c.
ASE-Deactivated	+29 volts d.c.
Power	
Operational	8.0 watts (maximum)
	6.0 watts (nominal)
Thermal Control (standby)	3.00 watts

deployment, as shown in Figure 2, and rotating handles on the staff assembly allow both the power- and the geophone-cable reels to rotate freely for cable deployment.

The thumper contains 21 Apollo standard initiators (ASI's), rated at 1 ampere "no-fire" and 3 amperes "all-fire." The ASI, as a component, generates a pressure of approximately 650 pounds per square inch in a 10-cubic-centimeter volume. The initiators are threaded into a magnesium mounting plate, which forms a portion of the thumper base. The ASI's are individually fired directly into a forged-aluminum impact plate, which is spring-loaded

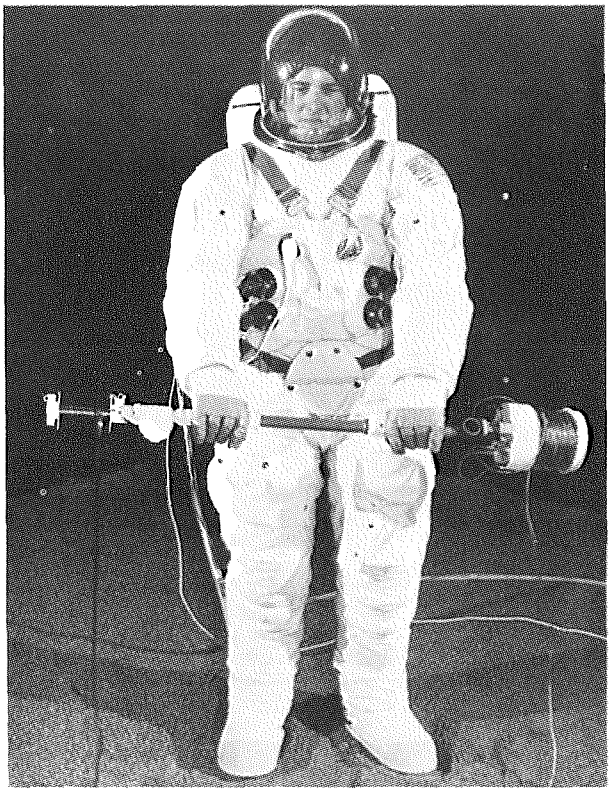

Figure 2 Deployment of Thumper/Geophone Assembly

against the mounting plate. As illustrated in Figure 3, the gas pressure resulting from an initiator discharge drives the impact plate sharply downward, imparting a thump to the adjacent lunar surface. The initiator-discharge gases are immediately vented around the edges of the impact plate and are deflected downward by a ring which is part of the mounting plate. A pressure switch, installed in the mounting plate, closes from the pressure generated from an initiator firing. The switch closure causes an RTE signal to be generated in the ASE central electronics, indicating the instant of explosion. The end of each ASI mounted in the mounting plate is covered with a coating of silicone rubber to protect the initiator from the pressure and debris from adjacent initiator

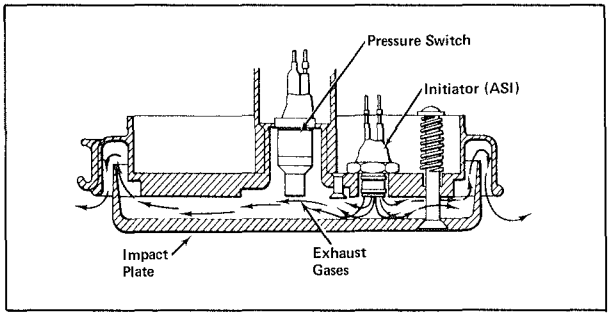

Figure 3 Operation of Thumper Base Section

firings, which might otherwise cause sympathetic deflagration. Extensive test firings have demonstrated the adequacy of this protection.

The thumper is so designed that all the initiators are internally shorted by the ASI rotary selector switch when the selector switch is in the zero position. In any other position (numbered 1 through 21), one ASI is connected to the firing circuitry and the other twenty remain shorted out. Simple rotation of the switch to a position other than zero will not in itself fire an ASI, even with power applied; a definite two-step firing operation with a time delay is required. After ASI selection by rotation of the selector switch to a numbered position, the thumper is armed by rotating the ARM/FIRE knob approximately 90 degrees and holding it at that position for a minimum of 4 seconds. This switch is then pushed in, applying a capacitor charge across the ASI and causing it to fire. The ARM/FIRE control is so designed that the firing switch cannot be actuated until the arming switch has been activated. If for any reason it should be necessary to stop the firing sequence after the thumper is armed, release of the ARM/FIRE control permits it to return to its normal unactivated position, and the arming capacitors are automatically discharged in a matter of milliseconds. In the normal position, the control provides a low impedance across the firing capacitors, both to prevent them from picking up a static charge and to discharge them if they are charged but have not fired through an ASI.

The thumper is shown in the firing position in Figure 4.

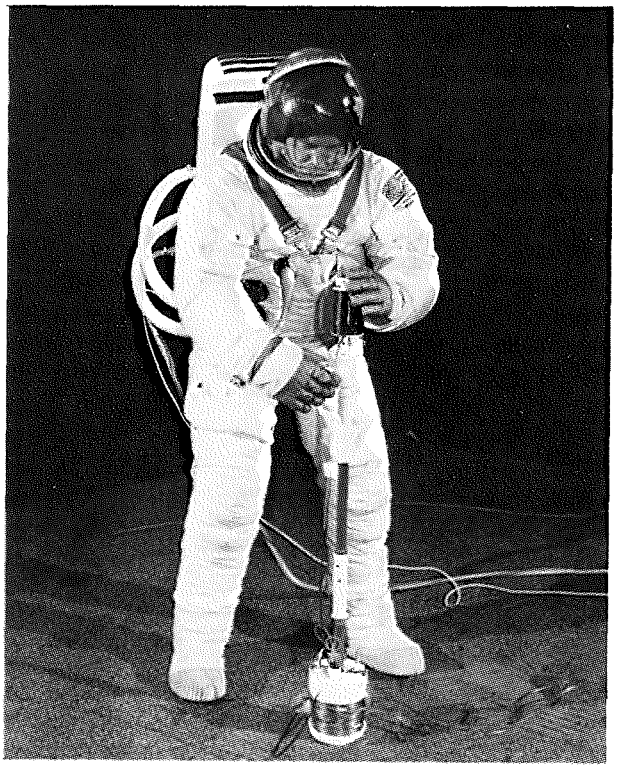

Figure 4 Thumper in Firing Position

Mortar Package Assembly (MPA)

The mortar package, shown in a deployed configuration in Figure 5, consists of a mortar box assembly and a grenade launch assembly (GLA). The mortar box is an L-shaped fiberglass box, with a magnesium frame and folding legs. The grenade launch assembly is made up of four fiberglass launch tubes, each containing a rocket-launched explosive grenade. The GLA is mounted in the mortar box. The mortar box contains the electronic circuitry for arming and firing the grenade rocket motors, along with a receiving antenna, two SAFE/ARM switches, and a thermal bag. The antenna, used in conjunction with the grenade transmitters, is mounted to the side of the mortar box and folded along the edge of the package during transport. A flag is mounted on the antenna top section to aid the astronaut during deployment. The two SAFE/ARM switches disable both the arming and the firing circuits and short out the rocket-motor firing capacitors and initiators for astronaut safety during lunar deployment. The forward end of the mortar box is beveled at 45 degrees,

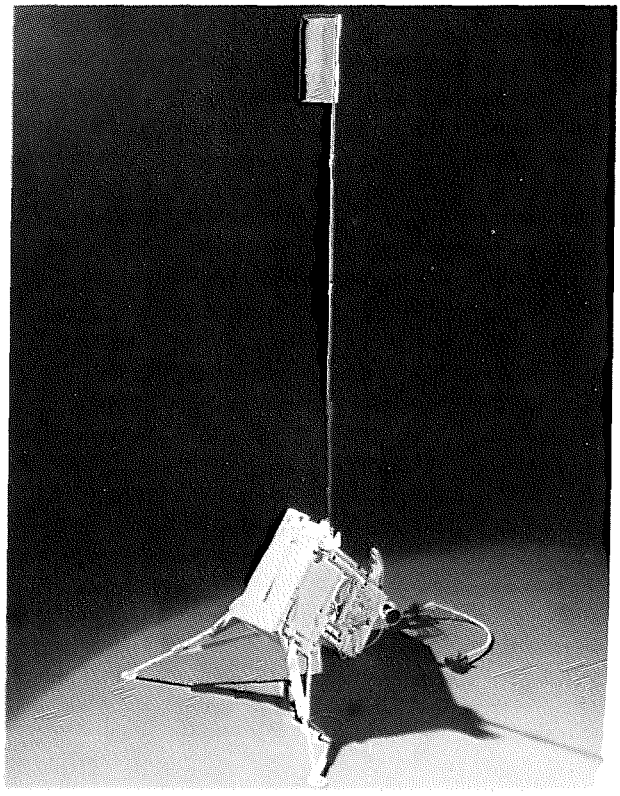

Figure 5 Deployed Mortar Package Assembly

and in the deployed position the MPA rests upon the 45-degree bevel. The remainder of the package is supported by two legs, which are stored along the side of the box during transport and folded down and locked into place during deployment. The mortar box is attached to an aluminum-skin pallet assembly in the final deployed configuration. The pallet has four 7-inch stakes mounted to its underside and, when placed on the lunar surface, provides a stable base for a 45-degree grenade launch.

The mortar package assembly is designed to survive on the lunar surface for a period of one year. A temperature ranging between -60°C during lunar night and +85°C during lunar day is maintained by a thermal control design incorporating thermal isolation and insulation as well as electronic heaters inside the mortar box. Isolation is provided by a multilayer aluminized-Mylar thermal bag, which is installed down inside the mortar box. The electronic heaters are mounted on the walls of this bag. Insulation is provided by a multilayer aluminized-Mylar fiberglass cover along the top of the mortar box. This cover remains in place throughout lunar storage until the first grenade is launched through it; it also serves as a radio-frequency-interference shield, completely enclosing the grenade launch assembly. The mortar-box firing circuits are designed with low-pass input filters, and all firing capacitors and initiators have resistors across them to reduce the effects of electrostatic charge. The fragile bottom of the thermal bag disintegrates when the grenades are launched. Two fiberglass blowout panels, each extending over two launch tubes, enclose the bottom of the mortar box and blow away upon grenade ignition.

GLA Configuration

The grenade launch assembly, pictured in Figure 6, is a fiberglass launch-tube assembly (LTA) consisting of four rocket-launched grenades, a grenade safety-pin assembly, three microswitches, three temperature sensors, and two vertical sensors. Each of the four launch tubes has a cross section of 3 inches. Two tubes are 9 inches long and the other two are 6.5 inches long. Around the outside of each tube is wound a range line, a thin stranded stainless steel cable, to which the grenade is attached. Two fine copper wires are looped around each range line, so spaced that the first breaks when the grenade is separated from the launch tube by about 16 inches and the second breaks when this distance is increased by exactly 25 feet. Loop-breaking starts and stops a range gate pulse, establishing a time interval for determination of grenade velocity.

Grenade construction is detailed in Figure 7. The four grenades are similar, differing only in the size of

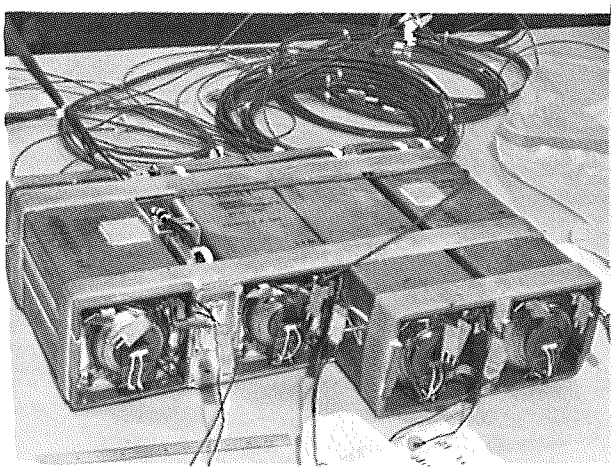

Figure 6 Grenade Launch Assembly

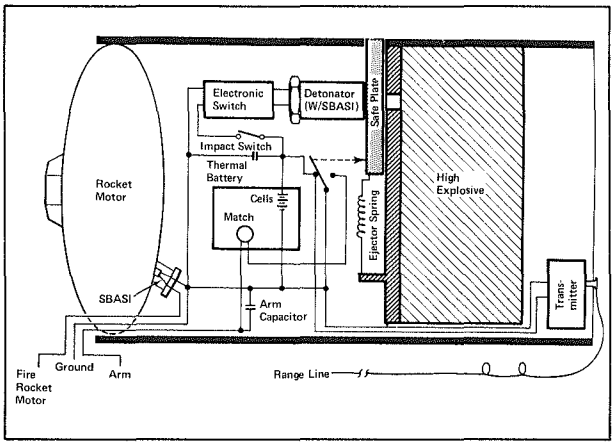

Figure 7 Grenade Construction

the motor and the amount of propellant and high explosive. Each has a thin fiberglass casing and a 2.7-inch-square cross section; they range in length from 4 to 6 inches. Inside the casing are the rocket motor, a safe-slide plate, a high-explosive charge, a detonating cartridge, an omnidirectional impact switch, a thermal battery, and a 30-megahertz transmitter. The range line is attached to the output terminal of the transmitter and serves as a half-wave end-feed antenna as it trails the grenade in flight.

The launch tubes for grenades 2, 3, and 4 each contain a microswitch that closes when the grenade is launched. Each switch connects the firing command from a sequential grenade-firing circuit to the next grenade to be launched.

Two temperature sensors are located between tubes 1 and 2 of the LTA; a third is located between tubes 3 and 4. One of the sensors provides an analog signal indicating GLA temperature to the data handling function of the Active Seismic Experiment. The other two sensors are part of the mortar-box heater control circuitry.

Two bubble-type electrolytic vertical sensors are mounted between tubes 3 and 4. These single-axis sensors indicate angular tilt (±12 degrees) in pitch and roll from the local vertical to provide grenade-launch-angle deviation from the 45-degree deployment angle. The vertical sensor is qualified for a 100-*g* shock resulting from grenade launch.

Grenade Launch

The mortar package is activated by ARM GRENADES and FIRE GRENADES commands from earth. The ARM GRENADES command is applied to and gated through the experiment central-electronics command gating to the grenade-arming circuit, which charges the regular and sequential firing capacitors in the mortar box and in each of the four grenades by applying a 24-volt arming signal. After arming, a FIRE GRENADE command for each of the grenades is applied to the command gating and gated to the appropriate firing circuit in the mortar box; this causes the firing capacitor to discharge and to ignite the grenade propellant through a single-bridgewire Apollo standard initiator (SBASI). As the grenade leaves the launch tube, the safe slide is spring-ejected; this permits a microswitch in the grenade to close, discharging the grenade-arming capacitor across a thermoelectric match and, in turn, activating the thermal battery. The thermal battery, when activated, provides internal grenade power for driving the transmitter and charging the detonator storage capacitors.

The first of the two range-line breakwires is broken upon grenade launch, initiating the range gate pulse to the real-time-event logic in the central electronics. Rocket propellant in the grenade is exhausted before the grenade exits the tube. The second range-line breakwire is broken when the grenade is 25 feet into trajectory; this terminates the range gate pulse to the real-time-event logic and provides time/distance data for subsequent determination of grenade velocity. The grenade transmitter, activated at launch and utilizing the grenade range-line as an antenna, transmits until it is destroyed upon grenade impact. The omnidirectional impact switch in the grenade allows the detonator capacitor to discharge, firing a detonator to set off the grenade high explosive upon impact. The 30-megahertz signal from the transmitter is received by the antenna mounted on the mortar box and is conducted by coaxial cable to the receiver in the Central Station electronics. The received signal is applied, through a level detector, to the real-time-event logic for application to the data handling function. The grenade transmitter signal provides an indication of time of flight and instant of detonation, and thus a second calculation of range, enhancing the confidence factor for the range calculation that is based on launch-angle and grenade-velocity data generated from the vertical sensors and the range-line breakwires.

Grenade 2 (3000 feet) is fired first, followed sequentially by grenade 4 (500 feet), grenade 3 (1000 feet), and grenade 1 (5000 feet). This firing order results in optimum mortar-package firing stability. A redundant arming and firing circuit is provided for sequential firing in the event of failure of one or all of the regular firing circuits. This so-called sequential circuit is armed by the normal ARM GRENADES command. A series of interlocking microswitches connect the sequential firing circuit to the next grenade-firing circuits as the grenades are launched.

Grenade Design Features

The safe slide in each grenade constitutes a mechanical block between the detonator and the explosive block. It is held in place while the grenade is in the launch tube and is spring-ejected at launch. While it is in place, inadvertent detonator ignition will not set off the high-explosive charge. The safe slide also keeps a microswitch so positioned as to isolate the thermal battery output from the high-explosive firing circuitry, and provides a low impedance to the firing capacitors to prevent their being charged by a static charge.

The thermal battery in each grenade contains a thermoelectric match, which has a no-fire rating of 0.75 ampere for 10 milliseconds and an all-fire rating of 2.0 amperes for 10 milliseconds. The hermetically sealed battery output is rated at a nominal 15 volts (a 13-volt minimum for 1-second activation to a maximum of 19 volts) and is capable of providing 100 milliamperes for 1 minute (minimum).

The grenade transmitter has a ruggedized, subminiature, encapsulated cordwood construction. It operates at a continuous-wave frequency of 30 megahertz ±100 kilohertz, with a power output of 200 milliwatts for a minimum of 1 minute. Both the transmitter and the thermal battery are designed to survive a grenade-launch shock of 2465 *g*'s and are qualified at 3200 *g*'s.

The grenade high-explosive charge is plastic-bonded hexanitrostilbene (HNS).* The selection of HNS for use in the Active Seismic Experiment was made on the basis of vacuum stability, thermal stability, friction sensitivity, impact (shock) sensitivity, shelf life, and radiation sensitivity. The material does not decompose in a vacuum, prolonged exposure resulting in a weight loss of less than 0.06 percent, and this due primarily to evaporation of residual solvents. From a

*Developed by the Naval Ordnance Laboratory, White Oak, Maryland.

thermal standpoint, HNS is an excellent explosive material. It does not begin to melt until exposed to temperatures well above 500°F for prolonged periods, making it extremely safe to handle in any normal temperature environment. It is in no way sensitive to friction, and as a raw material it is very insensitive to impact shock. It has been dropped from great heights onto solid concrete without detonating; its impact sensitivity as measured in Military Standard Laboratory tests is well above the minimum military standard of 60 centimeters. With respect to shelf life, military tests predict a decomposition of only 1 percent over a 500-year period at 212°F. Radiation sensitivity tests indicate that HNS is in no way sensitive to radiation. From these criteria, it was concluded that HNS could be handled, tested, flown on a spacecraft, and deployed by astronauts with relative safety. For the Active Seismic Experiment, raw HNS is blended with Teflon to yield a 90-percent-HNS/10-percent-Teflon composition. The blend is pressed into a plastic block under pressures of approximately 30,000 pounds per square inch, and the block is then machined into the flight configuration seen in the X ray of a completed grenade launch assembly shown in Figure 8.

Grenade design also features a fast-ignition motor, with an extremely short thrust duration (6 to 10.5 milliseconds) and a stable launch platform. Stability is attained by utilizing recoilless launch techniques, with open-end launch tubes operating on the rocket-motor action/reaction principle for grenade launch. During the development phase of the Active Seismic Experiment, a trade-off study was conducted and tests were performed to compare the feasibility of open-tube rocket-launched grenades with that of a closed-tube mortar approach. Mortar launch offered the advantage of good reproducibility, provided that a lightweight, stable platform could be achieved; moreover, all the propellant would burn while the grenade was still in the closed tube. However, the high reaction load imparted to the launch platform presented a problem in that it necessitated a mechanically strong and predictably heavy design. The logical alternative to the mortar approach was to attach a motor to the grenade to form a miniature rocket and use an open launch tube. The motor developed has so short a burn time that it is burned out completely by the time the grenade travels the length of the 6.5-inch or 9-inch tube. Since there is little reaction load on the launcher, the design is suitably lightweight. There are two basic motor sizes, with different propellant loadings to achieve the different burn times. Nozzle sizes of 0.5 and 0.8 inch are used for the two motors to yield the required thrust levels, the nozzle being an orifice rather than a conventional nozzle. A further requirement imposed on the motor is that it be hermetically sealed but ignite reliably even if the seal should be lost during the year of lunar storage. The motors are therefore individually sealed with a 0.003-inch stainless steel diaphragm stitch-welded across the nozzle; the diaphragm blows out upon ignition. The initiators are also welded in.

The solid propellant used* was selected for its burn rate, temperature stability, friction sensitivity, impact sensitivity, and vacuum stability. An extruded cylinder of the magnesium/Teflon-composition propellant 0.205 inch in diameter is sliced into wafers 0.013 to 0.018 inch thick, as dictated by thrust/time curve requirements. The wafers are retained behind a conical screen welded inside the motor assembly, in numbers varying from 570 to 2365. Two views of the rocket motor assembly and a cutaway showing the conical screen are seen in Figure 9. The motors are elliptical in shape, being formed by 2:1 elliptical

*A classified (NOTS PL6670) military propellant.

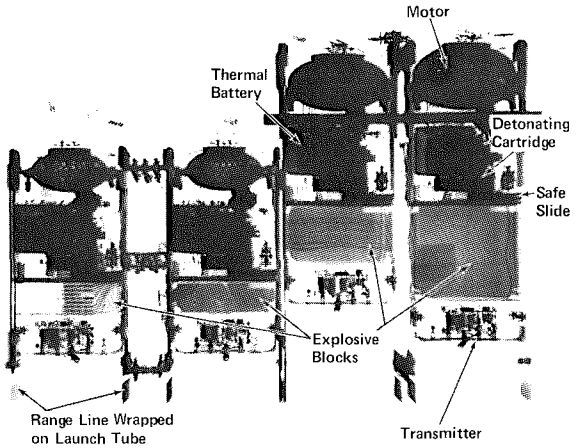

Figure 8 X Ray of Flight-Configuration Grenade Launch Assembly

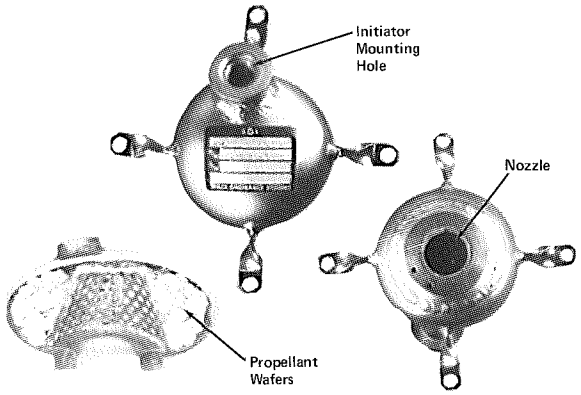

Figure 9 Grenade Rocket Motor

Parameter	Grenade			
	1	2	3	4
Range (ft)	5000	3000	1000	500
Weight (gm)	1261	1024	775	695
High-Explosive Charge Weight (lb)	1.0	0.60	0.30	0.10
Rocket-Motor Mean Peak Thrust (lb)	5000	2500	1700	1250
Mean Velocity (ft/sec)	163	126	73	52
Lunar Flight Time (sec)	44	32	19	13
Rocket-Motor Propellant Weight (gm)	42	27	15	10
Number of Propellant Pellets	2365	1520	620	570
Launch Angle	45°	45°	45°	45°
Rocket-Motor Thrust Duration (msec)	6.0	7.5	10.5	8.5

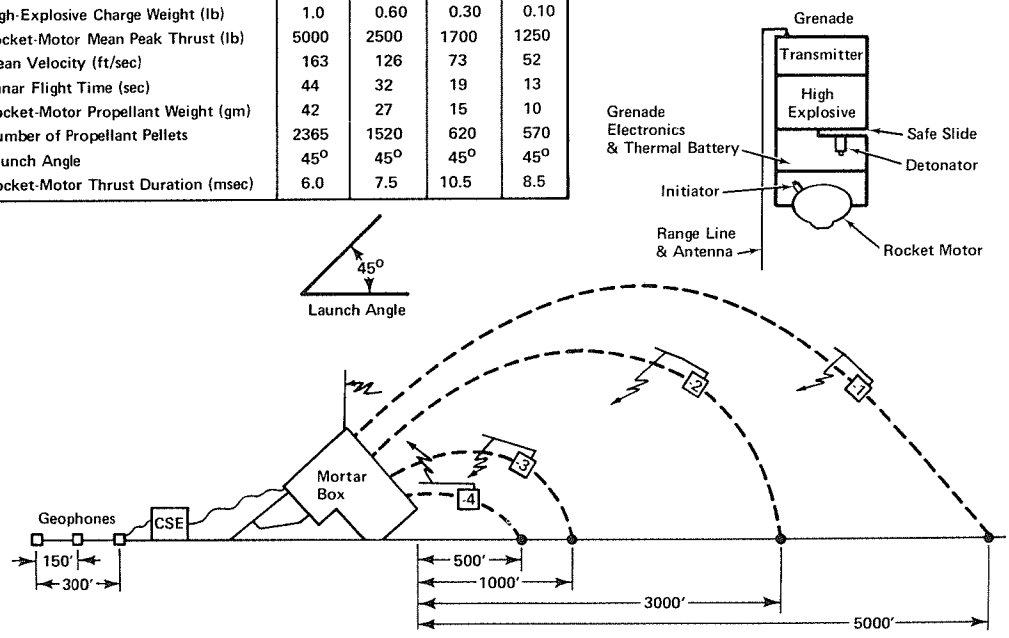

Figure 10 Grenade Design and Performance Parameters

domes of 4130 chrome/molybdenum steel, heat-treated to a minimum yield strength, welded together, of 180,000 to 200,000 pounds per square inch.

Grenade design and performance parameters are summarized in Figure 10.

Central Station Electronics (CSE)

The ASE central-electronics subsystem, shown in Figure 11, is hard-mounted to the ALSEP Central Station thermal plate and electrically and thermally controlled by that station. The subsystem contains power protection circuitry, temperature sensors, calibration, timing, and control-logic circuitry, and data handling and processing capability. Included as subassemblies are the 16-channel multiplexer and analog-to-digital converter, the ASE receiver, and the geophone amplifier.

The power protection circuitry contains current-sensitive relays that prevent overvoltage from damaging the ASE subsystems. It also prevents an ASE subsystem from overloading the ALSEP power distribution unit in the event of a malfunction. The circuitry is assembled on a printed-circuit board (power protection module). The circuits are designed to trip at an overload equal to 200 percent of the normal operating load. Operating and standby (survival) power is supplied to the Active Seismic Experiment from the ALSEP power distribution unit at +5, +15, - 12, and +29 volts d.c.

Two temperature sensors, mounted on the discrete-component board, provide central-electronics temperature data in the ON and SURVIVAL modes. The discrete-component board also includes arming and firing circuitry and calibration voltage circuitry. The calibration circuits perform two functions: They

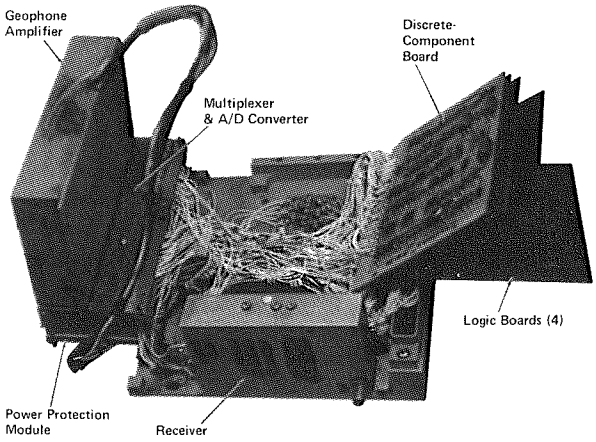

Figure 11 Active Seismic Experiment Central Electronics

provide a two-point calibration to the multiplexer and analog-to-digital converter, and, actuated by earth command, they provide a calibration signal to the geophones for lunar test and calibration comparison.

The timing and control circuitry is basically digital logic, which operates the Active Seismic Experiment using a 10.6-kilohertz clock signal in conjunction with seven commands from earth. The data rate of the ASE logic is 10.6K bits per second. The basic timing is obtained from the 10.6-kilohertz square wave received from the ALSEP data processor. The shift-register multiplexing logic selects the data to be loaded into the shift register through the analog-to-digital-converter frame, holding, and control gates. A START pulse is applied to the multiplexer and analog-to-digital converter from the decoder of the timing and control function. When a real-time event (RTE) occurs (as in the case of thumper firing, range-line-velocity START and STOP breakwires, or loss of transmitter signal upon grenade explosion), the RTE logic, in conjunction with the sequence counters and holding register, provides a MARK EVENT signal to indicate the event occurrence in the prior telemetry frame. The word and bit in which the event occurred are also identified.

Data handling and processing are accomplished by the application of 16 analog-voltage channels to the ASE multiplexer and analog-to-digital converter. Three analog channels are used for geophone outputs, two for mortar-box launch angle outputs, three for calibration, three for ASE temperature and power measurements, and the other five for ALSEP electric-power-subsystem temperature and power measurements. The analog signals are multiplexed, converted to digital signals, and formated for shifting to the ALSEP central data subsystem and downlink transmission.

Subword, word, and frame signals are derived from the sequence counters through the decoder of the timing and control function. The ASE data format is made up of 32 20-bit words per frame, each word consisting of four 5-bit subwords. Geophones 2 and 3 are sampled and read out in every word of the frame; geophone 1 is sampled and read out in all but the first word. In the first word, geophone 1 is sampled and stored, then read out in the first subword of the second word. The first two subwords of word 1 comprise a 10-bit frame-synchronizing signal. The first three bits of subword 1 of word 32 provide a mode-identification signal. The binary signals from the multiplexer converter are applied to the shift-register multiplexer gates, which are controlled by the shift-register multiplexing logic. A storage buffer is provided between the converter multiplexer and the shift-register multiplexer gates. The ASE data are shifted out in the 32-word telemetry-frame format to the biphase modulator of the ALSEP data subsystem for modulation and downlink transmission.

The ASE receiver is a subminiature, low-power r.f. receiver, capable of receiving a continuous-wave signal transmitted from the in-flight grenade transmitter. The receiver is located in the central-electronics package and is connected by coaxial cable to its antenna, which is mounted on the mortar box. The functions of the receiver are to acquire, track, and amplify the continuous-wave transmitter signal and to provide an output to the central electronics to indicate signal acquisition or loss. The receiver has a center frequency of 30 megahertz, with a minimum acquisition and tracking bandwidth of ±100 kilohertz.

The geophone amplifier assembly is a subassembly of the central-electronics subsystem. The amplifier, together with the geophones and cabling carried on the thumper, form what is known as the active seismic detection system (ASDS). Since the ASDS was designed, developed, and tested as a subsystem, it is described separately in the section that follows.

Active Seismic Detection System (ASDS)

The active seismic detection system is designed to monitor seismic waves in the frequency range between 3 and 250 hertz. Three electromagnetic geophones, three logarithmic-compression amplifiers, and the interconnecting cabling constitute its major elements. The geophones can be excited mechanically by natural or artificial seismic waves or electrically by a GEOPHONE CALIBRATE command. Sensing induced or natural seismic activity which creates motion in the lunar surface, each geophone generates an electric (a.c.) signal that is proportional to the amplitude and frequency of the ground motion. This signal is supplied to the geophone amplifier assembly in the central electronics, where it is first amplified by a linear amplifier. It is then filtered to eliminate frequencies of more than twice the sampling rate and to flatten the frequency response in the passband of 3 to 250 hertz by enhancing signals with frequencies below the geophone natural frequency. After filtering, the signal is logarithmically compressed by one of two identical logarithmic compressor circuits in each geophone-channel log compressor; two such compressor circuits are required – the one to process positive and the other negative signals – because the geophone signals are bipolar and logarithmic compression is a function of the instantaneous amplitude. The log-compressed signal is connected to a multiplexer gate, which is controlled by the ASE format-generator logic to properly time-sample the data.

Because ASDS response may change in the course of 1-year lunar operation and storage, a pulse-type calibration is included with the amplifiers to provide a relative-calibration function. This function is activated by applying a GEOPHONE CALIBRATE command to the ASE command gating. The command is gated to the calibration circuitry when a pulse 1 second in width is generated and applied to the ASDS calibrate driver, electrically exciting the geophones. Geophone excitation permits measurement of geophone resonant frequency, generator constant, and damping coefficient relative to the preflight calibration. A temperature sensor mounted in geophone 1 (that closest to the Central Station) provides temperature data whenever the ASE is not activated.

Geophone Design

The geophones developed for lunar use are of the moving-coil/magnet type. The coil is the inertial mass, suspended by springs in the magnetic field. Above the resonant frequency of such a device, its output is proportional to ground velocity; below its resonant or natural frequency, the output drops off at the rate of 12 decibels per octave.

Previously existing commercial geophone designs were evaluated but found to be unsuitable for lunar use. Spring parameters had to be changed to be compatible with lunar gravity. Moreover, it was apparent that significant increases in sensitivity could be achieved with simultaneous reductions in weight and size if better magnet materials and more efficient coil windings were used. Design changes were also suggested by such considerations as the methods available to the astronaut for implanting the device and the need to protect the springs from the vibration and shock levels encountered during testing and transit. The final design saw a significant increase in available signal power with some savings in size and weight, as well as the satisfaction of such other design objectives as the matching of the coil resistance to the optimum amplifier source impedance.

The design goal for overall ASDS response was that it be flat to ground velocity down to 3 hertz. The minimum resonant frequency for reliable operation of geophones of small size and weight can be expected to be somewhat higher than 3 hertz, particularly with the springs used for operation at lunar gravity. Preemphasis in the succeeding electronics was used to provide the desired response at frequencies below geophone resonance frequencies.

For state-of-the-art junction transistors in appropriate configurations, the power spectral density of the equivalent input noise is very nearly constant down to about 20 hertz. Below this frequency it increases with a slope of $1/f$. Preemphasis at frequencies lower than the resonance frequency thus amplifies the $1/f$ noise, decreasing the signal-to-noise ratio for signals at higher frequencies. This effect constitutes a strong incentive to select as the natural frequency of the geophone the lowest possible frequency consistent with small size and weight and adequate mechanical ruggedness. These constraints led to the choice of 7.5 hertz as the natural frequency for the lunar geophone.

Figure 12 is a cutaway view of the assembled geophone, showing the position of the coil in the magnetic flux path. The internal assembly is supported within the outer case by parts machined from Epon® 828 for thermal and mechanical stability. When the mass-lock button at the top of the case is held in the depressed position, three nickel/silver fingers extending inside the inner case assembly (the magnet cup) hold the coil firmly against the lower stops. This mass lock ensures that the unit can survive the shock and vibration encountered in environmental testing and transit to the moon. The spring-loaded mass-lock buttons are released automatically when the geophones are removed from the thumper and deployed by the astronauts.

®Epon is the registered trademark of Shell Chemical Corporation for a family of resins.

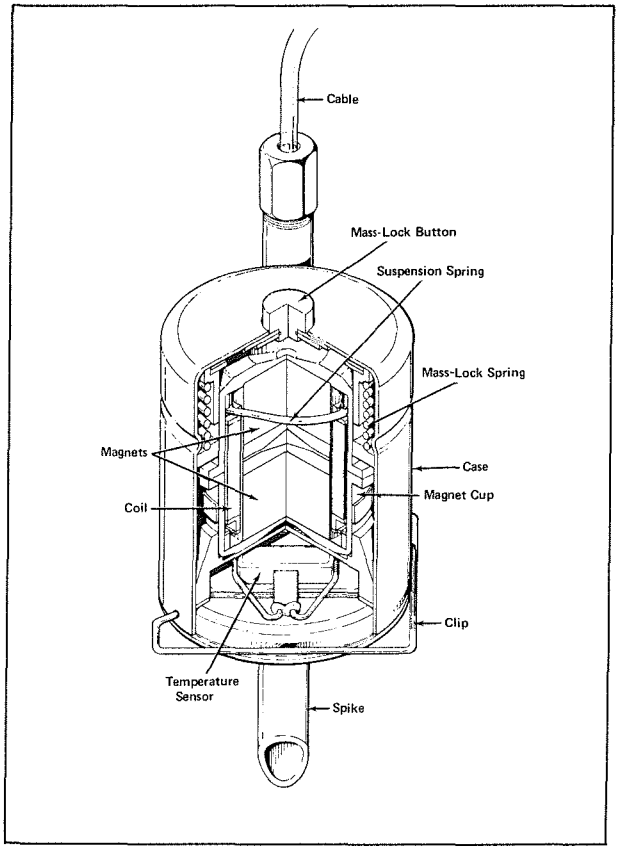

Figure 12 Cutaway View of Assembled Geophone

The coil is wet-wound, using Epon 828 on a mandrel between end pieces also cast from Epon 828, with nickel/silver-threaded inserts, encapsulated in them; 13,600 turns of No. 43-type ML copper magnet wire are used. The screws that secure the springs to the coil, and the springs themselves, serve as conductors from the coil. The two halves of the magnet cup are identical and include magnet pole pieces and pole caps, as shown in the figure. Fabricated of Alnico 9, they are so charged that the fields in the two halves oppose one another, creating a closed flux path for each half of the cup. The average flux in the gap for each half ranges from 19,000 to 20,000 maxwells. The sensitivity and frequency-response characteristics of the resulting geophone are excellent. An open-circuit generator constant of about 235 volts per meter per second is achieved, using a coil resistance of 6200 ohms; open-circuit damping is about 5 percent of critical. By way of comparison, a standard 4.5-hertz geophone* has a generator constant of about 24 volts per meter per second, with a coil resistance of 215 ohms and open-circuit damping of about 23 percent of critical. Adjusting for differing coil resistances and ignoring differences in open-circuit damping, the available signal power from the lunar geophone is about three times that from a commercial geophone. The magnetic cup assembly of the commercial unit is 1.88 inches high and 1.62 inches in diameter and weighs about 9.5 ounces. The lunar geophone is 1.25 inches high and 1.095 inches in diameter and weighs 4.16 ounces. Complete with outer case, the unit weighs 6.25 ounces.

Geophone Testing

Testing of the lunar geophone on earth presents a problem because the inertial mass rests on the lower stops in the earth's gravitational field. To overcome this problem, a device was developed which introduces into the coil of the geophone just enough direct current to offset about five-sixths of the weight of the inertial mass at earth gravity. The necessary current was accurately calculated for each geophone on the basis of its measured generator constant and was nominally 0.74 milliampere. High-voltage batteries and a large dropping resistance were used to obtain a quiet current source. Large capacitors were inserted in the amplifier input to block any d.c. flow from the amplifier.

Verification of geophone linearity at the very low signal amplitudes expected presents another problem. The system sensitivity is such as to provide clearly discernible signals in response to ground motions of 1 millimicron zero-to-peak at 10 hertz. Testing at these levels, which are lower than normal background seismic-noise levels on earth, requires the use of a quiet site and an isolation drive system to excite the geophones.

Low-level tests** were performed in a 50-foot-deep cased hole. The operating mechanism from a vertical seismometer† with a natural frequency of 0.8 hertz was used as the isolation drive unit. A signal generator was the driving source, and signal levels required for a given displacement were calculated, using the calibrated generator constant of the large seismometer. The three geophones were mounted directly to the 18-kilogram mass of the seismometer, and lunar gravity was simulated using the quiet current source previously described. Testing very late at night, good data were obtained down to displacements of 1 millimicron peak-to-peak at 10 hertz. There were no measurable deviations from linearity at these low amplitudes.

Cable Assembly

The geophone cable assembly consists of four twisted-pair, shielded polyimide-insulated cables. Three of the pairs connect the three geophones to their respective amplifier inputs; the fourth connects a temperature sensor in the near geophone to the proper data circuitry. The three geophones are spaced at 150-foot intervals on the cable, automatically providing the proper separation upon deployment by the astronaut. White markers on the cable indicate the thumper firing points.

Amplifier Design

A three-channel amplifier conditions the geophone signals prior to their conversion into digital format. Since the seismic thumper device is used for short-range shots (of the order of feet), seismic signals containing energy at frequencies of 100 hertz and higher can be generated. A system time resolution of ±1 millisecond was selected. This dictated a minimum sampling frequency of 500 hertz, which, in turn, specifies the filter response at high frequencies necessary to minimize data contamination from sideband folding. The low signal-to-noise ratio expected from the distant grenade explosions and uncertainty as to the character of the waveforms to be generated made it desirable to widen the frequency response as much as possible within the aforementioned constraint. The

*Hall-Sears model HS-1.

**For greater detail, see "The Active Seismic Detection System Final Report," Geotech Technical Report No. 69-44, Garland, Texas, 7 August 1969.

†The Johnson-Matheson vertical seismometer.

overall frequency response for the active seismic detection system is shown in Figure 13.

The wide dynamic range of the expected signals, the overall timing resolution desired, and telemetry bit-rate constraints suggested the desirability of some form of data compression prior to transmission to earth. The dynamic range of the linear system is nominally 80 decibels. The maximum bit rate available to the Active Seismic Experiment is 10.6K bits per second. With a minimum sampling frequency of 500 hertz, uniform sampling in time, and three channels of seismic data required, a maximum of only 5 bits per geophone-data subword would be available. In a linear digitization system, this would lead to unacceptably poor resolution at the very low signal levels expected from the distant grenade shots. Since signal levels are likely to be distributed throughout the dynamic range of the system, the compression scheme of choice was one that would give signal resolution as some constant fraction of signal amplitude. Logarithmic compression was selected because this is its principal characteristic.

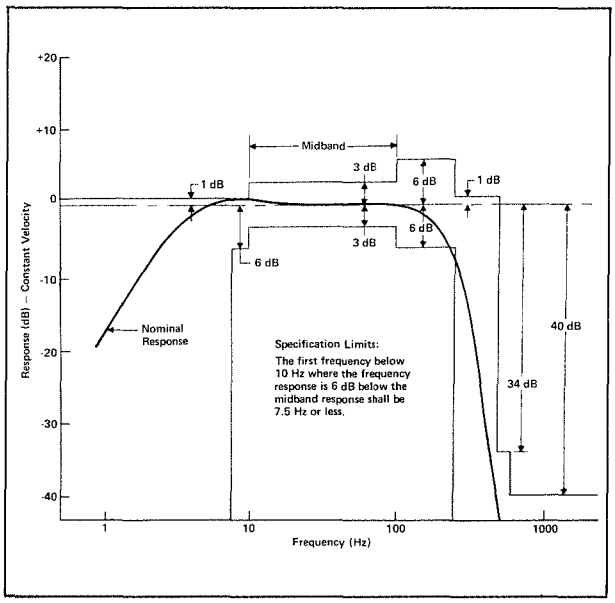

Figure 13 Active Seismic Detection System Nominal Frequency Response

The Charged-Particle Lunar Environment Experiment

A. D. ROBINSON
L. D. FERGUSON

The Charged-Particle Lunar Environment Experiment (CPLEE) deployed at Fra Mauro on 5 February 1971 by the Apollo 14 astronauts was one of the first experiments developed for investigating particles and fields on the lunar surface. The CPLEE monitors the flux of the electrons and protons that bombard the surface of the moon. Its design represented a considerable challenge from the standpoints of configuration, electronics, materials, and structural, thermal, manufacturing, and packaging considerations. This paper describes the particle spectrometer that was developed for the Apollo Lunar Surface Experiments Package (ALSEP) and details the constraints imposed on it by ALSEP mission conditions with respect to size, weight, power, outgassing, response to ultraviolet radiation, mechanical and thermal drift, signal-to-noise ratio, and measurement repeatability.

INTRODUCTION

The Charged-Particle Lunar Environment Experiment (CPLEE), deployed at Fra Mauro as a part of the Apollo 14 ALSEP system, was designed to measure electron and proton fluxes at the lunar surface resulting from solar wind, thermalized solar wind, cosmic rays from solar flares, and charged-particle clouds formed and trapped in the earth's magnetospheric tail. The characteristics measured include particle energies in the 40- to 70,000-electron-volt range, as well as angular distributions and time variations. The measurements are expected to provide information on a variety of particle phenomena to shed light on such matters as the origin of aurorae.

EXPERIMENT CONCEPT

The CPLEE, seen in Figure 1, is a remote particle-flux measurement system incorporating sensors and electronics in a deployable package. The package provides mechanical integrity during Apollo launch and protects the experiment subsystems on the lunar surface from the effects of solar radiation.

As shown in Figure 2, the experiment instrumentation includes two identical electron/proton energy analyzers,[1] one oriented vertical to the lunar surface and the other positioned to monitor particle fluxes from lunar east at an angle 60 degrees from vertical. Mounted below the analyzers are power supplies for the analyzers, pulse-counting circuitry for counting the electrons and protons at each of 18 energy levels over selected time intervals, and electronics for binary-encoding the flux data and for transferring them to the ALSEP telemetry system for transmission to earth.

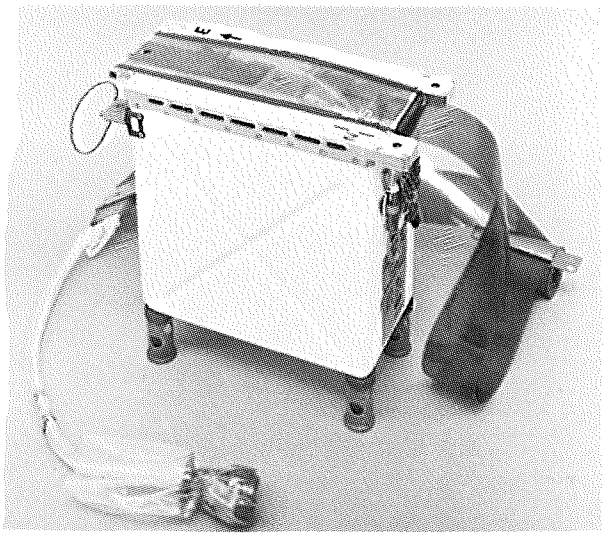

Figure 1 Flight Model of Charged-Particle Lunar Environment Experiment

Electrons and protons of all energies enter the analyzers through a three-aperture collimating slit system with a look angle of 4 degrees by 20 degrees (see Figure 3). The charged particles pass between a

---

The Charged-Particle Lunar Environment Experiment was conceived in 1965 by Principal Investigator Brian J. O'Brien, then associated with the Space Science Department at Rice University and now at the University of Sidney in Australia. The experiment is similar in concept and purpose to a series of experiments designed for satellite and rocket payloads to investigate causes and characteristics of auroral phenomena. The Co-Principal Investigator is David L. Reasoner of Rice University.

The Charged-Particle Lunar Environment Experiment was designed and fabricated at the Bendix Research Laboratories, Southfield, Michigan, under contract to Bendix Aerospace Systems Division, Ann Arbor, Michigan.

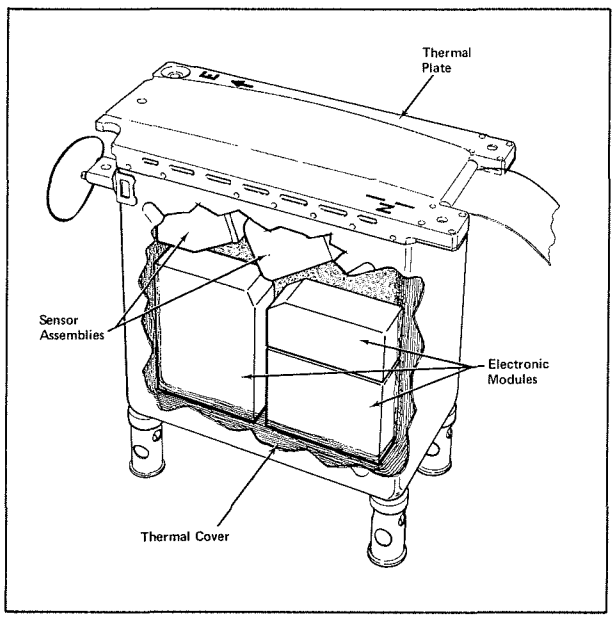

Figure 2 Charged-Particle Lunar Environment Experiment (Cutaway View)

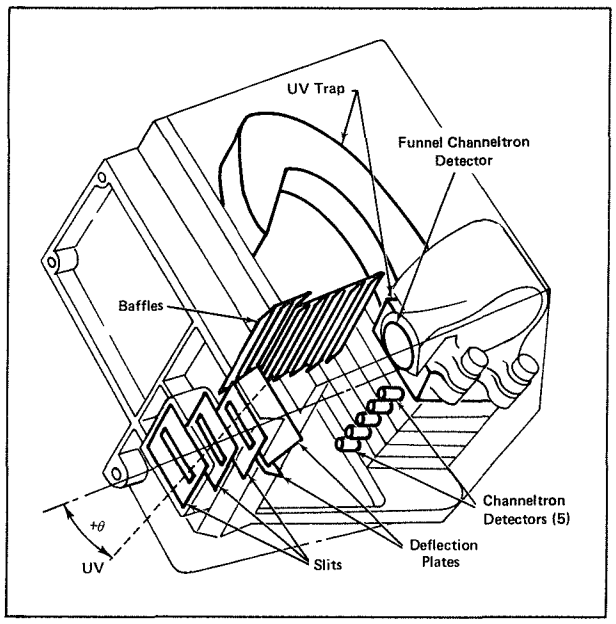

Figure 3 CPLEE Sensor Assembly

pair of electrostatic deflection plates and are dispersed, the amount of dispersion depending on particle energy, charge sign, and voltage on the deflection plates. Five Channeltrons® detect those particles that are dispersed below the sensor axis in five discrete energy bands; a single funnel Channeltron detects particles of opposite charge, which are dispersed above the axis in one broad energy band.

®Channeltron is the registered trademark of The Bendix Corporation.

Energy bands and deflection voltages are shown in Figure 4. With the lower deflection plate grounded and the upper plate stepped through eight voltage levels (three positive levels, zero, three negative levels, and back to zero), proton and electron energies are sorted into 18 different bands in the range between 40 and 70,000 electron volts. Sensors are calibrated and background measurements are made while the deflection plate is passing through the two zero-voltage levels in each complete energy-scanning cycle. With a deflection-plate dwell of approximately 2.4 seconds at each voltage level, and with the two analyzers alternately collecting data and reading out data into the ALSEP data handling and telemetry system, a complete analysis of electrons and protons occurs every 20 seconds.

To ensure the operational capability of the CPLEE in the extreme temperature environments of both lunar day and lunar night, careful attention was given to the structural/thermal design of the experiment. The temperature of the lunar surface rises to 250°F during lunar day and drops to -300°F during lunar night. The CPLEE detectors and electronics can operate safely over the temperature range -40°F to 160°F, dissipating 5 watts of power during operation; it was necessary, therefore, to balance such thermal processes as surface reflection and reradiation, insulation, and thermal conduction to maintain the required operating temperature range.

Solar radiation exhibits a strong vacuum-ultraviolet level, to which the Channeltron detectors react, giving rise to a substantial noise background. To reduce this background to an acceptable level, the analyzers were designed to shield the detectors from direct solar ultraviolet radiation and to substantially reduce the background from reflected ultraviolet radiation and ultraviolet photoelectrons.

The materials used in the CPLEE were selected for their low weight, their high structural stability, and their low outgassing rate in the vacuum radiation environment. Since the open-window Channeltron

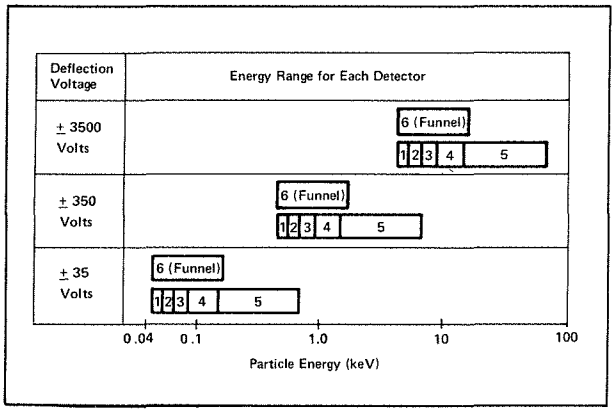

Figure 4 Sensor-Assembly Detector Passbands

detectors must operate in a vacuum below 10^{-5} Torr, materials with high outgassing rates could not be tolerated. Also enforcing this constraint was the fact that voltages of ±3500 volts and +3000 volts are applied to the deflection plates and Channeltron detectors, respectively; leakage currents at pressures above 10^{-5} Torr can contribute to background noise, and high current discharges could damage power supplies and detectors.

Very tight mechanical tolerances were imposed on the components of the analyzer assemblies by the need for a high degree of energy-band repeatability for individual detectors from one analyzer to another, with calibration limited to prelaunch exercising of the experiment.

DESIGN REQUIREMENTS

The primary design requirements for each sensor assembly are detailed in Table I. ALSEP system requirements limited maximum operating power for the instrument to 3.0 watts (plus 3.5 watts for active thermal control), and Apollo mission requirements limited its weight to 6.0 pounds. Thermal design requirements for deployment on the lunar surface also imposed severe constraints on instrument design, which had to minimize the loss of internal heat under lunar-night conditions and at the same time provide for efficient dissipation of electrically generated heat and for reflection of solar radiation during lunar day.

Table I Sensor Assembly Design Requirements

Parameter	Requirement
Field of View	4 degrees by 20 degrees.
Particle Energy Range	40 electron volts to 70 kiloelectron volts.
Maximum Detectable Flux	
C-Type Channeltron	10^{10} particles per square centimeter per second per steradian.
Funnel-Type Channeltron	8×10^{8} particles per square centimeter per second per steradian.
Minimum Detectable Flux	
C-Type Channeltron	10^{5} particles per square centimeter per second per steradian.
Funnel-Type Channeltron	8×10^{3} particles per square centimeter per second per steradian.
Count Rate	400,000 particles per second, with a pulse-pair resolution of 1 microsecond.
Cross Talk between Channels	Not more than 10 counts per second (with detector aperture covered) when adjacent channel is counting 500,000 parts per second.
Ultraviolet Rejection	10 counts in any channel when entrance aperture is irradiated with 5.1 ergs of ultraviolet radiation at 1216 angstroms.

EXPERIMENT DESCRIPTION

The Detectors

The Channeltron electron multiplier is the basic detector element in the CPLEE. The C-type detector is seen in Figure 5, and the funnel type is shown in Figure 6. These detectors are sensitive to both protons and electrons over the energy range required for the experiment; they operate at a counting rate of up to 1 megahertz.

The detector is a glass capillary tube having an inside diameter of about 1 millimeter and a length of 10 centimeters. A layer of special conducting material that has secondary-electron-emission characteristics is deposited over the interior surface of the tube. When a potential difference is applied between the ends of the tube, an electric field is established down its

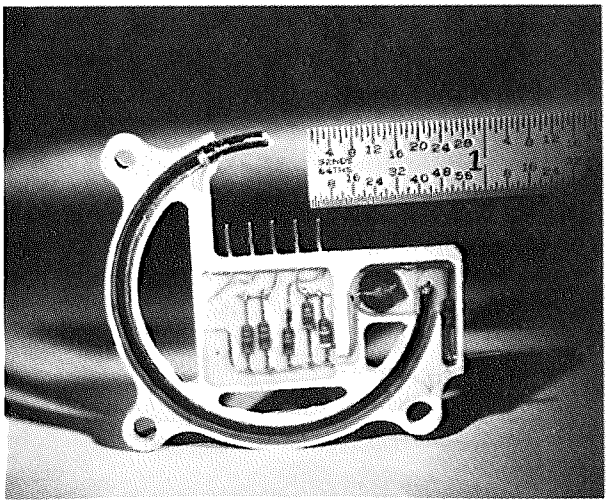

Figure 5 C-Type Channeltron Detector

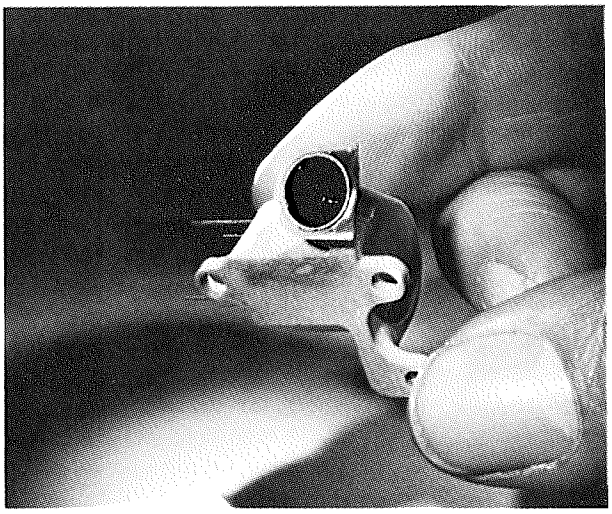

Figure 6 Funnel-Type Channeltron Detector

length. Any electron ejected from the inside surface by photoelectric or secondary emission is accelerated down the tube and simultaneously drifts across the tube with whatever lateral velocity is acquired in the ejection process. Electron multiplication occurs when the potential difference is such that these free electrons gain enough energy from the electric field between encounters with the surface to generate more than one secondary electron at each encounter. A single electron ejected at the low-potential end of the detector can result in an electron gain of about 10^8 at the high-potential end.

Figure 7 illustrates the typical electron-gain characteristics of a Channeltron detector. Note that the knee of the gain curve occurs at about 2700 volts. Between this knee and the saturation region, the amplitude and shape of the output pulses tend to be uniform and independent of the type or energy level of the radiation. Detector efficiency, however, does depend on particle energy level and on type of radiation.

Since the detector is sensitive to electrons, protons, X rays, and ultraviolet radiation, the output pulses from the detector contain no information concerning the type or energy of the primary radiation. The sensor assembly must therefore include some means of particle discrimination so that only particles of one polarity and one energy interval reach a given detector during any one measurement interval. This discrimination function is provided by the deflection plates, in conjunction with the six detector locations.

The Sensor Assembly

As was shown in Figure 3, each physical analyzer consists of a set of entrance slits, deflection plates, six detectors, an ultraviolet trap, and side-wall baffles; not shown in Figure 3 but also present are upper and lower secondary-electron particle stops, mounted on a magnesium frame. A lightweight cover encloses the sensor assembly.

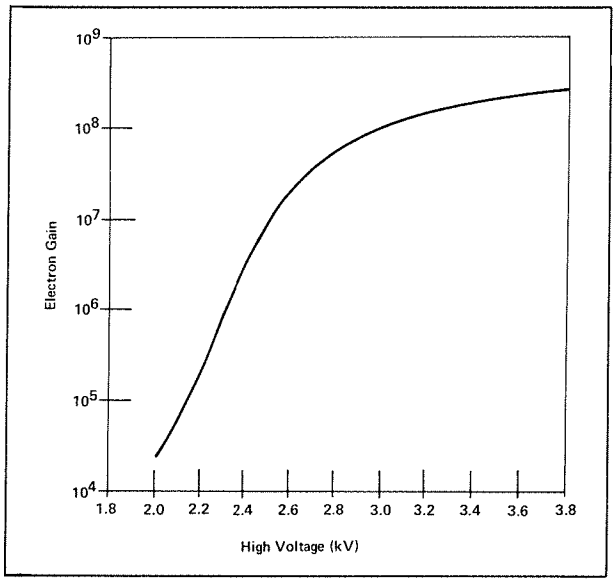

Figure 7 Channeltron Electron-Gain Characteristics

The three entrance slits confine the analyzer look angle to 4 degrees by 20 degrees, defined from a point on the analyzer axis between the funnel Channeltron and the closest C-type Channeltron. The deflection plates are deliberately tilted relative to the axis to permit the charged particles to be dispersed within a short distance (1.5 inches) without striking the plates. The six detectors are arranged about the axis to provide narrow- and wide-band coverage of the energy spectrum between 40 electron volts and 70 kiloelectron volts. The C-type detectors with preamplifiers are potted in metal/ceramic supramica holders 1/8 inch thick. The funnel detector and ultraviolet trap are fabricated to close mechanical tolerances and carefully stacked together in the analyzer frame to provide repeatability.

The on-axis ultraviolet trap and side-wall baffles were added to suppress the ultraviolet background noise. Secondary electrons resulting from the incoming low-energy electrons and protons impacting the walls of the analyzer are collected by the upper and lower particle stops before they reach the detectors.

Experiment Operation

The CPLEE simplified block diagram in Figure 8 illustrates experiment operation for one physical analyzer. Seen in the basic functional blocks are the sensor assembly, the Channeltron power supply, the deflection-plate power supply, the low-voltage power supply, the programmer, and the signal-processing electronics. The pulse output of each Channeltron detector is fed to a separate amplifier, and the pulses from each amplifier are gated to a counter. The high-energy and funnel detectors (detectors 5 and 6) have 20-bit counters; detectors 1 through 4 have 19-bit counters. The output from each counter is transferred to a shift register upon command of the programmer, and the count data from the shift registers are read out as serial digital data by the ALSEP telemetry system.

The operation of the charged-particle experiment as a whole is outlined in Figure 9. Notice that two physical analyzers must time-share the counting electronics, and a multiplexer consisting of twelve input gates is used to read in data. The time multiplexing operates as follows: The pulses from one sensor assembly are gated to the counters for one deflection-voltage level. Upon receipt of an even frame mark, the programmer directs the deflection-plate power supply to its next level, and couples the second

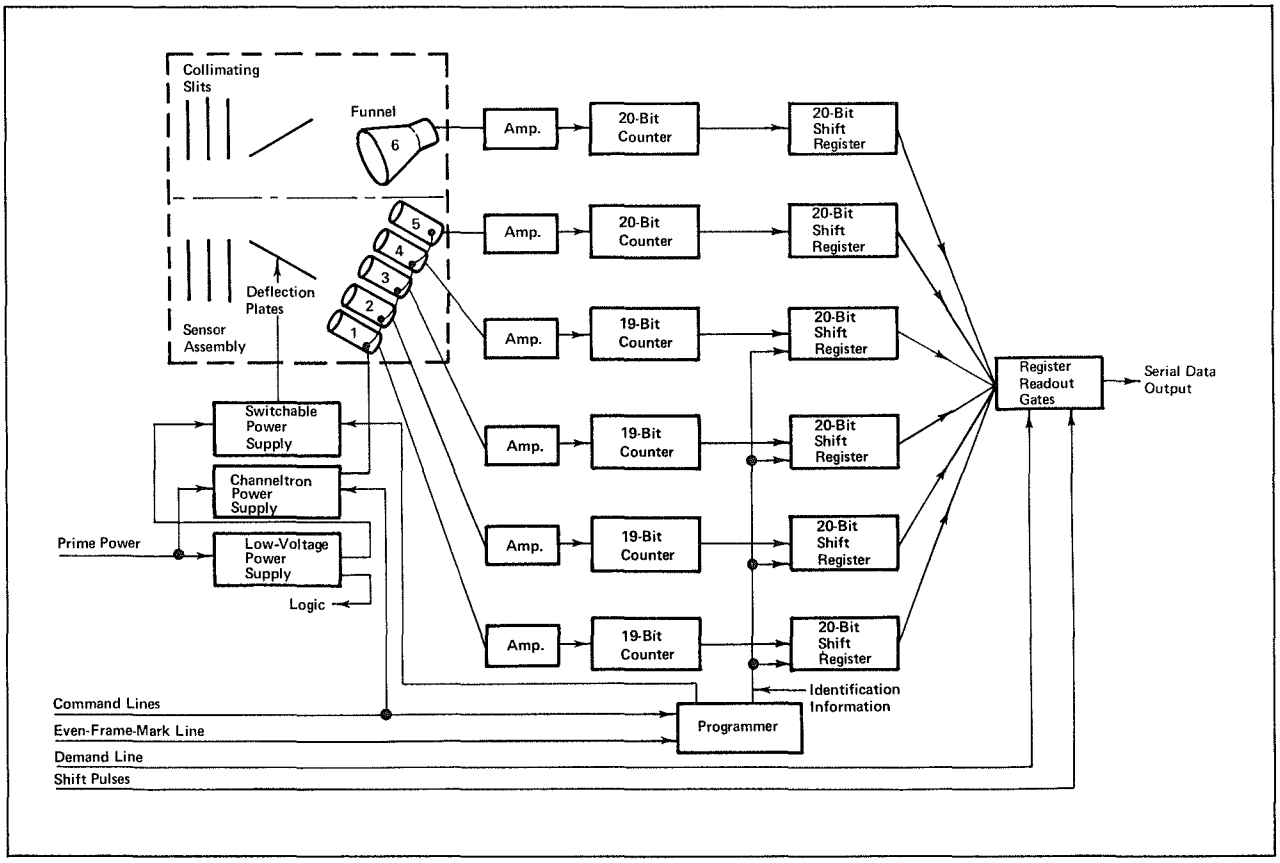

Figure 8 Single-Analyzer Operation in Charged-Particle Experiment

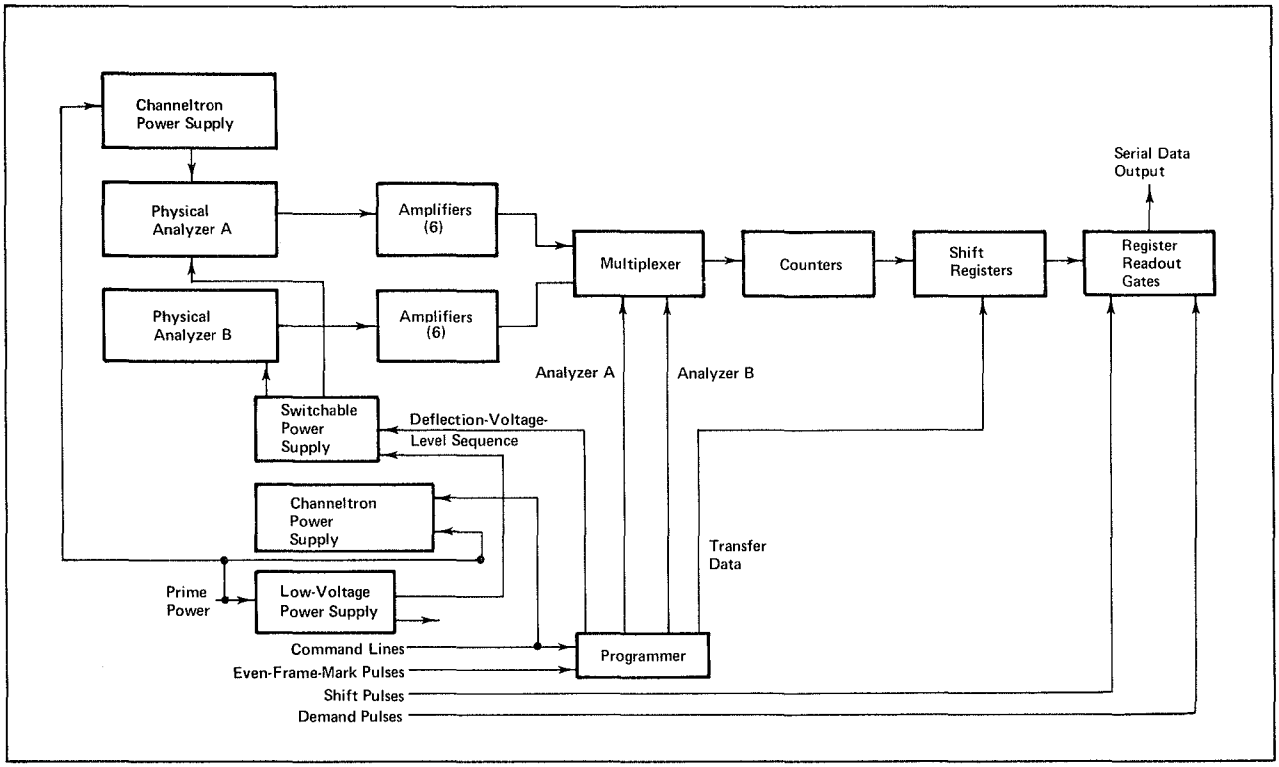

Figure 9 Full-System Operation of Charged-Particle Experiment

sensor assembly into the counters. At the same instant, the counter inputs are inhibited so that no more counts can be accumulated, and the transfer gates are enabled so that the counter contents are transferred to six 20-bit shift registers. After a suitable time delay to allow the power supply to reach its steady-state level, the counters are preset to the zero condition, and the inhibit pulse is removed. The counters then collect information from the second physical analyzer. The count data in each shift register are read out by the ALSEP telemetry system upon receipt of the demand pulse from the Central Station.

Figure 10 describes the timing sequence that is used in the automatic switching of deflection-plate voltage. Each ALSEP telemetry frame requires 0.604 second, so that the even frame marks occur every 1.2 seconds. The interval between even frame marks is the basic measurement time interval for the experiment. For purposes of illustration, let us assume that experiment operation starts with the application of +3500 volts to the deflection plates.* Analyzer A measures the charged-particle flux for a period of 1.21 seconds. Then analyzer B measures the radiation incident on it for 1.21 seconds, and during this time the measurement made by analyzer A is read out by the ALSEP telemetry system. Now the deflection voltage is automatically switched to +350 volts, and the measurement sequence is repeated. Since the total measurement period for the two sensor assemblies is 2.42 seconds at each deflection voltage, and since measurements are made at eight deflection-voltage levels, a complete operational sequence requires 19.4 seconds.

Performance Verification

Two features incorporated into the design of the charged-particle experiment serve to verify instrument performance.

During the negative zero-voltage period in the automatic switching sequence, a test oscillator checks the performance of all preamplifiers, amplifiers, counters, and shift registers. The output of the oscillator is fed to all twelve detector preamplifiers in parallel. Since the oscillator has a frequency of about 350,000 counts per second, it provides enough pulses to fill the last stage of each counter.

Performance can also be verified by means of two 5-millicurrie nickel-63 beta sources located in the experiment dust cover. The two sources are positioned in front of the entrance apertures of the two sensor assemblies, and an analysis of instrument response provides a rapid but thorough evaluation of overall instrument performance. A typical detector

*The timing sequence may start at any point when the experiment is turned on.

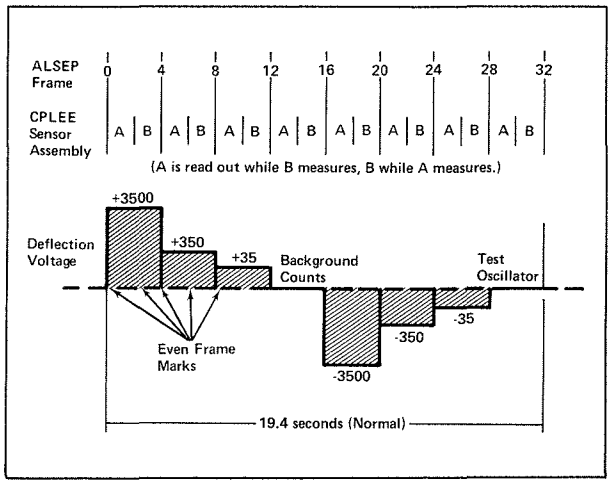

Figure 10 Time Sequence for Deflection-Plate Voltage Switching

count pattern for one complete cycle of operation is presented in Table II. The beta-source test is used to verify that there has been no change in the performance of the instrument subsequent to its calibration. The test can be performed at any time prior to removal of the dust cover from the experiment.

Commands from Earth

The charged-particle experiment is designed to respond to eight commands which can be transmitted to it by Mission Control at MSC through the ALSEP Central Station via the Manned Space Flight Network.

Only one of the eight commands – that providing for dust cover removal – is essential to the operation of the experiment. The dust cover, which serves to

Table II Typical Full-Cycle Detector Response to Nickel-63 Beta Source

Deflection Voltage, number of volts	Count per Detector					
	1	2	3	4	5	6
−3500	8	22	37	52	155	10
−350	1	0	2	5	37	31
−35	1	2	1	2	4	32
−0 (test oscillator)	350,936	350,936	350,936	350,936	350,936	350,936
+3500	0	3	0	0	0	989
+350	2	1	0	2	1	145
+35	0	0	0	2	0	28
+0 (background)	2	1	0	0	1	33

protect the Channeltron detectors and the thermal-plate surface from dust generated by the ascent of the Lunar Module, is a thin sheet of Mylar and H-film (Kapton), molded with two steel negator springs. The cover is held in place with monofilament nylon line, which is cut by two Atlas reefing line-cutters when the removal command is transmitted. The dust cover then coils up and rolls over one end of the thermal plate, carrying the beta-test sources with it. Once the cover is removed, experiment operation is automatic. A timer in the ALSEP Central Station provides a backup cover-removal command in case of uplink failure.

As previously described, the experiment normally operates in the automatic-switching mode, with the deflection-plate voltage switched through eight voltage levels every 20 seconds. For a situation in which it is desirable to study a particular range of particle energies with greater temporal resolution (2.4 seconds), however, a command from earth will stop automatic switching. Another command then permits the deflection voltage to be manually stepped to the range of interest. After the measurements at that voltage have been completed, still another command is sent to return the experiment to the automatic-sequencing mode.

Two commands are used to override the thermostat in the active thermal control system. The first of these turns on the operational heaters. To return to automatic thermal control, a standby command is transmitted, followed by a second command to turn on operating power.

Two commands provide the capability of increasing Channeltron operating voltage from 2800 to 3200 volts and then decreasing it again from 3200 to 2800 volts. The voltage increase would be necessary should the electron-gain characteristics of the Channeltrons degrade during the life of the experiment.

EXPERIMENT ENGINEERING AND DESIGN

The Sensor Assembly

The constraints imposed on CPLEE instrument design by ALSEP mission conditions and the extremes of the lunar environment proved highly challenging to design engineers. Materials and configurations for the experiment subassemblies – including the two sensor assemblies – had to be so selected as to eliminate unnecessary weight, power, and volume, while at the same time meeting requirements for structural integrity, mechanical tolerances, and optical, electrical, thermal, and vacuum characteristics.

The weight of the sensor assemblies was kept at a minimum by fabricating the analyzer frame and cover from magnesium. All unnecessary material was removed from the frame, leaving a web pattern to provide the required structural rigidity. The covers were formed from 0.010-inch sheet magnesium, and the assemblies were gold-plated to prevent corrosion. For the most part, mechanical tolerances were held tightly to better than 0.001 inch to ensure the accurate alignment of the three aperture slits, the deflection plates, and the Channeltron detectors, and, in turn, to ensure repeatable energy passbands and ultraviolet noise rejection.

Each of the six Channeltron detectors is mounted in a thin synthetic-mica holder, which also contains a preamplifier. Again, excess material was removed to keep weight at a minimum. The mica, which has excellent outgassing characteristics and optical-radiation-resistance properties, provides a rigid, thermally stable mount for the detectors and isolates the high-voltage components. The individual detector packages are separated by thin stainless steel shims, grounded electrically to prevent detector cross talk.

The most critical factor affecting analyzer design was the ultraviolet-rejection requirement.[2] A goal of less than 10 noise counts per second in each channel was established for an ultraviolet flux of 5.1 ergs per square centimeter per second of hydrogen Lyman-Alpha (1216 angstroms) incident on the entrance slits. The design task was difficult for several reasons. The large flux is roughly equivalent to 10^9 photons per second passing through a surface area of 0.01 square centimeter, the active area of the Channeltron detector. This flux, coupled with a pulse yield (electron pulses out per photon in) at 1216 angstroms of about 2 percent, could result in a noise count rate greater by a factor of 10^6 than the 10-count-per-second goal. Even though the six detectors in each analyzer are hidden from direct view through the entrance slits, most surfaces are highly reflective in the extreme-ultraviolet region, and a significant number of scattered ultraviolet photons can reach the detectors in a few bounces. Under these circumstances, the near-axis detectors would receive several thousand counts per second except for the preventive measures that have been taken.

Figures 11(a) and 11(b) show top and side cutaway views, respectively, of the sensor assembly. Note the locations of the side light-capturing baffles, the on-axis ultraviolet trap, the charged-particle deflection plates, and the three entrance slits. The ultraviolet response of detectors 1, 4, and 5 in the absence of side-wall traps, careful alignment and treatment of deflection plates, and razor-blade slits (configuration A) is plotted in Figure 12(a). The incidence angle θ is parallel to the plane of the long slit dimension. The incident photon flux is 8.8 ergs per square centimeter per second at 1236 angstroms, which is roughly

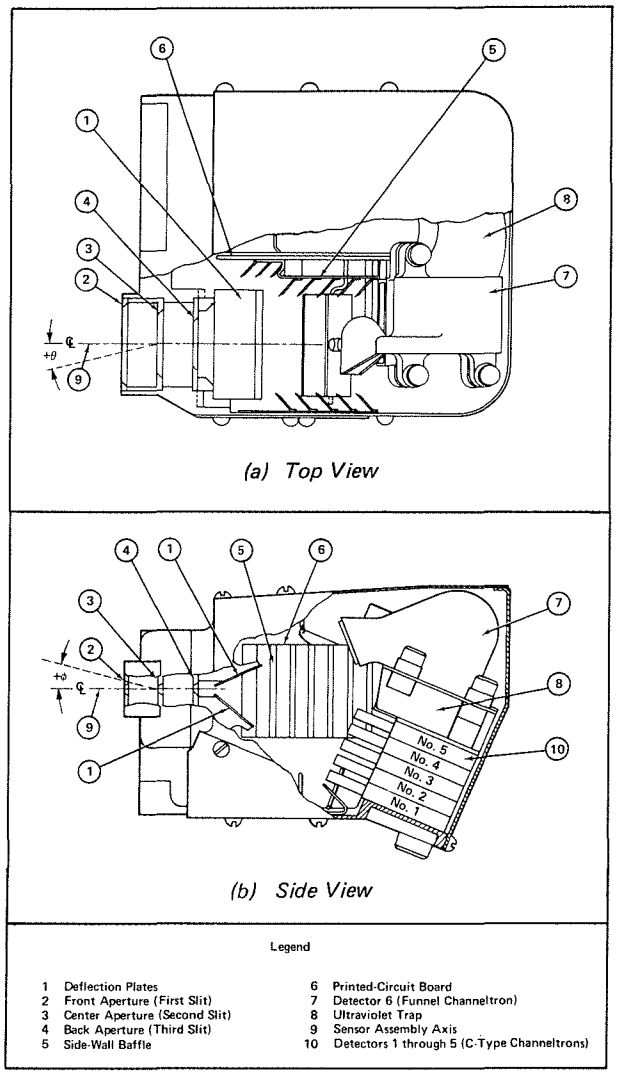

Figure 11 Sensor Assembly

equivalent to 5.1 ergs per square centimeter per second of hydrogen Lyman-Alpha at 1216 angstroms in its generation of background-noise count rate. Under these conditions, all the detectors display noise levels well in excess of 10^3 counts per second. The ultraviolet response of detectors 1, 4, and 5 after installation of side baffles with tilted razor blades, introduction of razor-blade slits with reduced reflection characteristics, and careful alignment of the deflection plates, vapor-blasted to produce diffuse optical reflections (configuration B), is shown in Figure 12(b). The corresponding response for an ultraviolet flux swept at an angle ϕ in the plane of the narrow slit dimension is shown in Figure 12(c). In the latter configuration, detectors 1 and 4 display acceptable noise levels. Although detector 5 displays a high noise count for a zero-degree incident ultraviolet flux, its response clearly indicates the importance of preventing ultraviolet reflections from the side walls. The high count at zero degrees is believed to be the result of reflections from the sharp entrance slits and of the fact that detector 5 is only a few thousandths of an inch removed from direct excitation by the ultraviolet beam.

The optical characteristics of the slit, baffle, deflection-plate, and ultraviolet-trap surfaces were individually tailored to reduce the ultraviolet noise background. To trap and absorb ultraviolet photons that strike the upstream sides of the two innermost entrance slits, the inner walls of the two chambers formed by the three slits were coated with a mixture of PC-15 urethane epoxy and carbon black, which gave the lowest reflectivity (highest absorptivity) of any surface coating studied. Ultraviolet radiation that passes through the entrance-slit openings can strike either of the side-wall baffles, enter the ultraviolet trap, or pass between the outer side-wall baffle and the detectors. The clean, specularly reflective surfaces of the side-wall-baffle razor blades trap the ultraviolet photons through multiple bounces between the blades and the mounting surface. Photons entering the crescent-shaped ultraviolet trap bounce from the gold-plated reflecting walls near the trap entrance and proceed further into the trap where they are absorbed.

Although the edges of the razor blades and the ultraviolet trap are sharp, so as to prevent back reflections toward the entrance slits, some reflection does occur from these edges and from the detector mountings and the detector-package cover. To prevent the back-scattered ultraviolet radiation from entering the detectors by specular reflection from the deflection plates, the plates are vapor-blasted with fine glass beads to produce a diffuse surface. Ultraviolet radiation striking this surface is scattered in all directions; thus the number of photons scattered in the direction of the detectors is reduced. Secondary photoelectrons are generated where photons impact baffle, deflection-plate, trap, and entrance-slit surfaces. These electrons leave the surfaces with energies of the order of 10 electron volts and represent a source of detector noise. To minimize this source of noise, the detectors are elevated to a bias level of - 16 volts and the side-wall baffles are placed at a +35-volt level relative to the sensor-assembly support structure and covers. The electric field thus produced provides a barrier against photoelectrons.

Mechanical/Thermal Design

Mechanically, the CPLEE consists of a thermal plate, a main frame which supports the electronics subassemblies, and a thermal cover.

The thermal plate, seen at the top in Figure 2, is the member through which the experiment is

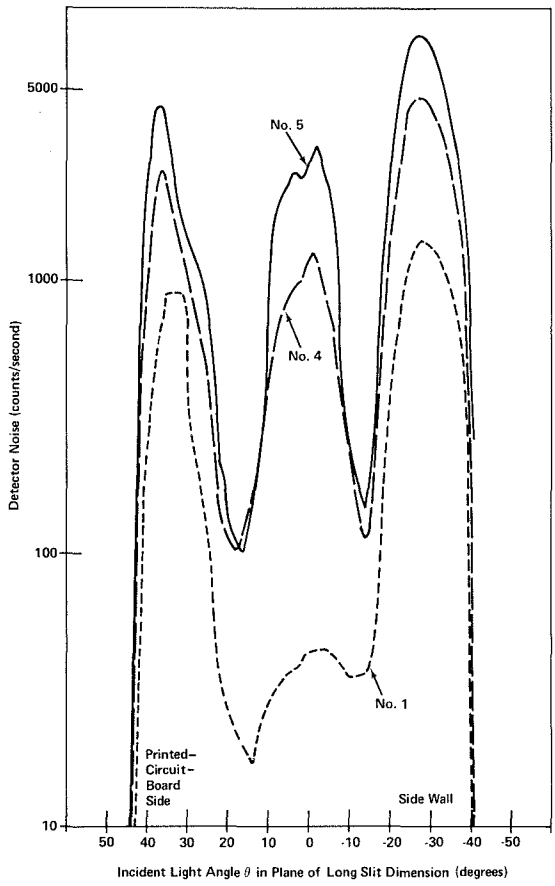

(a) Configuration A with Light Incident to Long Slit Dimension

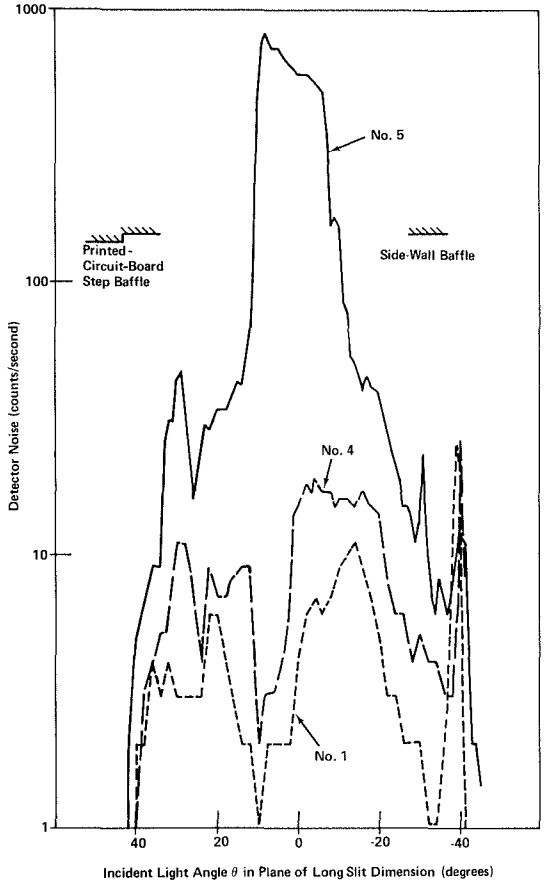

(b) Configuration B with Light Incident to Long Slit Dimension

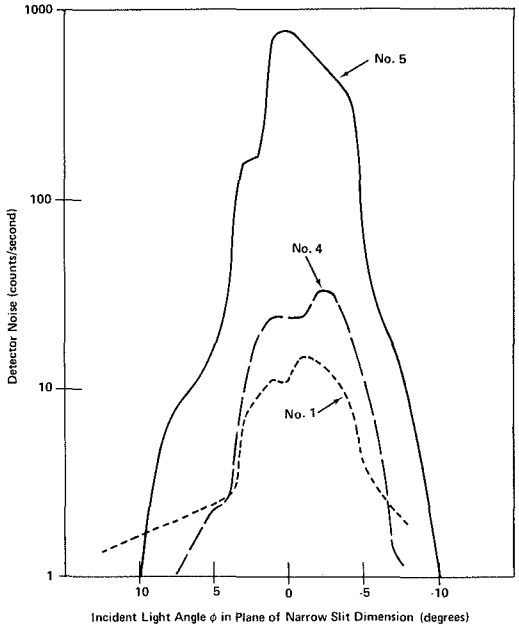

(c) Configuration B with Light Incident to Narrow Slit Dimension

Figure 12 Detector Response to Ultraviolet Radiation

mounted to the ALSEP Central Station. It forms a rigid box structure for the support of all the internal components and also acts as a heat sink, radiating into space the excess heat generated by the electronics. A center strip that runs the entire length of the top is gold-plated, as are the edges; the side areas are painted with a thermal coating. As a consequence, excess heat is radiated in the day-operating mode and heat loss is kept at an acceptable level under night conditions. Although the lunar surface temperature varies from -300°F during lunar night to +250°F at lunar noon, the interior electronics are kept at a temperature ranging from -40°F to +160°F. Low-power electric heaters maintain the interior temperature during lunar night.

The internal electronics are mounted to the main frame of the experiment, which also acts as a thermal stabilizer by providing a path for the conduction of excess heat to the thermal radiator. Fabricated from formed sheets of aluminum with flanges at the joint areas, the frame was designed for compactness, light weight, and high thermal conductivity. A dip-brazing process was used to fuse the joints, the result being essentially a one-piece structure with maximum thermal conductivity and joint strength. The frame panels, made of aluminum alloy 6061, were formed in an annealed condition and heat-treated to a T-6 condition. The complete frame was gold-plated prior to component assembly.

All external surfaces of the CPLEE are kept within the operating temperature range by passive thermal control. The experiment is encased on four sides and the bottom by a thermal cover made of low-thermal-conductivity fiberglass material and painted with a thermal-control coating. Between the fiberglass cover and the interior electronics package is a blanket of superinsulation composed of alternate layers of aluminized Mylar and dexiglas insulation; the result is very low thermal conductivity and minimum heat flow into and out of the electronics. The experiment is supported on four fixed fiberglass legs, which minimize heat flow between the experiment and the lunar surface.

Stowing and Deployment

Unlike any of the other ALSEP experiments, the CPLEE was designed to be stowed on the ALSEP sunshield, inverted with respect to its deployed configuration. This approach minimizes the structure weight required for mechanical support of the sensor assemblies. Because the Channeltron electron multipliers in the two sensor assemblies are the components most susceptible to damage due to shock and vibration, these assemblies are mounted directly to the thermal plate, which in turn is hard-mounted to the sunshield. In this configuration, a minimum of vibrational energy is transmitted to the sensor assembly from the ALSEP Central Station during launch.

The original deployment plan called for the astronaut to lift the CPLEE off the sunshield by grasping its support legs. The astronaut life-support system makes it impossible, however, for the astronaut to reach heights lower than 14 inches from the lunar surface; deployment via the support legs was therefore not feasible. Rather, the universal handling tool (UHT), which is 26 inches long, is used to lift the experiment from the sunshield and lower it to the surface.

Use of the universal handling tool introduced an interesting deployment problem. A tool socket along the bottom side of the experiment would make it easily removable from the sunshield with the UHT, but subsequent deployment, leveling, and alignment would then require that the UHT be withdrawn from the bottom socket and reinserted in a socket in the experiment top side. His life-support system does not allow the astronaut sufficient reach to install the tool by holding it in one hand and the experiment in the other; a trigger on the tool must be depressed to insert it into a socket, and the astronaut would be unable to "choke down" on the tool. The dilemma was resolved by designing a UHT socket for the CPLEE that could rotate 180 degrees, making it unnecessary to disengage and reinsert the tool to complete experiment deployment.

EXPERIMENT CALIBRATION

In speaking of particle fluxes,* one must distinguish between unidirectional fluxes, in which all the particles have the same direction of travel, and distributed fluxes, in which particles may arrive over a range of directions. Unidirectional fluxes are measured in particles per square centimeter per second – that is, the number of particles passing through a unit area normal to the beam direction per unit time. Distributed fluxes, on the other hand, are measured in particles per square centimeter per second per steradian – that is, the number of particles passing through a unit area per unit time whose arrival directions fall within a 1-steradian solid-angle cone.

The salient characteristics of a detection-system geometry are contained in the *geometric factor*, a quantity expressing the relationship between an incident particle flux and the number of particles per second striking the detector. For distributed fluxes,

*Much of the experiment calibration description in this section is taken from previously unpublished material supplied to the authors by David L. Reasoner, Rice University.

$$N = GF_o \cdot J \tag{1}$$

where N is the number of particles per second striking the detector, GF_o is the omnidirectional geometric factor, and J is the omnidirectional particle flux. Similarly, for unidirectional fluxes,

$$N = GF_u \cdot F \tag{2}$$

where GF_u is the unidirectional geometric factor and F is the unidirectional particle flux.

Dimensional analysis shows that GF_o is in units of area times solid angle, whereas GF_u is in units of area. Indeed, we can write

$$GF_o = A \cdot \Omega \tag{3}$$

and

$$GF_u = A \tag{4}$$

where A is the effective collection area of the detection system and Ω is the solid-angle response of the system. In other words, Ω expresses how large a cone the detector "sees"; thus, for a detection system sensitive to particles with arrival directions over an entire hemisphere, Ω is equal to 2π steradians.

Output response R is related to N, the number of particles striking the detector per second, by an equation of the form

$$R = K(N) \cdot N \tag{5}$$

It should be emphasized that K is, in general, a function of N; hence, overall system response may not be a linear function of the magnitude of the incident particle flux. The equations for overall system response thus become

$$R = K(N) \cdot GF_o \cdot J \tag{6}$$

$$R = K(N) \cdot GF_u \cdot F \tag{7}$$

or

$$R = K(N) \cdot A \cdot \Omega \cdot J \tag{8}$$

$$R = K(N) \cdot A \cdot F \tag{9}$$

The task of calibrating a detection system is that of determining the quantities A, Ω, and $K(N)$, either separately or in combination. An additional complication introduced in the case of the CPLEE arises from the fact that CPLEE responses are functions of particle energy; indeed, the response equations for this experiment should more properly be written

$$R(E) = K(N,E) \cdot A(E) \cdot \Omega(E) \cdot J(E) \tag{10}$$

$$R(E) = K(N,E) \cdot A(E) \cdot F(E) \tag{11}$$

The system used to calibrate the CPLEE, shown diagrammatically in Figure 13, consisted of a large vacuum chamber, an electron gun, a movable mounting fixture, an SDS-92 computer which runs the calibration automatically and collects the data, and the circuitry required to control the instrument and to interface the instrument and system with the computer. The electron gun was capable of producing a uniform, unidirectional electron beam of any energy between 30 and 30,000 electron volts. Beam intensity was measured with a Faraday cup that could be placed between the beam and the instrument. The CPLEE mounting fixture was capable of tilting the instrument in two orthogonal directions relative to the beam; the angular position of the fixture was varied by means of stepping motors and was read by a.c. synchro resolvers.

The entire system was controlled by the SDS-92 computer. Computer instructions were encoded to provide for such functions as positioning the mounting fixture at a desired angle, moving the Faraday cup into the beam and reading the cup current, reading various analog voltages with a DVM-multiplexer system, and interrogating the CPLEE to read out the accumulators. The calibration data were recorded on magnetic tape for later analysis.

Complete angular instrument response was measured for electrons of a particular energy by tilting the instrument with respect to the beam. The angular response grid was ±15 degrees in the long axis with 1-degree steps and ±10 degrees in the short axis with 0.5-degree steps. The data from one such response scan were used to calculate the quantities Ω and $K(N) \cdot A$ and thus to determine the values of GF_o and

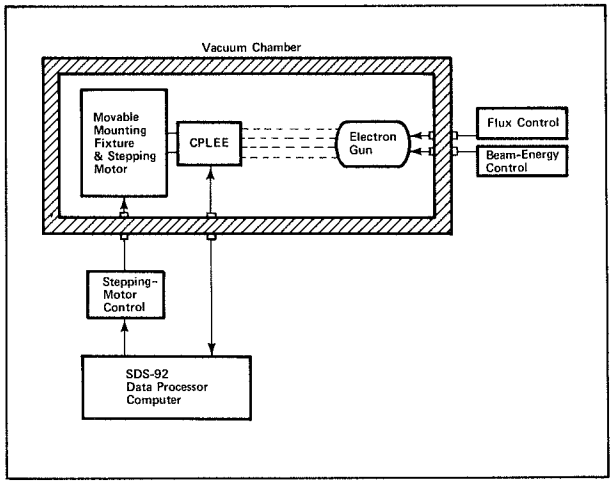

Figure 13 CPLEE Calibration System

GF_u for that particular electron energy. By repeating the sequence for a number of beam energies, it became possible to plot a curve of $GF_o(E)$ versus E for a particular channel at a particular deflection voltage; this curve was the energy passband of the channel. Ten beam energies were used to define each passband; thus measurements were made on a total of 360 energy values.* Since the angular grid stepped through at each of these energies represented 1271 individual data points, complete calibration of the CPLEE instrument required approximately 500,000 separate measurements. From these data, the required geometric factors were calculated, along with such other vital information as cross-channel rejection and electron-scattering contamination.

The curve that results from plotting $GF_o(E) \cdot K(E)$ versus E is, in effect, a plot of the energy passband of a particular channel at a given deflection voltage for a particular type of particle. Typical of the 72 such curves generated for each CPLEE instrument (6 channels x 6 deflection voltages x 2 analyzers) are those shown in Figure 14, which represent the passbands of channels 1 through 5 for electrons at a deflection voltage of -350 volts.

Calibration data on three flight models verified excellent reproducibility between instruments. Such parameters as center energy location and passband width vary by no more than 10 percent. The parameter relating flux to counting rate [the product of $GF_o(E)$ and $K(E)$] may vary by as much as 200 percent, but this is to be expected since the quantity $K(E)$ is a function of individual Channeltron characteristics. Channeltron efficiencies, and hence the absolute geometric factors, appear to be stable to within ±20 percent over periods of months.

*Based on 10 energies per deflection voltage, 3 deflection voltages per channel, 6 channels per analyzer, and 2 analyzers per system.

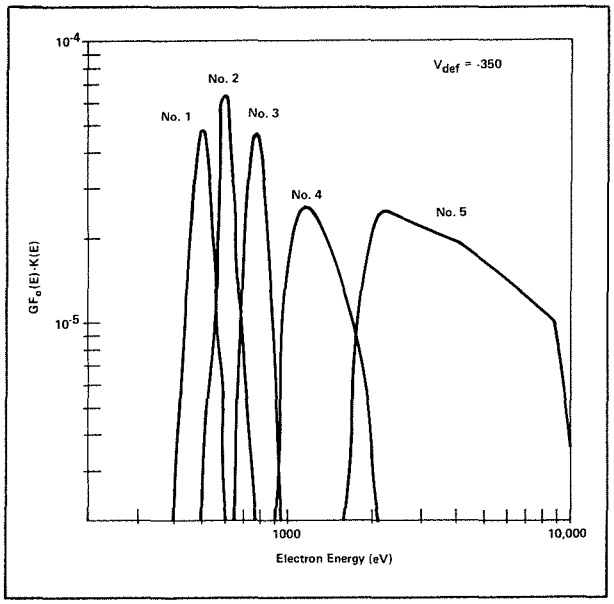

Figure 14 Typical Experiment-Calibration Passband Curves

REFERENCES

1. B. J. O'Brien et al., "SPECS, A Versatile Space-Qualified Detector of Charged Particles," *Review of Scientific Instruments* 38, 1058 (August 1967).

2. L. D. Ferguson, M. C. Johnson, J. L. Pfeifer, and W. G. Wolber, "Techniques for Suppressing Anomalous Response to Vacuum Ultraviolet Radiation in the Charged-Particle Lunar Environment Experiment," *Bendix Technical Journal* 1 (No. 1), 89 (Spring 1968).

SYMBOLS

A	effective collection area of detection system
E	electron energy
F	unidirectional particle flux
GF_o	omnidirectional geometric factor
GF_u	unidirectional geometric factor
J	omnidirectional particle flux
$K(E)$	detector response as a function of E
$K(N)$	detector response as a function of N
N	number of particles striking detector per second
R	detection-system output response
θ	angle of incidence in plane of long entrance-slit dimension relative to centerline
ϕ	angle of incidence in plane of narrow entrance-slit dimension relative to centerline
Ω	solid-angle system response

The Lunar Heat Flow Experiment

B. D. SMITH

A heat-flow instrument was included in the Apollo Lunar Surface Experiments Package (ALSEP) flown on the Apollo 15 mission, and similar instruments will be placed on the lunar surface during Apollo missions 16 and 17, to implement the study of heat flow from the moon through temperature and conductivity measurements in the moon's subsurface. Ambient temperatures and temperature gradients are measured electrically on platinum resistance-bridge sensors mounted in two probes. Thermal conductivity is determined by energizing heaters in the probes and measuring the temperature response of the sensors, which is a function of the conductivity of the surrounding lunar soil. This paper describes the construction and operation of the instrument and the techniques that have been developed to achieve the required measurement precision.

INTRODUCTION

The flow of heat from the lunar surface, and the associated subsurface temperature fields, have evolved from the conditions that existed when the moon was formed, under the influence of accumulated thermal and structural developments, including those deep in the interior. A knowledge of the present level of surface heat flow may therefore place some important limits on the range of feasible lunar models. To determine this level, an instrument capable of making lunar subsurface measurements from which local heat flow can be derived was carried to the moon on the Apollo 15 mission, and similar instruments will be carried on Apollo missions 16 and 17.

EXPERIMENT THEORY

The heat-flow instrument performs measurements to determine the mean vertical temperature gradient dT/dz and the effective thermal conductivity k of the material across which the measured gradient is developed. Conducted heat flow J diffuses down a temperature gradient in accord with the relationship between these two quantities in one dimension,

$$J = -k(dT/dz) \qquad (1)$$

Table I Predicted Experiment Ranges

Temperature Gradient dT/dz, °K/meter	Heat Flow J, watts/square meter	Thermal Conductivity k, watts/meter°K
0.1	4.2×10^{-3}	42×10^{-3}
12	25×10^{-3}	2.1×10^{-3}

Table I lists ranges of predicted density of heat-flow rates and soil thermal conductivities,[1,2,3] with the corresponding limits of average temperature gradients.

The average absolute temperature at any point in the subsurface (regolith) results from the balance between the solar heat influx and the total heat outflow acting through the regolith. Solar radiation power incident at the lunar surface varies from 1.45 kilowatts per square meter at one extreme to zero at the other. Resultant moon surface temperatures vary from approximately 400°K at lunar noon to 100°K at lunar night, with an annual modulation of about 8°K caused by the elliptical orbit of the moon around the sun. The attenuations and phase shifts of these periodic variations as they propagate into the moon are determined by the diffusivity of the regolith materials. Nonperiodic variations will also occur, the result of changes in the infrared emittance and solar absorptance of the surface when it is disturbed by the astronauts as well as of heat generated during instrument emplacement operations – hole drilling, in particular. To meaningfully extract the average gradient from the composite temperatures that may exist at practical lunar measuring depths, the temperature-measuring instrument must have a wider range than

---

Principal Investigator for the ALSEP Heat Flow Experiment is Marcus G. Langseth, Jr., Lamont-Doherty Geological Observatory, Columbia University, Palisades, New York. Coinvestigators are John Chute, Jr., Lamont-Doherty Geological Observatory, and Sydney P. Clark, Jr., Yale University, New Haven, Connecticut.

Arthur D. Little, Inc., Cambridge, Massachusetts, built the heat-flow probes and the probe test apparatus. Gulton Industries, Albuquerque, New Mexico, built the heat-flow electronics. Rosemount Engineering Company, Minneapolis, Minnesota, produced the sensors. Aerospace Systems Division of The Bendix Corporation, Ann Arbor, Michigan, has overall responsibility for hardware development and integration.

the gradients in Table I indicate, readings must be recorded frequently for more than a year, and absolute measurement accuracy must equal the relative accuracy requirement for the lowest mean temperature gradient expected.

Two different approaches are used in measuring lunar subsurface thermal conductivity by means of the heat-flow instrument. In the first approach, the thermal response of *in situ* lunar material to known heat sources is tested. In the second, vertical strings of temperature sensors record the characteristics of the periodic propagations into the surface to determine diffusivity; with this diffusivity information and good estimates of soil mass density and specific heat, thermal conductivity can be calculated.

The first of these approaches takes into account local inhomogeneities, and measurements should sample the volume of material that immediately influences the temperature gradient. Two variations within this approach are required to cover the conductivity range of expected subsurface lunar materials. For soils with low conductivities ($<5 \times 10^{-2}$ watt/meter°K), a tubular heater wound around one of a pair of temperature sensors vertically separated by 0.5 meter is energized with a small amount (2 milliwatts) of power. The rate of rise and steady-state value of the heated sensor temperature relative to the undisturbed reference level is a function of the thermal coupling from the heater to the lunar material and the thermal conductivity of the surrounding lunar soil. The temperature rise is inversely proportional to both thermal conductivity and absolute temperature level.[4] Useful range is limited at higher thermal conductivities by reduced sensitivity and the magnitude of the radiative and conductive thermal resistance of the coupling paths from instrument to soil. For materials such as rock, with conductivities greater than 2×10^{-2} watt/meter°K, the heater is powered to 0.5 watt; the transient and steady-state response of the lunar medium between the heat source and a "remote" sensor 0.1 meter away is determined by subtracting the characteristically short time constant response of the intervening sensor support structure from the overall response.

EXPERIMENT DESCRIPTION

The optimum site configuration for the Lunar Heat Flow Experiment is depicted in Figure 1. Two hollow fiberglass borestems, 2.5 centimeters in diameter, are drilled into the lunar surface to a depth of 3 meters at a distance of 10 meters from one another. Four sets of temperature sensors, spaced along a probe consisting of two flexibly joined rigid sections, occupy the bottom meter of each hole. The flexible joint permits the probe to be folded for transportation to

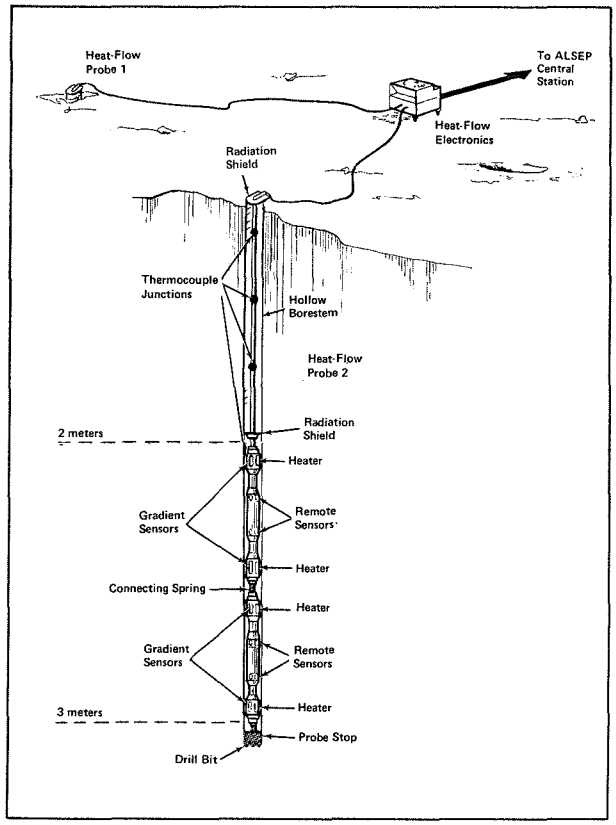

Figure 1 Optimum Site Configuration for Lunar Heat Flow Experiment

the moon. The sensors, which are primarily radiatively coupled to the borestem and lunar soil, are connected electrically by 8-meter woven cables to a package of electronics on the surface. Each cable carries four precisely located thermocouple junctions in the borestems above the probes. The electronics unit is connected by a flat ribbon cable, 9 meters long, to the Apollo Lunar Surface Experiments Package (ALSEP) Central Station, which formats all the data from and controls the operation of all the scientific-station instruments on command from earth.

The heat-flow instrument returns data giving average-temperature, differential-temperature, and low- and high-thermal-conductivity information from four locations on each probe, with the thermocouples supplying readings for temperature determinations in the upper part of the boreholes. Instrument performance requirements for these measurements are summarized in Table II. In the normal operating mode, the heat-flow instrument gathers ambient and high- and low-sensitivity differential temperature data from the "gradient" sensors situated at the ends of each half-probe section and samples the thermocouple outputs during the 7.25-minute measurement sequence. Various subsequences can be selected (e.g., measurements on one probe only), but most of them

Table II Heat-Flow-Instrument Performance Requirements

Measurement	Requirement			
	Range	Resolution	Accuracy[a]	Minimum Stability
Temperature Difference across 0.5-Meter Probe Section in Lowest Meter of Hole	±2°K (high sensitivity) ±20°K (low sensitivity)	0.0005°K (high sensitivity) 0.005°K (low sensitivity)	±0.003°K	0.003°K/year
Ambient Temperature of Probe in Lowest Meter of Hole	200–250°K	0.02–0.08°K	±0.1°K	0.05°K/year
Temperature of Thermocouples in Upper 2 Meters of Hole	90–350°K	±0.17°K	±0.5°K	0.5°K/year
Thermal Conductivity of Material Surrounding Probes	0.002–0.4 watt/meter°K	±20%	±20%	——

[a] Maximum probable error.

would not normally be used. Low-conductivity experiments are performed on command, with each heater activated in turn to 0.002 watt for about 40 hours. The normal measurement sequence is unchanged. The high-conductivity mode of operation requires the selection of measurements on the remote sensors in any half-probe section, the type of data returned alternating between high-sensitivity differential and absolute temperature measurements. Either of the adjacent heaters at the ends of the probe half may be activated by command. Each heater should be on for about 6 hours, but this depends on the conductivity experienced.

The experiment data, collected for a year, require detailed analysis – including processing through finite-difference models of the thermal transfer functions relating lunar soil, heaters, and sensors – before they can be interpreted in a geophysical context to produce a single value for the heat-flow rate from the moon.

PROBE AND SENSOR CONSTRUCTION

The platinum resistance sensors used in the heat-flow-instrument probe contribute significantly to the quality of the measurements obtained. The approach

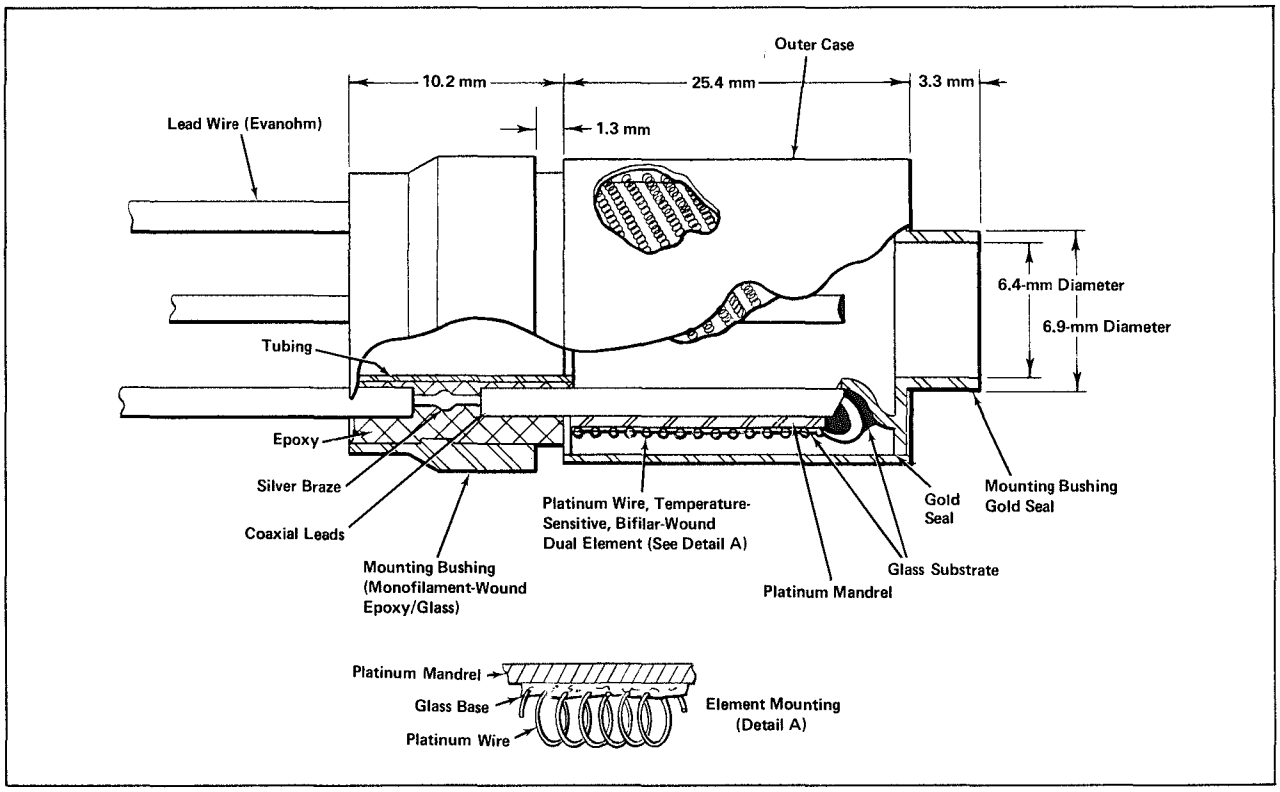

Figure 2 Gradient-Sensor Construction

to sensor construction is not new: Siemens described a platinum resistance thermometer, with wire wound on a clay cylinder enclosed in a wrought-iron tube, at a meeting of the Royal Society of London in 1871.[5] Whereas present commercial thermometers have stabilities of 10 to 100 millidegrees Kelvin per year with normal use,[6] the lunar gradient measurements require stabilities of the order of 1 millidegree Kelvin. These have been achieved in standards laboratories for some time, but with sensors that are susceptible to quite low levels of shock and vibration, and with substantial precision equipment required to obtain accurate readings.

Two types of platinum resistance thermometer are used in the heat-flow instrument, the so-called *gradient* sensor and the *ring* or *remote* sensor. The gradient sensor, the construction of which is detailed in Figure 2, incorporates a unique method of supporting the resistance wire[7] to reduce instability normally induced by mechanical or thermal stress. Pure annealed 0.04-millimeter-diameter platinum wire is mounted, coiled in a 0.3-millimeter-diameter helix extended to 0.07 millimeter pitch, on a glass-insulated platinum mandrel. The base of each loop is arranged so that only 10 percent of the turn is embedded in the substrate. The mandrel and glass have the same expansion coefficients as the coil, and the assembly is annealed at 673°K for 15 hours before sealing. The platinum coil is isolated from contamination by an atmosphere of pure helium contained within a gold-sealed platinum outer case. Platinum-wire coaxial leads extend through ceramic-insulated tubes for silver brazing to Evanohm and Manganin connecting wires. Each sensor assembly houses two separate elements, effectively bifilar wound, with nominal resistances of 500 ohms at 273.16°K (0°C).

The remote sensor, the construction of which is illustrated in Figure 3, consists of two 500-ohm-nominal-resistance platinum wires set in a ceramic glaze around a thin platinum ring. Because its intended use is in the short-term high-conductivity

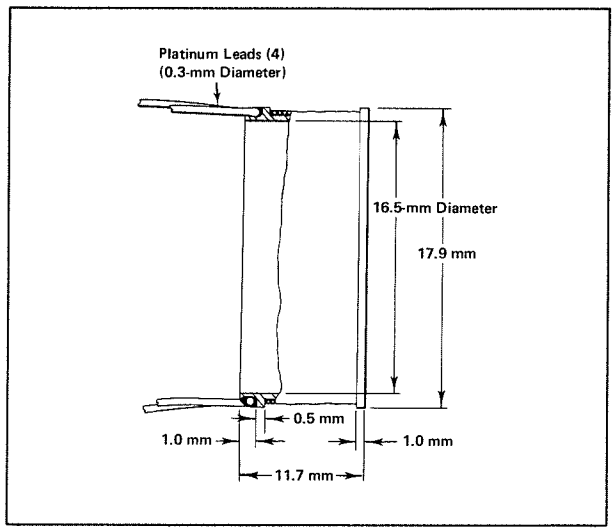

Figure 3 Ring- or Remote-Sensor Construction

experiments, it has a less stringent stability requirement (0.002°K/6 hours) than the gradient sensor. Unexpectedly, however, it has demonstrated a long-term stability comparable to that of the gradient sensor.

The sensors are mounted as shown in Figure 4, which illustrates the configuration common to the ends of all half-probe sections. The gradient assembly is epoxied at the mounting bushing at the sensor-lead exit end to the inside of the probe end-sheath. The small tube on the opposite end (also shown in Figure 2) is supported by a snugly fitting fiberglass bushing, which permits strain-free differential expansion with good mounting support. Associated with each gradient sensor is a 1000-ohm Karma wire heater, wound concentrically with the gradient sensor on the thin section of the end sheath. The ring-sensor platinum band is partially cemented internally to a filler sheath, which, in turn, is attached to the outer sheath of the probe. A tube joins the two end pieces to form a probe half-section.

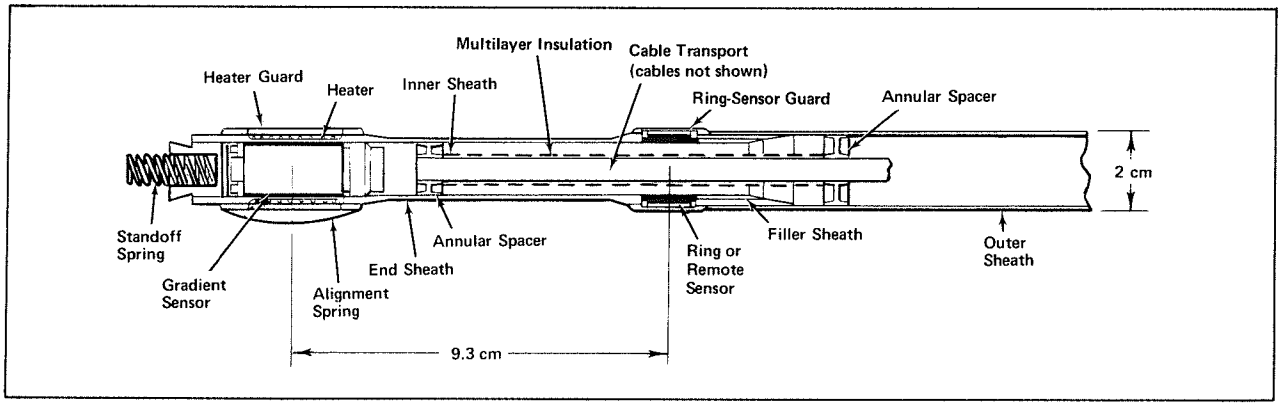

Figure 4 Half-Probe End Section

The structural components providing the span between the sensors are manufactured from low-conductivity thin-walled filament-wound epoxy fiberglass. All cabling is carried through the probe body inside the split inner sheath, which is shielded with multilayer insulation to reduce radiative coupling between the wiring and probe wall, particularly during conductivity experiments with a heater on. The areas around the sensors are partially enclosed with guards for protection during handling.

A probe assembly is 1.09 meters long when unfolded at the closely coiled extension spring that joins the two half-sections. The complete unit is coated with a matt-black thermal control paint. An assembled probe, with its 8-meter 35-conductor connecting cable, weighs less than 0.5 kilogram.

Gradient and ring sensors are each interconnected within a probe half with AWG 23 Evanohm wire to form bridges, the opposite arms of which are physically situated in the same sensor assembly at a common temperature. A schematic of this resistance-bridge arrangement is shown in Figure 5 (left), where T_1 is the temperature of one sensor assembly and T_2 the temperature of the other. The gradient-sensor assemblies, which form one bridge, are separated by 47 centimeters; the remote-sensor assemblies, which form the other, are located 29 centimeters apart and 9 centimeters from the heater windings.

Six wires connect each bridge to the electronics unit. Those from a lower half-probe are conveyed in the upper section through the hollow sensor assemblies. Evanohm wire is used because it has a remarkably small temperature coefficient of resistance (0.00002/°C), with closely controllable resistivity and a thermal conductivity that is low for an electrical conductor.

SENSOR CHARACTERISTICS

In Callendar's empirical parabolic equation[8,9]

$$T = 100[(R_T - R_0)/(R_{100} - R_0)] + \delta[(T/100) - 1](T/100) \quad (2)$$

the constant δ defines the characteristics of an individual platinum resistance thermometer over the temperature range 0°C to 630°C, where T is temperature in degrees Centigrade, R_T is resistance at temperature T, R_0 is resistance at 0°C, and R_{100} is resistance at 100°C. The Callendar constant is determined by calibration at three fixed points: the triple point of water (0.0100°C), the steam point (100°C), and the boiling point of sulfur (444.600°C). For use between 0°C and -183°C, a correction term devised by Van Dusen is added to the Callendar equation to give[10]

$$T = 100[(R_T - R_0)/(R_{100} - R_0)] + \delta[(T/100) - 1](T/100) + \beta[(T/100) - 1](T/100)^3 \quad (3)$$

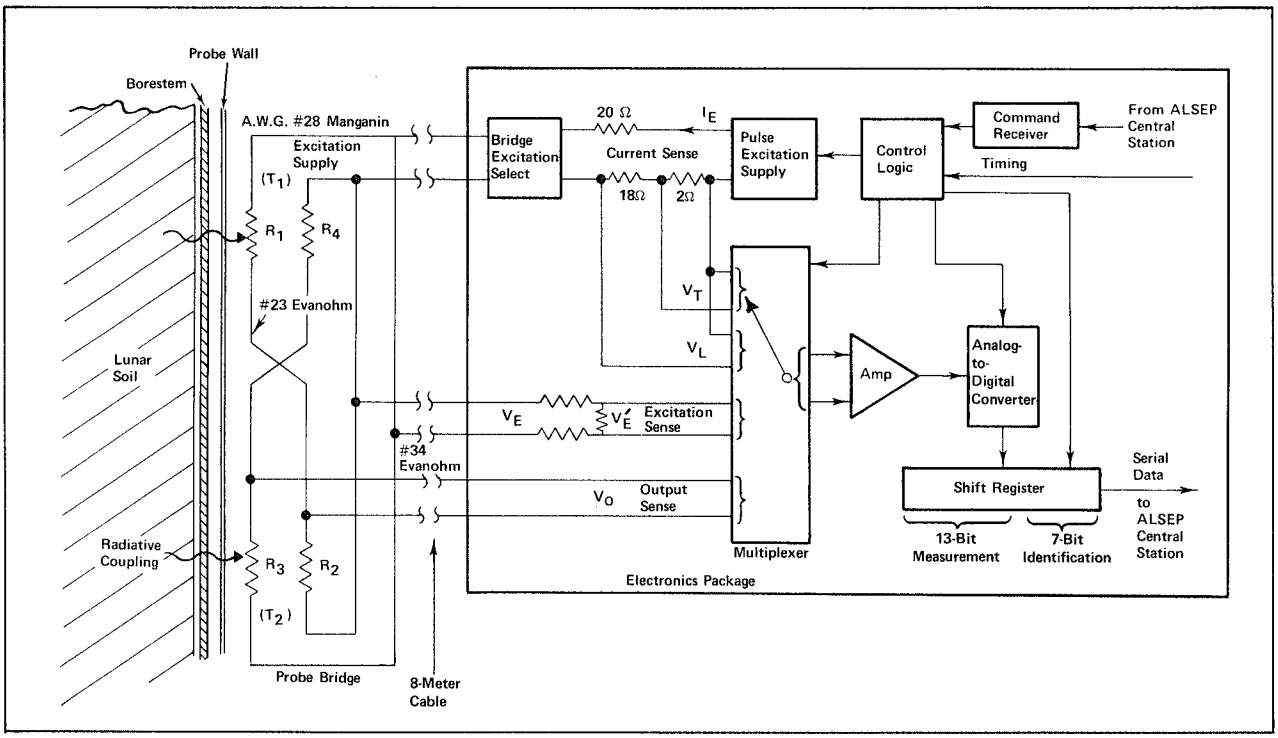

Figure 5 Schematic for Electronics Measurements on Bridge Sensors

where the constant β for an individual thermometer is found by calibrating at the boiling point of oxygen (-182.97°C). The resistance of one platinum element at temperature T relative to its resistance at 0°C is therefore

$$R_T/R_0 = 1 + (1/100)[(R_{100}/R_0)-1] \left\{T - \delta[(T/100)-1](T/100) - \beta[(T/100)-1](T/100)^3\right\} \quad (4)$$

Referring to Figure 5, the bridge voltage ratio is defined

$$V_O/V_E = (R_1R_4-R_2R_3)/[(R_1+R_3)(R_2+R_4)] \quad (5)$$

where R_1, R_2, R_3, and R_4 are Wheatstone bridge arm resistances, V_E is the excitation voltage across the bridge, and V_O is the output voltage. By combining equations (4) and (5) and eliminating small terms, the following simplified expression is obtained,

$$(V_O/V_E)R_B = A_1 + A_2T + A_3T^2 + A_4\Delta T + A_5\Delta T(\Delta T+2T) + A_6[\Delta T(4T^3-300T^2)+\Delta T^2(6T^2-300T)+\Delta T^3(4T-100)+\Delta T^4] \quad (6)$$

where R_B is total bridge resistance, T is the temperature of one sensor assembly expressed in degrees Centigrade, ΔT is the temperature differential between sensor assemblies in degrees Centigrade, and A_1, A_2, A_3, A_4, A_5, and A_6 are constants. Similarly, bridge resistance R_B can be related to temperature T and temperature differential ΔT by the simplified expression

$$R_B = B_1 + B_2T + B_3T^2 + B_4\Delta T + B_5\Delta T(\Delta T+2T) + B_6(T-100)T^3 \quad (7)$$

where B_1, B_2, B_3, B_4, B_5, and B_6 are constants. Equations (6) and (7) are transcendental in T and ΔT. To find absolute and differential temperatures, an iterative simultaneous solution of both calibration equations is required.

THE ELECTRONIC MEASUREMENT SYSTEM

System Operation

It can be seen from equations (6) and (7) that the electrical measurements required to solve for T and ΔT are total bridge resistance R_B (measured as a single element), excitation voltage V_E, and differential output voltage V_O. The system by which these measurements are made is represented in the simplified block diagram in Figure 5, which incorporates the essential features of the bridge measurement method, although it includes only one of the eight probe bridges and omits thermocouple circuits, power supplies, and the bulk of the logic and control circuits.

Each of the bridges is selected through reed relays for excitation by direct current. The bridges produce a differential output-to-input voltage ratio V_O/V_E of approximately $\pm 5.8 \times 10^{-3}$ for a dynamic range of ±2°K. With 8 volts applied to the bridge excitation cables, the data-chain maximum input requirement is set at ±34 millivolts. The gradient-bridge low-sensitivity range of ±20°K requires 0.8 volt excitation for a similar output maximum. Measurements for total bridge resistance are made at the 8-volt supply level. Excitation voltage V_E is reduced to the maximum level of the output voltage by an attenuator in the excitation sense circuit.* The output impedance is arranged to be the same as the bridge differential output impedance. At the low-sensitivity excitation level of 0.8 volt, the attenuator output V_E' is one-tenth the maximum bridge unbalance voltage V_O at ±20°K temperature extremes. To effectively normalize these readings and at the same time avoid attenuator switching or gain changes, excitation current I_E is sensed. This current is combined with the total bridge resistance value, determined from readings at 8 volts excitation made within a short time of the current measurement, to calculate the low-level-excitation supply voltage. Low-sensitivity current is found from the potential difference V_L developed across a precision 18+2-ohm resistance in the supply line; high-sensitivity current is found from the potential difference V_T across the 2-ohm resistor only. The latter value is used with the attenuated bridge-excitation-voltage measurement to determine total bridge resistance R_B. Differential output voltages are read directly.

These various measurements are presented sequentially through a low-level field-effect-transistor (FET) multiplexer to the input of the common signal amplifier, which has a gain of 288 and full-scale output of ±10 volts. The amplified signal is converted to a 13-bit digital number and clocked into a shift register along with a 7-bit mode-identification and binary-measurement code. The resulting 20-bit number is serially shifted into the ALSEP Central Station for insertion as two 10-bit words into the ALSEP data stream for transmission to earth. On earth, the binary numbers are converted back to the sensor temperatures from which they originated by applying the calibration factors for each bridge or thermocouple and each measuring channel. The sources of error to which the reconverted temperature values may be subject are outlined in Table III.

*The series elements of the attenuator include cable resistance that does fluctuate slightly with the large surface-temperature variations, but the proportion of cable resistance in the temperature-matched attenuator is small, and very high attenuation-ratio stability is achieved.

Table III Sources of Error in Experiment Data

Platinum-Bridge Error Sources • initial calibration accuracy • element stability with age • dissimilar-metal EMF's at sense-wire connections
Measurement-System Error Sources • initial calibration of electronics • system noise • spurious EMF's in multiplexer • excitation voltage stability sense-attenuation stability bridge heating • amplifier common-mode rejection gain and offset stability linearity settling time • analog-to-digital converter linearity reference-voltage stability quantizing magnitude
Data-Processing Error Sources • truncation errors • iterative solution accuracy of bridge equations

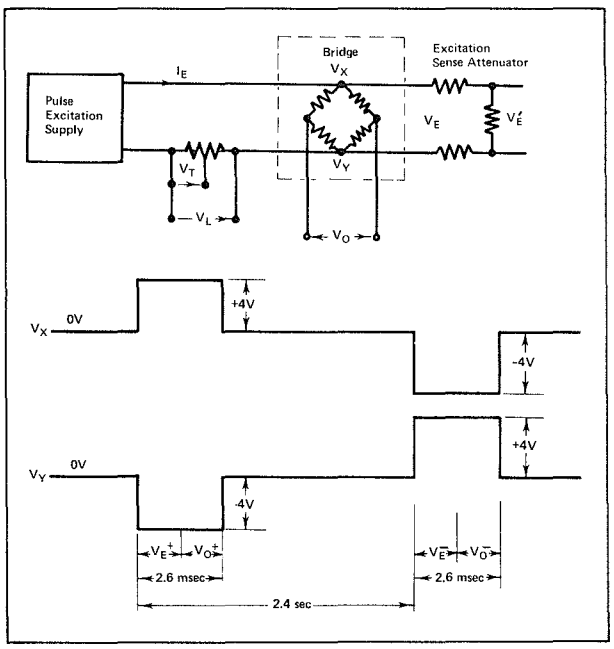

Figure 6 Typical Sequence for Bridge Measurements

The Ratio Measurement Technique

Errors due to long-term system gain and offset instability are circumvented by a scheme that paradoxically amounts to a calibration of each measuring channel by the unknown signal being measured. A ratio technique is used, which eliminates system gain and offset as factors in the reconstitution of the original bridge ratio, depending for its success only on gain and offset stability during the brief measurement period. All measurements are made twice, at two different levels. To utilize the full system range and obtain maximum resolution, it is convenient for each bridge input and output measurement to be made at reversed polarity, with equal bipolar excitation levels. The bridge is pulsed twice in 2.4 seconds for 2.6 milliseconds at a maximum duty cycle ($0.2\text{x}10^{-3}$), which limits self-heating to an acceptable 0.1 microwatt; two measurements are made during each excitation pulse. The sequence outlined in Figure 6 for a high-sensitivity differential measurement is typical of all measurements. Power is applied to the bridge from the excitation-pulse supply at bipolar 4-volt levels, giving a positive 8-volt total excitation. After 1 millisecond to allow the system to settle, the attenuator output $V_E'^+$ corresponding to excitation level V_E^+ is converted to a digital number N_1. Output voltage V_O^+ is then selected for measurement, and, after a 2.3-millisecond positive pulse duration, V_O^+ conversion to N_2 is executed. The entire process is repeated 2.4 seconds from the start of the sequence, with the pulse-excitation supply output reversed to -8 volts; during application of this negative pulse, $V_E'^-$ and V_O^- are converted to digital numbers N_3 and N_4, respectively.

If G represents amplifier and analog-to-digital-converter gain,

$$\begin{aligned}(N_2-N_4)/(N_1-N_3) &= [(V_O^+ + \epsilon_0 + \epsilon)G - (V_O^- + \epsilon_0 + \epsilon)G]/[(V_E'^+ + \epsilon_1 + \epsilon)G - (V_O^- + \epsilon_1 + \epsilon)G] \\ &= (V_O^+ - V_O^-)/(V_E'^+ - V_E'^-) \\ &= (V_O^+/V_E'^+)[1-(V_O^-/V_O^+)]/[1-(V_E'^-/V_E^+)] \end{aligned} \quad (8)$$

where ϵ is the amplifier and analog-to-digital-converter offset, ϵ_0 is the output-sense-line offset, and ϵ_1 is the excitation-sense-line offset. Since the temperature of a bridge in the lunar regolith will not change during the 2.4-second measurement period,

$$V_O^+/V_E'^+ = V_O^-/V_E'^- = C \quad (9)$$

where C is a constant regardless of the excitation magnitudes of V_E^+ and V_E^-. Rearranging equation (9) to read

$$V_O^-/V_O^+ = V_E'^-/V_E'^+ \quad (10)$$

and combining equations (8) and (10) results in

$$(N_2-N_4)/(N_1-N_3) = V_O^+/V_E'^+ \quad (11)$$

where $V_O^+/V_E'^+$ is the ratio between measured bridge signals, independent of gain and offset. The required bridge ratio V_O/V_E is obtained by applying the excitation-sense measurement attenuation factor Z, the

accuracy and stability of which clearly affect the result. Since $Z = V_E'/V_E$,

$$V_O/V_E = V_O/ZV_E'$$

Other Design Features

The use of excitation-polarity reversal, with one data converter for all measurements, eliminates some major sources of error and obviates the need for separate periodic calibrations on the moon and additional circuitry with which to perform them. Nevertheless, numerous sources of error remain. It is therefore pertinent to summarize here the more significant features of the principal components of the data chain, which account for demonstrated measurement accuracies of better than 0.02-percent-full-scale probable error over a temperature range of 0°C to 60°C.

The pulsed-power supply produces 4.000-volt± 1-millivolt bipolar pulses, which are stable to within 0.002 percent during bridge excitation and output measurements. The supply operates from positive and negative reference levels, derived from constant-current-driven low-temperature-coefficient zener diodes, which are switched by the control logic for positive and negative bridge excitation outputs from two series-connected operational amplifiers, each having a push/pull output stage to supply the 20-milliampere bridge current.

The multiplexer for the heat-flow instrument is a double-tiered N-channel field-effect-transistor (FET) commutator, with 32 differential input pairs. It is divided into four sections, one for each probe set of gradient sensors and one each for the remote sensors and the thermocouples. Each FET section is powered only when necessary to restrict the effects of a single-channel failure. Field-effect-transistor temperature-dependent offset voltages and mismatched differential impedances, which act with circuit impedances and amplifier bias currents to introduce variable offset voltages for each channel and different offsets between channels, are cancelled by the ratio measurement technique previously described.

The most basic design trade-offs in analog-to-digital converter design are speed and accuracy. Neither is of great consequence in this application, where extreme linearity, stability, and sensitivity are the only critical requirements. Digital conversion of the amplified sensor signals is achieved by 13-bit successive approximation to the sum of a generated +10.000-volt± 1-millivolt offset supply and the ±10-volt full-scale output from the data amplifier. The offset binary number produced is linear to within 0.0075 percent full scale, with a resolution of 2.4414 millivolts per bit. Conversion speed is 20 microseconds per bit. The device is a conventional successive-approximation analog-to-digital converter, with the two most significant bits of the ladder network trimmed to remove errors due to voltage drops across the switches.

The signals are amplified by a differential-input single-ended-output two-stage amplifier, with differential and common-mode impedances exceeding 50 and 20 megohms, respectively, at frequencies below 5 kilohertz. The common-mode rejection ratio is greater than 120 decibels over the same frequency range. The characteristics most important to the ratio technique are linearity, which is within 0.005 percent full scale, and short-term stability, which is better than 0.001 percent for 5 seconds at a maximum rate of temperature change of 0.01°C per second. The common-mode rejection ratio becomes important when bridge current is sensed at 8-volt excitation levels.

Constant-current sources are supplied to each base of the differential input pair to compensate for the bias current required by the matched semiconductors, but the more usual constant-current-source common-emitter supply is replaced with a variable current source that maintains the combined collector currents constant. The differential output from the collectors connects to an operational amplifier, the output of which feeds back to the emitters of the input stage to force the total of the collector currents to divide equally between the two halves of the differential pair. Stable operating points are thus established independently of common-mode inputs over a wide temperature range. The first-stage gain is 100. After filtering, the signal is applied to the input of the second-stage amplifier, which normally operates with a gain of 2.88. The total amplifier gain of 288 is used for all bridge measurements.

Thermocouple measurements require an input range of ±10 millivolts rather than ±34 millivolts. During thermocouple sequences, therefore, the second-stage gain is changed from 2.88 to 10 by switching a field-effect transistor to introduce a potential divider in the feedback path of the second stage.

THERMOCOUPLE MEASUREMENTS

Eight constantan and two chromel wires from the thermocouple junctions in the probe cables connect to Kovar leads at an isothermal block inside the electronics package. The Kovar leads convey the thermocouple voltages to the multiplexer. The isothermal block also contains a platinum/Evanohm bridge thermometer with two constant-value resistance arms. A schematic representing one probe-cable set of thermocouple junctions and the reference-temperature bridge is presented in Figure 7.

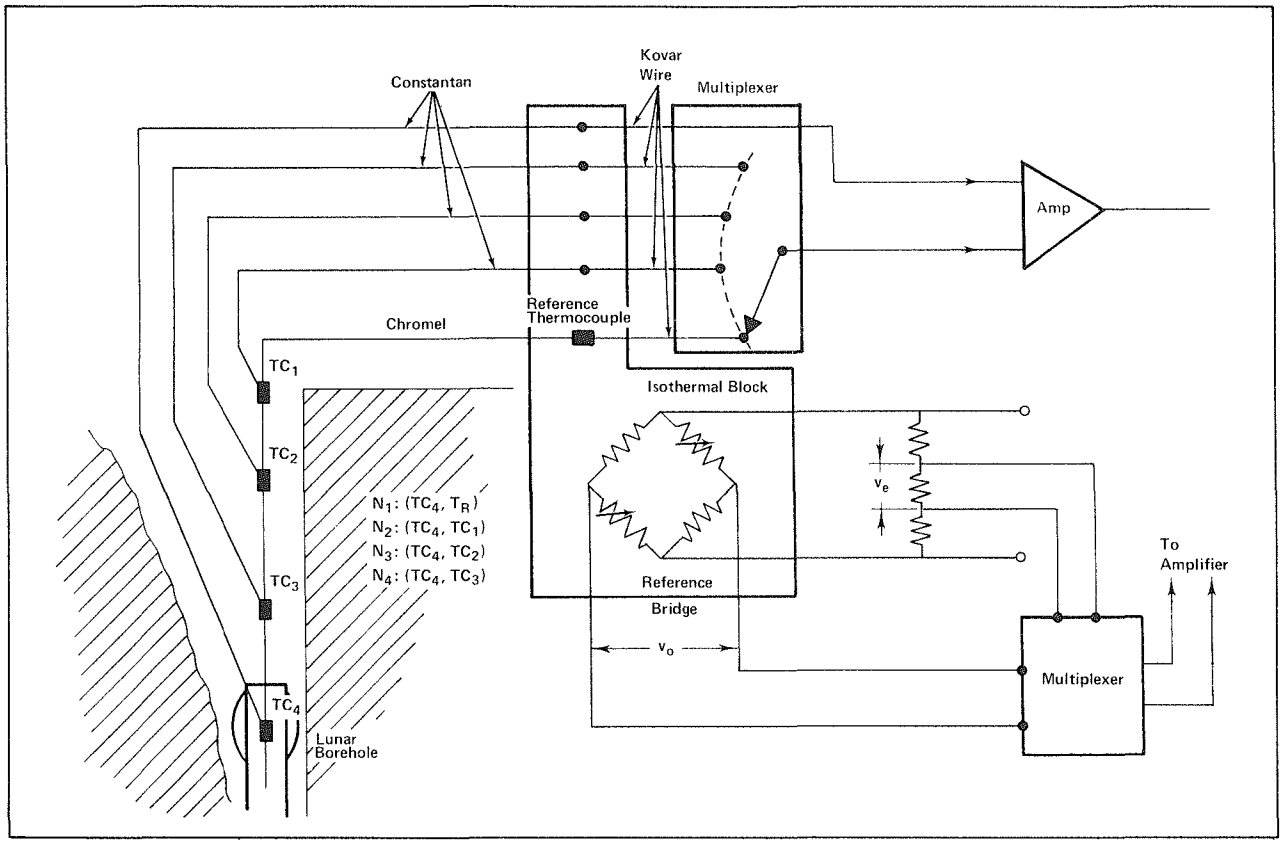

Figure 7 Schematic for Thermocouple and Reference-Temperature-Bridge Measurements

Thermocouple measurements of absolute temperature have an inherent accuracy an order of magnitude lower than platinum resistance measurements, in part because of thermocouple instability but primarily because of difficulties in measuring low-level voltage sources. Since the ratio technique is not applicable to thermocouple measurements, a calibration method is used to establish system gain and offset during the measurement sequence to find the isothermal block temperature with the bridge thermometer.

Measurements on the reference-temperature bridge follow the same pattern as those on the probe bridges, except that the amplitude of excitation is attenuated to give a ±10-millivolt full-scale output, which is the range of the thermocouple voltages. An amplifier nominal gain of 1000 is selected for reference-bridge and thermocouple measurements. To find system gain and error offset values, it is assumed that the attenuated positive and negative bridge-excitation voltages v_e are of known, equal, and opposite magnitudes since they are derived from the precisely controlled pulsed-power supply and are connected to the bridge by short leads within the electronics package.

The sensed excitation signals v_e^+ and v_e^- are converted by the analog-to-digital converter to binary numbers N_1 and N_3 in accord with the relationships

$$N_1 = [(v_e^+ + v_{off})G]/u$$

$$N_3 = [(v_e^- + v_{off})G]/u$$

where v_{off} is error offset voltage referred to the amplifier input and G is system gain. The full-scale 13-bit binary output count is 0 to 8191, which corresponds to an offset amplified signal range of 0 to 20 volts, giving a digit resolution u of 2.4414 millivolts. Gain is found from

$$G = u(N_1 - N_3)/(v_e^+ - v_e^-)$$

when the offset voltages cancel. To find the error offset voltage v_{off}, the offset binary outputs N_1 and N_3 are converted to positive and negative numbers by subtracting offset count 4096. If $N_1' = (N_1 - 4096)$ and $N_3' = (N_3 - 4096)$, then $v_{off} = u(N_1' + N_3')/2$.

The use of known balanced inputs in the reference-bridge measuring sequence thus establishes system gain and offset. The measured outputs are converted through electronics calibration data, and the bridge voltage ratio is then used to solve iteratively a third-order calibration equation for reference-bridge temperature and hence for isothermal-block and reference-thermocouple temperature. Measurements

of thermocouple voltages made shortly thereafter (in the sequence N_1, N_2, N_3, N_4, as shown on the Figure 7 schematic) are processed, using calculated gain and offset values, to arrive at true thermocouple voltage outputs.

The output from the chromel/constantan reference junction in the isothermal block is measured relative to only one of the junctions in the cable – that inside the hollow of the gradient sensor at the top of the probe. The remaining three junctions in each probe cable are also measured relative to this top junction. The double-referencing arrangement is designed to center the mean of the thermocouple-output extremes close to 0 volts for maximum measurement resolution. The predicted temperature range for the thermocouple junction at the top of the probe is 200°K to 260°K; the full-scale thermocouple range is 90°K to 350°K, and the isothermal-block temperature is controlled to between 278°K and 328°K.

The voltage/temperature characteristics of the thermocouples are described by calibration correction factors applied to standard tables of the National Bureau of Standards (NBS).[11]

PACKAGE CONSTRUCTION AND THERMAL CONTROL

The heat-flow instrument operates from a 29-volt d.c. supply and requires data-interlace and mode-control signals from the ALSEP Central Station. The unit is otherwise self-contained with respect to logic and power management for all the sensor measurements and for probe-heater control. A description of these ancillary circuits is beyond the scope of this paper.

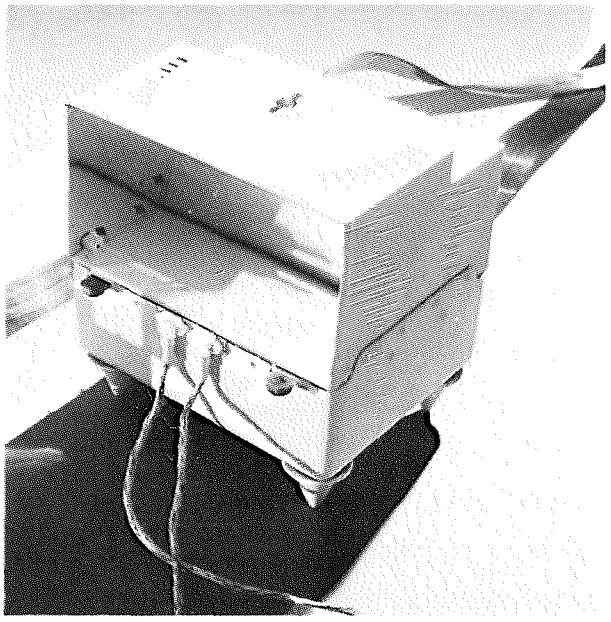

Figure 8 Heat-Flow-Instrument Package

In the deployed configuration, a ribbon cable made up of 40 flat copper conductors in a plastic film extends from the instrument package across 9 meters of the lunar surface to the ALSEP Central Station. This cable is connected to an astromate connector, which the astronaut mates with the Central Station outlet for power to and communication with the heat-flow instrument.

The two probe cables are each made up of 35 unshielded conductors, interwoven for a uniform stress distribution so that the weight of the astronaut can be supported without degradation in cable performance. These cables are very flexible, exhibiting little residual torque when extended, and they are covered with a woven Teflon sleeve to provide a low coefficient of friction during deployment. Heat leaks from the cables on the lunar surface to the probes and the electronics package are small since the conductors are made from low-thermal-conductivity wire.

The complete surface package, shown in Figure 8, weighs 7.0 pounds (3.2 kilograms) and is 9.5x10.0x11.0 inches (24x25x28 centimeters) in size, including the feet. The astromate connector, ribbon cable, and spool weigh 1.4 pounds (0.6 kilogram).

Electronics Package

The electronics package, shown in Figure 9, is made up of five multilayer printed-circuit boards, joined in a stack by interlocking spacers bonded to each board. The stack is 2.5x7.6x5.6 inches (6x19x14 centimeters) in size, the boards consisting of up to twelve layers, each 0.004 inch (0.1 millimeter) thick. The layers of circuit tracks are interconnected through plated holes in the composite board, and as many as 210 component subpackages are mounted on one board. The components are in physical contact with a heavy printed-circuit conductor, which forms a heat path to the interlocking

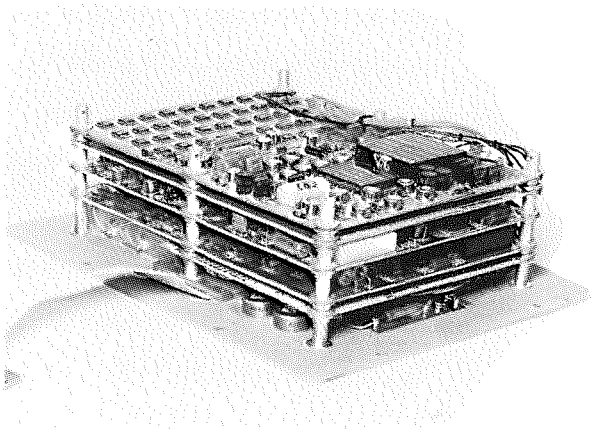

Figure 9 Heat-Flow-Instrument Electronics Package

spacers. Column screws pass through the spacers to a metal plate, which serves both as a thermal control plate and as a support for the board stack. A d.c./d.c. converter for the instrument power supplies is packaged on a board that is bonded to the thermal control plate. Heating elements are also mounted in good thermal contact with the plate. A short length of Manganin cable (at left in Figure 9) provides thermal insulation from the copper conductors in the ribbon cable. Bonded to the thermal control plate at the other side of the unit is a 70-pin isothermal connector to which the two probe cables are soldered. When the unit is assembled, the board stack is enclosed by a metal cover with a compressible, electrically conducting gasket to provide a barrier to electromagnetic interference.

The electronics unit weighs 3.3 pounds (1.5 kilograms).

Thermal Control Design

A thermal insulation bag, shaped as a container for the metal cover surrounding the board stack, is hooked by velcro pads to a low-thermal-conductivity mounting ring fitted around the inside edge of the thermal plate. The bag is constructed of twelve layers of closely spaced high-reflectivity shields having very low transverse conductivity; bridal-silk netting separates the layers and covers the inside and outside of the bag. The infrared emissivity of the 1/4-mil aluminized Mylar used for the shields is approximately 0.02.

The electronics assembly is supported and protected by a thin fiberglass outer case, which is connected to the mounting ring by low-conductivity joints. When the unit is standing on the feet on this outer case, the well-insulated electronics compartment is situated beneath the exposed thermal control plate. Internally generated heat is conducted to the plate and radiated from a spectrally selective surface coating (S-13G) having a high infrared emittance (ϵ_{IR} = 0.9) and a low absorptance (α_s = 0.2) at frequencies where solar power is most intense.

This simple thermal control arrangement could not modify the extreme heat of solar radiation as well as the cold of deep space in the tenuous atmosphere of the moon to meet the required electronics-temperature operating range of 278°K to 328°K without using excessive power during lunar night or permitting the upper limit to be exceeded during lunar day. The thermal plate is therefore protected from direct solar radiation by a sunshield fitted over the assembly as shown in Figure 8. The sunshield is an insulated box with one open side, which is placed to face away from the equator with its edge aligned in the east/west direction. The numbered marks on the sunshield are used as a shadowgraph with the shadow cast by the universal handling tool, which fits into the center socket. A specular reflector slopes from the top edge of the sunshield at an angle 57 degrees from vertical to almost touch the thermal plate. The reflector increases the view of the thermal radiator plate to the near-absolute-zero temperature of space and minimizes the lunar-surface-radiation reflections that reach the thermal plate from the exposed inside surfaces of the enclosure. The side curtains adjoining the sloping reflector are also specular surfaces. The reflecting mirrors are produced by thinly depositing aluminum onto polished fiberglass by a vacuum process. The back of the reflector and the thermal control plate inside the sunshield are heavily blanketed with aluminized Mylar, layered in the same way as in the thermal bag. The concealed interior surfaces of the sunshield are also vacuum-metalized to reduce radiant interchange of infrared energy inside. The exterior surfaces of the entire package are covered with S-13G thermal control coating.

A mask of multilayer insulation is attached to the edge of the thermal plate to prevent direct sunlight from reaching it in the event of moderate misalignment from an east/west line or instrument-leveling error. To aid in leveling in the stark lighting on the moon, the bubble level situated at one corner on a recessed platform is illuminated by reflection of sunlight from the vertical wall of the step.

The thermal control design for the heat-flow instrument is dictated largely by the power dissipation of the unit at lunar noon. The average dissipation is minimized by gating off as many circuits as possible when they are not required for measurements. During power gating, the average operational power dissipation is 3.9 watts. The power-sharing mode is set to switch in when thermal-plate temperatures exceed 300°K. During lunar night, when the electronics temperature falls below 290°K, additional power is dissipated by the heaters on the thermal control plate. The total power demanded by the instrument at lunar night is 10.5 watts. Should the 29-volt operational supply be switched off under abnormal circumstances, a separate survival line can be activated to a part of the thermal-plate heater for a power dissipation of 4 watts.

The thermal control system is designed for instrument deployments between lunar latitudes of ±45 degrees.

CALIBRATION AND TESTING

To ensure that the heat-flow instrument will meet its performance requirements, the calibration and test program is extensive and thorough. Indeed, a substantial part of the large array of calibration and test

apparatus used was developed specifically for this purpose. The sensors, probes, and electronics are subjected to worst-case mission environments and calibrated as subunits before assembly as flight instruments. The subassembly calibrations are verified by tests on the complete unit, which then undergoes a further series of tests closely simulating all the conditions anticipated for travel to and operation on the moon. The stability of the instrument following exposure to such critical environments as system vibration is carefully checked.

The Sensors

The platinum resistance thermometers are calibrated as a bridge by a comparison method.* Each sensor is immersed, along with a standard thermometer, in an isothermal bath of trichloroethylene. The baths have separate temperature controls so that temperatures can be independently set for each thermometer of the differential bridge. The standard thermometers are interchanged for several measurements to determine offset. The degree Kelvin is established from NBS-calibrated standard thermometers. Secondary absolute-value resistance standards of 1000 ohms, referred to an NBS standard, are maintained as a reference for the electrical measurements.

To check for random errors, each gradient bridge is calibrated at 42 points, which are least-squares fitted to equations (6) and (7) to yield the 12 constants in these equations. The standard deviation of the least-squares fit to the data points in equation (6) does not exceed 0.48×10^{-3}°K for any of the sensor assemblies tested, and more than 60 such assemblies have been produced. The gradient bridges are calibrated at differential temperatures of +20, +10, +2, 0, -1, -2, -10, and -20°K at absolute temperatures of 200, 212.5, 225, 237.5, and 250°K. The equivalent differential-temperature drift of some randomly selected gradient sensors tested periodically at 200°K and 270°K over a 3-year period is approximately 0.3×10^{-3}°K. The average absolute-temperature drift for individual sensor elements over the same 3-year period has been found to be 0.5×10^{-3}°K.

The ring sensors are calibrated at a minimum of 14 points to calculate 12 calibration constants.

Thermal-plate reference-temperature bridges in the electronics package are calibrated at -20, 0, +25, +50, and +90°C to yield the constants X_1, X_2, X_3, and X_4 in the relationship

$$V_O/V_E = X_1 + X_2(T_R) + X_3(T_R)^2 + X_4(T_R)^3$$

where T_R is the reference-bridge temperature and V_O/V_E is the bridge voltage ratio. During reference-bridge calibration at 0°C, all eight cable thermocouple junctions are immersed in an isothermal bath for calibration at 90, 200, 250, and 350°K.

The Electronics

Testing of the electronics data chain involves adjustment by resistance-value selection for zero offset, common-mode rejection, and gain. A calibration factor is found for each measuring channel by calibrating the channel as it will be used – that is, by performing ratio measurements. A set of resistance networks, calibrated to an accuracy of 0.002 percent, substitute for bridge and line resistances to simulate high-sensitivity and low-sensitivity ratios and bridge resistance. The various types of measurement are made through separate channels. Calibration is performed at nine different differential-ratio amplitudes and five levels of bridge resistance, and at least ten measurements are made for each of the input ratios. The mean $\bar{m}$ and standard deviation σ of the output ratios for a constant input are calculated, and a linear calibration factor is found from the mean values corresponding to ratios near the limits of channel range (n = 1 and n = 9 in Figure 10). The ideal transfer function of the channel is the calibration factor. The error at any point n is defined as the difference between the ideal output $R_I(n)$ and the mean output $\bar{m}(n)$, summed with the standard deviation $\sigma(n)$. To verify system linearity, these measurements are made at temperature intervals throughout the operating range of the heat-flow instrument. A maximum error of 0.0375 percent full scale is specified, but the typical maximum for instruments tested to date is 0.02 percent. Calibration factors are modified for the actual bridge-lead resistances. Thermocouple channel

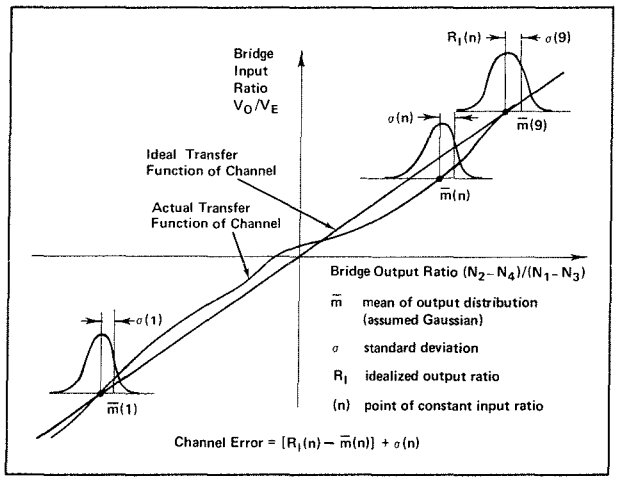

Figure 10 Error Definition for Instrument Measuring Channels

*Intercomparisons of NBS standards indicate that accuracies afforded by this method approach those obtained by absolute fixed-point calibration.

accuracy is also checked by multiple measurements at nine points throughout the ±10 millivolt input range.

The Probes

Assembled probes are characterized over ambient- and differential-temperature operating ranges in a temperature-gradient apparatus or gradient chamber, which has an overall height of 11 feet (3.4 meters) and a diameter of 2 feet (0.6 meter). The probes are inserted in a gradient tube 2.5 centimeters in internal diameter, in which a positive or negative temperature field can be developed. A liquid-nitrogen bath surrounds the gradient-tube assembly to provide a constant-temperature heat sink for heat introduced in developing average and linear differential temperatures. A double-vacuum shell minimizes heat leaks and permits the probe to be inserted without unduly disturbing the thermal equilibrium. Thermocouples and thermopiles in the gradient tube, along with associated readout instrumentation, provide temperature measurements to accuracies that approximate those of the heat-flow instrument. Probe-measured differential temperature is compared with apparatus-measured differential temperature in the form of a "shorting" ratio, which is approximately a linear function of the absolute temperature along the gradient, the probes being radiatively coupled to the gradient tube. This shorting ratio varies from bridge to bridge, depending on small differences in probe construction. The probes are tested at mean ambient temperatures of 205, 225, and 245°K, with linear gradients of 0, 2, and 18°K across each probe half-section. At least five tests are performed with each flight-instrument probe, including two in which the probe is integrated with the electronics. Gradient-chamber tests at 0°K check the zero offset of the gradient bridges and determine the offset values for the ring bridges, the cables of which are shortened during probe assembly. Each of the probe heaters is turned on at the 0.002-watt level by the electronics to characterize the "low-conductivity" performance of the probe in an infinitely conducting environment, which the gradient-tube apparatus represents since it is an almost perfect heat sink.

Thermal conductivity testing is also performed in an apparatus that simulates the properties of the lunar regolith. In essence, this thermal conductivity test apparatus is a 10.5- by 3-foot (3.2- by 0.9-meter) Dewar flask, with inner-vessel-wall cooling to the temperature range 200°K to 250°K. A probe boretube extends into a bed of glass microbeads in the inner container. The outer cavity and the boretube are evacuated, and the thermal conductivity of the glass-bead bed is varied over the anticipated lunar range by controlling the gas-filling pressure. Two such thermal conductivity test units have been constructed to permit the simultaneous testing of the two probes of a heat-flow instrument.

The Heat-Flow Instrument

For functional testing of the probes and the heat-flow instrument as a whole, thermal simulators are used to provide a stable temperature environment for the probes in the lunar-temperature operating range. Each simulator is an insulated container 8 feet (2.5 meters) deep, filled with solid carbon dioxide and ethanol, in which a heavy-metal double boretube is vertically situated. The ethanol fluid stabilizes at the temperature of the subliming dry ice that it surrounds. Since the temperature of sublimation is a function of pressure, the fluid temperature increases with depth to impose a gradient along the boretubes. Thermocouples and thermopiles within the metal block measure the temperature profile along the tubes. The laboratory thermal-simulator apparatus has a compartment for the electronics package so that the whole instrument can be operated in a vacuum. When inserted into the boretubes, the two probes of the instrument are in a similar, uncontrolled but slowly changing temperature field, and comparisons can be made of processed measurements on the probe bridges at given heights in the bath.

A similar simulator has been built into an adjunct to a 27- by 20-foot (8.3- by 6.2-meter) thermal vacuum chamber. During ALSEP system testing, the heat-flow electronics package is deployed inside the main chamber, with the probes situated in the stabilized thermal-simulator boretubes. The entire ALSEP system, including the heat-flow instrument, is exposed to the temperature conditions of lunar dawn, lunar noon, and lunar night in a vacuum of 5×10^{-8} Torr. Cold space is simulated in the chamber by pumping liquid nitrogen under pressure through black, optically tight panels. The sun is represented by carbon arc lamps, and dust degradation on instrument surfaces is simulated by subjecting them to additional infrared radiation.

Table IV presents a comparison of thermal-simulator temperature measurements made in a changing temperature environment by the heat-flow-instrument probes and electronics package during simulated lunar-night testing of the Apollo 16 ALSEP system. The means of the differences between the temperatures measured by adjacent bridges, corrected for bridge shorting ratio, and the standard deviations from the means are tabulated. The very small differences noted may have been caused by differences in the transient responses of the two probes, by different probe responses to nonlinear gradients, or by slightly different temperature fields, the result either

Table IV Apollo 16 Heat-Flow-Instrument Test Results in Lunar-Night Environment[a]

Sensor Data	Upper Gradient Bridge (°K)	Lower Gradient Bridge (°K)	Upper Remote Bridge (°K)	Lower Remote Bridge (°K)
Absolute Temperature, Mean Difference[b]	−0.002	−0.020	−0.028	−0.036
Absolute Temperature, Standard Deviation[c]	0.016	0.037	0.034	0.032
High-Sensitivity Temperature Differential, Mean Difference[b]	0.001	−0.001	0.003	0.002
High-Sensitivity Temperature Differential, Standard Deviation[c]	0.0002	0.0002	0.0021	0.0010
Low-Sensitivity Temperature Differential, Mean Difference[b]	0.001	−0.003		
Low-Sensitivity Temperature Differential, Standard Deviation[c]	0.002	0.002		
Cycles	8	8	10	10
Thermocouple Data (9 Cycles)	**Thermocouple 1 (°K)**	**Thermocouple 2 (°K)**	**Thermocouple 3 (°K)**	**Thermocouple 4 (°K)**
Thermocouple Temperature, Mean Difference[b]	−0.073	1.946	−2.928	0.343
Thermocouple Temperature, Standard Deviation[c]	0.190	0.193	0.220	0.193

[a]Test performed on 26 July 1971.
[b]Mean difference in readings of two opposed sensors.
[c]Standard deviation of difference in readings of two opposed sensors about the mean difference.

of inherent differences between the apparatus boretubes or of different times of measurement. Outside of these factors, the probe-measurement differences reflect the consistency of total instrument calibration, stability, and signal processing.

The low-sensitivity measurements on the upper gradient bridges illustrate an effect of data averaging that is generally seen in heat-flow-instrument test results. Although resolution in the ±20°K range is ten times less than in the high-sensitivity range, a fact reflected by the standard deviations, the averages are about the same in the two ranges. The number of measurements that do not follow this pattern decreases as the number of data cycles increases. Thus, system resolution is effectively increased by multiple-measurement averaging in both the low and the high sensitivity ranges. Use of this technique can result in an effective resolution better than analog-to-digital-conversion quantization would allow for a single measurement.

During the simulated lunar-night test in which these results were obtained, the probe cables were lying in an uncontrolled temperature zone. There is little value, therefore, in comparing thermocouple readings 2, 3, and 4. However, the mean of the measurement differences for the thermocouples situated at the top of the probes (0.073°K) relative to the single-measurement resolution of 0.17°K again demonstrates the data-averaging effect. The readings also provide a good comparative check of the thermocouples.

INSTRUMENT PACKAGING

All the components of the heat-flow instrument that will be placed on the moon during the Apollo 16 mission are pictured in Figure 11. These include a packing container for the probes and an emplacement tool to be used by the astronaut to insert the probes into the borestems. Overall package design is strongly influenced by the requirement for deployability by a suited astronaut, as evidenced by the various pull rings, handles, and carry straps seen in the photograph.

The probes are folded, with two molded packing pieces secured by nylon cloth and velcro pads holding the sections slightly apart. They are stored for transportation in two thin aluminum containers, which are carried to separate deployment sites on the lunar surface, each with one probe inside. The probes are held within the containers in nylon bags by soft foam bulkheads, so spaced along the folded probe as to suppress the first free-bending mode of the probe.* The cables are coiled around the inside of the probe containers in troughs formed by an inner wall on each side.

One probe container has provision for stowing the collapsed emplacement tool – four telescoping fiberglass tubes that lock when extended to give a tool

*Damping is effected by the hysteresis in the foam walls of the polyurethane foam supports. Tests have demonstrated that air-pumping by the cells does not contribute to the damping action.

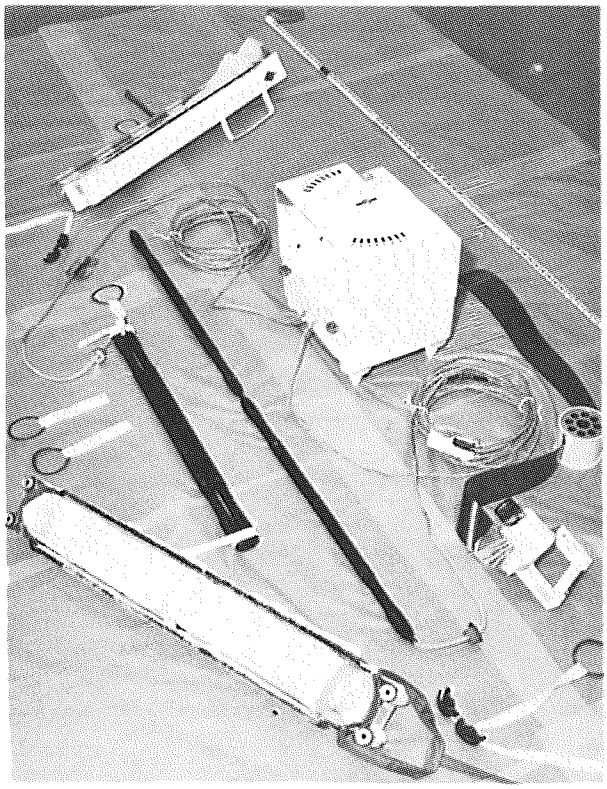

Figure 11 Apollo 16 Heat-Flow-Instrument Components

length of 224 centimeters. A slotted piece of fiberglass at the end of the smallest-diameter tube fits over the probe cable to implement probe deployment. The tool is white, with alphanumeric markings at 2-centimeter intervals and a bright orange band to indicate the depth to which the probe should be pushed.

The two probe containers fit together to form a single package, strengthened by the emplacement tool inside. The package is covered with white thermal-control paint and secured by velcro straps with pull rings. A complete probe-container assembly is 3.4x4.5x25.5 inches (8.6x11.4x64.8 centimeters) in size, excluding handles, and weighs 3.5 pounds (1.6 kilograms).

Carried to the moon in an equipment bay of the Lunar Module, the heat-flow instrument is mounted via quick-release fasteners to a subpallet, which stands vertically on a pallet as shown in Figure 12, supported by energy-absorbing mounts. The electronics package has shock-absorbing washers fitted to the four lugs protruding from the mounting ring. The probe package is secured through tubes at the four corners of the box. The astromate connector and cable (coiled inside the reel) are seen in the figure beneath the electronics package. The nylon cover on the electronics package, which serves to protect the thermal control surfaces from lunar dust, is removed

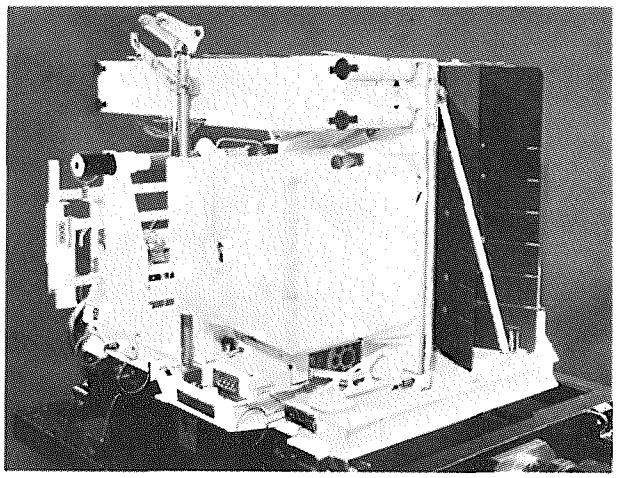

Figure 12 ALSEP Subpackage 2 Heat-Flow-Instrument Subpallet

before final leveling and alignment of the instrument on the moon.

CONCLUSION

An instrument of the type described in this paper was deployed on the lunar surface as a part of the Apollo 15 mission. It will operate for a year at the Plain of Hadley near the east bank of Hadley Rille to provide the data that are required for the first subsurface determination of heat flow from the moon. Instruments to be deployed on Apollo missions 16 and 17 will provide data for two subsequent determinations.

ACKNOWLEDGMENT

The author is grateful to colleagues at the National Aeronautics and Space Administration Manned Spacecraft Center, at Gulton Industries,[12] at Arthur D. Little, Inc.,[13] at Rosemount Engineering, and at Aerospace Systems Division of The Bendix Corporation for their assistance in the preparation of this paper. Discussions with Rodman P. Gilson have been especially useful. Marcus Langseth and John Chute have provided invaluable guidance.

REFERENCES

1. M. G. Langseth, Jr., K. A. More, and W. E. Johnson, "An Experiment to Measure Heat Flow from the Interior of the Moon," *Bendix Technical Journal* **1** (No. 1), 33-43 (Spring 1968).

2. M. G. Langseth, Jr., et al., "Apollo 13 Lunar Heat Flow Experiment," *Science* **168** (No. 3928), 211-217 (10 April 1970).

3. M. G. Langseth, Jr., "Lunar Heat Flow Experiment," presentation before the American Astronautical Society Conference, Ann Arbor, Michigan, 1968, AAS68-207, American Institute of Aeronautics and Astronautics, New York, New York.

4. D. Nathanson and R. Merrian, "Performance Prediction and Analysis of the Lunar Heat Flow Probes," Final Report submitted by Arthur D. Little, Inc., Cambridge, Massachusetts, to Lamont-Doherty Geological Observatory, Columbia University, Palisades, New York, January 1970.

5. C. W. Siemens, "On the Increase of Electrical Resistance in Conductors with Rise of Temperature," *Proceedings of the Royal Society (London)* **1871**, 444 (April 1871).

6. L. Klaven, L. Lofgren, and P. Felsenthal, "A Rugged, Stable, Differential Platinum Resistance Thermometer," *Review of Scientific Instruments* **41** (No. 4), 541-544 (April 1970).

7. U. S. Patent 3,114,125, dated 18 April 1961, granted to Rosemount Engineering Company, Minneapolis, Minnesota.

8. H. L. Callendar, "On the Practical Measurement of Temperature," *Philosophical Transactions (London)* **1887**, 161-230 (June 1887).

9. H. L. Callendar, "On the Construction of Platinum Thermometers," *Philosophical Magazine (London)* **32** (No. 194), 105-113 (July 1871).

10. D. Robertson and K. A. Walch, "Calibration Techniques for Precision Platinum Resistance Thermometers," in C. M. Herzfield (ed.-in-chief) and F. G. Brickwedde (ed.), *Temperature: Its Measurement and Control in Science and Industry*, Reinhold Publishing Corp., New York, 1962, Volume III, Part I.

11. R. K. Adams and E. G. Davisson, *Smoothed Thermocouple Tables of Extended Significance (°C)*, ORNL 3649, Oak Ridge National Laboratory, Oak Ridge, Tennessee, 1965, Vol. 2, Sect. 2.6.

12. "Heat Flow Electronics," Final Report on Subcontract 0243, prepared by Gulton Industries, Inc., Data Systems Division, Albuquerque, New Mexico, for The Bendix Corporation, Aerospace Systems Division, Ann Arbor, Michigan, January 1969.

13. "Lunar Heat Flow Probes for the ALSEP Heat Flow Experiment," Final Report on Subcontract 0242, prepared by Arthur D. Little, Inc., Cambridge, Massachusetts, for The Bendix Corporation, Aerospace Systems Division, Ann Arbor, Michigan, April 1969.

SYMBOLS

$A_{1...6}$	platinum bridge constants determined by calibration
$B_{1...6}$	platinum bridge constants determined by calibration
C	constant
dT/dz	mean vertical temperature gradient
G	system gain
I_E	bridge excitation current
J	heat flow
k	thermal conductivity
$\bar{m}$	mean value
n	point of constant input ratio
$N_{1...4}$	digital numbers
$N'_{1...4}$	$N - 4096$
R_0	resistance at 0°C
$R_{1...4}$	Wheatstone bridge arm resistances
R_{100}	resistance at 100°C
R_B	total bridge resistance
R_I	idealized output ratio
R_T	resistance at T°C
T	temperature in degrees Centigrade
T_R	reference-bridge temperature
TC	thermocouple
u	digit resolution (2.4412 millivolts)
v^+, V^+	positive voltage
v^-, V^-	negative voltage
v_e	sensed reference-bridge excitation voltage
v_o	reference-bridge output voltage
v_{off}	error offset voltage referred to amplifier input
V_E	bridge excitation voltage
V'_E	sensed bridge excitation voltage
V_L	potential difference across 20-ohm resistance for current I_E
V_O	bridge output voltage
V_T	potential difference across 2-ohm resistance for current I_E
V_X	voltage at connection point X
V_Y	voltage at connection point Y
$X_{1...4}$	calibration constants for reference bridge
z	vertical distance
Z	attenuation ratio V'_E/V_E
α_s	solar absorptance
β	Van Dusen calibration constant
δ	Callendar calibration constant
ΔT	temperature difference in degrees Centigrade
ϵ	system error offset
ϵ_0	output-sense-line offset
ϵ_1	excitation-sense-line offset
ϵ_{IR}	infrared emittance
σ	standard deviation

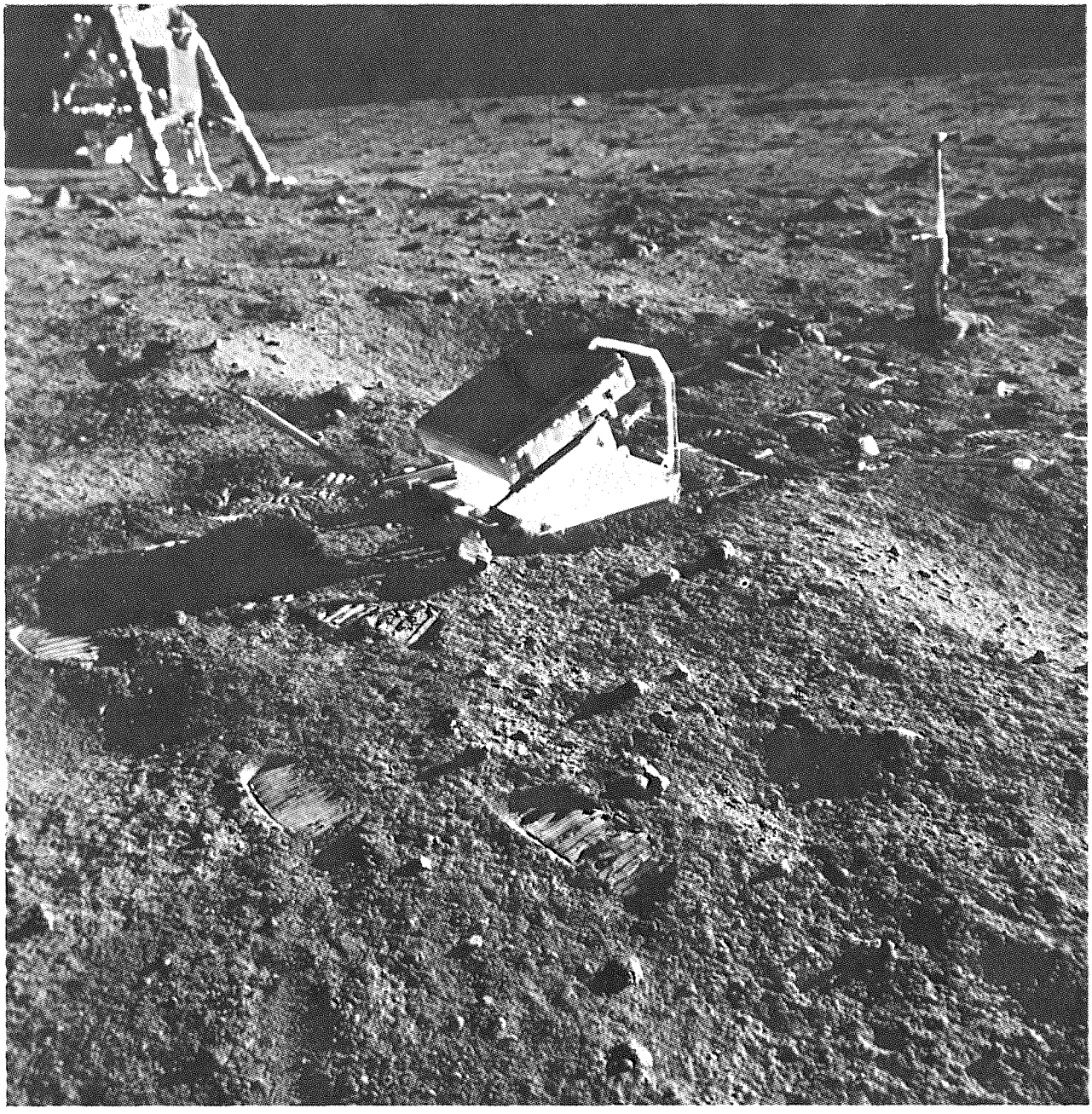

The Laser-Ranging Retroreflector

J. M. BRUEGER

The optical corner cube, or retroreflector, is a device that reflects an incident light beam – such as a laser beam – directly back to the beam source. The time interval between beam transmission and receipt of the return beam is a measure of the distance between the beam source and the retroreflector. This paper describes three laser-ranging retroreflector (LRRR) instruments, which were deployed on the lunar surface as part of Apollo missions 11, 14, and 15 to provide data on earth/moon distance variations. Array design, structural support, and deployment and alignment are discussed in detail. The development of passive thermal control for the arrays and related optical performance are also described.

INTRODUCTION

The Laser-Ranging Retroreflector (LRRR) Experiment represents the latest and most promising effort on the part of man to accurately measure variations in the distance between the moon and the earth over long periods of time. Such measurements, which are expected to provide new insight into earth and moon motions,[1] have been made by means of radar since 1957 to accuracies of ±0.7 mile. Subsequently, light from ruby lasers was transmitted to the moon through telescopes, by a group at MIT in 1962 and by another in Russia in 1964, and weak return signals were detected. The first distance measurements based on this technique were made by the Russians in 1965 to accuracies of about 600 feet, though it was recognized that a laser beam returned from the irregular curved lunar surface had inherent accuracy limitations.

Conceptually, the LRRR experiment originated at Princeton University in 1959, when a group there formulated a proposal for making precise optical measurements of satellite position by means of a retroreflector on the satellite and an earth-based light. In 1965, this same group proposed that a retroreflector be placed on the moon to implement distance measurements, this on the basis of a suggestion first made when the MIT group reported its ruby-laser success in 1962.[2] Shortly thereafter, the Lunar Ranging Experiment (LURE) group[1] was formed. The number and diversity of the scientific areas that are represented among the members of this group reflect the broad applicability that is anticipated for the experimental measurement data.

[1] The Principal Investigator for the Laser-Ranging Retroreflector, J. E. Faller of Wesleyan University, suggested the basic preliminary array design in a proposal submitted to the National Aeronautics and Space Administration by the Lunar Ranging Experiment (LURE) group in 1965.

EXPERIMENT CONCEPT

In principle, the optical retroreflector or *corner cube* functions like a bicycle taillight reflector or a luminous traffic sign; it reflects light back to the source, almost regardless of source location. Internally, the perpendicular back faces of the retroreflector operate on a light beam much as the walls and ceiling at the corner of a room operate on a ball thrown directly at the corner, the light returning on a line parallel to the path on which it entered the retroreflector, as illustrated in Figure 1.

Two considerations dictated that the retroreflectors in the LRRR array have small diameters – of the order of 1.5 inches. First, thermal gradients in the retroreflector result in optical distortion of the return signal, and the amount of this distortion is directly related to the diameter of the retroreflector. Second, because relative motion between the earth station and the moon displaces the center of the return signal, the signal must have a diffraction pattern wide enough to include the earth station in the return beam; diffraction-pattern width is a function of retroreflector size,

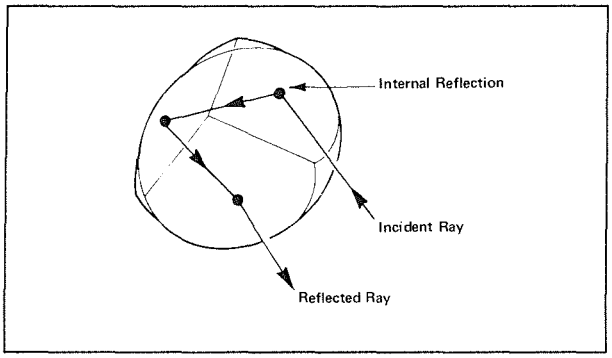

Figure 1 Typical Path of Laser Ray in Retroreflector

and although any diameter of less than 5 inches provides a wide enough pattern, diameters of less than 1.5 inches result in too great a pattern spread and, in turn, in too low a signal strength at the earth station. Signal strength could be increased by increasing the number of retroreflectors, but experiment-package size and weight constraints place an upper limit on this number. Signal strength could also be enhanced by coating the back faces of the retroreflectors, but this alternative was rejected because such coatings have a questionable lifetime and might result in thermal degradation.

At the laser-transmitting and -receiving station on earth, a telescope is used both in conjunction with beam generation and in conjunction with return-ray reception, as illustrated in Figure 2. Without the telescope, the beam transmitted would be spread over a diameter of about 300 miles on the moon; with a 100-inch telescope, beam divergence is reduced to the limit set by atmospheric turbulence under good viewing conditions, estimated to be a little more than a mile in diameter at the lunar surface. Thus more light is concentrated on the retroreflector package. A telescope is also used to collect the diverging light beam reflected from the retroreflector array and to direct it by optical means to a detector system. The accurate measurement of the time interval between laser-pulse transmission and return permits one to arrive at an accurate distance measurement. Pulse-length and time-measurement accuracies of the order of nanoseconds are currently achieved, and subnanosecond accuracies are anticipated for the future. The current distance accuracies are of the order of ±6 inches (±15 centimeters).

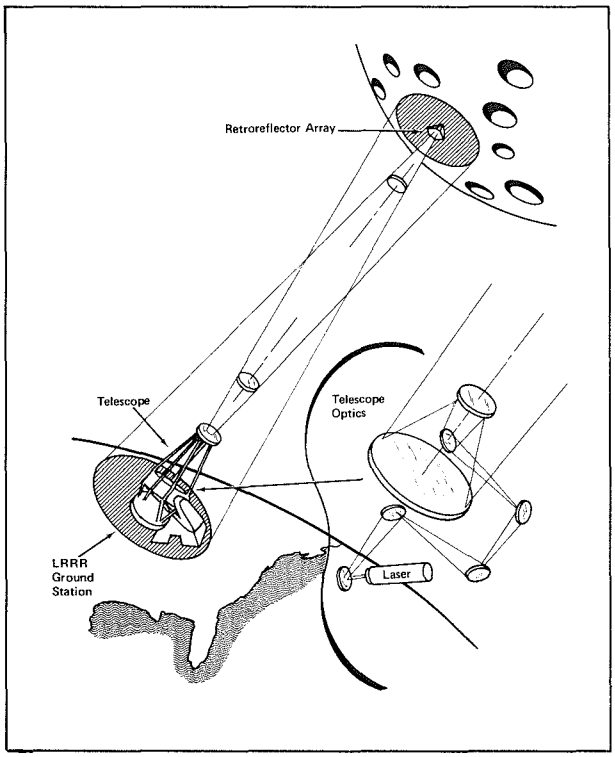

Figure 2 Optical Path of Laser Ray in Laser-Ranging Distance Measurement

THE APOLLO 11 RETROREFLECTOR

The Laser-Ranging Retroreflector was one of the two scientific instruments in the Early Apollo Scientific Experiments Package (EASEP), which was deployed on the lunar surface by the Apollo 11 astronauts in July 1969. Its selection for that mission – experiment planning for which began less than a year before launch – was based on the relative simplicity of its design, the completely passive nature of its operation, and, in particular, the broad applicability of the data it would provide to the scientific community in this country and abroad.

Constraints were imposed on the design of the LRRR both by the Apollo mission on which it was to be flown and by the experiment itself. To be flown on Apollo 11, the scientific package was to be mounted in the descent stage of the Lunar Module. It had to meet constraints with respect to envelope, weight (65 pounds), and center of gravity. It had to be capable of surviving mechanical and thermal environmental extremes. It had to be deployable on the lunar surface by a single life-support-suited astronaut within a 5-minute period. The very short time that was available for developing the EASEP imposed two further requirements unique to the Apollo 11 instrument: It had to use an existing ALSEP subpackage 2 pallet as the primary support structure, and it had to be capable of installation in the narrow confines of the spacecraft/Lunar-Module-adapter (SLA) section of the Apollo launch vehicle.

The performance requirements were those unique to the experiment itself. The LRRR was to provide an array of 100 retroreflectors. A machined-block array structure was dictated by the need to minimize design effort and schedule risk. Provision had to be made for aiming the array toward earth from any one of five equatorial lunar landing sites and for leveling the package without external tools or devices. Thermal control was to be passive, using a fixed-louver configuration with a height-to-width ratio (L/D) of 0.5* and such thermal coatings, finishes, and insulating materials as might be required. The performance requirement – expressed in terms of energy-return efficiency relative to an isothermal retroreflector over the lunar time cycle – was an 80 percent minimum return for 75 percent of the lunar cycle and a minimum return at any time in the cycle of 30 percent.

*This requirement was based on previous LURE group studies, the results of which are detailed in Reference 3.

The desired operating life of 10 years was not imposed as essential because of lunar environment uncertainties.

A flight model of the instrument that was developed to meet the above constraints is seen in Figure 3. Its final weight was 51.9 pounds. Design details and associated analyses are presented in the sections that follow.

Retroreflector Development

Verification tests of individual retroreflectors, conducted by the LURE group in 1966,[4] confirmed the optical performance of the small-diameter retroreflector and demonstrated retroreflector endurance over extreme thermal cycles. A new and more rapid technique for conducting interferometer tests on individual retroreflectors was also developed, which made possible more rapid production.

The retroreflectors used in the Apollo 11 array were fabricated and tested under the direction of the LURE group and provided to this facility as Government-furnished equipment for installation in the LRRR models. To ensure a compatible retroreflector mount design, requirements governing envelope, weight, and mounting-interface dimensions were defined in an interface control drawing. Each retroreflector was machined from a diagonally halved cube of quartz, with three circular segments left on its periphery as mounting tabs. A high-purity quartz* obtainable only from West Germany was used, along with unique final finishing techniques, proprietary to the supplier. Back-face flatness was held to $\lambda/10$ and top-face flatness to $\lambda/4$, λ being the wavelength of the laser light (6943 Å).

Individual retroreflector testing was limited to demonstration of wavefront deviation performance, using an automatic measuring technique.[5] For the Apollo 11 retroreflectors, back-face perpendicularity – in terms of maximum root-mean-square wavefront deviation of a reflected beam – was specified at $\lambda/14$. The performance actually achieved exceeded this specification to such an extent that only retroreflectors with deviations of $\lambda/18$ or less were used in the flight model. For retroreflectors in subsequent LRRR arrays, the specification was increased to $\lambda/20$.

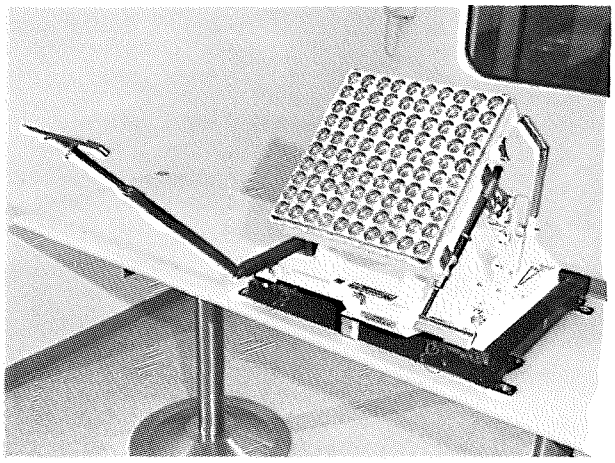

Figure 3 Apollo 11 Laser-Ranging Retroreflector

Array Design

The retroreflector array functions to support and align the retroreflectors, to protect them from the Apollo mechanical environment, and to provide thermal control in the lunar environment.†

For the Apollo 11 array, a structure was required that would support 100 retroreflectors in a mount design compatible with retroreflector shape and tab configuration. Alignment of each retroreflector was to be maintained within ±2 degrees of the mean retroreflector alignment, which, in turn, was to be within ±0.25 degree of an array reference direction. The mount was to be so designed as to minimize thermal conduction and to permit relative motion between the reflectors and the mount components for minimum thermally induced loads. Array support brackets, with specified orientations, were to be provided at four designated places on the underside of the array. Close-tolerance mounting of two additional brackets was required for later installation of the array-aiming handle.

The array panel structure was machined from a solid 6061-T6 aluminum block 4 inches thick and 18 inches square (see Figure 3). The choice of material and alloy was based primarily on considerations of availability, strength/weight ratio, machinability, corrosion resistance, and desirable thermal properties. Machining was favored over other techniques because it simplified fabrication control. The finished structure was composed of 4-inch-deep orthogonal webs, spaced about 3.5 inches apart, with a 0.05-inch-thick diaphragm left at midheight to provide lateral stiffness. The orthogonal pattern of 100 circular cavities in the upper section of the panel is so laid out that web continuity is fully maintained across all dimensions. Mounting brackets are bolted directly to the lower edge of the webs at locally thickened intersections. Tooling was used to machine the holes that interface with the LRRR support structure. Holes drilled in the top face between cavities to

*Amersil's Supersil I Special Grade.

†Retroreflector-array design studies were undertaken by the LURE group and the LRRR contractors as early as 1967. These initial efforts were based on integration of the experiment with the mainline ALSEP system and included development of thermal analysis techniques and preliminary thermal and structural design studies.

reduce weight were covered for thermal control reasons.

The mount design for the individual retroreflectors, shown in Figure 4, utilizes two Teflon rings, one above and one below the tapered tabs on the retroreflector. An indexing tab on the top face of the lower ring fits against the back face of the retroreflector to control rotational position. The lower ring sits on a shelf machined into the cavity; a slot in its lower edge mates with a pin protruding from the shelf. The retroreflector/Teflon-ring assembly is confined to its cavity by a threaded aluminum retainer ring and locked in place by the deformation of a number of threads in the panel. An axial clearance of 0.002 to 0.003 inch, provided to minimize thermal conduction, permits finite movement of the retroreflector; however, no damage results. The axial length of the Teflon rings and the taper of the retroreflector-mount tabs are such that, as the mount assembly experiences temperature change, the differential thermal expansions (radial and axial) between the quartz, Teflon, and aluminum are complementary, and mount clearance does not change significantly.

Thermal/Optical Design

Once the Laser-Ranging Retroreflector is deployed on the lunar surface, its optical performance is dependent on passive thermal control. Temperature gradients in a retroreflector cause spatial variations in its index of refraction, which reduce the central irradiance of the return-beam far-field diffraction pattern. The goal of the passive thermal-control design, therefore, was to maintain each retroreflector in a nearly isothermal condition in the changing lunar thermal environment.

Retroreflector temperature gradients can result from radiative and conductive heat transfer between the retroreflector and the array structure, from solar

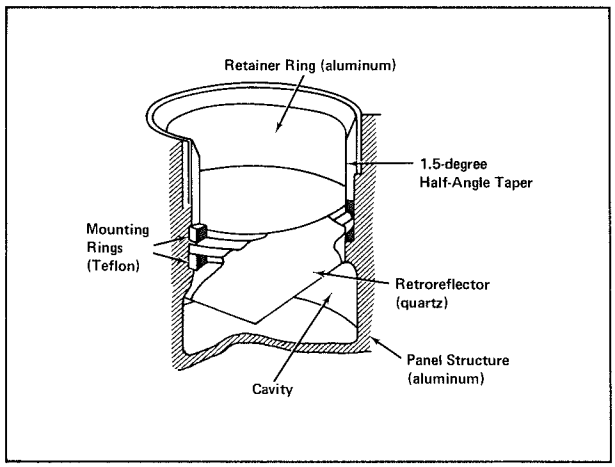

Figure 4 Apollo 11 Retroreflector Mount

radiation, from infrared radiation from the lunar surface, and from radiation emitted by the retroreflector to space. Early thermal-control analyses identified as most promising a design concept in which the retroreflectors are recessed in cylindrical cavities that act as louvres, partially shielding the retroreflector from incident solar radiation and restricting the view between the retroreflector and space. Further thermal isolation is achieved by using low-conductance mounts, by minimizing the emittance of the cavity surface below the retroreflector, and by insulating the bottom and sides of the array structure.

Thermal design parameters were established and optical performance of the selected design was predicted from thermal/optical analyses involving three distinct computer programs. A thermal analysis program was used to predict the temperature distributions in the retroreflectors as a function of sun angle and array-design parameters. A ray-trace program was used to develop the phase shift of a number of rays passing through the thermally perturbed retroreflector. These phase-shift data were then used in a Fourier transform program to obtain the irradiance distribution in the far-field diffraction pattern.

The thermal model used in the thermal analysis program to represent thermal coupling with the retroreflector is shown in Figure 5. A seven-sided prism, developed from a tetrahedron and divided into five zones, was used to represent the retroreflector. Confidence in the thermal-analysis computer program was established by running single-retroreflector-mount conductance tests. The computer central-irradiance program was verified by comparing computer results with an analytical solution of the *linear vertical temperature gradient* case.

The thermal design that resulted from parametric analysis was intended to thermally isolate the retroreflector from heat sources and to minimize retroreflector thermal gradients by heat transfer. Conductance through the mount rings was minimized by fabricating the rings from Teflon and by permitting axial clearance in the mount assembly. Machined 6061 aluminum provided a low-emittance cavity surface to minimize heat transfer between the cavity and the back surface of the retroreflector when the sun angle is such that solar heat is not retroreflected. To maximize heat transfer to space and to the top surface of the retroreflector, the retainer ring was given a high emittance by using a clear anodize on an 1100-series aluminum, the intent being to decrease the structure temperature and to balance the heat being emitted to space by the top surface of the retroreflector. Structure heating, which tends to increase retroreflector temperature gradients, was further minimized by the low solar absorptance of the polished top surface of the aluminum array structure. Absorption of solar

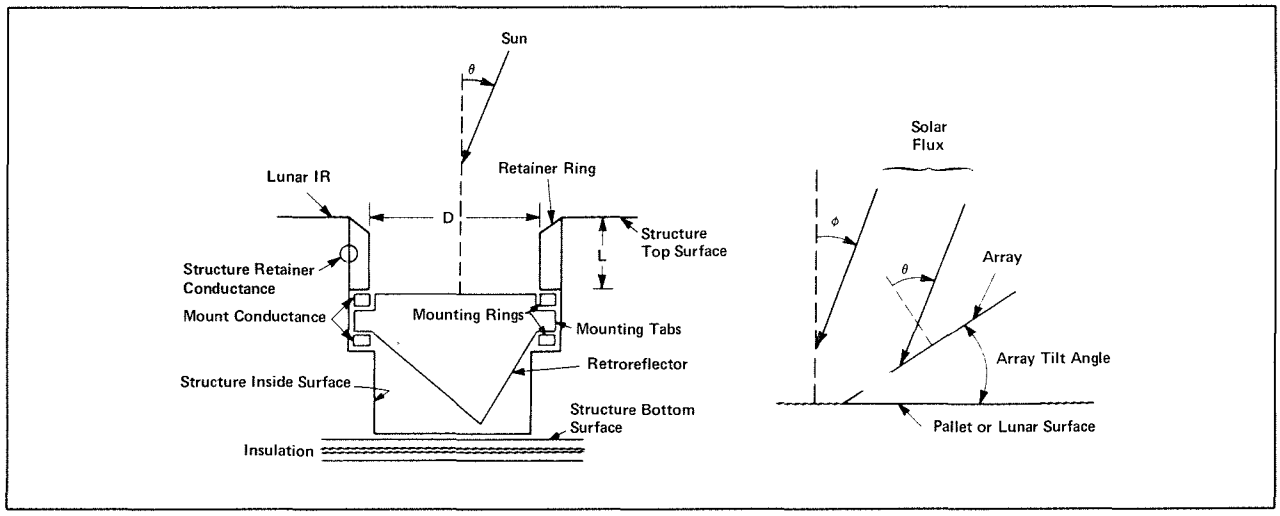

Figure 5 Retroreflector-Array Thermal Model

and lunar-surface radiation on the back and side faces of the array was minimized by a multilayer insulation blanket, constructed as shown in Figure 6.

An evaluation of the effect of heat conduction to the support structure revealed that, in general, retroreflector temperature gradients are reduced as heat is transferred out of the array. A separate system thermal analysis was used to calculate the temperature levels of the array and the support structure and the resultant heat exchange. The model for this analysis included array thermal characteristics that were obtained from the array thermal analysis described above. The results provided data on net heat flow as a function of sun angle and array orientation for the various potential lunar landing sites. On the basis of these results, a Z-93 thermal coating was selected for the top of the support structure to minimize net heat flow into the array at any of these sites. It was estimated that, at the primary landing site, support-structure temperatures would be lower than array temperatures for most of the lunar day; heat would be expected to flow into the array only when the sun direction was normal to the array top surface, in which case solar radiation is retroreflected, or when the sun direction was 70 degrees or more away from normal, in which case the cavity walls most effectively block solar radiation from entering the cavities. Array temperatures fall to their lowest lunar-day levels under these circumstances.

Thermal/optical performance at the prime landing site was predicted in a final analysis, using the array/support-structure heat exchange data and the thermal design parameters selected for the array. The results are presented in Figure 7, where central irradiance (relative to that of an isothermal retroreflector) is plotted against sun angle for arrays with and without array/support-structure heat exchange. It can be seen that heat exchange generally upgrades performance in terms of central irradiance. The curves have a shape characteristic of a retroreflector in a cavity. The two low-performance regions correspond to solar-radiation angles of incidence outside the range in which solar radiation is retroreflected. Retroreflection occurs when angle θ in Figure 5 is between -16

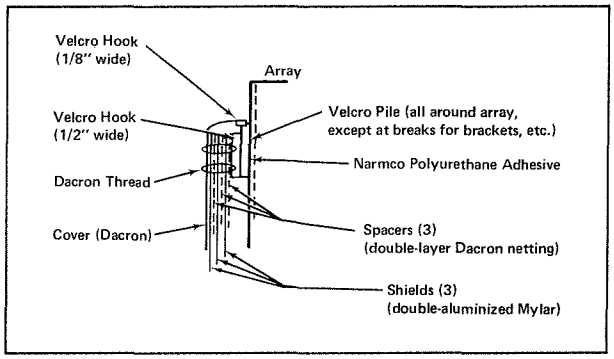

Figure 6 Retroreflector-Array Multilayer Insulation Blanket

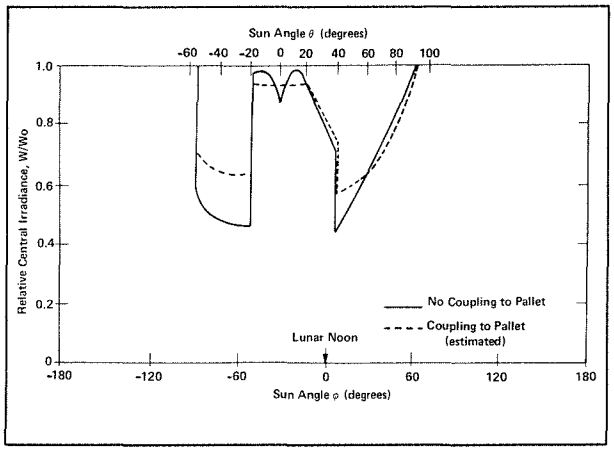

Figure 7 Predicted Thermal/Optical Performance (Apollo 11 LRRR)

degrees and +45 degrees if the retroreflector real back-edge is oriented toward the lower array edge. The degraded performance is terminated by the sun falling below the horizon or by solar radiation being cut off by the cavity walls.

An additional thermal requirement was imposed late in the development program, when a final decision was made as to how far the EASEP would be deployed from the Lunar Module. Based on this distance, it was predicted that the LRRR would be exposed to a heating rate of 1 to 2 BTU per second per square foot for 10 seconds during Lunar Module ascent-stage lift-off. Since it was anticipated that deterioration of the array insulation assembly might result, the flight-model array was given the additional protection of a blanket composed of aluminized Kapton film and layers of beta-fiberglass cloth and netting.*

Structural Support

The Apollo 11 LRRR structural support hardware, shown in Figure 8, was designed to support the array during storage, transportation, handling, testing, loading into the Lunar Module, space flight, lunar deployment, and a possible 10 years of lunar surface operation.

Program schedule requirements dictated that an existing ALSEP subpackage 2 pallet be used as the primary support structure. This aluminum honeycomb pallet had an aluminum machined-channel edge frame and four titanium interface fittings designed to mate with four interface pins in the Lunar Module. Slide bars on the Lunar Module projected through the forward pallet fittings to lock the pallet on the pins. An astronaut-operated handle on the Lunar Module removed the slide bars to permit deployment on the lunar surface.

The structural interface between pallet and array consisted of four adhesive-bonded posts, each of which provided a clevis to mate with the bracket on the array. The two pins through the forward interfaces acted as structural tie-down pins and as pivots during array tilting. The two pins through the rear fittings also acted as structural tie-downs but had to be removed by astronaut operation of two deployment handles to permit array tilting. Constraints on post location and maximum tilt-angle requirements established the height of the posts. The design proved to be simple and reliable, though it did not represent a minimum-weight approach.

The angle-indicator bracket and the sun-compass plate, to be described later, were fastened to the pallet using removable fasteners and locating indices to make possible the easy exchange of these items within the space constraints of the SLA. Such exchange would have been required to minimize array-aiming errors had there been changes in launch date and/or landing site. A forward tie-down bracket for the alignment handle was permanently mounted to the pallet by fasteners and adhesives. The astronaut carry handle, riveted to the edge frame and already assembled on the pallet, had provisions for pin tie-down of the boom-attachment assembly. Two rear-support tie-down brackets were mounted to the pallet, using fasteners and adhesives, to provide female fittings for the rear-support assembly. Quick-release pins fastened the rear support to the brackets to facilitate assembly in the SLA prior to installation in the Lunar Module. Envelope constraints in the SLA made it necessary to install both the rear-support and the boom-attachment assemblies on the LRRR at the Lunar Module scientific equipment bay door.

Alignment and Deployment Mechanisms

Having reached the moon, the Apollo 11 LRRR package was to be removed from the scientific equipment bay in the Lunar Module and carried to a deployment site about 60 feet south of the Lunar Module. Here the protective cover was to be removed and the array was to be unlocked, rotated to a tilt or elevation angle appropriate to the landing site, and locked in this position. The package was then to be lowered to the lunar surface and moved along the surface until it was aligned in the proper azimuth and

*Beta cloth is a high-temperature material used in astronaut spacesuits. The upper limit of its useful temperature range is 1200°F.

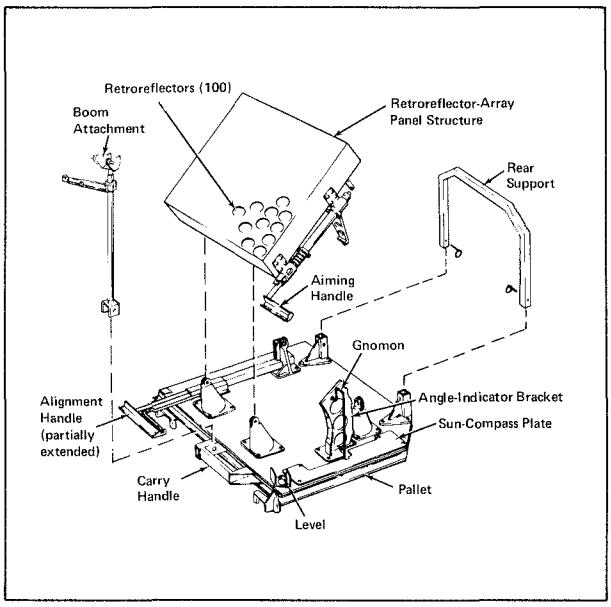

Figure 8 Mechanical Assembly (Apollo 11 LRRR)

the Apollo 11 LRRR, but it was to be stowed on a vertical bulkhead in Quad I of the Lunar Module. It was to have the Apollo 11 array design, but a maximum weight of 48 pounds and a lower center of gravity and envelope height. The support structure and deployment mechanisms were to be compatible with this lower weight as well as with a single deployment site (Fra Mauro) and the use of the ALSEP universal handling tool for alignment and leveling. Finally, the package was to be capable of withstanding the vibration environments unique to its Quad I location as well as all other environments to which the Apollo 11 instrument was exposed.

The Laser-Ranging Retroreflector developed to meet these requirements is seen in Figure 9. The final weight of the package was 45.6 pounds. Its components and its thermal/optical performance are discussed in the sections that follow.

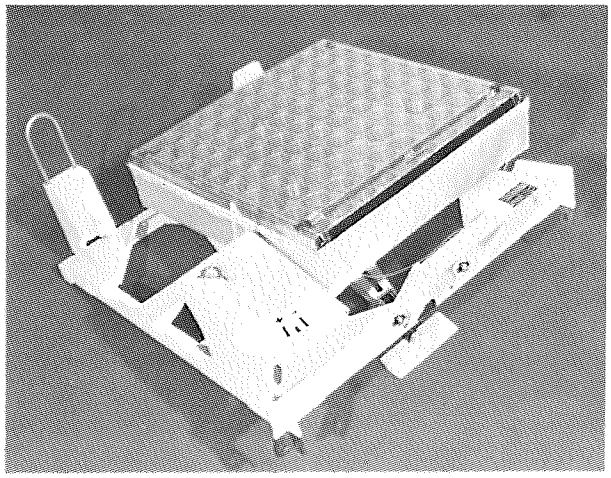

Figure 9 Apollo 14 Laser-Ranging Retroreflector

Retroreflectors and Retroreflector Array

As was the case for the Apollo 11 array, the retroreflectors were fabricated and tested under the direction of the LURE group and supplied to this facility as Government-furnished equipment. Because their extremely high quality had been previously established, the wavefront deviation requirement was increased to $\lambda/20$.

The basic Apollo 11 array design was used except that, at the suggestion of the Principal Investigator, the cavity taper above the retroreflector was increased to decrease the obscuration of the cavity walls at off-axis earth positions throughout lunar day and night. Some degradation in thermal performance was expected to result, since solar-radiation blockage would be reduced during limited periods of the lunar day, but analysis and test confirmed that the level of degradation (a 5 to 6 percent performance loss)

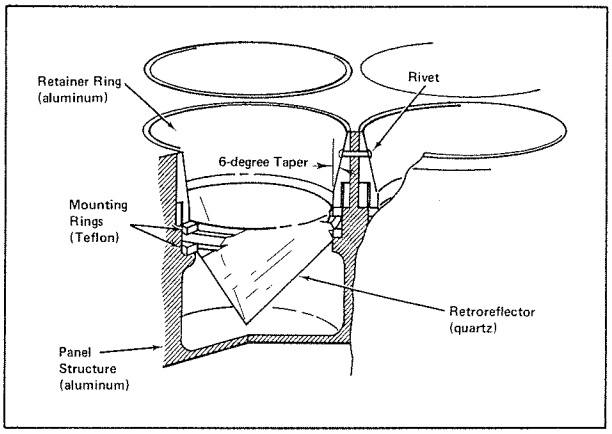

Figure 10 Apollo 14 Retroreflector Mount

would be acceptable and that structural integrity would not be compromised. Overall gains due to decreased obscuration were estimated by the Principal Investigator to be of the order of 30 percent over the total lunar cycle.

The modified mount design is shown in Figure 10. Note that the inside taper of the retainer ring is a 6- rather than a 1.5-degree half-angle and that there are minor changes in retaining-ring upper configuration and in array-cavity configuration. Note too that the retainer rings are retained by rivets rather than by thread-staking as in the Apollo 11 array.

Structural Support

Preliminary design evaluation suggested the advisability of using a simple frame structure as the basic Apollo 14 LRRR structural support. Although not as efficient as a honeycomb pallet from a structural-stiffness standpoint, the frame structure permitted greater design freedom and facilitated the development of a lighter, simpler package within cost and schedule constraints.

The Apollo 14 LRRR mechanical components are shown in Figure 11. The support structure is a riveted assembly of aluminum channel sections, with four titanium Lunar-Module-interface fittings and four aluminum array-interface fittings. The four array tie-down brackets are attached to the frame at these fittings by means of bolts that do not require release at the time of deployment; frame and array are tilted as a unit. All alignment and deployment mechanisms except the array protective cover are riveted to the frame.

Alignment and Deployment Mechanisms

The Apollo 14 LRRR had essentially the same mechanical requirements for alignment and deployment as the Apollo 11 LRRR. Provision for its

leveled so that the tilted array pointed toward the center of the earth's libration pattern.

The tilt-angle and tilt-axis-azimuth parameters for array deployment were determined from analyses of the geometry involved in directing the array, from a given coordinate point on the lunar surface, toward a point in space representing the center of the earth's libration pattern. Parameters for sun-shadow index markings were developed, based on the sun position anticipated at the nominal deployment time, to permit the astronaut to accomplish azimuthal array orientation by aligning the index markings with a shadow cast by a vertical gnomon. These parameters were established for five potential Apollo 11 lunar landing sites and for a variety of launch-date periods.

The mechanisms by which deployment and alignment are accomplished, seen in Figure 8, include the following:

- *Astronaut Carry Handle:* Attached to the edge frame of the pallet, the handle is shaped to conform to the gloved hand of the astronaut and is normally used to carry the package to the deployment site. By astronaut choice, the Apollo 11 package was actually carried by the tubular boom-attachment assembly, which is attached to the carry handle in the stowed configuration.
- *Boom-Attachment Assembly:* Interfaced with the Lunar Module boom, the assembly is usually used to lower the package from the scientific equipment bay of the Lunar Module.
- *Alignment Handle:* Initially, the handle releases the left rear array tie-down and locks, to provide a left-hand support for the astronaut while he is tilting the array with his right hand. In its second mode of operation, the handle extends to permit controlled lowering of the package to the lunar surface and movement of the package along the lunar surface to achieve alignment. In still a third mode, the handle locks in a raised position and remains within the reach height of the astronaut for initial package alignment and later adjustment.
- *Aiming Handle:* This handle is used initially to release the right rear array tie-down. It is subsequently used to tilt the array to the proper elevation angle and to lock it into this position.
- *Angle-Indicating Bracket:* On the bracket are index holes and visible markings for use in conjunction with the aiming handle to set the array tilt angle. The bracket on the Apollo 11 LRRR was marked for five sites. This bracket also supports the gnomon, the shadow of which is used to align the package.
- *Sun-Compass Plate:* This plate provides the sun-shadow index markings that are used in conjunction with the gnomon to align the package in azimuth. The plate on the Apollo 11 LRRR was marked for five sites.
- *Bubble Level:* By means of this bubble in a contained liquid (highly refined kerosene) and appropriate index markings, the array can be leveled to within ±1 degree. A light deflector diffuses incident sunlight for level illumination at low sun angles.
- *Array Protective Cover:* This cover provides nonhermetic protection from dust, debris, and contaminants within the scientific equipment bay of the Lunar Module prior to and during flight. It also protects from lunar dust during early phases of deployment.
- *Rear-Support Assembly:* A U-shaped assembly mounted at the rear of the pallet, this support permits the undeployed package to be set down on the lunar surface without overturning and prevents the array from coming into contact with lunar surface materials.

Lunar Surface Operation

The Apollo 11 Laser-Ranging Retroreflector was deployed with ease on the lunar surface in July 1969. First returns were received on 1 August 1969 through the 120-inch telescope at the Lick Observatory in California, a station that operated only during the initial acquisition phase. Returns were also received later in the month through the 107-inch telescope at the McDonald Observatory in Texas and through the 60-inch telescope at the Air Force Cambridge Research Laboratory in Tucson, Arizona. The McDonald Observatory is currently the primary station operated by the LURE group for the continuous acquisition of data.

THE APOLLO 14 RETROREFLECTOR

The LURE group recognized even before deployment of the Apollo 11 LRRR that additional laser reflectors deployed at widely separated locations on the moon would permit more accurate differentiation of lunar libration motion (wobble) from lunar orbital motion. Accordingly, a low-cost short-schedule program of LRRR development was begun in March 1970, with delivery scheduled for August and Apollo 14 launch scheduled for October. The basic Apollo 11 instrument design was to be modified to yield an instrument that would be lighter in weight and smaller in envelope size, the latter because of a new stowage location in the Lunar Module; it was to be deployable at an off-equator site, and its deployment was to require even less astronaut effort.

Specifically, the Apollo 14 LRRR was to have the same mechanical interface with the Lunar Module as

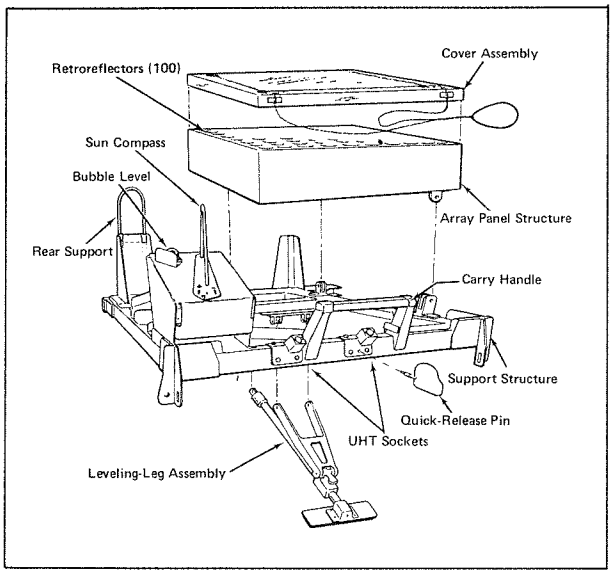

Figure 11 Mechanical Assembly (Apollo 14 LRRR)

removal from the Lunar Module was to be made via a Lunar Module adapter* to which the LRRR was to be mounted, the interface design being that used for the Apollo 11 package. This adapter, in turn, was to be mounted directly to fittings in the Quad I bay of the Lunar Module. Instead of the integral handles provided on the Apollo 11 LRRR, use of the ALSEP universal handling tool for lowering and maneuvering the package outside astronaut reach limits was to be implemented.

The mechanisms provided for deployment and alignment include the following:

- *Astronaut Carry Handle:* This handle permits the package to be removed from the Lunar Module adapter, carried to the deployment site, and handled during array-cover removal and leveling-leg deployment. Offset to place it over the package center of gravity, the handle is shaped to conform to the gloved hand of the astronaut.
- *Rear-Support Assembly:* This support prevents the package from tipping over when set on the lunar surface prior to deployment and protects the array from contact with the surface. Its tubular cross section and clear anodized finish minimize thermal radiation into the adjacent array cavities.
- *Leveling-Leg Assembly:* This assembly supports the array and its support structure at the proper array tilt angle after deployment. Locked in its stowed configuration by a ball-lock pull pin which the astronaut can remove by pulling on the ring attached, the leveling leg lowers itself and locks into position at a preset stop. A footpad on the leg permits the astronaut to assist in the lowering process if necessary. In the deployed configuration, the footpad combines with the lower edge of the support-structure frame, on which it hinges at two points, to form a stable triangular "footprint" capable of supporting loads somewhat larger than the maximum load an astronaut can apply through the UHT, even in a worst-case situation.
- *Sun-Compass Assembly:* This assembly consists of the index-marked sun-compass plate, the gnomon, and the bubble level, all of which are used to level the package and to align it in azimuth. The base of the assembly is formed-aluminum sheet metal. The assembly can be adjusted to meet the tolerance on the angle between the sun-compass top reference surface and the top array surface. A bubble-level indication of LEVEL means that the array is tilted at the angle prescribed for pointing from that specific Apollo 14 landing site. Because it was necessary to accommodate only a single site, it was possible to minimize the effects of variations in deployment time by using for alignment purposes a gnomon tilted into the plane of the sun so that its shadow is essentially time-independent. Pointing parameters for required sites and for a variety of launch dates were determined analytically. The bubble level, equipped with a light deflector, is identical in design to that used in the Apollo 11 LRRR.
- *Array Protective Cover:* The protective cover for the Apollo 14 LRRR array was identical to that used for the Apollo 11 array.

Thermal/Optical Performance

Design changes having been made in array orientation, in cavity configuration, in the number of thermal paths between array and support structure, and in the orientation of the support structure relative to the lunar surface, it was necessary to analyze thermal/optical performance once again to ensure that predicted performance was within specification limits.

It was found that the Apollo 14 LRRR array would be subjected to generally higher temperatures as a result of the higher solar absorptance and lower infrared emittance associated with the array-cavity design change. The structural support, thermally controlled by a Z-93 inorganic coating, was also expected to reach higher temperatures because of increased radiation heating by the lunar surface and reduced radiation losses to space. However, the maximum temperatures predicted did not exceed those to which

*Supplied by the Lunar Module contractor.

the Apollo 11 array and structure had been exposed in thermal/vacuum tests. The introduction of the two new thermal paths between the array and the support structure was expected to enhance heat leakage between the two.

The general impact of these changes was to improve overall thermal/optical performance, as shown in Figure 12. Although some degradation occurs at sun angles nearly normal to the array, performance remains high because the solar radiation to the array is nearly totally reflected by the retroreflectors, reducing array temperature.

Lunar Surface Operation

The Apollo 14 Laser-Ranging Retroreflector was successfully deployed at Fra Mauro on 5 February 1971. The McDonald Observatory, the prime data-acquisition station, has been receiving returns from it since that night.

THE APOLLO 15 RETROREFLECTOR

The decision to carry still a third laser reflector on either the Apollo 15 or the Apollo 16 flight was made while the Apollo 14 LRRR program was in progress. On the strong recommendation of the LURE group, the new array was to be made up of 300 retroreflectors and be located off the moon's equator. The greater size of the array would increase its optical efficiency and permit the use of subnanosecond pulses, which have inherently less energy but increase ranging accuracy. It would also increase the rate of data acquisition by increasing the probability of obtaining returns under less-than-optimum seeing conditions at the ground station. Finally, it would permit ranging by smaller telescopes (down to diameters of approximately 40 inches), freeing the telescope at the prime station in the United States for other observing

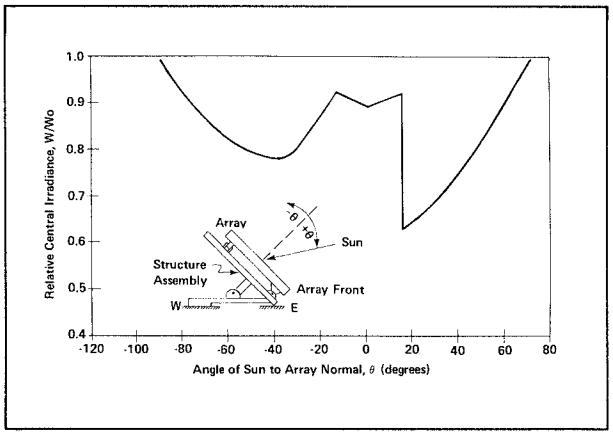

Figure 12 Predicted Thermal/Optical Performance (Apollo 14 LRRR)

programs and increasing foreign participation; the latter was important because the measurement of earth wobble and rotational variations is dependent on frequent returns at worldwide stations. The emplacement of this third array, at a point off the equator of the moon, would make available three noncollinear reflectors, which would permit still better differentiation of longitudinal and latitudinal moon librations from moon orbital motions. It might also permit separation of lunar tidal effects, and could provide evidence of irregular fluctuations in lunar rotation rate and polar position, which relate to the possibility of a fluid core and free librations of the moon.

Since the proposed landing site for the Apollo 15 flight was a desirable location for a third Laser-Ranging Retroreflector, every effort was to be made to meet the Apollo 15 schedule of deadlines. Nevertheless, the design was to be flexible enough to provide for pointing from any of the then anticipated Apollo landing sites. Long-lead retroreflector procurement began in July 1970, design efforts were initiated in August, and the program went into full operation in September.

The requirements imposed on Apollo 15 LRRR design were similar to those imposed on previous designs, with the following exceptions:

- Weight was not to exceed 97 pounds.
- Center-of-gravity requirements were changed by Lunar Module requirements, but envelope constraints remained the same.
- A greater vibration-survival-capability requirement was imposed by a new stowage position in Quad III of the Lunar Module.
- The array was to contain 300 retroreflectors, mounted as in the Apollo 14 LRRR.
- The alignment mechanisms were to be flexible enough to permit deployment at any landing site then being considered for future Apollo flights.

The Laser-Ranging Retroreflector that was designed to meet these requirements is seen in Figure 13. The final package weight was 79.8 pounds. Design details are presented in the sections that follow.

Retroreflector Procurement

The performance requirement imposed on retroreflectors for the Apollo 15 LRRR array was identical to that imposed on those for the Apollo 14 array – namely, a wavefront deviation of $\lambda/20$ or less. Schedule constraints permitted the fabrication and test of only enough flight-quality retroreflectors to implement the flight model; retroreflectors for the qualification-model arrays were fabricated from a lower quality quartz and to the interface dimensions only.

Array Design

Schedule constraints had predominated over weight constraints in array design for the Apollo 11 LRRR and were largely responsible for retention of the same design in the Apollo 14 LRRR. Now the very rigid weight constraints imposed on the Apollo 15 LRRR required that basic array design be critically reviewed. Since a threefold increase in the number of retroreflectors to be mounted had to be accommodated in a package weighing only about 50 percent more than the Apollo 11 package and 100 percent more than the Apollo 14 package, a higher mounting efficiency was obviously needed. In addition, a multisite aiming capability had to be incorporated. Weight constraints thus acquired a higher priority than schedule.

Two major design changes were made: The main array structure became the primary support structure as well, and a staggered or close-packed array-cavity spacing was substituted for the original orthogonal arrangement. Envelope constraints required that more than one panel be used; to keep weight as low as possible, the decision was made to use two panels, hinged to facilitate deployment. Center-of-gravity requirements permitted the off-center mounting of the upper panel, and provision was made for its permanent removal in recognition of the possibility that weight constraints might be further tightened for later Apollo flights.

Like the earlier arrays, the Apollo 15 arrays were machined from solid 6061-T6 aluminum blocks. The large main panel is 25.8 inches by 21.8 inches in size and contains 204 retroreflector cavities. The smaller upper panel is 12.4 inches by 21.8 inches in size and contains 96 retroreflector cavities. The basic cavity design is that used on the Apollo 14 array, except that the cavities are orthogonally arranged in alternating rows only. The effect is to provide a closer packing of the cavities, as seen in Figure 13. Six thin-walled sections, all nominally 0.035 inch thick at the upper section of the cavity, are thus associated with each cavity, rather than four as in the previous design. This spacing required that extreme care be exercised in final machining and that the manufacture of spare array panels be closely scheduled. The structural/thermal mount design used is that shown in Figure 10.

Structural Support

The main array serves also as the primary support structure in the Apollo 15 LRRR. Both arrays have orthogonal vertical webs below the cavity section and a horizontal diaphragm between these webs and the cavity section to provide lateral stiffness. Titanium fittings, bolted to the main array by high-strength

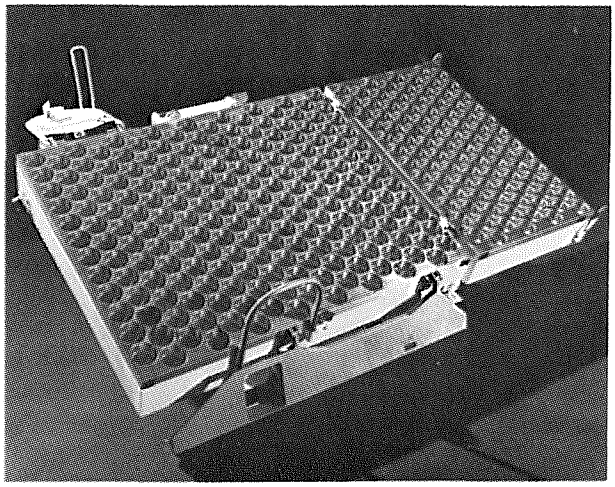

Figure 13 Apollo 15 Laser-Ranging Retroreflector

fasteners, serve as interface attachments to mate with the Lunar-Module-adapter interface pins and the astronaut-operated slide bars. The small upper array is supported on the large main array at two hinges and two tie-down brackets. The astronaut handle, sun-compass assembly, leveling-leg assembly, and rear-support assembly are all bolted to the front and rear webs of the main array.

Thermal/Optical Design

A preliminary thermal analysis, assuming the use of multilayer thermal insulation on the arrays and support of the arrays by the hinged leveling leg, revealed an unacceptable level of thermal/optical performance, in terms of reflected-signal relative central irradiance. The multilayer insulation and the high thermal resistance of the leveling-leg hinge interface had the effect of essentially decoupling the arrays from the lunar surface temperature environment. The resulting array temperatures were generally higher than those predicted for the Apollo 14 array except at times when direct solar radiation was being retroreflected by the Apollo 15 array.

It was necessary, therefore, to conduct a parametric trade-off study on the various thermal design techniques that could be used to implement heat transfer to the relatively cool lunar surface in the shadow behind the deployed arrays. The shadow is present throughout most of the lunar day, since the package faces nearly directly south from the prime site, a north-latitude site. Based on the results of the study, which are summarized in Figure 14, a Z-93 thermal coating was applied to the webs and undersides of the arrays and no multilayer insulation was used on the arrays. It was predicted that this thermal design would yield optimum performance, not only

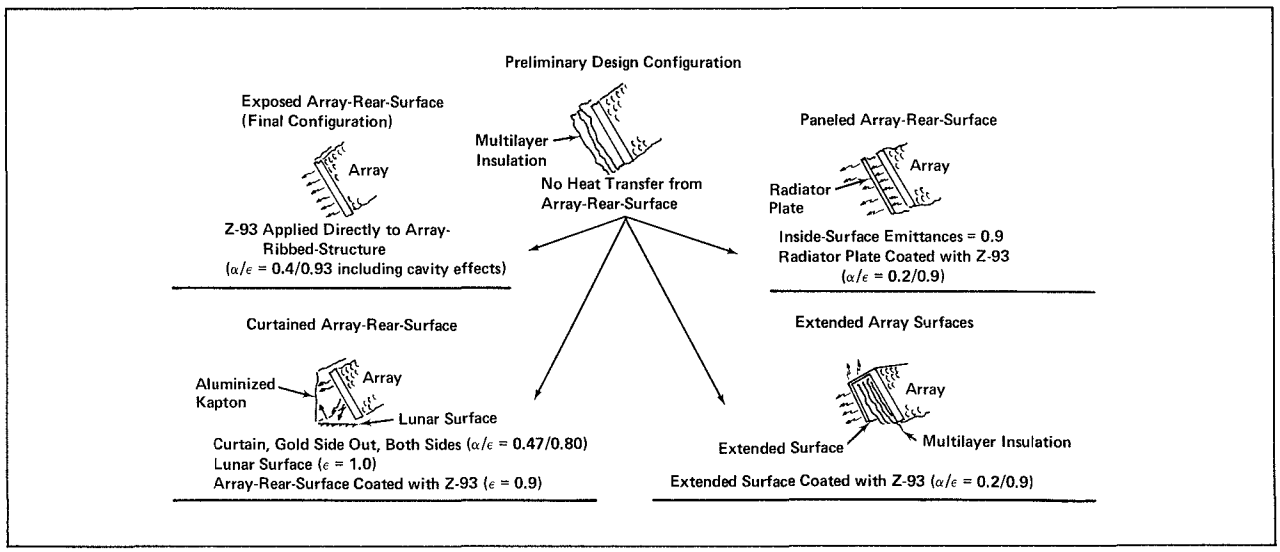

Figure 14 Candidate Techniques for Apollo 15 LRRR Thermal Control

at the prime deployment site – Hadley Rille – but also at alternative equatorial sites such as Marrius Hills, where direct solar radiation would impinge on the array bottoms at low sun angles.

For the Hadley Rille site, final predicted performance for the Apollo 15 LRRR (see Figure 15) surpassed specified thermal/optical performance requirements. The temperatures attained by the arrays should be well below those used in the thermal/vacuum tests (169°F as compared with 250°F).

Alignment and Deployment Mechanisms

In addition to the alignment and deployment functions for which mechanisms had to be provided in previous LRRR packages, provision had to be made in the Apollo 15 package for unlocking the small array and rotating it into the deployed configuration and for unlocking the sun-compass assembly from its stowed position, permitting it to move automatically to the deployed position. Other innovations resulted from the requirement that the alignment devices be

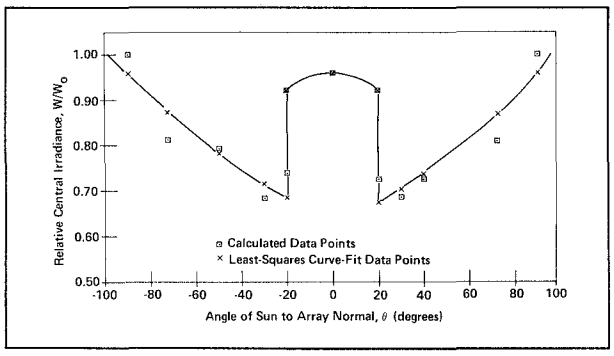

Figure 15 Predicted Thermal/Optical Performance (Apollo 15 LRRR)

flexible enough to implement array alignment at any Apollo lunar landing site. To this end, it had to be possible – just prior to stowage on the Lunar Module and without replacing any parts – to adjust the leveling leg, the sun-compass index markings, and the angle of the sun-compass reference surface for the appropriate site.

The innovative design features incorporated in the Apollo 15 LRRR deployment and alignment mechanisms include the following:

- *Small-Array Deployment Mechanisms:* To deploy the small array, the astronaut pulls on a lanyard stowed on the carry handle, thereby releasing two ball-lock pull pins that carry shear loads across the fore and aft tie-down brackets during stowage. The two arrays are hinged, and a handling knob is provided on the small array to facilitate its rotation into the plane of the large array. Spring-loaded plungers mate with latches to lock the small array into the deployed position.

  Sun-Compass Assembly: Because of LRRR envelope limitations, this assembly is hinged to the front of the large array and locked in the stowed position by a ball-lock pull pin. When the astronaut pulls a ring to remove the pin, the spring-loaded assembly automatically swings into the preset deployed position. The position stop is adjusted prior to stowage on the Lunar Module to provide an angle between the sun-compass reference surface and the array top surface such that, when the bubble level on the sun-compass assembly reads LEVEL, the array is at the desired tilt angle for pointing. A threaded adjustment and a lock nut implement the position-stop setup.

- *Leveling-Leg Assembly:* This assembly, which provides a triangular support for the arrays in the deployed configuration, is hinged at two places along the rear web and at one place on the front web of the large array. The assembly consists of two essentially rigid sections, a leg/footpad section that pivots at the array rear and a brace assembly that pivots at the array front and slides along the leg at its other end. The two sections are held in place by a ball-lock pull pin, inserted in the front end of the assembly. When the astronaut pulls and removes the pull pin, the leg section pivots down and the brace section pivots and slides along the leg until it is locked at a predetermined location by a keeper assembly. The rear support is designed to keep the arrays above the lunar surface. The length of the brace section and the position of the keeper assembly can be adjusted to yield the most structurally favorable section lengths. The leveling-leg setting provides the nominal array tilt angle; fine adjustment is then accomplished by maneuvering the package, using the universal handling tool, to embed the appropriate portion of the leg in the lunar surface until the level bubble is centered.
- *Array Alignment Mechanisms:* On the top surface of the sun-compass assembly is a plate, adjustable in azimuth and locked in place by threaded fasteners, on which index marks are inscribed and a gnomon is mounted. To properly align the arrays in azimuth, the astronaut inserts the universal handling tool into a socket on the LRRR, and, using it as a handle, maneuvers the package until the gnomon shadow is aligned with the center index mark and the level bubble is centered. Compass rose markings are provided on the compass base to assist in the prelaunch orientation of the index marks to an azimuth appropriate to the landing site. As in earlier programs, array-pointing parameters were generated by computer analysis of pointing geometry and site conditions.
- *Rear-Support Assembly:* Like the Apollo 11 and Apollo 14 LRRR packages, the Apollo 15 package is equipped with a U-shaped rear support to prevent its tipping over when set down on the lunar surface prior to deployment. Surface finish and shape were selected to minimize thermal effects.
- *Array Protective Covers:* Because of the possibility of off-loading the small array should that prove necessary, each of the two arrays was provided with a protective cover. Cover removal is accomplished by astronaut activation of lanyards.

Lunar Surface Operation

The Apollo 15 Laser-Ranging Retroreflector was deployed without incident at Hadley Rille on 31 July 1971. The McDonald Observatory team acquired the initial return signal on 3 August, when atmospheric conditions first permitted ranging; signals were acquired that same evening from the Apollo 11 and Apollo 14 instruments as well, demonstrating the present capability of a single ground station to range on all three sites. The fact that every subsequent attempt to range on the Apollo 15 LRRR has been successful may be largely due to the strength of its return signal. This signal strength – together with the existence of prominent landmarks near the Apollo 15 site, which simplify telescope aiming – is expected to encourage foreign use.

REFERENCES

1. J. E. Faller and E. J. Wampler, "The Lunar Laser Reflector," *Scientific American* **222** (No. 3), 38-49 (March 1970). These authors also summarize man's attempts to measure earth/moon distances during the past 2000 years.

2. C. O. Alley, P. L. Bender, R. H. Dicke, J. E. Faller, P. A. Franken, H. H. Plotkin, and D. T. Wilkinson, "Optical Radar Using a Corner Reflector on the Moon," *Journal of Geophysical Research* 70, 2267-2269 (May 1965).

3. "Analysis of Thermal Control Designs for Retro-Reflector Array," Final Report C-70472, prepared for the University of Maryland, Department of Physics and Astronomy, by Arthur D. Little, Inc., Cambridge, Massachusetts, 1968.

4. "Confirmation of Predicted Performance of Solid Fused-Silica Optical Corner Reflectors in Simulated Lunar Environment," Progress Report to the Planetology Subcommittee of the National Aeronautics and Space Administration, prepared by the Department of Physics and Astronomy, University of Maryland, College Park, Maryland, October 1966.

5. R. A. Jones and P. L. Kadakia, "An Automated Interferogram Analysis Technique," *Applied Optics* 7 (No. 8), 1477-1482 (August 1968).

ALSEP Human-Engineering Design Criteria

R. L. REDICK

The development of human-engineering design criteria for crew operations was one of the most challenging aspects of preparing for manned lunar surface exploration. This paper details some of the human-engineering guidelines that were developed for crew interface with the Apollo Lunar Surface Experiments Package (ALSEP). It traces in particular the development of the versatile universal handling tool, and describes briefly the crew-engineering mock-up used for human-factors evaluation and the astronaut trainer used for crew training.

INTRODUCTION

The emphasis placed on human engineering in the Apollo program in general, and in the development of the Apollo Lunar Surface Experiments Package (ALSEP) in particular, proved a considerable challenge to this infant profession. Little was known about human dimensions forty years ago. The airlines industries, as they emerged, developed rules of thumb with respect to cockpit reach and chair height, and airframe designers conducted studies leading to selected crew parameters. Still, at the time the Apollo program was initiated, the technical literature on human engineering was sparse and the accuracy of much of the existing data was questionable.

The Mercury program rapidly changed this picture. Some very ambitious human-engineering programs were undertaken by the armed forces, the National Aeronautics and Space Administration (NASA), and their industrial suppliers. By 1959, the old Joe and Josephine charts were both inadequate and out of date. The quantity and scope of the new data demanded a different format, more complex and more encyclopedic. Charts of the type shown in Figure 1 were developed, detailing, for example, anthropometric data for the adult American male and female.* Documentation efforts on the part of industrial and Government specialists led to the publication of some very excellent compendia of human-engineering information.[2,3,4,5] They, in turn, provided a point of departure for the development of design criteria for ALSEP hardware and astronaut tasks.

*Figure 1 is reproduced from Reference 1.

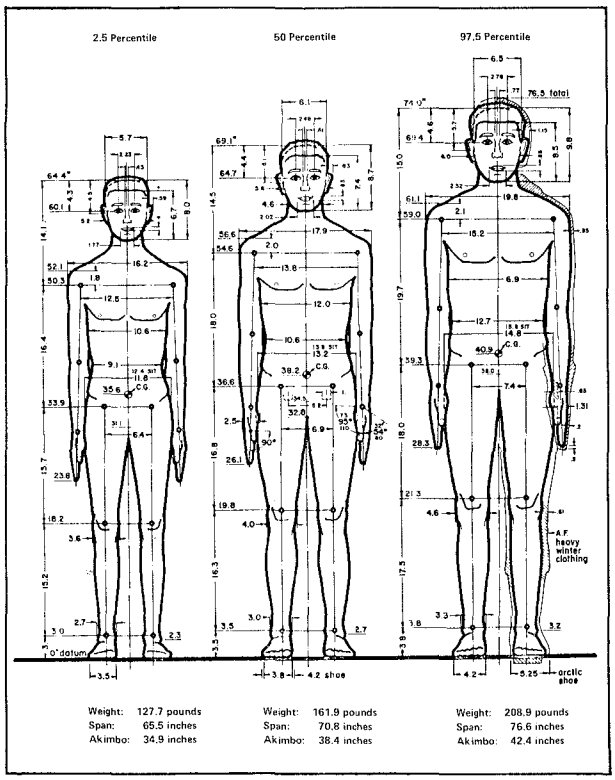

Figure 1 Anthropometric Data for Standing Adult Male

HUMAN-ENGINEERING DESIGN GUIDELINES

We at this facility were commissioned by NASA in 1965 to design, build, and test the Apollo Lunar Surface Experiments Package, which was to be transported to the lunar surface aboard the Lunar Module.

On the moon, the astronaut was to remove the package from the Lunar Module and deploy and properly orient the individual experiments. The experiments would then remain on the moon, operating after departure of the astronauts to complete the scientific mission.

Experiment design required that specifications be developed, establishing the most effective interface between the experiments package and the astronaut. These specifications were to be so defined as to optimize astronaut performance, minimize skill requirements and training time, maximize overall astronaut/equipment reliability, and foster design standardization within the system. They were to be flexible enough to permit interpretation and implementation by crew-engineering specialists should unanticipated situations such as landing-site changes or prime-crew preferences make this necessary.

The astronaut interface with the ALSEP occurs during extravehicular activity on the lunar surface. Insofar as overall system requirements and constraints permitted, it was desirable that ALSEP hardware enhance the effectiveness of the astronaut in experiment deployment and that astronaut tasks require a minimum of knowledge, skill, training, and procedural data. The human-engineering constraints imposed on both hardware and task design involved such parameters as mental and physical skill, crew training, science objectives, and Apollo mission psychophysical stresses. Consideration also had to be given to the psychomotor limitations imposed on the astronaut by the extravehicular mobility unit (EMU), the ergonomic limitations imposed by the portable life-support system / oxygen purge system (PLSS / OPS), and the effects of the lunar environment and the EMU on the visual, auditory, tactile, kinesthetic, vestibular, and thermal sensory modalities. Certain of the guidelines that were developed for hardware and task design are discussed in the sections that follow.

Mechanical Guidelines

To prevent mechanical degradation of the extravehicular mobility unit, the exterior of the ALSEP was to have no sharp edges, corners, protuberances, burrs, or abrasive surfaces in areas that the astronaut might reasonably be expected to contact. A minimum radius of 0.03 inch for any external edge or corner was specified, with beading recommended for those edges and corners where material thickness would not permit such a radius. Masking with Teflon tape was considered an acceptable alternative approach. Guards to preclude pinching or cutting the EMU were to be provided on all hinged surfaces and other moving parts.

Thermal Guidelines

Two potentially hazardous thermal conditions were to be precluded in the design of ALSEP equipment and deployment tasks. The astronaut was not to be brought into close proximity with any high-heat source that, through radiation, might cause thermal overloading of the PLSS or damage to the spacesuit. In addition, both astronaut and EMU were to be kept from physical contact with high-temperature surfaces that, through conduction and compacting of the insulating layers in the spacesuit, might damage the spacesuit or harm the astronaut. Where thermal analysis and/or thermal tests indicated the potential presence of such hazards, deployment operations and equipment were to be so designed as to isolate the astronaut from them to the greatest possible extent, assuming his adherence to prescribed task procedures and his exercise of normal caution.

The maximum heat flow to the skin of the astronaut that can be allowed to result from spacesuit contact with a hot surface is 18 BTU per square foot per minute. Spacesuit design permits safe contact with surface temperatures ranging from 250°F to -250°F, with a loading of 2.0 pounds per square inch, for a period of 3 minutes. Equipment to be held by the astronaut in such a way that the layers of his spacesuit are compressed for longer than 3 minutes was to be thermally controlled to yield a surface temperature range of 60°F to 103°F, ensuring that body pain thresholds for heat and cold (113°F and 50°F, respectively) are not exceeded.

All equipment surfaces that might represent a thermal hazard for either astronaut or EMU were to be monitored by a device that would provide a temperature-status readout to the astronaut.

Ordnance Guidelines

Astronaut interface design was to incorporate no device containing high explosives or combustibles that would require activation prior to experiment deployment or crew departure from the lunar surface. Any actuators and initiators included in experiment design were to comply with the following requirements:

- They were to be Apollo-approved and standardized.
- They were to be incorporated into the system in accord with the latest regulations for range safety.
- Their operation was to be protected by at least two nonstorable commands from the ground.
- Their firing circuits were to be isolated in the ALSEP system and were to contain protection from induction, stray voltage, and interference from other system circuits.

Operating Force Guidelines

ALSEP components – controls and actuation devices, in particular – were to be so designed as to require for their operation a minimum of energy expenditure on the part of the astronaut, with no exposure to such dangers as loss of balance.

Specifically, the astronaut was not to be called upon to exert more than 20 pounds of force in any given direction. Where experiment design required the application of a greater force, a lever arm or geared assist device was to be provided. The lanyard used in ALSEP cask removal, seen in Figure 2, is such a device.

Special care had to be exercised in designing astronaut-operated equipment to keep the level of force required for equipment operation below that required for moving or lifting the equipment. It would not be feasible, for example, to use a 5-pound pull-to-release pip pin to secure a part of a subsystem weighing 24 pounds on earth; on the moon the subsystem would weigh 4 pounds (one/sixth its earth weight), and the exertion of the necessary 5 pounds of pull force would actually lift the subsystem rather than release the fastener.

It was also specified that mechanical design take into account man's strength capabilities, and, where necessary, incorporate physical restraints to prevent the astronaut from imposing a force exceeding the tensile strength or inertia limits of the equipment. Under lunar gravity conditions, an astronaut can exert a static load of 20 pounds and, in extreme circumstances, dynamic loads as high as 60 pounds.

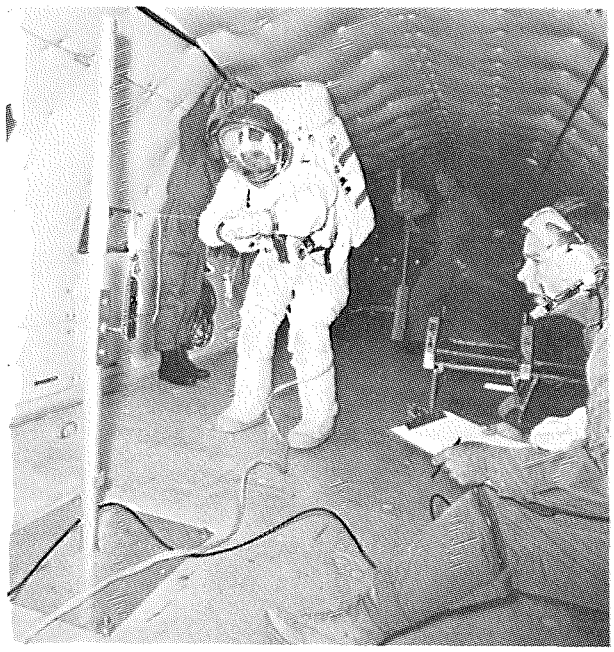

Figure 2 ALSEP Cask Lanyard Test on KC-135 Aircraft

Similarly, fine-adjustment mechanisms were to be constructed of materials capable of withstanding maximum torque loads, taking into consideration the fact that an astronaut can exert a 20-pound load when employing only one hand to operate an adjustment mechanism.

To ensure tactile feedback to the astronaut, he was not to be required to exert a force of less than 3 pounds at the point of application on any component or assembly, whether full-hand or fingertip. He was also not to be required to exert a torquing force in excess of 3.8 pounds on any component 0.75 inch in diameter or diagonal (for circular or rectangular cross sections, respectively); maximum torquing force was specified at 5.0 pounds for diameters or diagonals of 1.00 inch, at 7.6 pounds for diameters and diagonals of 1.25 inches, and at 9.6 pounds for diameters and diagonals of 1.50 inches. Finally, the astronaut was not to be required to exert a dynametric (gripping) force in excess of 10 pounds.

Other Guidelines

Similar human-engineering design parameters were developed in other areas for lunar surface operation in the EVA mode. Specifications were arrived at for leveling and alignment provisions; for astronaut tools, connectors, and switches; for such visual aids as numerals, sundials, gnomons, and decals for astronaut cuing; and for mobility constraints. The development of the prime astronaut tool will be discussed here in some detail. For a detailed review of the other parameters, the reader is referred to Interface Control Specification IC 314134 for Apollo 17.[6]

THE UNIVERSAL HANDLING TOOL

Human-engineering design studies yielded the requirement that integral and detachable tools and work aids be provided, which would permit the astronaut to deploy the ALSEP from a standing position. Such tools were to be suitable for use within the constraints imposed on the astronaut by the extravehicular mobility unit. These constraints, and a high center of gravity, limit the minimum reach height on the lunar surface to 22 inches for a work task and to 16 inches for a short-term operation such as grabbing or ring-pulling.

Tool Description

The universal handling tool (UHT), seen in Figure 3, was designed to implement fastener release; experiment removal, deployment, emplacement, leveling, and alignment; and ALSEP-subpackage and -component manipulation and adjustment. Utility and

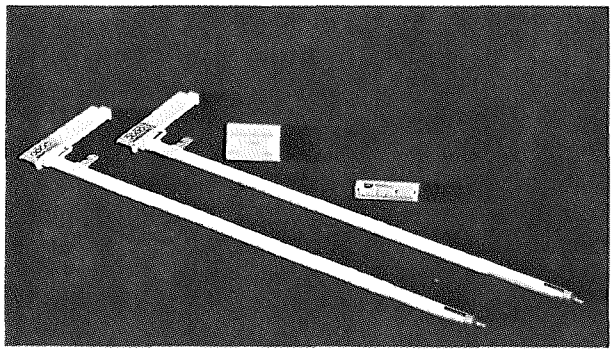

Figure 3 The ALSEP Universal Handling Tool

simplicity of operation were to be emphasized. Two such tools were to be provided for ALSEP deployment, one for each astronaut.

The tool shaft was to be 26.5 inches in length and capable of engagement near the tool head. Engagement was to be controllable from the opposite end of the shaft by trigger action. Tool design was to include a modified T-handle grip and nonslip grip tape on the shaft to aid in astronaut handling.

Fixed or rotatable interface sockets for the universal handling tool were to be provided as required on the Experiments Package and subpackages and on the various experiments, along with UHT engagement markings. The sockets on the subpackages were to be located near the carry handle and so oriented as to permit engagement and disengagement for emplacing the subpackages either horizontally or vertically. The sockets on the subpallets, on the radioisotope-thermoelectric-generator cable reel, and on other such units were to be as close to the deployed-configuration center of mass as was feasible, taking into account other design constraints, in order to maximize equipment maneuverability.

Tool Development

The universal handling tool, the evolution of which is shown in Figure 4, originated as a 4-inch experiment handling tool (EHT), developed early in the program to deploy the ALSEP experiments. The EHT had an L-shaped handle and a pushbutton-to-release system. A separate 21-inch tie-down release tool (TDRT) was used to release the experiment tie-down Calfax-type fasteners.

As the program progressed, tool length was increased to 10 inches to accommodate crew-reach parameters and changes in experiment design, and then to 14 inches to implement additional stowage and astronaut-task requirements. When it became obvious that still greater length would be needed, provision was made for attaching the EHT to the TDRT to give a combined length of 35 inches. The task of

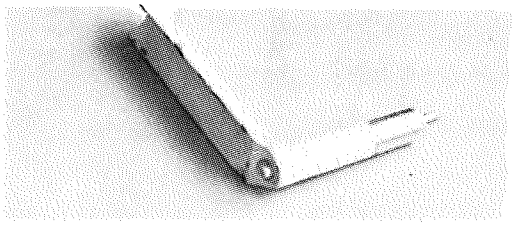

(a) 4-Inch Experiment Handling Tool

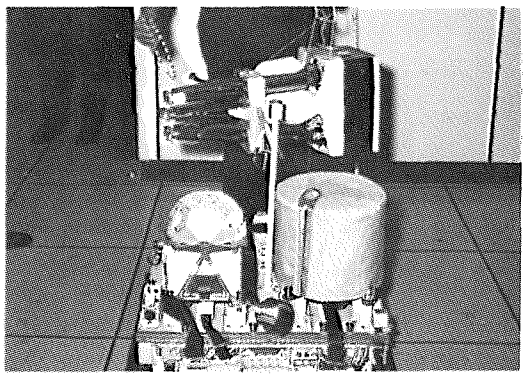

(b) 21-Inch Tie-Down Release Tool

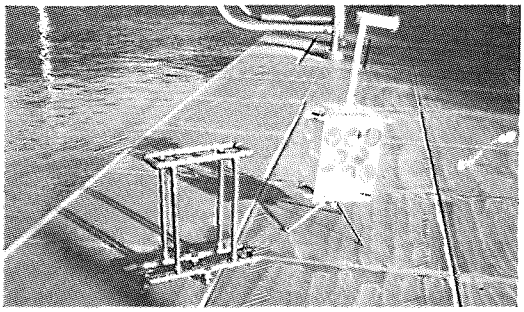

(c) 10-Inch Experiment Handling Tool

(d) 14-Inch-EHT/21-Inch-TDRT Combination

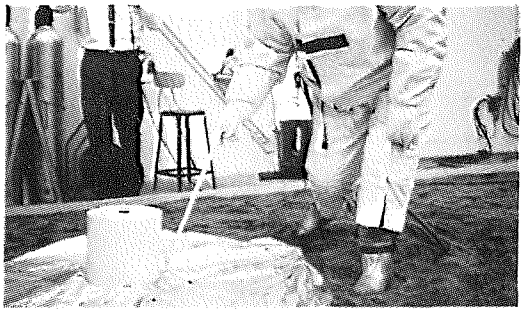

(e) 25.5-Inch Universal Handling Tool

Figure 4 Evolution of the Universal Handling Tool

connecting and disconnecting the two tools proved to be cumbersome and time-consuming for the astronauts, however, and as a result, tool design underwent a dramatic change. The experiment-carry and fastener-release functions were combined into a single 25.5-inch tool, appropriately called the universal handling tool in recognition of its extraordinary utility. The incorporation of Boyd bolts to replace the Calfax fasteners constituted a major improvement. The Calfax fastener has a larger tool interface than the Boyd bolt (a blade-type head rather than a hex-type head); whereas its release requires a 540-degree counterclockwise rotation, release of the Boyd bolt requires only a 75-degree counterclockwise rotation. The 25.5-inch tool also incorporated a trigger release system, with a full trigger guard and an angular handle.

Final design changes resulted from stowage constraints and the decision to carry two such tools. Shaft length was increased to 26.5 inches, a modified right-angle handle was incorporated, and the trigger guard was partially removed. Tools of this final design have been carried on every Apollo mission since the flight of Apollo 12.

DESIGN VERIFICATION

Human-factors engineering plays an important early role in ALSEP design verification. Well before the mechanical and electrical engineer have a qualification model with which to work, the human-factors engineer conducts shirt-sleeved and pressure-suited crew-engineering tests on a *crew-engineering mock-up*, built from engineering-model drawings. This mock-up provides an excellent test bed for crew-reach parameters and deployment-task mechanical interfaces, identifying any science requirement that cannot be met by a pressure-suited astronaut. A typical suited crew-engineering test is seen in Figure 5. The mock-up is evaluated extensively at 1 *g* and is flown in a KC-135 aircraft in a simulated 1/6-*g* environment. The tests are conducted early enough to permit crew-engineering improvements to be incorporated in later engineering prototypes and qualification models and in the flight unit.

ASTRONAUT TRAINING

Crew training for ALSEP deployment begins at NASA ten months prior to launch. The *astronaut trainer*, necessarily a prototype since its design is completed a year prior to launch, is constantly updated as changes are incorporated in flight-model design. Every effort is made to implement ease of deployment in the original crew-training model, but each crew, in the course of its training, introduces

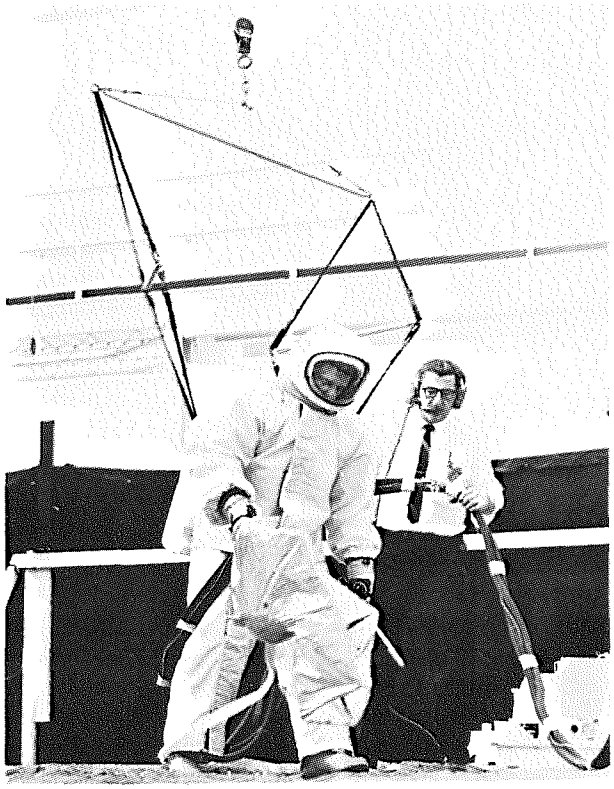

Figure 5 Suited Test in Crew-Engineering Laboratory

major and minor design changes peculiar to its own needs; as a result, each ALSEP crew interface is ultimately custom-built for an individual crew to the extent that science constraints permit.

The training unit is normally deployed about 25 times by the prime crew and about 15 times by the backup crew, both shirt-sleeved and pressure-suited. A final mechanical-fit check, conducted at Kennedy Space Center, provides the crew with a close look at actual flight hardware; the prime crew personally performs a white-glove deployment of the flight unit prior to its stowage aboard the Saturn V. This experience is designed to make all deployment movements on the lunar surface flow freely and logically in spite of such factors as reduced unit weights, reduced gravity, and lunar surface terrain peculiarities. That the goal is achieved is evidenced by the success and ease with which four ALSEP deployments, one of them pictured in Figure 6, have been accomplished.

SUMMARY

Crew engineering has become a more exact discipline – one that applies the knowledge of the psychologist, the physiologist, and the systems engineer to the development of design parameters. It minimizes the time, money, and effort that are required for hardware development and crew training

prior to flight. It also reduces the possibility of human error during deployment, since human error is frequently the result of suboptimum system design. If its primary function is not to keep the tasks of the astronauts simple, it nevertheless ensures that the man will not have to fight the system.

The significant quantities of new human-engineering design data accumulated in the course of ALSEP design should have great utility in future space-related programs as well as in numerous commercial applications.

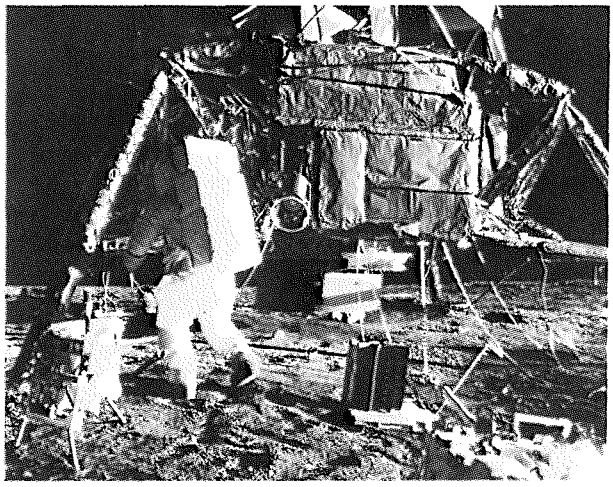

Figure 6 Deployment of Apollo 14 ALSEP at Fra Mauro (February 1971)

ACKNOWLEDGMENT

The author is indebted to Major Joseph H. Roberts, United States Air Force, who served for three years with the Crew Procedures Division of the NASA Manned Spacecraft Center in Houston, for his counsel and assistance in the preparation of this paper.

REFERENCES

1. H. Dreyfuss, *The Measure of Man*, Whitney Publications, New York City, 1960.
2. Wesley E. Woodson, *Human Engineering Guide for Equipment Designers*, University of California Press, Los Angeles, 1954.
3. Paul Webb (ed.), *Bioastronautics Data Book*, NASA-SP-3006, National Aeronautics and Space Administration, Washington, D.C., 1964.
4. Emanuel M. Roth (ed.), *Compendium of Human Responses to the Environment*, NASA-CR-1205, National Aeronautics and Space Administration, Washington, D.C., 1968.
5. *Design Handbook for Personnel Subsystems*, AFSC DH 1-3, Air Force Systems Command, Andrews Air Force Base, Maryland, 1969.
6. L. D. Marrus, "Interface Control Specification for Astronaut/ALSEP Array E," IC 314134, The Bendix Corporation, Aerospace Systems Division, Ann Arbor, Michigan (8 June 1971).

ALSEP Data Management

C. R. MURTAUGH
W. K. STEPHENSON*
B. L. SHARPE*

Nine million measurements a day are transmitted from each functional ALSEP on the moon and continuously collected on earth for use in long-term scientific analysis. Periodically, this massive flow of intricate data is examined on a real-time basis to evaluate ALSEP performance and to study the need for new commands to any of the ALSEP systems. A worldwide complex of facilities and personnel has the challenging task of efficient and timely data processing and dissemination. This paper describes facility characteristics and support activities and details certain constraints imposed on ALSEP hardware design by data handling requirements. The highlights of the first two years of lunar data management are reviewed.

INTRODUCTION

On the moon, the Apollo Lunar Surface Experiments Package (ALSEP) collects scientific and engineering data, encodes these data, and transmits them to earth in the form of a continuous downlink radio signal. On the earth, the signal is received and the data are extracted and subjected to engineering evaluation and scientific analysis. The engineers and scientists may decide, from the data and previously established ground rules, to modify ALSEP operation by transmitting uplink radio commands. This remote-control capability, using feedback from actual measurements with human judgment in the loop, results in a high degree of ALSEP flexibility and versatility. To ensure maximum scientific output from the lunar-laboratory/terrestrial-computation-and-analysis combination, earth-based operations must be characterized by short-term responsiveness and long-term continuity.

A short-term, quick-response command/control capability enhances system productivity by facilitating the correction of conditions that might otherwise shorten system life and by improving data collection during system life. In the first instance, prompt detection of malfunctions and degradations permits corrective action to be applied by command. In the second instance, early enough observation of transient scientific events permits setting changes to be commanded while the event is in progress to better the measurement of sensitivity, gain, offset, or spectrum region.

Long-term measurement continuity is essential to most lunar experiments because scientific conclusions are often based on time-dependent trends, on the position of the moon relative to the sun/earth line, or on statistical data analysis. Measurement continuity also ensures the recording of sporadic scientific events, regardless of when they occur.

DATA HANDLING EQUIPMENT

An overview of basic ALSEP data operations is presented in Figure 1.† With no provision for data storage other than shift registers, all ALSEP measurements are transmitted to earth almost immediately and must be recorded promptly if they are not to be lost. Recording is done on magnetic tape 24 hours a day at one of the several S-band receiving stations in the worldwide Manned Space Flight Network (MSFN) of the National Aeronautics and Space Administration (NASA). The tapes are shipped to the NASA Manned Spacecraft Center (MSC) in Houston, Texas, for further processing and distribution.

At scheduled intervals, live data are relayed from the receiving station – through the NASA Goddard Space Flight Center (GSFC) – to the Mission Control Center (MCC) at MSC for real-time monitoring, evaluation, and control. At the Control Center, the incoming data words are sorted and converted for presentation on a variety of digital and analog displays for operator interpretation and control decisions. When required, a command message is generated by a push-button input on a console at Mission Control Center, operating through a computer; this message is relayed through GSFC to the appropriate MSFN station, where a station computer processes it and passes the corresponding bit pattern to the uplink transmitter.

*National Aeronautics and Space Administration Manned Spacecraft Center, Houston, Texas.

†The discussion in this and subsequent sections is applicable to the Early Apollo Scientific Experiments Package (EASEP) carried to the moon on Apollo 11 as well as to the ALSEP systems placed on the lunar surface on Apollo missions 12, 14, and 15. These discussions do not reflect changes in ALSEP data management which have occurred since the beginning of the Apollo 15 mission.

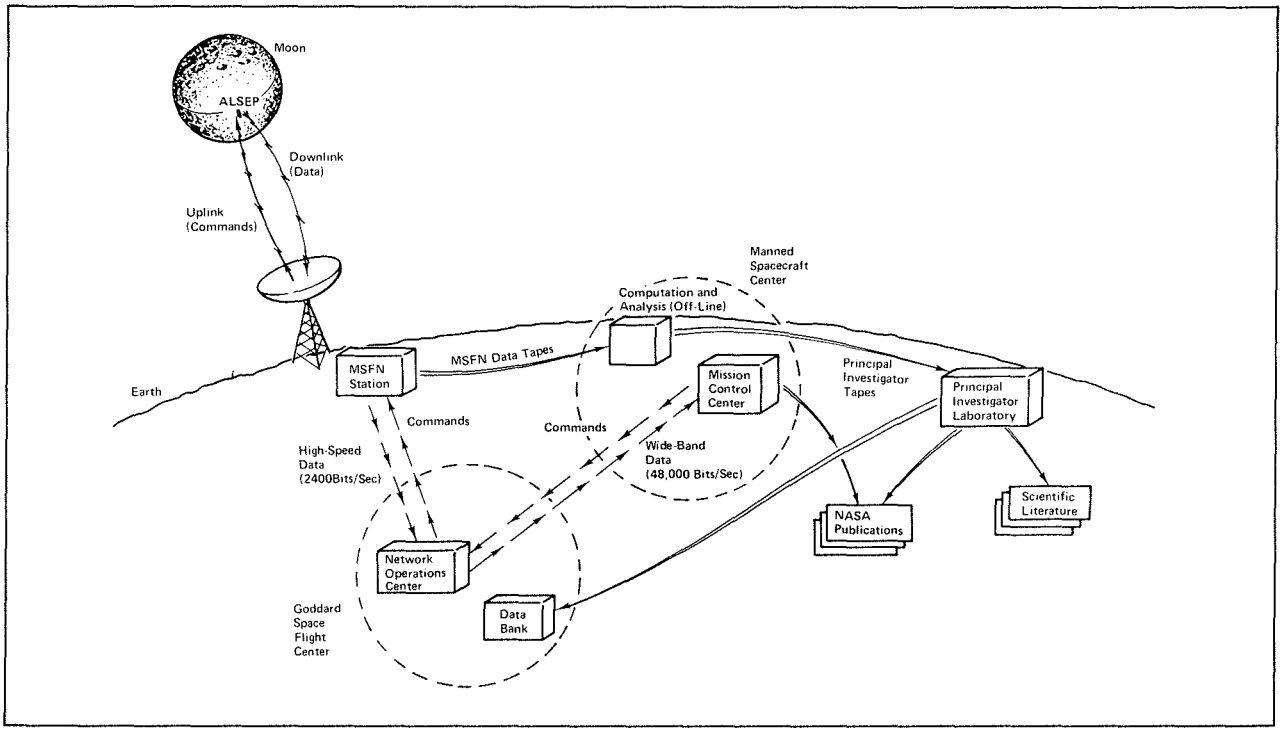

Figure 1 Overview of ALSEP Data Management

The availability of the communications facilities and operating procedures developed for the Apollo program proved useful in the development of the ALSEP data management system but also imposed certain constraints on ALSEP design. A second set of constraints was imposed by the need for communicating with multiple ALSEP systems. Together, these constraints led to the following ALSEP-downlink characteristics:

- *A unique transmitter frequency for each ALSEP, to avoid mutual interference between the ALSEP systems and with Apollo communications, in the S-band range of the MSFN receivers.*
- *A unique identification code for each ALSEP, transmitted in the downlink data to facilitate proper data processing.*
- *An ALSEP-downlink-carrier modulation compatible with MSFN receivers.*

Two ALSEP-uplink characteristics also resulted from the MSFN constraints:

- *Uplink-command transmission to all ALSEP systems on a single S-band frequency, with an address code included to direct to the proper ALSEP.*
- *An ALSEP-uplink-carrier modulation identical with the Apollo modulation except for the deletion of the 70-kilohertz intermediate frequency.*

Finally, two characteristics in the ALSEP antenna, through which both uplink and downlink signals pass, evolved from the MSFN constraints:

- *An antenna beamwidth wide enough to accommodate the effects of lunar librations.* Because of these librations, the earth (as seen from the moon) appears to oscillate over a period of 28 days within a rectangle 14 degrees by 16 degrees, in a pattern that repeats only every 6 years. Allowing for misalignment tolerances, the antenna beamwidth was tailored to achieve, at 11 degrees off-axis, a gain only 4.2 decibels less than the boresight gain.
- *Antenna mounting on an aiming mechanism that provides for crew adjustment over the range of Apollo landing locations.* The aiming mechanism permits alignment by the astronaut to the mean earth direction – i.e., to the effective center of the libration pattern. Dial settings for this alignment are computed in advance as a function of the expected lunar location and sun angle at the time of alignment.

With the gain of the ALSEP antenna fixed by beamwidth considerations, and with the performance parameters of the receiving stations established, the selection of ALSEP transmitter power and receiver sensitivity was dictated by signal-to-noise-margin, or bit-error-rate, requirements in the communications links.

ALSEP Downlink Characteristics

The data carried on the ALSEP downlink include the outputs of the scientific sensors (designated scientific data), interspersed with equipment performance measurements (the so-called engineering data). One data word, the basic unit of communication, has for ALSEP a length of 10 binary bits; 64 words (640 bits) constitute one ALSEP data frame. Within the data frame, each ALSEP has a unique format or word assignment for the individual experiments. These assignments are fixed (hard-wired) within the frame; should an individual experiment fail or be commanded OFF, the spaces assigned to it in the format remain unused – i.e., they carry filler bits of all ONE's or all ZERO's, depending on circuit characteristics, and cannot be used by another experiment. Although word assignment to an experiment within the frame is fixed, each individual experiment programs the manner in which its words are used, achieving flexibility typically by the subcommutation of measurements. Because of this subcommutation, interpretation of a given ALSEP word often requires reference to other words and sometimes to other frames. Moreover, some measurements exceed the 10-bit word length and must be split between two words in successive frames. Many of the experiments make a sequence of measurements covering several ALSEP frames before repeating; for example, one complete sample of measurements from the Suprathermal Ion Detector Experiment requires 256 ALSEP frames (2.5 minutes) for transmission.

In the normal mode, the downlink data rate is 1060 bits per second – one frame every 0.60377 second. A contingency rate of 530 bits per second can be selected by command to improve marginal signal conditions. A third rate – 10,600 bits per second – is used to handle data from the Active Seismic Experiment in its scientific mode. Handling these three data rates, extracting the individual words from the data format, and properly identifying their content are tasks that challenge the earth phase of ALSEP data processing.

ALSEP Uplink Characteristics

There are several built-in features in the ALSEP system designed to protect the equipment, restore operation in case of malfunction, adjust sensors in response to changing measurements, and help ensure data quality. Nevertheless, changing conditions in the lunar environment and realistic concern over possible failures dictate a capability for receiving commands by uplink from the earth. Approximately 75 functions of each ALSEP system can be controlled by such uplink commands for purposes of overcoming malfunctions, increasing flexibility, making scientific adjustments, or maintaining more positive control over data quality. Since the same function, requiring the same command, may exist in more than one ALSEP system operating on the moon, an address code is inserted into each command message to properly direct it.

An ALSEP command takes the form of a momentary switch closure rather than a proportional control or uplink-data input. Depending on the function being controlled, a single command may be used to step through as many as 16 states by repetitive application. Thus, the number of functional modes or circuit configurations that can be obtained by command in a single ALSEP system is extremely large.

MSFN Station Configuration

The two-way flow of ALSEP data – downlink for real-time performance evaluation and uplink for control commands – involves the same facilities and many of the same people that support Apollo mission operations. Twelve land-based stations and one ship station in the Manned Space Flight Network are available for use. Three of the land stations have 85-foot-diameter antennas; the others have antennas 30 feet in diameter which under normal circumstances are satisfactory for ALSEP reception. Most of the stations have a multiple capability, with four receivers connected to a single antenna; hence, four downlink signals of different frequency – one Apollo signal and signals from three ALSEP systems, for example – can be received and recorded simultaneously. When fewer than four signals are being monitored, the extra receivers serve as backup.

Because of the rotation of the earth, a single station can receive data from the moon only for a period of six to twelve hours. Sequential stations operate simultaneously for periods of up to several hours. During these overlap intervals, both stations receive and relay ALSEP data to MCC via GSFC; the source whose data are processed is selected on the basis of convenience and data quality.

The functional configuration of a typical MSFN station is diagrammed in Figure 2.

Downlink Operation

Downlink signals are received by unified S-band (USB) receivers, and demodulated signals are fed to the pulse-code-modulation (PCM) decommutators, one for each of up to three operating ALSEP systems. The PCM data stream is then fed to the station computer, which identifies the individual ALSEP data frames and stores them in buffers for subsequent transmission to Mission Control Center. These data

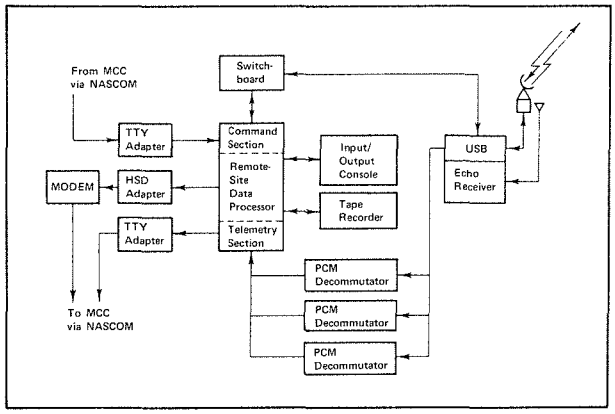

Figure 2 Manned Space Flight Network Station Configuration

streams are also recorded continuously on magnetic tape for later shipment to the MSC off-line data processing facility.

Data in the buffers is fed periodically through a high-speed-data (HSD) adapter and a modulator/demodulator (MODEM) into the NASA Communications (NASCOM) network. Each station is normally equipped with three HSD circuits, which operate at a data rate of 2400 bits per second through a combination of land lines, undersea cables, microwave relays, and satellite relays.

The HSD rate of 2400 bits per second is derived from the Apollo downlink data rate of 200 8-bit words per frame and one frame per second. Timing pulses at 1-second intervals control the HSD circuits and allow single 1600-bit frames of Apollo data to be relayed through the network, along with such overhead information as time of receipt at the station and address required for network routing. A network software modification permits the transmission of ALSEP data consisting of 640 bits per frame at a normal data rate of 1060 bits per second. The modified software also provides for the simultaneous transmission of data from two ALSEP systems to Mission Control Center. Five consecutive frames from each of the two systems are stored in the buffers; at 3-second intervals, this 6400-bit block of data, together with its time and address overhead, is transmitted through a single HSD circuit, which has a 3-second capability for 7200 bits. The frames from the two systems alternate in the data block, so that when only one system is transmitting, every other frame in the ten-frame block is blank.

This adaptation of MSFN hardware and Apollo software involves one complication. The HSD circuit can accept from each ALSEP 160 frames every 96 seconds (32 data blocks), but it receives only 159 from the moon. In place of the missing frame, a filler frame is substituted, properly identified for deletion in MCC data processing.

The real-time transmission of data from the Active Seismic Experiment to Mission Control Center at its data rate of 10,600 bits per second would exceed the available link capacity. Consequently, an editing process is incorporated in the station computer software by means of which approximately 85 percent of the geophone output readings are discarded; the remaining 15 percent, along with selected engineering data, are sent through a single 2400-bit-per-second HSD circuit. The resulting format precludes the simultaneous transmission from that MSFN station of data from any other ALSEP system. Since the Active Seismic Experiment monitoring period is only a few hours in duration, this limitation is acceptable, as is the sacrifice of the high-frequency-range geophone measurements deleted in the editing process. All the high-bit-rate data, as well as the data transmitted simultaneously from other ALSEP systems, are preserved on the magnetic tape record of the station.

Certain ALSEP downlink data, notably the command verification words (CVW), are segregated in the station computer and forwarded to MCC on teletype-quality circuits (TTY). Support summary messages are also sent via TTY at the end of the station support period.

Station equipment identical to that shown in Figure 2 is used to support Apollo missions. The ALSEP and Apollo signals are received through the same USB antenna but are processed separately.

Uplink Operation

Command messages are sent from Mission Control Center via NASCOM to MSFN stations for transmission to the ALSEP systems on the moon. The command software checks the incoming message for errors and converts it to the binary code used in uplink modulation.

The error check is designed to detect garbled messages, nonexistent commands (those not in the station's inventory), and critical commands (those in the inventory but not enabled by a specific prior request). When an error is detected, a SITE VALIDATION light at MCC fails to illuminate, and the cause is identified by printout at the station. Voice communications are then used to evaluate whether the command should be attempted again or whether trouble-shooting is in order.

If no error is detected in the command message, the appropriate modulation is applied immediately to the USB transmitter. A small antenna mounted in front of the station's main antenna picks up the radiated signal, and, through an echo receiver, verifies proper transmission. In case of failure, a GROUND REJECT status is identified.

Most commands transmitted to the ALSEP systems result in a command verification word (CVW) in the next frame of downlink data. The station computer watches for the CVW, and if it fails to appear within 5 seconds, a SPACECRAFT REJECT status is identified. A few ALSEP commands, particularly those that interrupt the downlink transmission or cause loss of data synchronization, are expected to result in SPACECRAFT REJECT or loss of CVW.

The MSFN station software for command transmission is a good example of the influence of Apollo development work on ALSEP operations. Apollo command messages have several standard lengths, one of them being 75 binary bits. To circumvent the need for preparing and maintaining additional software, the ALSEP 61-bit command message was modified to fit existing Apollo software by adding 14 trailing filler bits, easily generated in a subroutine.

Network Operations Center

All communications – including voice communications – between the MSFN stations and Mission Control Center go through the Network Operations Center at Goddard Space Flight Center (GSFC). The data flow through this facility is shown in Figure 3. ALSEP data received from MSFN stations (one or more) on HSD circuits are stored temporarily in the polynomial buffer terminal (PBT) and are then relayed to MCC on a wide-band-data (WBD) circuit operating at 48,000 bits per second. Data are interlaced on the WBD circuit, using a time-multiplexing technique; thus 3-second blocks of ALSEP data from different stations are compressed into separate 0.15-second blocks prior to relay. A single ALSEP data frame, transmitted from the moon originally in 0.60377 second, is compressed into 0.01333 second when it arrives at MCC.

The time compression inherent in the multiplexing technique is rectified by a reconstruction technique during real-time data processing at MCC. The time delays that result from buffering, on the other hand, cannot be rectified, and there may be as much as 9 seconds of delay between the time data are received at the station and the time they arrive at MCC because of buffering at various points in the network. This delay adds to the 1.3-second moon-to-earth transit time of the radio signals, but its overall effect on data evaluation at MCC is negligible, as is that of the similar but shorter overall delay in uplink commands.

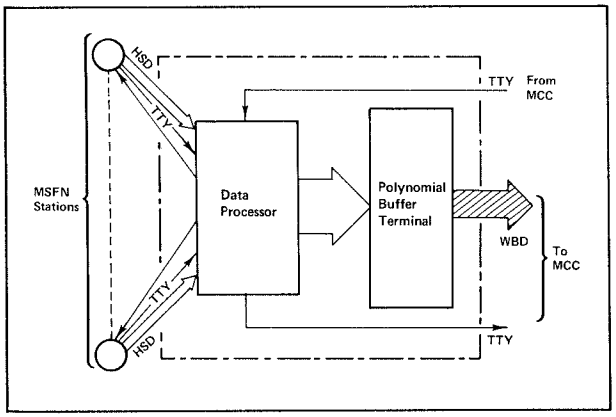

Figure 3 GSFC Network Operations Center Configuration

Mission Control Center

The MSC Mission Control Center houses the large numbers of consoles, computers, displays, and communications channels that are required for the support of Apollo real-time operations. Its functional configuration is shown in Figure 4. The key activities for directing and conducting ALSEP missions are performed here and parallel those of the Apollo missions. These activities include real-time assessment of mission status, consultation with scientific and technical experts when required, and execution of command decisions.

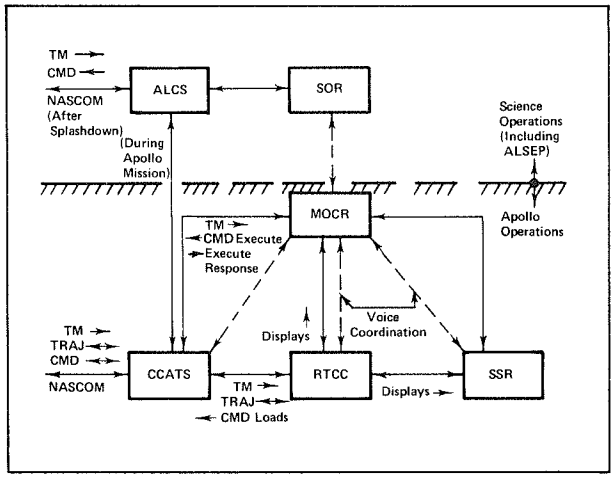

Figure 4 MSC Mission Control Center Configuration

Science Operations Room

The Science Operations Room (SOR) is the center for science mission control. It accommodates ALSEP control facilities, mission science management personnel, and the scientists and supporting personnel whose task it is to monitor the lunar traverses of the astronauts. The 30-foot-by-30-foot control area, shown in Figure 5, features a console flanked by numerous display devices, among them several analog recorders and a computer-driven high-speed printer.

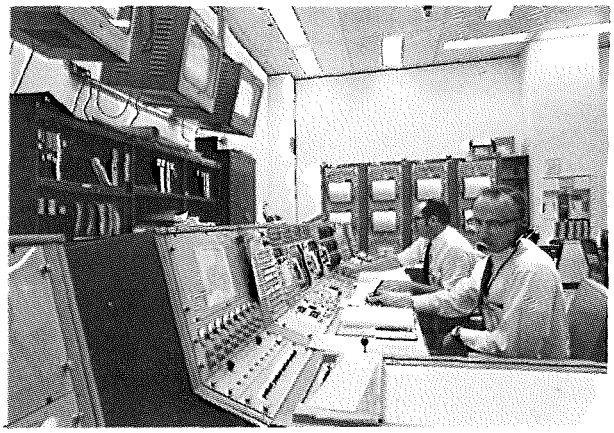

Figure 5 ALSEP Control at Mission Control Center

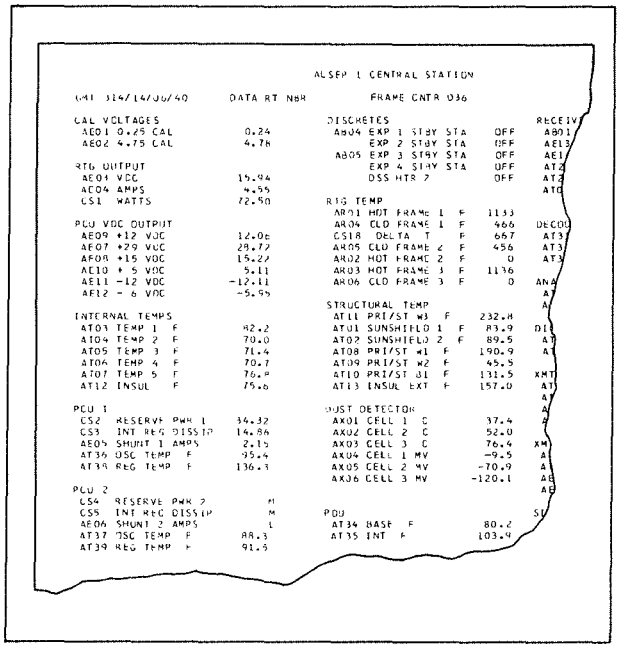

ALSEP 1 CENTRAL STATION

GMT 314/14/00/40 DATA RT NBR FRAME CNTR 036

CAL VOLTAGES			DISCRETES		RECEIVE
AE01 0.25 CAL	0.24		AB04 EXP 1 STBY STA	OFF	AB01
AE02 4.75 CAL	4.78		EXP 2 STBY STA	OFF	AE13
			AB05 EXP 3 STBY STA	OFF	AE1
RTG OUTPUT			EXP 4 STBY STA	OFF	AT2
AE04 VDC	15.94		DSS HTR 2	OFF	AT3
AE04 AMPS	4.55				AT4
CS1 WATTS	72.50		RIG TEMP		
			AR01 HOT FRAME 1 F	1133	
PCU VDC OUTPUT			AR04 CLD FRAME 1 F	466	DECOD
AE09 +12 VDC	12.06		CS1R DELTA T F	667	AT3
AE07 +29 VDC	28.72		AR05 CLD FRAME 2 F	456	AT3
AE08 +15 VDC	15.27		AR02 HOT FRAME 2 F	0	AT3
AE10 + 5 VDC	5.11		AR03 HOT FRAME 3 F	1136	
AE11 -12 VDC	-12.11		AR06 CLD FRAME 3 F	0	ANA
AE12 - 6 VDC	-5.95				A
			STRUCTURAL TEMP		A
INTERNAL TEMPS			AT11 PRI/ST W3 F	232.8	A
AT03 TEMP 1 F	82.2		AT01 SUNSHIELD 1 F	83.9	DIG
AT04 TEMP 2 F	70.0		AT02 SUNSHIELD 2 F	89.5	AT
AT05 TEMP 3 F	71.4		AT08 PRI/ST W1 F	190.9	AT
AT06 TEMP 4 F	70.7		AT09 PRI/ST W2 F	45.5	
AT07 TEMP 5 F	76.8		AT10 PRI/ST B1 F	131.5	XMT
AT12 INSUL F	75.6		AT13 INSUL EXT F	157.0	AT
					A
PCU 1			DUST DETECTOR		A
CS2 RESERVE PWR 1	34.32		AX01 CELL 1 C	37.4	A
CS3 INT REG DISSIP	14.86		AX02 CELL 2 C	52.0	
AE05 SHUNT 1 AMPS	2.15		AX03 CELL 3 C	76.4	XM
AT36 OSC TEMP F	95.4		AX04 CELL 1 MV	-9.5	A
AT38 REG TEMP F	136.9		AX05 CELL 2 MV	-70.9	A
			AX06 CELL 3 MV	-120.1	AE
PCU 2					AE
CS4 RESERVE PWR 2	M				
CS5 INT REG DISSIP	M		PDU		SE
AE06 SHUNT 2 AMPS	L		AT34 BASE F	80.2	
AT37 OSC TEMP F	88.3		AT35 INT F	103.9	
AT39 REG TEMP F	91.5				

Figure 6 Typical High-Speed-Printer Data Format

These displays present all the current engineering and science data that are required by the flight controllers. The data are used to make control decisions and to monitor the response of the ALSEP to commands. During normal periods, the support team consists of two to three people, but the area can accommodate up to five flight controllers and eight experiment investigators. The console is equipped with a large number of event lights that respond to discrete changes in housekeeping data – typically, to the ON/OFF status of switches.

The ALSEP computer system (ALCS) processes data for the ALSEP real-time displays in the SOR. The displays can handle up to four ALSEP systems, two at a time, a capability that is adequate for normal data flow through NASCOM. The data arrive in time-compressed blocks on the WBD circuit, and, after processing, are reconstructed to achieve realistic timing – i.e., they are read out at the proper speed for display on analog chart recorders. The ALCS also converts engineering data from the original binary-bit code, through calibration curves, into more intelligible form – voltages or degrees of temperature, for example. It has a limit-sensing capability that permits it to identify values that lie outside selected ranges and an arithmetic-computation capability that permits it to compute measurement sums, differences, or products, as required.

At MCC, most of the ALSEP data are preserved on sheets prepared by the high-speed printer in a format such as that shown in Figure 6. Upon console-push-button activation, the printer transfers the latest update of data from its memory buffers to the data sheet or printer format assigned to the particular ALSEP system and individual experiment involved. A single sheet can be printed in approximately 1 second; data updating may take from a few seconds to several minutes, depending on the experiment. The Central Station data are completely updated every 54 seconds. Should the ALCS detect a serious irregularity in these data, an automatic printout of the format containing the abnormal reading is made.

Other Areas

The other areas that make up Mission Control interface with the ALCS and SOR as shown in Figure 4.

The Mission Operations Control Room (MOCR) is the focal point for flight control activity during an Apollo mission and is equipped with consoles for the Flight Director and a team of supporting specialists. Backup resources for the MOCR are accommodated in a number of Staff Support Rooms (SSR), where detailed data monitoring and evaluation are pursued by personnel with specific responsibilities for particular areas – propulsion, communications, navigation and control, and the like.

The Real-Time Computer Complex (RTCC) processes Apollo telemetry (TM) and trajectory (TRAJ) data and generates special command (CMD) loads such as updates for the spacecraft on-board navigation equipment.

The Command, Control, and Telemetry System (CCATS) serves as a switchboard for sorting WBD and other data received from NASCOM and routing it to the appropriate computer/user. It also provides an interface for commands sent from MCC to NASCOM. During an Apollo mission, ALSEP data from NASCOM are sorted by CCATS and routed to ALCS; when no mission is in progress, ALCS performs the interface function.

DATA HANDLING PROCEDURES

The collection and distribution of ALSEP data are accomplished through many of the facilities developed for the Apollo program and involve a sizable body of personnel with Apollo or Apollo-related backgrounds. ALSEP data-handling procedures are the product both of the manned space programs and of the unmanned space programs previously developed to collect scientific data of the ALSEP type. As a consequence, the ALSEP data-handling approach, philosophy, and techniques are hybrids that contain some elements of both these sources.

Mission Preparation

Throughout the ALSEP development program, Mission Control Center personnel have an active role in the system design process through participation in formal reviews as well as in day-to-day design analyses. Flight controllers not only receive classroom instruction covering ALSEP systems and components but also formulate and conduct extensive reviews of operational handbooks, procedures, and mission rules prior to each mission. The Principal Investigators, various NASA organizations, and contractor representatives all participate in related mission planning and preparations. The hardware and software for real-time displays are developed and verified by synthetic (taped) inputs. Operational simulations, using a computerized mathematical model of the mission ALSEP system, are conducted to confirm the readiness of personnel, documents, hardware, and software. The final prelaunch check-out at Kennedy Space Center includes a radio-frequency uplink/downlink interface test, operating through the Merritt Island MSFN receiving station, to prove closed-loop compatibility with MCC.

Real-Time Operation

Data are always being received and recorded at one of the MSFN stations, but the relay of data to MCC for real-time monitoring and command/control decisions goes on only part of the time. Real-time activity is continuous during the first 45 days after ALSEP start-up on the moon. This 45-day period, which ends shortly after sunset on the second lunar day of ALSEP operation, provides one complete sunset-to-sunset cycle of baseline performance data.* The lunar equipment can subsequently be monitored on an intermittent basis against this well-defined baseline with a high degree of confidence and at minimal cost.

Real-time activity following the 45th day is typically scheduled for 2 hours every day during lunar daytime, for 1 hour every other day during lunar night, and for longer periods at each terminator crossing (lunar sunrise and sunset). This schedule is subject to modifications, both planned and unplanned, and a support period can be extended to obtain measurements of unusual interest or to meet other extenuating circumstances.

Performance Evaluation

Since sudden changes in ALSEP performance are rare, most control decisions are based on a thorough study of recent history and trends as compared with performance during previous lunar cycles.

The majority of serious problems, anomalies, and failures can be acted upon by application of a mission rule. The mission rules are published prior to each mission and dictate corrective actions for a large number of contingencies. If a problem arises that is not covered by a mission rule, a team of experts determines what action to take on the basis of design, test, and lunar data.

All abnormal conditions and the investigations associated with them are documented for NASA records. The investigations usually result not only in immediate corrective action but also in a recommendation for preventing recurrence of the problem in this or any other ALSEP system.

Command Activities

Both normal and abnormal conditions may necessitate command intervention. Gains or scales of the scientific instruments can be adjusted by command should the data warrant such adjustment. Sensors can be periodically calibrated to help ensure measurement validity. Certain temperature conditions can be modified as needed by commanding heaters ON or OFF or by selecting or bypassing thermostatic controls. Redundant components or alternate modes of operation can be activated in cases of equipment failure. In the absence of abnormal conditions, commands are transmitted on a schedule dictated by past experiment performance and investigator needs.

As of 1 September 1971, the number of commands processed totalled 10,600 for the Apollo 12 ALSEP system, 3500 for the Apollo 14 ALSEP system, and 1700 for the Apollo 15 ALSEP system. Most of these were associated with scientific-data-collection functions. Their number (more than 17 per ALSEP system per day) reflects the degree of human decision-making that goes into the operation of these lunar laboratories.

*The period from start-up to the first sunset is discounted as atypical.

Control Center Records

The continuous flow of ALSEP data into Mission Control Center results in the rapid accumulation of real-time records – printer output sheets, analog chart recordings, and numerous handwritten logs noting commands sent, difficulties encountered, and unexpected measurement changes. To reduce the bulk of this accumulation, data summaries are generated and a monthly lunar "script" is prepared, in which all known significant events are detailed and periodic checkpoints for trends are identified.

Off-Line Data Analysis

Although performance can be evaluated and science data preliminarily interpreted on the basis of the real-time data displayed at MCC, final scientific interpretation is normally the result of more extensive data analysis, using specialized high-speed computer programs. For purposes of such analysis, the tape records from the MSFN stations are processed by off-line facilities at MSC into separate tapes for the individual experiments, formated as prescribed by the Principal Investigator for the experiment. These tapes are subsequently processed by the Principal Investigator at his own facility.

The manner in which the data are processed varies from experiment to experiment because each has unique time constants that relate to its peculiar scientific phenomena and instrumentation.

Dissemination of Experiment Results

Early ALSEP experiment results are published in the NASA Preliminary Science Report for each Apollo mission. This report contains for the most part quick-look evaluations of the real-time data rather than conclusions based on comprehensive off-line analyses. More detailed results are presented by the individual investigators at the NASA-sponsored Annual Lunar Science Conference, the Proceedings of which are published. Thereafter, each investigator is free to discuss his conclusions at scientific symposia and to publish them in the scientific literature.

All data processing results are compiled on magnetic tape or reproducible charts, which are stored in the NASA Data Bank at Goddard Space Flight Center and are available to the scientific community.

OPERATIONAL EXPERIENCE

The ALSEP systems placed on the moon by the crews of Apollo missions 11, 12, and 14 continued to function long after the astronauts returned to earth.

The Apollo 11 seismometer, powered by solar cells, provided pioneering lunar seismic data during lunar daytime in July and August 1969. Loss of command capability around noon of the second lunar day terminated the scientific output, but engineering data were received through dawn of the sixth lunar day (December 1969), at which time the downlink signal disappeared.

The Apollo 12 ALSEP system – five experiments powered by a radioisotope power supply – has operated continuously since November 1969 and, as of September 1971, shows no sign of deterioration, far outliving its design life of 1 year. During its first year of operation, the system was monitored in real time on a scheduled or unscheduled basis for 2300 hours, 26 percent of its total operating time. Three of the experiments are still producing useful data, and operational support is planned through 1971. This system has provided more than six billion measurements, which have contributed significantly to our knowledge of the moon and the earth and their interactions with the particles and fields emanating from the sun.

The Apollo 14 ALSEP system – also five experiments powered by a radioisotope power supply – made possible for the first time the correlation of data obtained by two instruments operating simultaneously at a distance of 181 kilometers from one another. Such seismic events as a presumed meteorite impact and the impact of the Apollo 14 Lunar Module ascent stage have been recorded by both the Apollo 12 and the Apollo 14 seismometers; the meteorite impact was also recorded by the ion detectors in the two ALSEP systems.

Over and above the direct scientific and engineering information these ALSEP systems have provided, a number of interesting applications have been found for their downlink signals. These signals serve as a boresight reference for calibrating the gimbals on S-band antennas of the Air Force Eastern Test Range; as a navigation beacon for aircraft operating over the polar regions; as a frequency and signal-strength reference for the development of precision measuring techniques; and as a tracking reference for obtaining better geographic-coordinate locations for the MSFN and Deep-Space S-band receiving stations.

The acid test for real-time data processing came on 5 February 1971 when the Apollo 14 ALSEP began operation in concert with the Apollo 12 ALSEP. During the critical turn-on and adjustment period for the new experiments, there was no lack of timely data on which to base decision making and performance evaluation; nevertheless, attention was not completely diverted from the older experiments package. This compatibility may reflect in part the operational stability of the two systems, but it also substantiates the capabilities of the facilities and procedures involved.

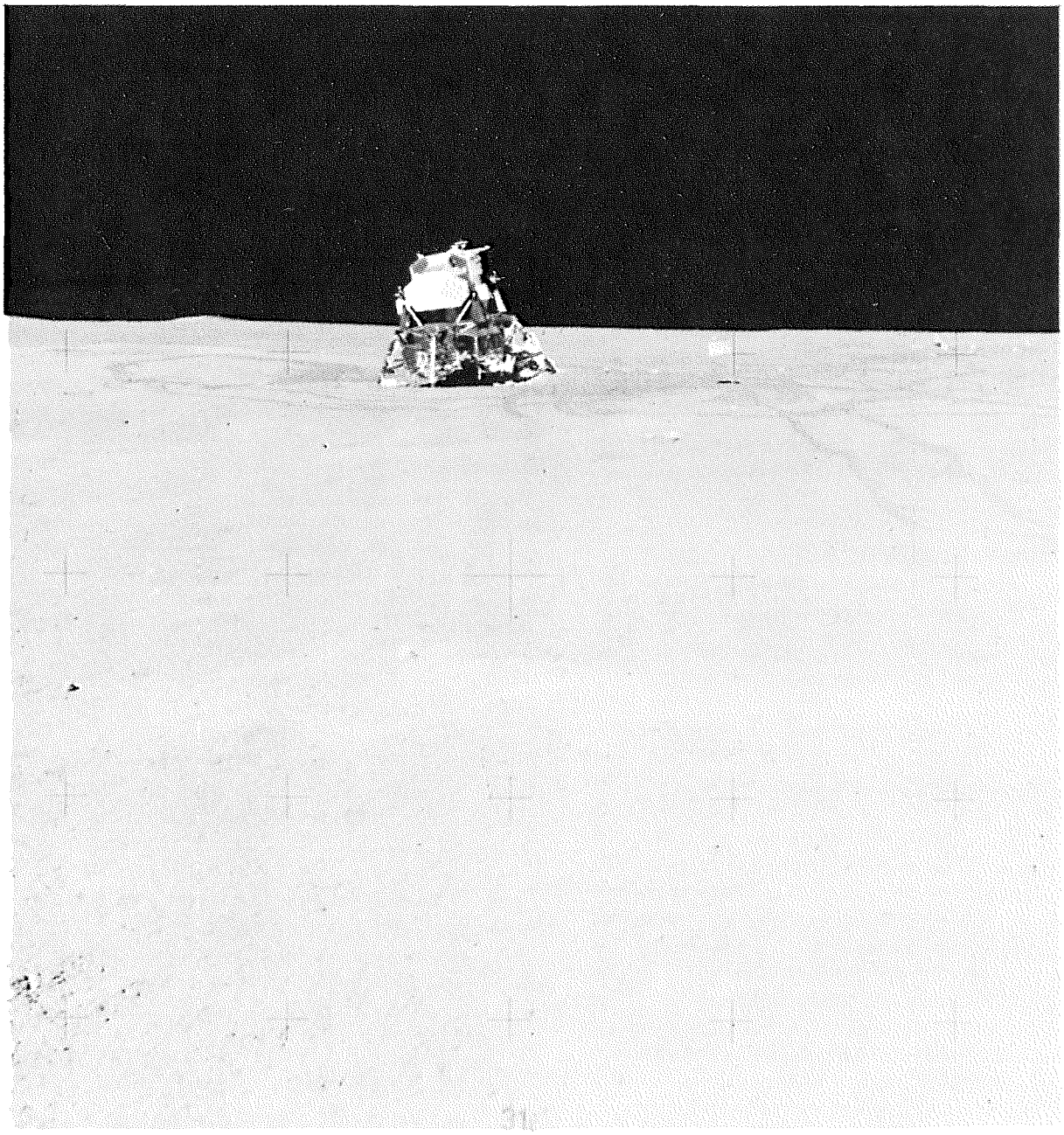

The Lunar Ejecta and Meteorites Experiment

L. GALAN

INTRODUCTION

The Lunar Ejecta and Meteorites (LEAM) Experiment will determine the speed, direction, mass, and flux density of cosmic dust particles in the vicinity of the earth/moon system. It will also measure the flux density and orbital parameters of lunar material ejected whenever meteorites strike the lunar surface. The experiment is part of ALSEP array E, which is scheduled for launch on Apollo 17 late in 1972. The sensing elements, controls, self-calibration features, and data processing techniques* were successfully tested on the Pioneer 8 dust detectors. This note presents a brief description of the dust detector, its principle of operation, and the engineering design carried out to adapt the instrument for lunar operation, including deployment by an astronaut.

SENSOR DESCRIPTION AND OPERATION

Figure 1 is a schematic representation of the basic cosmic dust detector, which consists of two film-grid arrays spaced 5 centimeters apart. In the front array, four very thin metallized film strips are positioned equidistant between four pairs of grid strips, and the entire assembly is sandwiched between two suppressor grids. The collector-grid pairs are positively biased and run perpendicular to the film strips which are negatively biased, forming a 4x4 matrix that is used to identify the particle impact area. The rear array is also a 4x4 film-grid matrix, but the metallized film strips are bonded to an impact plate of sufficient mass to arrest the particles of interest. A crystal microphone bonded to the rear surface of the impact plate picks up a signal related to the momentum of the particle. The front and rear film-grid arrays together form a total of 256 possible identifiable sensor combinations for use in determining particle time-of-flight and direction. Some of these combinations cannot be used in practice because of necessary structural obstructions; others may be deliberately shielded to provide important sensor controls.

*Developed by LEAM Principal Investigator Otto E. Berg; see O. E. Berg and F. F. Richardson, "The Pioneer 8 Cosmic Dust Experiment," *The Review of Scientific Instruments* 40 (No. 10), 1333-1337 (1969).

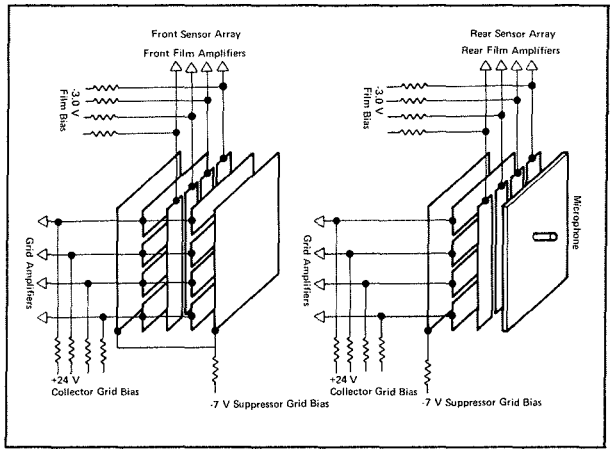

Figure 1 Pioneer 8 Cosmic Dust Detector Schematic

If a particle striking the front film has sufficient momentum, it will penetrate the very thin film and continue on toward the rear impact plate. As the metallized thin film is penetrated, an ionized plasma is produced and the particle loses some of its kinetic energy. The positive ions and electrons in the plasma are collected by the electrically biased films and grids, respectively, producing two coincident pulses. These are individually amplified and processed in the experiment electronics to identify the area of impact, to initiate time-of-flight measurement, and to analyze the pulse height of the positive film signal (which is related to the particle energy loss). Some of the particles that penetrate the front film intercept the rear film also, depending on their trajectory angle, and generate a plasma and a microphone pulse. These coincident signals are individually amplified and processed in the experiment electronics to identify the area of impact, to stop the time-of-flight clock, to analyze the height of the microphone signal (which is related to particle momentum), and to analyze the pulse height of the rear film (which is related to particle remaining energy).

Signals from the collector grids and film strips are threshold-detected and digitally recorded in predetermined storage register accumulators. Peak-height and

time-of-flight measurement data are also computed and recorded. Recognition of an impact causes all storage register bits except those in the accumulators to reset before new data are stored. The stored data are shifted to ALSEP, serially upon demand, in the form of two 10-bit NRZ-C digital words each telemetry frame, at a normal rate of 1060 bits per second or a contingency rate of 530 bits per second.

The LEAM experiment, seen in Figure 2, is made up of three sensors. Two have dual-film assemblies to measure time of flight. The third has a rear array only. One of the dual-film sensors faces up when deployed on the lunar surface and the other faces eastward. The single-film sensor faces westward.

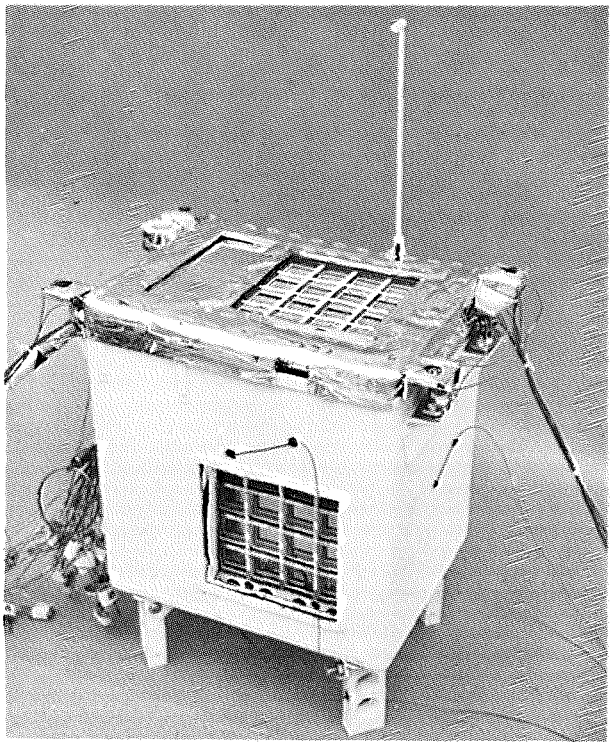

Figure 2 The Lunar Ejecta and Meteorites Experiment

STRUCTURAL AND THERMAL DESIGN

The fundamental LEAM-experiment design is based substantially on the Pioneer 8 dust detector, which is operating successfully in a spin-stabilized satellite placed into a heliocentric orbit of approximately 1 astronomical unit by a thrust-augmented delta vehicle. Since the launch-and-boost environment of the Pioneer 8 spacecraft was more severe than that anticipated for Apollo, the delicate sensor structural design is the same in every essential detail. However, the thermal environment of the LEAM experiment will be quite different from that of Pioneer 8 because the LEAM will be deployed on the moon whereas Pioneer 8 spins in space at a rate of approximately 1 revolution per second. The LEAM experiment will experience the 28-day lunation cycle for a latitude somewhere between - 45 and +45 degrees.

To withstand the expected design-limit accelerations, shock, and vibration, each of the three sensors and the central-electronics package are rigidly mounted on a support structure, which in turn mounts to ALSEP subpackage 2 through four vibration isolators. The dual-film sensors include dynamic isolation of the front film frames; thus the thin films, which are the most delicate elements of the experiment, are doubly isolated from high-frequency boost-induced accelerations. The front thin film of each dual-film sensor is a laminate made by vacuum deposition of aluminum on Parylene C* substrate, with an overcoat of vacuum-deposited silicon monoxide. The film laminate is bonded to a 95-percent-transparent one-eighth-inch-square mesh of 0.006-inch beryllium copper, which provides both structural support and thermal conduction for the film.

The LEAM thermal control system is completely passive in the heat-rejection mode and uses resistive electric heaters during lunar night. The thermal control design incorporates proven ALSEP techniques, including multilayer superinsulation to contain the electronics, low-conduction mounts between the inner and outer structures, a second-surface-mirror space radiator, low-conduction manganin wire cable feedthrough, S-13G white thermal coating on solar-illuminated external surfaces, and vacuum-deposited aluminum on internal surfaces. Because approximately 20 percent of the exposed outer surface of the LEAM experiment is open to admit microparticles, the electronic packages cannot be completely enclosed in a thermal blanket. Each of the three sensors requires an aperture of approximately 25 square inches in the thermal blanket, but two of the sensors have a thin front film that, together with its support frames, covers up the entire aperture. These front films are coated with vacuum-deposited aluminum, which is opaque to visible and infrared radiation. The third sensor does not have a front film as a shield; as a result, the rear impact plate and the sensitive crystal microphone bonded to it are subjected to direct sun and space exposure.

It can be shown analytically that to survive direct sunlight on the moon, a one-inch-square thin film less than 5000 angstroms thick made of Parylene with a metal deposition must have a solar-absorptivity/infrared-emissivity (α/ϵ) ratio of less than 2.5 at its ex-

*Parylene C is a polymer series developed by Union Carbide Corporation.

ternal surface if the film provides the only conduction path. With the supplementary conduction provided by the beryllium copper grid, however, experiments revealed that the α/ϵ ratio could be greater than 6.0 without exceeding the film design temperature limits. The increased conduction coupling provided by the support grid affects the thermal balance of the entire experiment package such that films with high values of α and ϵ require more heater power at night than films with low α and ϵ values. The selected aluminum deposition film with an outer coat of silicon monoxide provides a solar absorptivity α of 0.35 and an infrared emissivity ϵ of 0.09. The combined heat leak through the two front films is about 25 percent of the total.

The single-film-sensor thermal balance also made necessary careful selection of the surface optical properties and conduction path. Because the impact plate must be mechanically isolated from the experiment structure, natural conduction paths were difficult to implement. Conduction coupling with minimum acoustic coupling was achieved by bonding one edge of 0.0015-inch-thick pure aluminum foil strip to the periphery of the plate and the other edge to the structure, with a separation of approximately one-eighth inch. Aluminum is vacuum-deposited on the molybdenum film strip, providing an emissivity of 0.05 and an absorptivity of 0.12. The nighttime heat leak is about 17 percent of the total. The temperature excursion of the crystal microphone is predicted to be between 137°F and -22°F.

THIN FILM DEVELOPMENT

The front-film configuration incorporated in the LEAM experiment differs from that used in the Pioneer 8 cosmic dust detector and resulted from a development program made necessary primarily by the fact that no experimental data were available on the behavior of Pioneer-type front film in the lunar thermal environment. Analysis showed that films of the Pioneer type with α/ϵ ratios greater than 2.5 could not survive direct sunlight on the moon. Moreover, considerable experimentation with plasma-producing depositions had taken place in the United States and abroad subsequent to 1967 when Pioneer 8 was launched; this work indicated that other metals, some of which are more easily deposited than the copper used on Pioneer 8, could be applied to produce equal or better ionization pulses. Finally, the availability of improved thin-film substrate materials, such as the much stronger Parylene C, suggested that it might be possible to reduce the mass cross section of the front film, thereby increasing the dynamic range of the detector. A program was therefore established to define and verify through test a composite capable of meeting the mechanical and thermal requirements, while at the same time minimizing mass cross section and maximizing ionized-plasma production.

Several film samples of different thicknesses of the Parylene C substrate, with and without a 95-percent-transparent beryllium copper support grid, were tested under sinusoidal and random vibrations to assess their mechanical properties. It was concluded that to survive launch and boost a support grid was needed, and that with such a grid, the Parylene C film substrate could be as thin as 1000 angstroms.

A much more extensive variation in film samples was required to assess the thermal properties of thin films. The objective of the thermal investigations was to find an opaque film whose external optical properties provided an α/ϵ ratio of 2.5 or less while minimizing α and ϵ. With a Parylene C substrate thickness fixed at 2000 angstroms, samples of three different metal deposits – gold, silver, and aluminum – were tested for optical properties, with deposit thickness, deposition rate, outer-coat material, and outer-coat material thickness varied for each metal. Film configurations with and without a support grid were also tested in a calorimeter. The calorimeter tests showed that, with a support grid, the α/ϵ ratio of the film could be significantly higher than 2.5 without its yield point being exceeded in direct sunlight. The principal conclusions drawn from the thermal tests were that the film should have a support grid and that either silver or aluminum, with or without an outer coating of Parylene C or silicon oxide, is satisfactory. From overall experiment thermal-control considerations, the silver film is preferred because of its lower emissivity and absorptivity.

Representative samples of gold, silver, aluminum, and lithium chloride salt were tested in the Goddard 2-megavolt electrostatic accelerator to assess the electrical properties of the new films. The plasma-producing qualities of all the samples proved to be the same as those of the copper film used in the Pioneer 8 dust detectors.

Methods of film-laminate production were also investigated to determine which provided the best reproducibility for quality control. By virtue of their physical properties, some materials can be vacuum-deposited on a thin Parylene C pellicle with reasonable uniformity in the free-standing state whereas others cannot. It was also found that some film composites are easily mounted in a reasonably loose state whereas others tend to mount tightly. Experience has shown that loosely mounted thin films survive cold LN_2 temperatures; tightly mounted films tend to fracture at temperatures below -78°C.

The film finally chosen for the LEAM experiment is a composite of nominally 2000-angstrom Parylene

C and 750-angstrom aluminum, with a 3000-angstrom coating of silicon oxide over the aluminum. This film is bonded to a beryllium copper grid of one-eighth-inch mesh. The aluminum and silicon oxide are vacuum-deposited at rates of 6.5 and 10 angstroms per second, respectively, with the Parylene substrate in a free-standing state.

ELECTRONICS DESIGN

The electronics design is fundamentally the same as that used in the Pioneer 8 dust-detector experiment. The basic differences are in the circuitry required to operate with the ALSEP Central Station and in design refinements that reflect a more advanced state of the art, such as the use of low-power, highly reliable microelectronic components.

The timing and control logic provides the analog and digital interface with the ALSEP Central Station. Engineering data are multiplexed on three analog data lines, and science data are serially shifted on one digital data line. Each analog line is sampled once every 90 data frames by the ALSEP data subsystem. Up to ten engineering analog data signals are multiplexed on two lines, and survival temperature is continuously monitored on the third. Two 10-bit NRZ-C digital words are provided every 64-word ALSEP telemetry frame in response to a demand pulse per word and in synchronism with the ALSEP data sequence of 90 frames. The experiment uses ten words to transfer a complete set of data. Thus, eighteen complete sets of experiment data and one set of engineering data are transmitted for every 90-frame ALSEP sequence, the transmission time required being about 54 seconds under normal conditions or 108 seconds in the slow-rate contingency mode.

The dual-film sensor logic consists of a measurement section and a buffer section. The measurement section contains identification-pulse storage latches, accumulators, pulse-height-analysis (PHA) conversion counters, and a time-of-flight (TOF) conversion counter. The buffer section is a parallel-in/serial-out shift register that shifts on demand only. The shift repeats transmission of old data, which are never cleared until replaced by new data or by calibration data. New data from a hit on any film or main microphone will initiate a measurement cycle unless flip-flops (FF) and latches are still holding data from a previous hit not yet fully processed. The OR function of all the hit signals triggers a one-shot that has three functions: (1) to provide a gate for the front- and rear-film PHA counters; (2) to provide a synthetic rear-film signal after a certain amount of time, permitting the TOF measurement logic to progress whenever the rear-film signal is missing; (3) to prevent premature issuance of the measurement-completion signal. When the measurement operation ends, four flip-flops that control the transfer of the data into the shift register are set. Whenever two events occur in close proximity, transfer into the shift register is held up until the earlier data have been sent. Once conditions are right, with the appropriate flip-flops in the set state and the current frame available, the sequencer states are traversed, clearing the shift register, copying the measurement flip-flops into the shift register, and then clearing all the measurement-storage devices except the accumulators.

The most difficult problem involved in adapting an essentially existing and proven electronics design to a new application on the lunar surface is noise. The concept of using coincidence detectors and control shielding was introduced in the original Pioneer dust detector to eliminate noise-induced signals. In the case of ALSEP, the problem of noise interference with other experiments as well as that of noise susceptibility had to be considered.

Radiated interference from the LEAM experiment is negligible because the currents and voltages are low and the highest frequency generated is from the 25-kilohertz clock, which is easily shielded with 0.04-inch solid copper. Additional radiative shielding is provided by the aluminized thermal enclosure. Conducted-interference sources such as the d.c./d.c. converter were systematically eliminated or minimized through redesign following breadboard testing.

The most serious noise problem is the susceptibility of the high-impedance, sensitively triggered amplifiers. Radiated noise is picked up through the three large sensor openings and through the 30-foot cable that ties the experiment to the ALSEP Central Station. The radiated-noise sources to which ALSEP is tested have frequencies of 15 kilohertz to 10 gigahertz. The sensor amplifiers cut off at a frequency of about 12 megahertz. In that the sensor outer grids provide an effective shield up to 1 gigahertz, a certain amount of natural filtering is inherent in the design. In addition, the sensor amplifiers have a high common-mode noise rejection of about 74 decibels minimum. Two design approaches will be evaluated during prototype testing to further reduce radiated-noise susceptibility. That favored at this writing ties the signal return to the experiment housing. The alternative approach, which is used with other ALSEP experiments, ties the experiment housing to chassis return, with the actual grounding taking place at the Central Station.

LUNAR DEPLOYMENT

The LEAM experiment is transported to the moon, mounted upside down on ALSEP subpackage 2 and

held down by four quick-release fasteners. The subpack is first off-loaded from the Lunar Module and taken by the astronaut to its deployment site where it is placed upon the lunar surface. To deploy the experiment, it must be removed from the pallet, transported to its deployment site about 25 feet away, placed on the lunar surface, and coupled to the Central Station via a 30-foot flat cable. These operations are designed to take a single astronaut no longer than 10 minutes.

To remove the experiment from the subpack, the astronaut first releases four fasteners with the universal handling tool (UHT); he then couples the UHT to a swivel socket, making it possible for him to raise the experiment without bending over. Before actually removing the experiment, the astronaut plugs a 37-connector flat cable into the ALSEP Central Station, using an astromate connector with a large handle so that he need not bend over. He now lifts the experiment by the UHT handle and carries it to its deployment site, trailing behind the unreeling flat cable. At the deployment site, he performs two pull-and-release functions for which two large lanyard rings are provided on the side of the experiment, secured by velcro tape. The first lanyard unlocks the UHT swivel socket, permitting the experiment to rotate 180 degrees to its upright position. The other lanyard releases two latches to extend the four legs and gnomon bar. The astronaut then lowers the experiment to the surface on its legs and, with the UHT still attached, performs two simple leveling and alignment operations. While watching a bubble level, he presses downward and twists with the UHT, causing the appropriate leg to sink into the soil until the experiment is level. He approximates correct north and south alignment when he places the experiment on the surface, using his own shadow as a guide; he then accomplishes fine alignment by moving one end of the experiment with the UHT while watching the shadow of the gnomon rod on a compass rose painted on the experiment dust cover. Photographs are taken of the gnomon shadow and bubble level for later use in data reduction.

The Lunar Mass Spectrometer Experiment

R. D. ORMSBY
C. E. DeHAVEN, JR.

The Lunar Mass Spectrometer (LMS) is a small, lightweight, low-power, highly sensitive instrument being developed to fly on Apollo 17 and designed to identify the constituents of the lunar surface atmosphere. Its function will be to determine the global distributions and the diurnal variations of the lunar atmosphere and thus to test theories of planetary exosphere dynamics. Since the lunar atmosphere is a classical exosphere, these gas distributions can provide a reasonable check on exospheric transport theories, which play an important part in terrestrial exospheric problems. In addition, the LMS will provide valuable clues as to the origin of the lunar atmosphere and, by simultaneously monitoring the carbon monoxide (28 atomic mass units) and the sulfur dioxide (64 atomic mass units) constituents, will isolate volcanic activity.

The LMS is basically a magnetic-deflection mass spectrometer with three ion detection systems covering mass ranges of 1 to 4 atomic mass units, 12 to 48 atomic mass units, and 27 to 110 atomic mass units, respectively. It is capable of detecting partial pressures ranging from 10^{-8} to 10^{-13} Torr. The overall instrument sensitivity is greater than 1×10^{-5} ion amperes per Torr, with unit resolution at 82 atomic mass units.

MASS SPECTROMETER CONFIGURATION

As shown in Figure 1, the LMS consists of two major subsystems, the electronics section and the gas analyzer section, the latter of which contains a gas ionizing assembly, the ion-separating magnetic assembly, and the ion detection assembly.

The two subsystems are joined to a common baseplate, with each subsystem having its own fiberglass cover. The electronics subsystem is contained in a thermal bag, covered by a second-surface-mirror radiator plate to provide thermal control. This control will maintain electronics subsystem temperatures between 0°F (lunar night) and 150°F (lunar day). The gas analyzer subsystem contains no thermal control and is subject to the lunar temperature range of -300°F to +250°F.

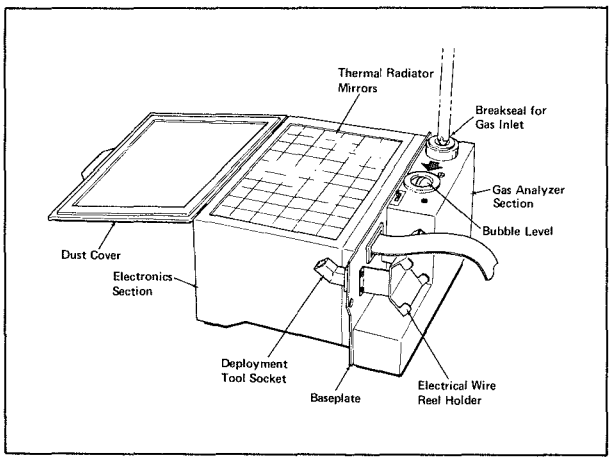

Figure 1 Lunar Mass Spectrometer Configuration

There are two heater assemblies on the LMS. One, designated the *survival heater,* is attached to the radiator plate and is used to supply heat to the electronics subsystem should it be required during lunar night. The second, designated the *bake-out heater*, is attached to the ion source and serves to remove contamination that may accumulate by raising the temperature of the ion source. The LMS functional block diagram in Figure 2 identifies the major electronic functions and the electrical interfaces with the gas analyzer.

Figure 3 is a schematic of the gas analyzer section. As the gas molecules enter the inlet, they are ionized in the ion source, drawn out of the source, focused into an ion beam, and accelerated through a slit assembly leading to the drift tube. In the drift tube, the ions are deflected by a permanent magnet and collected by three electron multipliers at three exit-slit locations. The mass spectrum is scanned by varying the ion accelerating voltage in the ion source in a stepwise manner and counting the number of ions impinging on each detector at each voltage step. The magnitude of the count determines the concentration

The Lunar Mass Spectrometer design is based upon concepts developed by John Hoffman of the University of Texas at Dallas. The flight hardware is being designed and built jointly by the University of Texas and Bendix Aerospace Systems Division, Ann Arbor, Michigan, under the sponsorship of the National Aeronautics and Space Administration Manned Spacecraft Center.

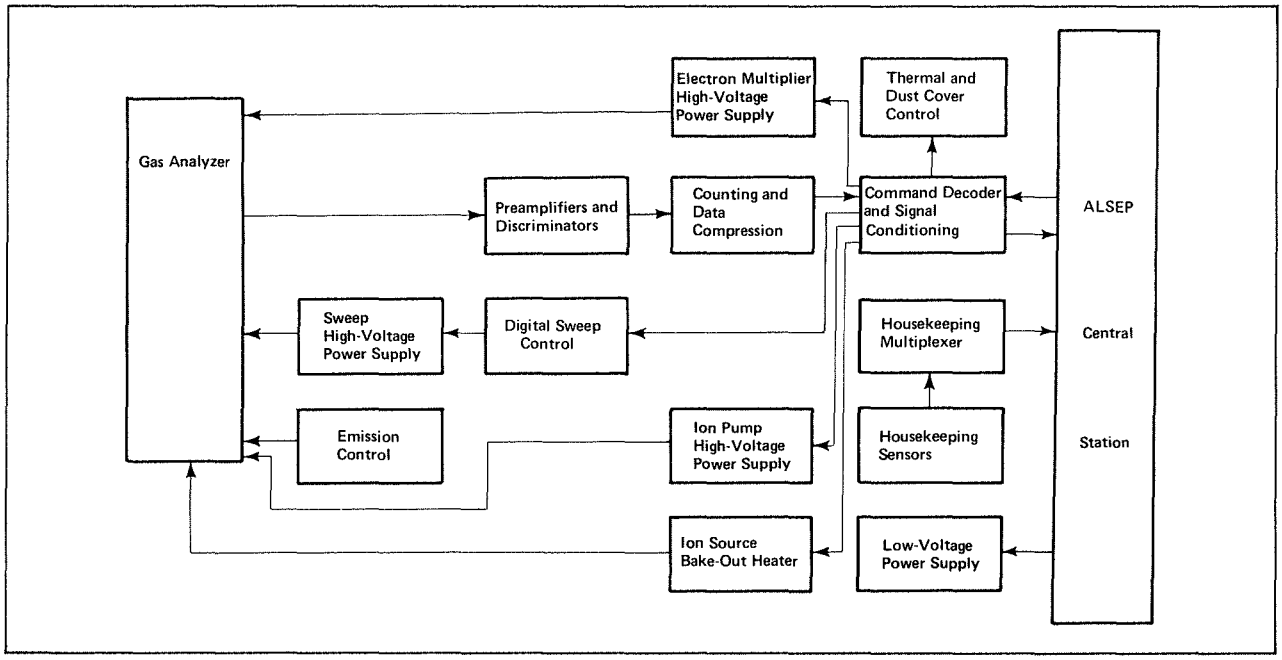

Figure 2 Lunar Mass Spectrometer Functional Block Diagram

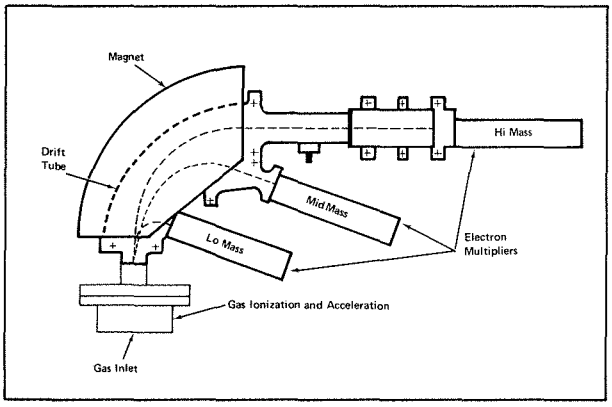

Figure 3 Gas Analyzer

of each constituent of the gas sample in the ion source, and the voltage step number is calibrated to identify that constituent.

MASS SPECTROMETER DESIGN

Atmospheric gas molecules collected by the inlet aperture of the mass spectrometer are ionized by electron impact in an open ion source, using a Nier-type electron source. Thermionic electrons, produced by passing 1 ampere through a tungsten/rhenium filament, are collimated by a small 350-gauss permanent magnet. A second tungsten/rhenium filament assembly applies a positive voltage and acts as an electron trap; this filament can be switched to become the thermionic emitter in case the other filament experiences burnout. The current detected by the electron trap is used to provide active emission control of the filament current. The differential voltage applied to the filament assemblies provides the force necessary to accelerate the electrons through the ion source to develop an energy level of approximately 80 electron volts.

After the gas molecules are ionized, they are drawn out of the ion source past a series of slits, as illustrated in Figure 4. This is accomplished by placing a positive voltage on the entire ion source and providing an opening in it to permit the positively charged ions to accelerate toward a ground-potential slit; this slit is called the object slit since it also serves as the object for the ion optics of the mass spectrometer. Between the object slit and the ion source is a second slit called a J-plate; this slit is analogous to an optical

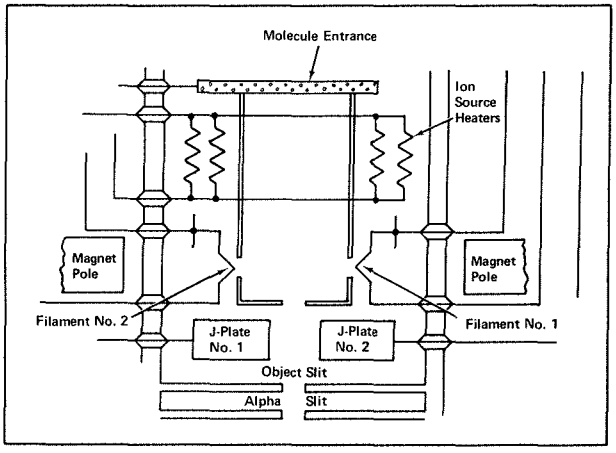

Figure 4 Ion Source

lens and is used for fine-focusing of the ion beam. A third slit, called the alpha slit, is between the object slit and the drift tube and serves to limit the ion optic aberrations. The object slit and the alpha slit are at ground potential; the J-plate potential is 90 to 95 percent of the ion source voltage. In order for the instrument to sweep the mass range, the ion source voltage is varied in a stepwise manner to impart different momenta to the ions as they leave the ion source and pass into the drift tube. The voltage sweep starts with a pedestal voltage of +320 volts and increases to +1420 volts in 1330 steps.

After the ion beam passes through the slit assembly, it enters the analyzer portion of the instrument, where it is deflected by a 4300-gauss permanent magnet in accord with the following equation,

$$M/E = KB^2R^2/V \qquad (1)$$

where B is magnetic field strength, R is ion-trajectory radius of curvature in the magnetic field, V is ion accelerating voltage, K is a constant, M is ion mass in atomic mass units, and E is electronic charge. Exit slits with ion detectors are located on three circular trajectories having radii of 0.478 inch, 1.653 inches, and 2.500 inches, as illustrated in Figure 3. This combination provides for the simultaneous monitoring of carbon monoxide and sulfur dioxide on the medium and high mass ranges, respectively.

The density of each gas species is a function of the number of ions detected at each voltage step. Electron multipliers provide a pulse output for each ion input. This output is the input to a charge-sensitive amplifier, in series with a discriminator and a 21-bit counter. Since electron multipliers cannot be operated safely at pressures above 1×10^{-5} Torr, the pressure in the analyzer is determined prior to electron-multiplier turn-on by monitoring the current of a 0.15-liter/second-appendage ion pump.

Upon command from the Central Station, the data in the counter are compressed and relayed to the Central Station for telemetry back to earth. The magnitude of the ion count indicates the partial pressure of the gas species at each voltage step. The instrument is calibrated to relate ion count to gas pressure and voltage step to gas being detected.

Figure 5 is a photograph of the gas analyzer section of the LMS engineering model. A sample of the data obtained from this unit and presented in analog form on a strip-chart recorder is shown in Figure 6.

ENGINEERING REFINEMENTS

Program final design required that weight and power be reduced to a minimum. A major reduction was achieved in the weight of the analyzer magnet (from 6.0 to 3.75 pounds) by substituting in the flight design Alnico 9 material for the Alnico 7 used in the engineering model.

Previous mass spectrometers for space have used a squib-activated "can-cutter" to remove the protective cover over the entrance to the ion source. On the

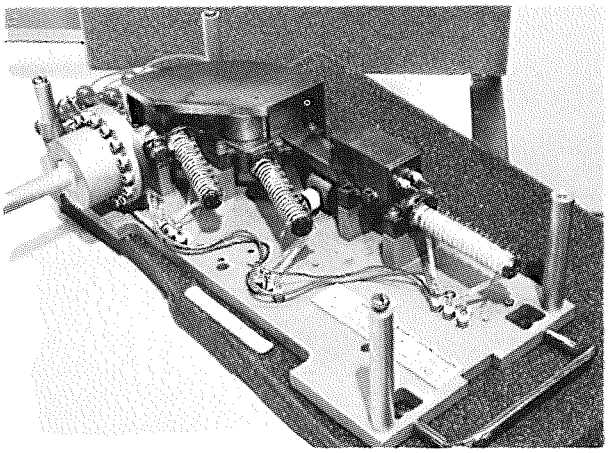

Figure 5 Gas Analyzer Section of Engineering Model

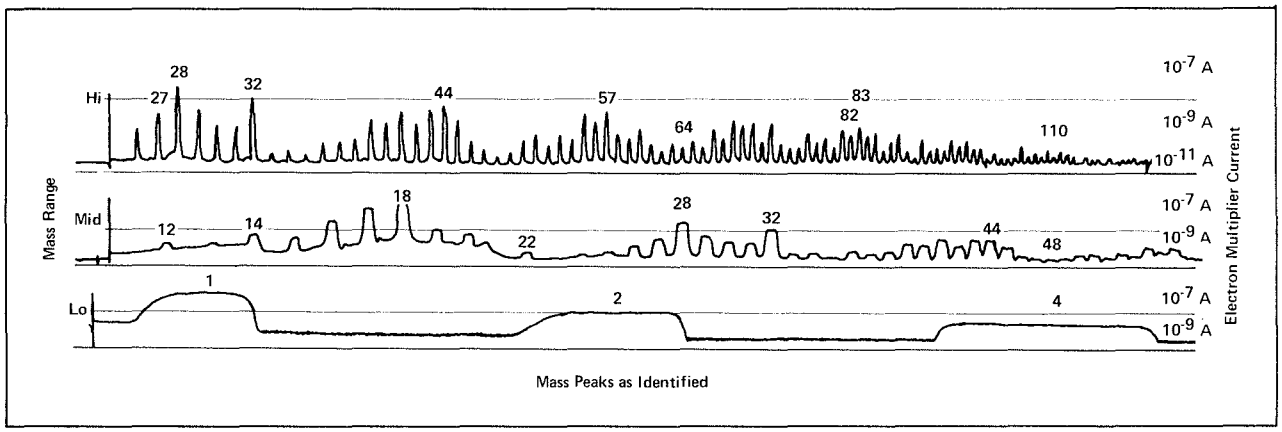

Figure 6 Analog Data Output

ALSEP spectrometer, this is replaced by a simple astronaut-actuated breakseal, which eliminates the need for electronic circuits, reduces the weight of the device, and, most important, increases reliability.

The second-surface-mirror radiator plate is equipped with a cover to protect it from dust contamination both during astronaut deployment and during Lunar-Module ascent. This cover must be removed after the Lunar Module has departed from the moon. Squib actuators, which are commonly used for remote releasing, are a source of contaminating gas that could degrade the scientific data. It was necessary, therefore, to develop another form of dust-cover tie-down and release. A Dacron cord is used, around a small section of which is coiled a Nichrome resistive heating element. After the Lunar Module leaves the surface of the moon, a current of approximately 250 milliamperes is run through the Nichrome strip for 15 seconds; resistive heating occurs, the Dacron cord is burned through, and a preset spring forces the dust cover open.

EXPERIMENT OPERATION AND DATA RETURN

The ALSEP telemetry frame contains 64 10-bit words, which are transmitted at a rate of 1060 bits per second. At the beginning of each frame, a pulse from the Central Station is used to step the digital sweep control by one step. Thus, the dwell time on each voltage step is approximately 0.6 second, and during this time the three 21-bit counters accumulate data from the three electron multipliers. The 21-bit counters are then parallel-loaded into shift registers, which compress the data into three coded 10-bit words. Upon receipt of a data-demand pulse from the Central Station, the three scientific data words are serially transmitted to the Central Station for downlink transmission as ALSEP words 17, 19, and 21. The LMS has been allocated ALSEP word 5 for transmission of a status flag word to indicate the condition of the instrument. Various temperature and housekeeping-current monitors are transmitted as analog data on ALSEP word 33.

CONCLUSION

The first mass spectrometer to be placed on the lunar surface, the LMS is scheduled to fly on Apollo 17 in December 1972. It is a high-performance gas analysis instrument that weighs only 20 pounds and requires 12 watts for operation in the extreme lunar-surface environment. The new scientific data it collects on the lunar atmosphere should serve to help us better understand the atmosphere of our own earth as well.

The Lunar Seismic Profiling Experiment

J. E. DYE

The Lunar Seismic Profiling Experiment (LSPE), now under development and scheduled for deployment on the moon as a part of the Apollo 17 mission, is an advanced version of the Active Seismic Experiment, described elsewhere in this issue.* The LSPE consists of eight packages, each containing an explosive charge, and a central-electronics package, which is housed within the ALSEP Central Station. The explosive charges weigh from 1/8 pound to 6 pounds and are approximately equivalent to TNT in energy per pound. They will be deployed from the Lunar Roving Vehicle (LRV) by the astronauts at distances of 500 meters to 3.5 kilometers from an array of four geophones emplaced on the lunar surface. The charges will be detonated after the astronauts leave the lunar surface by an r.f. command from the ALSEP Central Station.

The detonations will generate waves of seismic energy, the velocities of which will be determined to depths of 3 to 4 kilometers on the basis of geophone detection measurements. The data obtained, in combination with known velocity/density relationships, are expected to reveal much concerning the internal structure and composition of the lunar surface. According to present plans, the Apollo 17 landing site should be near a major planetary ridge – one comparable in extent to the midoceanic ridges on earth – which may be the surface manifestation of a fundamental internal process of lunar evolution, such as differentiation and/or convection.

The Lunar Seismic Profiling Experiment and the Active Seismic Experiment have the following important similarities and differences:

- The LSPE has a maximum explosive-charge weight of 6 pounds, whereas that in the ASE is 1 pound. As a consequence, the LSPE charges can be deployed at a greater maximum distance from the geophone array – 3.5 kilometers for the LSPE as compared with 1.7 kilometers for the ASE – to yield seismic velocity measurements at greater lunar-surface depths.
- The ASE explosive charges are rocket-propelled. Those of the LSPE are carried to the desired deployment site aboard the LRV and emplaced on the lunar surface by the astronauts.
- The ASE charges detonate on impact with the lunar surface after rocket propulsion initiated by ground command. The individual LSPE charges are armed by two mechanical timers that are started by the crew at the time of deployment. Time runout and arming occur well after the crew has left the lunar surface. Detonation is accomplished via a ground-controlled r.f. link between the ALSEP Central Station and a receiver in each explosives package.
- The ASE geophone array is linear, 300 feet in length, and consists of three geophones spaced at 150-foot intervals. The LSPE geophone array is triangular in shape, with one geophone positioned at each of the apices of an equilateral triangle 300 feet on a side; a fourth geophone is positioned at the triangle center. The LSPE array provides a capability for determining the arrival angle of the induced seismic energy.
- The LSPE geophones are identical to the ASE geophones but are stowed in a different manner for transport to the lunar surface and deployment by the astronauts.
- The LSPE central electronics are similar in function and construction to the ASE central electronics. They differ in that, whereas the ASE contains a receiver, the LSPE contains a transmitter that transmits a pulse-coded r.f. signal to a receiver in the explosives package to actuate detonation at a precise time.

EXPERIMENT DESCRIPTION

The LSPE explosives package is seen in Figure 1, and a cutaway view is shown in Figure 2. The Lunar Seismic Profiling Experiment contains eight such packages, all identical except for the size of the high-explosives charge and the preset runout time of the mechanical timers. The high-explosives charge is contained within a nickel-plated fiberglass housing, which forms the bottom portion of the explosives package. The top portion – the electronics and SAFE/ARM

Robert L. Kovach, Department of Geophysics, Stanford University, is Principal Investigator for the Lunar Seismic Profiling Experiment as well as for the Active Seismic Experiment.

*J. R. McDowell, "The Active Seismic Experiment."

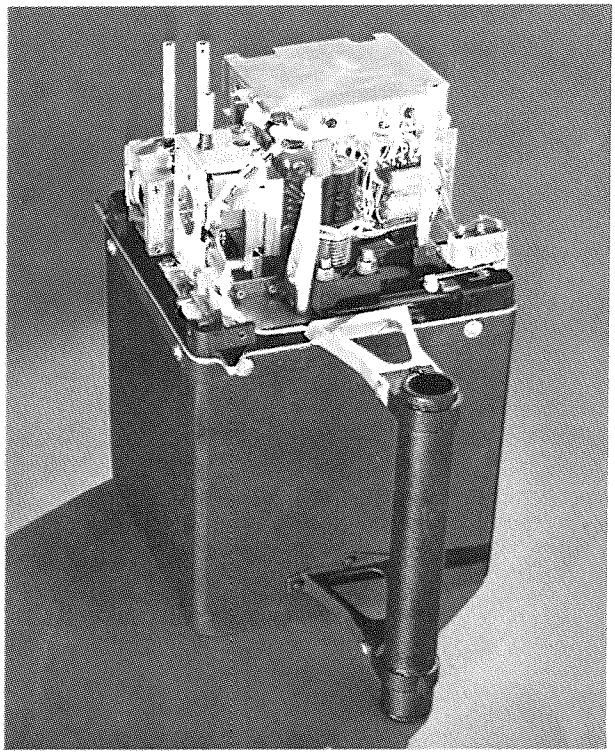

Figure 1 Lunar-Seismic-Profiling Explosives Package (Cover Removed)

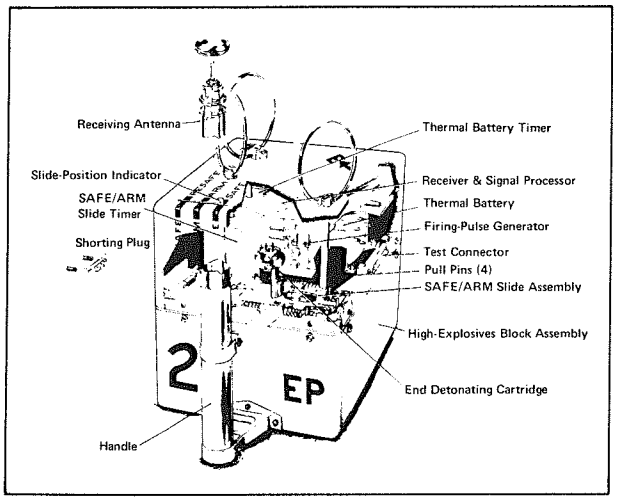

Figure 2 Lunar-Seismic-Profiling Explosives Package (Cutaway View)

assembly – consists of a magnesium baseplate upon which are mounted the following components:

- the *end detonating cartridge (EDC)*, the first component of the explosives train;
- the *SAFE/ARM slide*, the second component of the explosives train, which contains an explosive lead;
- a mechanical *SAFE/ARM slide timer*, which moves the lead into line with the EDC to complete, or arm, the explosives train;
- *receiving antenna, receiver, signal processor, and firing-pulse generator*, which function to receive the pulse-coded FIRE signal transmitted from the ALSEP Central Station, to process this coded signal, and to provide a firing pulse that fuses a bridgewire in the EDC to actuate the explosives train;
- a *thermal battery*, which supplies power to the above circuitry;
- a *thermal battery timer*, which activates the battery via impact of a firing pin onto a percussion primer in the battery.

A temperature ranging between 40°F and 170°F will be maintained for these components over the period from lunar morning to lunar noon during which the package is to be exposed to the lunar environment. Solar input at high sun angles will be minimized by multilayer insulation inside a fiberglass top cover and by a coating of white thermal paint on the exterior of the upper portion of the cover. The remaining exterior surfaces of the explosives package are painted black to permit rapid initial warm-up of the packages, which will be deployed at low sun angles when temperatures are near the minimum operating limit.

The astronauts start the two mechanical timers at the time of deployment by removing two separate pull pins. Another pull pin provides a safety back-up to the SAFE/ARM slide timer by constraining the SAFE/ARM slide in its SAFE position. A fourth pull pin, contained within the thermal battery timer, serves as a safety back-up against the possibility of premature functioning of the battery timer by constraining the firing pin from activating the battery. Each of these pins is held by a retaining-spring force that must be overcome by the astronaut during pin removal. Removal of the SAFE/ARM slide pull pin requires both rotation and pull, the two actions in sequence being constrained by a retaining-spring force. Locking features are incorporated in all pins to prevent their removal in the event of component malfunction. Should either of the timers have started to run, its pin would be locked in place and impossible to remove. Should the slide not be constrained in the SAFE position by the SAFE/ARM slide timer, the SAFE/ARM slide pull pin would lock and could not be removed. Should the firing pin be prematurely released by the timing mechanism, the pull pin constraining the firing pin within the thermal battery timer would lock in a similar manner.

EXPERIMENT OPERATION

A block diagram describing the operational sequence within an LSPE explosives package is presented in Figure 3.

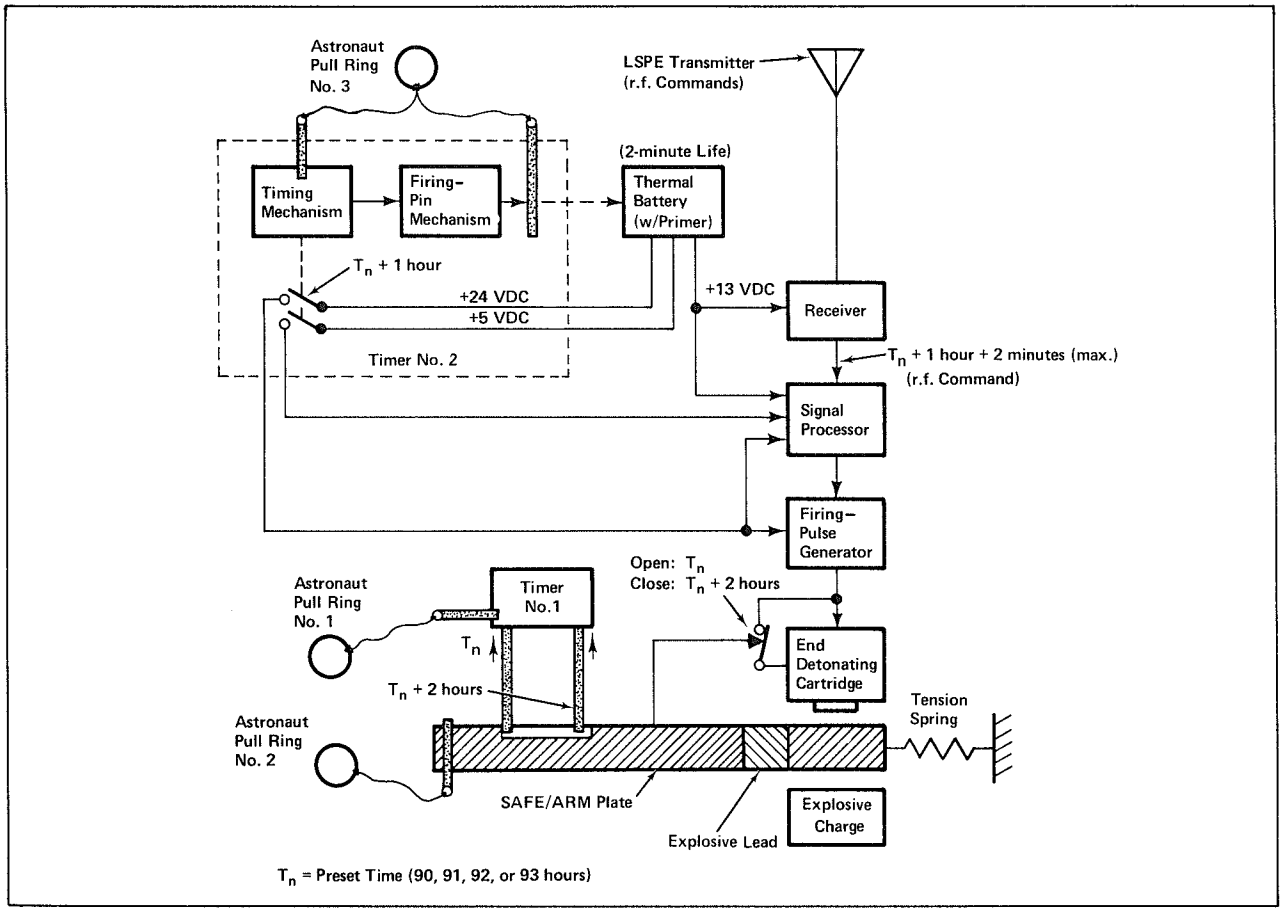

Figure 3 Explosives Package Block Diagram

When the astronaut removes the four pull pins at the time of deployment, the mechanical timers start, which, after a 90-hour timeout, remove the safety constraints holding the SAFE/ARM slide and the battery firing pin in the locked position; the prescribed order of pull-pin removal maximizes the safety that is inherent in the pull-pin locking features. The SAFE/ARM slide timer is preset to function for 90 hours, a period that assures – even in a contingency situation – that the crew will have left the lunar surface prior to the arming of any explosives package. Once this period has elapsed, a pin constraining the spring-loaded SAFE/ARM slide is retracted by the timer, permitting the slide to move to its ARM position. Motion of the slide opens a microswitch that to this point has shorted the electrical leads of the EDC. The thermal battery timer is preset to function, independently, at 91 hours, 1 hour after the SAFE/ARM slide timer has placed the slide in its ARM position. A spring-loaded firing pin within the timer is released, striking a percussion primer within the battery and activating the battery. Concurrently, two microswitches within the timer are closed, connecting the thermal battery output to the electric circuits.

The LSPE transmitter, which is located within the ALSEP Central Station, transmits a repetitive pulsed carrier signal, the time characteristics of which are detailed in Figure 4. A series of three pulses properly spaced in time is required to elicit a FIRE signal out of the signal processor within the explosives package and detonate the explosives train. Should the first set of pulses fail to accomplish this, the battery life of 2 minutes permits three additional attempts to be made. Since the seismic data subsequently collected must be accurately referenced to the instant of detonation, it is necessary to establish which specific set of pulses is effective. This is done by comparing known times of pulse-set transmission with the time of arrival at the geophones of the initial seismic data. Pulse sets are spaced at 29.55-second intervals to make such identification possible without ambiguity.

In the event of a dud, the SAFE/ARM slide timer mechanism retracts a second pin and the slide moves to a RESAFE position; this occurs at 92 hours, 2 hours after initial release of the SAFE/ARM slide. A linkage extending through the top cover of the explosives package and connected to the SAFE/ARM slide

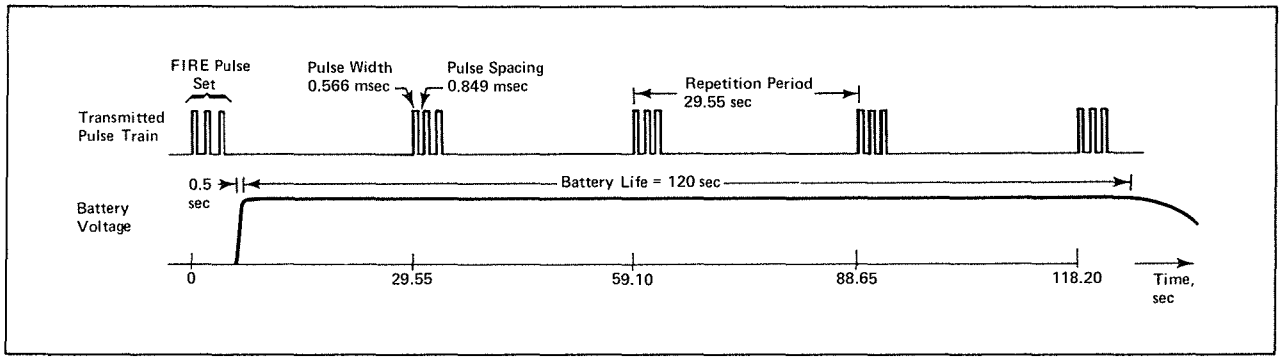

Figure 4 Time Characteristics of LSPE Transmitter Signal

indicates to the astronauts that the slide is in its initial SAFE position.

It should be noted that the explosives package is so designed as to eliminate any possibility of premature detonation endangering the lives of ground handling personnel or of the astronauts during deployment. The locking features of the pull pins and their order of removal preclude any mechanical timer-action output should either or both timers operate prematurely. Subsequent to pull-pin removal, premature detonation could occur only if both timers were to time out prematurely, each within a window of 2 hours, and if a pulse-coded spurious r.f. signal within the narrow 10-kilohertz bandwidth of the receiver were to be received during the 3-minute window of maximum battery life.

The LSPE geophones, which are identical to those used for the Active Seismic Experiment, are stowed in a geophone module as shown in Figure 5. The universal handling tool is used by the astronauts to carry this module to a deployment site about 30 feet away from the ALSEP Central Station. The tool is also used to remove the module cover; to pick up, carry, and emplace the individual geophones; and to spool out the geophone cable, which is wound on a ball-bearing-supported reel.

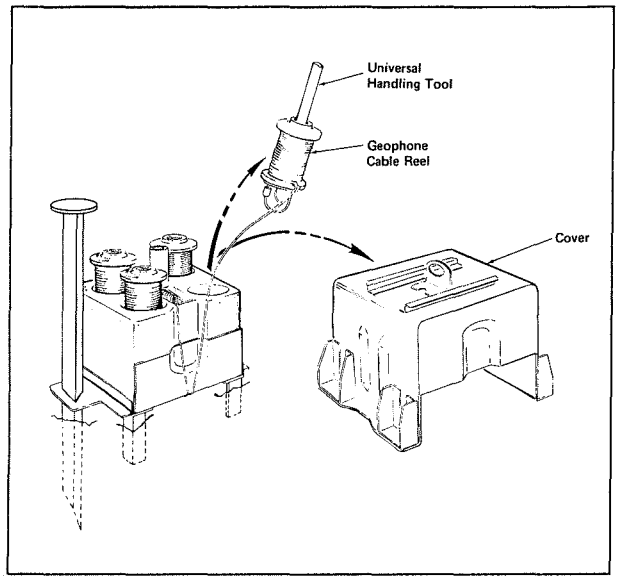

Figure 5 Geophone Module Deployment

The Lunar Surface Gravimeter Experiment

H. K. HSI
W. E. CROSMER

INTRODUCTION

The Lunar Surface Gravimeter (LSG) Experiment is an extremely sensitive experiment designed to accomplish the following tasks:

- To search for gravitational radiation from cosmic sources, which may excite low-frequency free oscillations of the moon, in the frequency range upward from 1 cycle every 15 minutes.
- To obtain information on the internal structure of the moon by measurement of lunar deformations associated with tidal forces.
- To obtain vertical-axis seismic data up to frequencies of 16 hertz.
- To determine the ratio of lunar gravitational force to earth gravity with a precision of 1 part in 10^5.

The Lunar Surface Gravimeter has three basic components: a LaCoste-Romberg gravity meter, a structural/thermal-control package, and an electronics package.

THE GRAVITY SENSOR

The gravity meter uses the LaCoste-Romberg type of spring-mass suspension to sense changes in the vertical component of local gravity. A schematic diagram of the meter is shown in Figure 1.

In the LaCoste-Romberg instrument, the major fraction of the force supporting the sensor mass (beam) against the local gravitational field is provided by the zero-length spring. A zero-length spring is one in which the restoring force is directly proportional to the spring length. Small changes in force tend to displace the beam up or down. This imbalance is adjusted to the null position by repositioning the spring pivot points by means of micrometer screws.

The sensor mass can be modified by the addition or removal of small weights, permitting the range of the sensor to be extended from earth to lunar operation.

The electronic sensing portion of the instrument consists of a set of capacitor plates. Two plates are

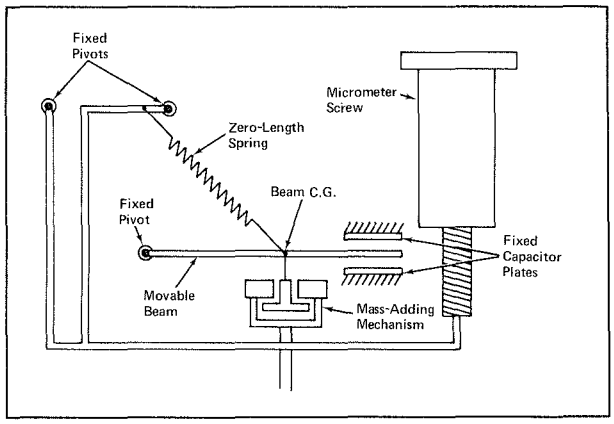

Figure 1 Lunar Gravity Meter Schematic

fixed to the frame of the sensor, geometrically concentric with a third plate of similar size which is attached to the movable beam of the sensor. The plates are so arranged that the center plate is located exactly between the two outer plates when the beam is exactly horizontal.

The LSG has two servo systems. A null-seeking servo system provides an electrostatically generated restoring force to balance the change in gravitational forces and recenter the beam to its reference position, equidistant between the two outer capacitor plates. The spring suspension point is adjusted by means of a motor-driven micrometer-screw servo system and is so set up that the center plate is zeroed when the input perturbation signal is midway between its extreme values. Micrometer-screw position is detected by readout of shaft encoders coupled to the screws.

The sensor-spring constant, and thus the restoring force, is affected by temperature. However, there is a point of inflection on the spring-constant-versus-temperature curve at which the spring constant is least sensitive to temperature changes; this point is called the spring inversion temperature point. To minimize the effects of temperature on the data output, the sensor will be operated near this temperature (50°C) and its setpoint will be maintained with a short-term (30-minute) stability of ±0.001°C and a long-term (one-lunation) drift of ±0.01°C.

The Lunar Surface Gravimeter Experiment was conceived by Principal Investigator Joseph Weber of the University of Maryland.

INSTRUMENT CONFIGURATION

To operate properly, the gravimeter sensor must be finely leveled and its temperature and pressure must be maintained within very close limits. A cutaway view of an instrument design to satisfy these requirements is shown in Figure 2.

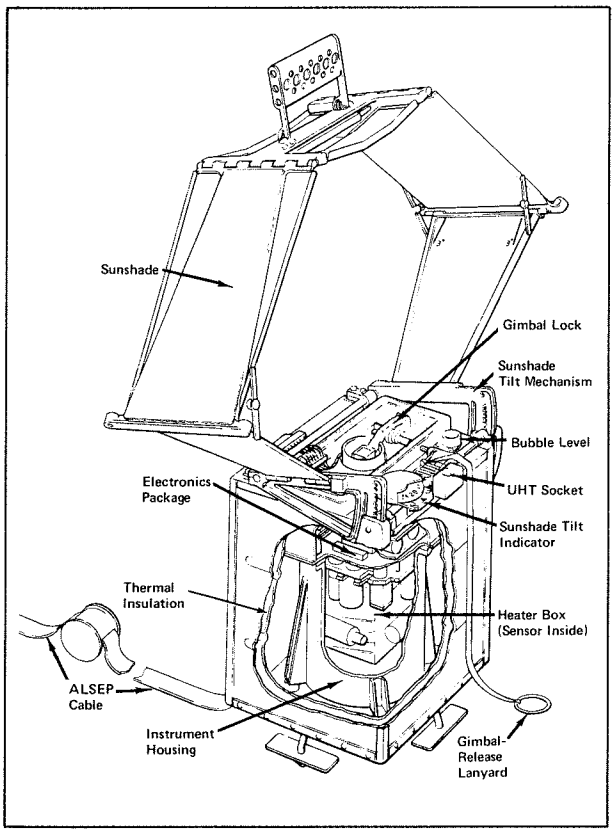

Figure 2 Lunar Surface Gravimeter Configuration

In essence, the sensor is surrounded by three containers. The innermost is the heater box, which contains in addition to the gravimeter sensor the basic heating elements and drive mechanisms. Figure 3 is a photograph of an early model of this unit. Located on the outside of the heater box are motors for driving the micrometer screws, for mass adding, and for adjustment of tilt angle. The box is suspended in the sealed instrument housing, which is evacuated and back-filled with nitrogen to a nominal pressure of 10 Torr. This small amount of gas provides the damping necessary for operating the sensor and the servo systems. The four fiberglass straps by which the box is suspended provide conductive thermal isolation from the instrument housing. The electronics package is mounted on top of the instrument housing. A pressure sensor for monitoring internal pressure is located in the instrument-housing cover. Power and signal connections between the pressure sensor, the heater

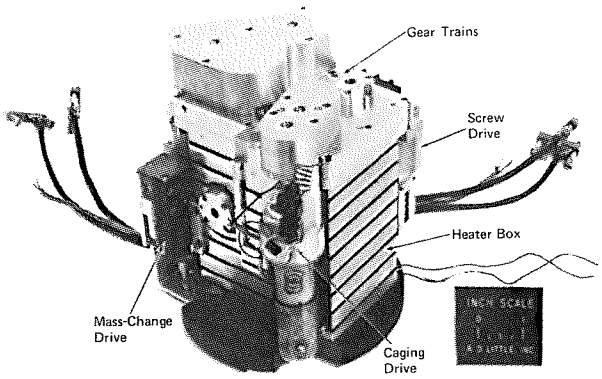

Figure 3 Heater-Box/Sensor Assembly

box, and the electronics package pass through two hermetically sealed connectors in the cover.

The total instrument-housing and electronics-package assembly is suspended from a gimbal for self-leveling. For fine adjustment, the center of gravity of the gimbal-suspended mass is adjusted by driving small, weighted motors attached to the heater box along a screw to a new position. The clearance between the instrument housing and the outer container permits a swing of slightly more than 3 degrees in all directions without interference. In the stowed configuration, the gimbal is locked and the entire suspended mass and gimbal are depressed into small cones located in the insulation between the two outer containers.

The container that encloses the entire suspended mass is composed of insulation between two aluminum shells. Four feet, used for lunar emplacement, project from the bottom of the container. The top has a cavity that contains the thermal radiator and the gimbal-actuator mechanism. Also located on the top of the unit are a bubble level, the handling-tool socket, the sunshade with its tilt mechanism, the tilt indicator, and detents for locking in a tilted position. On the side of the outer container is a bracket that retains the cable spool and cable linking the unit to the ALSEP Central Station.

The sunshade is a five-element mechanism that has three functions: It prevents direct solar radiation from impinging on the cavity, it provides a means for mounting the entire instrument to the ALSEP support structure, and it transmits the gimbal-locking preload of 1200 to 2000 pounds. The top element of the sunshade has an astronaut handle to facilitate deployment. This handle is hinged to fold down flat during transit. A gnomon or sun-angle indicator is marked on the sunshade for azimuth alignment. The sunshade tilt indicator is calibrated in degrees of latitude, permitting the astronaut to tilt the sunshade to accommodate landing-site latitude variations of ±25 degrees from the lunar equator.

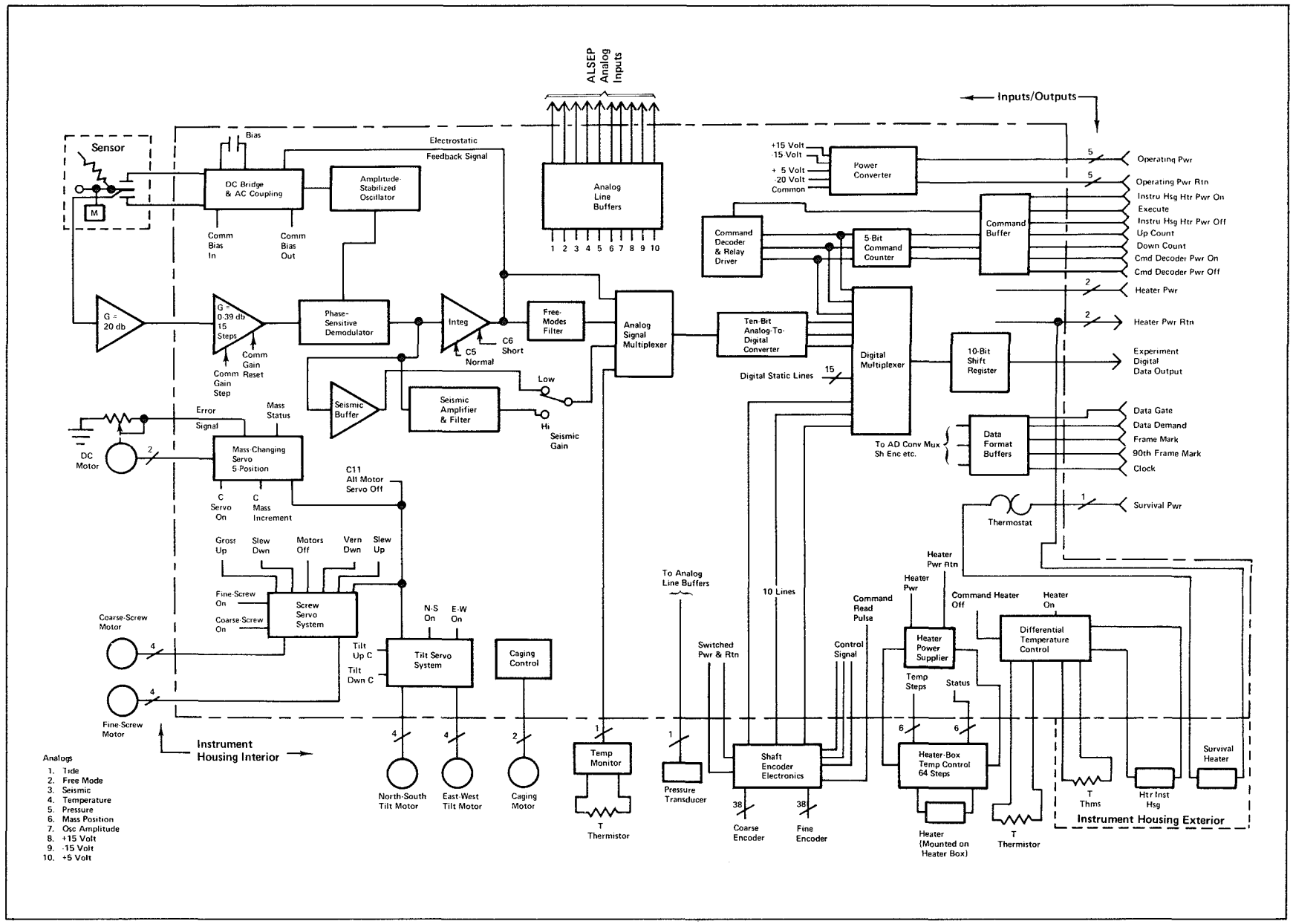

Figure 4 Lunar Surface Gravimeter Electrical Block Diagram

To keep the sensor near its inversion temperature with a short-term stability of ±0.001°C, a linear control system – consisting of an adjustable thermistor bridge circuit driving a high-gain amplifier, with a power output stage controlling the heater current – is used to control the heater winding on the heater box. The thermistor bridge circuit is adjustable through 64 steps of 0.05°C, decoded from the combinations of six relay commands. This makes possible an adjustment of ±1.6°C around the nominal operating point for determining the sensor inversion temperature on the lunar surface in the event that drift should occur during earth storage or lunar transit and operation. The instrument-housing temperature is controlled to within ±0.05°C at a temperature setpoint approximately 0.5°C lower than the heater-box temperature. A bridge circuit, provided with fixed thermistors in two of the reference lines, controls the current to the heater as referenced to the heater box. The heaters are a combination of four bifilar-wound blanket heaters and four resistors mounted on the external surface of the instrument housing.

FUNCTIONAL OPERATION

The Lunar Surface Gravimeter detects and measures the vertical component of gravity at three different frequency levels–tidal (d.c. to 0.008 hertz), free-modes (0.0008 hertz to 0.12 hertz), and seismic (0.05 hertz to 16 hertz). These signals are detected with an accuracy of 1 part in 1000, with a resolution of 2 microgals for the tidal signal, 0.008 microgal for the free-modes signal, and 0.001 micron for the seismic signal.

A functional block diagram for the Lunar Surface Gravimeter is presented in Figure 4. The five timing and control signals received from the ALSEP Central Station–frame mark, 90th frame mark, data gate, data demand, and shift pulses–are buffered by the digital line buffers and used throughout the electronics for timing and control. Seven command lines are provided. Four commands are generated directly via the ALSEP uplink. The other three command lines are used to step a command counter (up or down) and generate a command-execute function. In this way, more than thirty-six commands can be accommodated with a minimum requirement on lines to the receiving station. The ALSEP data format consists of 64 10-bit words transmitted every 9.4 milliseconds at a bit rate of 1060 bits per second. The LSG has been assigned 36 words in this format. To provide the seismic frequency response desired, every even-numbered word except word 2 is seismic data. Word 25 has been assigned to tidal data, word 27 to free-modes data, word 29 to sensor-temperature monitoring, word 35 to experiment operational status, and word 37 to command counter status. In a special mode of operation, all the data words are assigned to readout of the shaft encoder position for 90 frames.

The measurement of lunar gravity consists of centering the gravimeter mass in preparation for operating with the electrostatic servo system. The incremental masses added by command to the sensor mass, and the position of the coarse and fine micrometer screws as read out by the shaft encoder logic, provide the gravity measurement.

The deflection of the beam is detected by a differential capacitor whose center plate is attached to the beam. The differential capacitor is driven by a balanced a.c. signal. The magnitude and phase of the signal from the center plate indicate the displacement of the beam from center. This signal is amplified and converted to a d.c. signal by a series of amplifiers and a demodulator. The demodulator output is passed through a low-gain amplifier to detect large motions of the beam during initial setup of the experiment.

In order to operate over a wide input range and to make the operation independent of small changes in the electronics, a feedback voltage applied to the capacitor plates balances the input force and brings the beam back to a near-center position. The restoring force is obtained by modulating a constant voltage bias across the plates. The electrostatic force generated is directly proportional to the feedback voltage, which is obtained by integrating the beam-position signal from the demodulator. At low frequencies (tidal and free-modes motions), where the integrator has sufficient time to follow, the output is directly proportional to the gravity change. The output of the integrator is of sufficient amplitude to provide an accurate measurement of the tidal data; the free-modes data have a much lower intensity, however, and require that the integrator output be further amplified and filtered.

The seismic signals are of a higher frequency than the tidal or free-modes signals. Since these input frequencies are higher than the natural frequency of the sensor, the beam will remain fixed in space because of its inertia. The detection of seismic signals is based on the motion of the fixed plates relative to the beam. The error signal generated as a result of this motion is a direct indication of the seismic input. Since such signals are low-level, a second amplifier is used to amplify and filter the demodulator output.

The outputs of the free-modes filter, the integrator, the seismic filter, and the temperature sensor are analog signals. To process, transmit, and display these data in digital form, an analog-to-digital converter is required. The voltage-comparison technique is the basis for the converter, and the successive-approximation method is used because of its relative speed and

conversion accuracy. A digital-to-analog converter provides a variable reference voltage which follows the input analog voltage.

THE DEVELOPMENT PROGRAM

The LSG experiment is scheduled for deployment on the lunar surface as part of the Apollo 17 mission in December 1972. The development program currently underway at this facility was preceded by over five years of research and development elsewhere.* The program includes design, assembly, and test of an engineering model, a qualification model, and the flight instrument.†

Of the extensive tests that are planned, the most significant will be in the areas of thermal vacuum and noise performance. The thermal vacuum tests will establish the capability of the thermal control system to maintain sensor temperature and pressure within the close limits required for successful operation of the experiment. The noise performance tests will verify that the electronics noise is sufficiently low that it will not limit the ability of the experiment to detect the very small signals expected to result from gravitational radiation.

---

*Conducted by Weber, Larson, Richard, and Giganti at the University of Maryland.

†Major subcontractors are Arthur D. Little, Inc., for the structural/thermal components and LaCoste-Romberg, Inc., for the gravimeter sensor.

AUTHORS

Donald K. Breseke
Aerospace Systems Division
Ann Arbor, Michigan

Experiment Supervisor, ALSEP Passive Seismic Experiment. B.S. in Physics, Purdue University, 1956. Currently supervising activities associated with the fabrication and testing of the Passive Seismic Experiment and its integration into the Apollo Lunar Surface Experiments Package. Was previously responsible for systems engineering and analysis in the Advanced ALSEP study program and for navigation systems in lunar-roving-vehicle study programs. Formerly affiliated with ITT Laboratories in its Astrionics Laboratory.

John M. Brueger
Aerospace Systems Division
Ann Arbor, Michigan

Manager, Viking Upper-Atmosphere Mass Spectrometer program. B.A.E. and M.S. in Aeronautical Engineering, Rensselaer Polytechnic Institute, 1952 and 1958. Was responsible for development of Laser-Ranging Retroreflectors flown on Apollo missions 11, 14, and 15, serving as program manager. Previously served as Engineering Mechanics Supervisor in planetary experiments studies and supervised special-project mechanical design engineering in the ALSEP program. Directed development of payload/launch-vehicle interfaces for the Emergency Rocket Communication System. Has also been responsible for launch-vehicle and rocket-motor design and development in various missile programs. Member: American Institute of Aeronautics and Astronautics; Tau Beta Pi; Society of Sigma Xi.

Walter E. Crosmer
Aerospace Systems Division
Ann Arbor, Michigan

Systems Engineering Supervisor, Lunar Surface Gravimeter Experiment. B.S. in Physics and Mathematics, Valparaiso University, 1956. Currently involved in the Apollo Lunar Surface Experiments Package development program for Apollo 17, with responsibility for systems engineering for the Lunar Surface Gravimeter and monitoring of two major subcontractors. Has previously participated in a number of instrument and system development programs for lunar and Mars exploration, among them the Viking Pyrolysis/Mass-Spectrometer Experiment, the Apollo Lunar Surface Experiments Package for Apollo 12, and a variety of lunar vehicle development programs. Has authored a number of papers on lunar mission analysis and system development planning.

Clark E. DeHaven, Jr.
Aerospace Systems Division
Ann Arbor, Michigan

Experiment Engineer, Lunar Mass Spectrometer program. B.S. in Physics, Michigan State University, 1968. Currently responsible for Lunar Mass Spectrometer design analysis and functional verification testing. Previously conducted design analyses and test verification on a Martian-soil pyrolysis and gas-analysis instrument for the NASA Viking program. Has also performed preliminary design analyses and development testing for radiographic systems, among them the Bendix-Ray XM-105.

Jack E. Dye
Aerospace Systems Division
Ann Arbor, Michigan

Program Manager, Lunar Seismic Profiling Experiment. B.S.E.E., Washington University (St. Louis), 1949; M.S.E.E., University of Maryland, 1953. Currently responsible for development of the Lunar Seismic Profiling Experiment for the Apollo Lunar Surface Experiments Package (ALSEP). Has previously served as ALSEP Assistant Program Manager, as Systems Manager for the Apollo 12 ALSEP, and as Manager, ALSEP Experiments. Formerly managed the Information Sciences and Electronics Department. Prior to joining Bendix, worked on weapons development at Emerson Research Laboratories and at the Naval Ordnance Laboratory at White Oak. Member: Institute of Electrical and Electronics Engineers; Tau Beta Pi; Pi Mu Epsilon; Society of Sigma Xi.

Lowell D. Ferguson
Bendix Research Laboratories
Southfield, Michigan

Manager, Program Development. B.S. in Engineering Physics, Ohio State University, 1958; M.S. in Physics, Ohio State University, 1960. Was responsible for the design and fabrication of the electron/proton energy spectrometer used in the ALSEP Charged-Particle Lunar Environment Experiment. Also directed the development of a complex mass-analysis system for extracting and analyzing short-lived, high-temperature neutral and ionic gas products formed in the wake of hypervelocity projectiles. Has conducted experimental investigations on the feasibility of obtaining time-coherent focused ions at the detector of the time-of-flight mass spectrometer by means of a pulsed electrostatic lens, and holds a patent related to this spectrometer.

Louis Galan
Aerospace Systems Division
Ann Arbor, Michigan

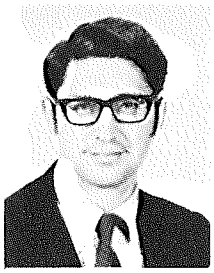

Manager, Lunar Ejecta and Meteorites (LEAM) Experiment program. B.S.M.E., Massachusetts Institute of Technology, 1951; M.S.A.E. and M.S.M.E., University of Michigan, 1954 and 1955. Currently responsible for development of the LEAM experiment for Apollo 17. Previously participated in management of lunar-roving-vehicle design studies and full-scale-model fabrication and testing. Has also participated in the preliminary design and integration of missile and spacecraft systems and in the development of ballistic rocketborne weather reconnaissance and communications payloads, with emphasis on structures, aerodynamics, thermodynamics, and propulsion. Author of several formal publications on lunar vehicles and lunar environmental design. Registered Professional Engineer, State of Ohio. Member: Phi Kappa Phi; Pi Tau Sigma; Tau Beta Pi; Society of Sigma Xi.

Hwei-Kai Hsi
Aerospace Systems Division
Ann Arbor, Michigan

Program Manager, Lunar Surface Gravimeter Experiment. B.S. and M.S. in Mechanical Engineering, University of Michigan, 1954 and 1955. Currently directing the development of the Lunar Surface Gravimeter for the Apollo Lunar Surface Experiments Package for Apollo 17. Previously Manager of the Apollo Lunar Surface Experiments Package Experiments Department. Also Program Manager for the Apollo 11 Early Apollo Scientific Experiments Package Passive Seismic Experiment. Prior to work on Apollo programs, served as Manager for the Viking Pyrolysis/Mass-Spectrometer Experiment and Supervisor of the Space Power group. Has authored a number of papers on space power systems.

Lynn R. Lewis
Aerospace Systems Division
Ann Arbor, Michigan

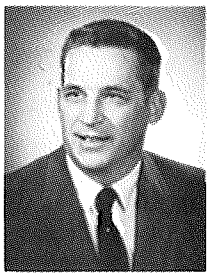

Assistant ALSEP Systems Manager. B.S. and M.S. in Physics and Mathematics, State University of New York (Albany), 1954 and 1955. Currently involved in design and development problems associated with experiment integration and system testing for the Apollo 17 ALSEP. Was Engineering Department Manager for ALSEP systems to be flown on Apollo missions 16 and 17, with responsibility for electrical, mechanical, and thermal designs. Managed Design Integration and Test Department and directed flight testing of packages flown on missions 11, 12, and 13. Coordinated assembly and test of ALSEP qualification models for missions 12, 13, and 14. Has also been responsible for electrical design definition and compatibility, engineering model tests, and engineering support for all system-level tests. Prior to work on ALSEP, conducted scientific mission studies on lunar surface science, and experiment-feasibility studies for hard-landing lunar probes. Was also systems integration engineer for the OV3 satellite series.

John Lewko, Jr.
Aerospace Systems Division
Ann Arbor, Michigan

Instrument Engineer, Space Systems Directorate. Diploma in Communications and Television Engineering, Radio Electronics Television School, 1950. Currently responsible for the design of an advanced triaxial seismometer instrument for the Viking Mars Lander program, employing seismic data compression concepts, digital filtering, and large-scale integration techniques to produce a miniaturized, lightweight, low-power seismometer system. Formerly Manager, Space Seismology Equipment Department, with responsibility for the redesign, fabrication, integration, and test of the ALSEP Passive Seismometer system. Also managed the Single-Frequency-Repeater and Traveling-Wave-Tube-Repeater Communication Satellite programs.

Jack R. McDowell
Aerospace Systems Division
Ann Arbor, Michigan

Project Engineer, Apollo Lunar Surface Experiments Package program. B.S.E.E., University of Denver, 1950. Responsible for the design and development of the Active Seismic Experiment. Previously Group Supervisor in the Systems Design Department, assigned to develop new concepts and preliminary designs for advanced aerospace systems. Served as Program Manager for the Navy Tactical Probe System, directing operations analysis, conceptual design, and feasibility studies. Prior to joining Bendix, worked on the Titan program at Martin Marietta Corporation and on the SHRIKE and RASCAL programs at Bell Aircraft.

James L. McNaughton
Aerospace Systems Division
Ann Arbor, Michigan

Engineering Group Supervisor, ALSEP Structural, Thermal, and Crew Group. B.S.M.E., University of Michigan, 1961; M.S.M.E., San Diego State University, 1964. Currently responsible for structural, thermal, and crew-engineering design aspects associated with the ALSEP data subsystem, the nuclear power system, and experiment packaging. Previously directed thermal control design for the ALSEP experiments, the central electronics, and the nuclear generator and cask structure. Work involved thermal design studies and analyses and thermal vacuum testing, and participation in mission evaluation of lunar-based equipment. Member: American Institute of Aeronautics and Astronautics.

Clyde R. Murtaugh
Aerospace Systems Division
Ann Arbor, Michigan

Mission Support Supervisor, Apollo Lunar Surface Experiments Package program. B.S.E E., Ohio State University, 1943; M.S. in Aeronautics, California Institute of Technology, 1947. Currently responsible for field personnel assigned to the NASA Manned Spacecraft Center for ALSEP mission operations. Has previously conducted conceptual design studies to establish structural and mechanical configurations for scientific satellites. Author of a number of papers on spacecraft, lunar roving vehicles, launch vehicles, and aerodynamic testing. Associate Fellow and past-Director, American Institute of Aeronautics and Astronautics.

Ralph D. Ormsby
Aerospace Systems Division
Ann Arbor, Michigan

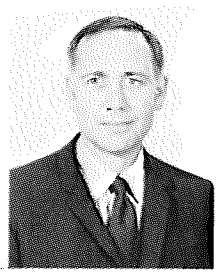

Manager, Lunar Mass Spectrometer program. B.S.E.E. and M.S.E.E., Purdue University, 1952 and 1954. Currently responsible for design and development of the Lunar Mass Spectrometer to be flown on Apollo 17. Previously directed development of the Early Apollo Scientific Experiments Package (EASEP) for Apollo 11 and was in charge of preliminary design and development planning for Advanced ALSEP and Mars Surface Experiments. Has also worked on preliminary design of scientific satellites, of spacecraft for deep-space operation, and of military systems for intelligence and reconnaissance. Served as Project Engineer for development of the electrically suspended gyroscope and other navigation and control projects. Member: American Institute of Aeronautics and Astronautics (Associate Fellow); Institute of Electrical and Electronics Engineers.

Ronald L. Redick
Aerospace Systems Division
Ann Arbor, Michigan

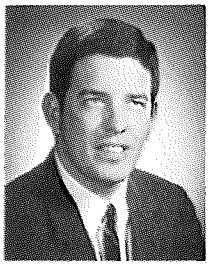

Crew-Engineering Supervisor, ALSEP Crew-Engineering Group. B.S. in Biology, Eastern Michigan University, 1960. Directs the operation of the crew-engineering laboratory, with responsibility for development, coordination, and planning of human-engineering design for ALSEP personnel subsystems. Activities include astronaut/system interface analysis, design, simulation, and test. Has been responsible for crew training for the ALSEP program since 1965. Is a qualified suited subject for the Apollo II pressure suit and the KC-135 zero-gravity aircraft. Previously participated in early development of human-factors requirements for airborne communications in fixed-wing and rotary aircraft. Member: Institute of Biological Sciences; Human Factors Society.

Albert D. Robinson
Aerospace Systems Division
Ann Arbor, Michigan

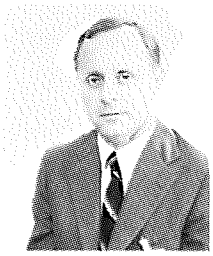

Principal Engineer. A.B. in Physics, Indiana University, 1950. Currently Engineering Project Manager for the Earth Resources Technology Satellite (ERTS) bulk processing subsystem, a special ground processing system for converting video-tape recordings of experimental ERTS data into latent images on 70-millimeter film. Previously Project Engineer for the ALSEP Charged-Particle Lunar Environment Experiment and the Solar Wind Experiment. Prior experience includes work on the Celescope experiment for the Orbiting Astronomical Observatory, the Ultraviolet Radiometer for the TRUMP program, and the Lunar Geophysical Probe project at the Sarasota Division of EMR. Was also Project Engineer for the AN/APS-104 radar project at Bendix Electrodynamics Division and Senior Engineer on the TALOS Guidance System project at Bendix Missile Division.

Burton L. Sharpe
NASA Manned Spacecraft Center
Houston, Texas

Head, Lunar Surface Section, Flight Control Division. B.S. in Aeronautical Engineering, University of Colorado, 1957. Currently supervises real-time monitoring and control of the Apollo Lunar Surface Experiments Packages. Is also involved in real-time direction of Apollo-astronaut scientific activities on the lunar surface, in traverse planning, and in lunar-roving-vehicle systems monitoring. Before joining NASA in 1966, was associated with the Atlas development program at Convair-Astronautics and with the Gemini-Agena program at Lockheed Missiles and Space Company. Member: American Institute of Aeronautics and Astronautics.

Bruce D. Smith
Aerospace Systems Division
Ann Arbor, Michigan

Project Engineer, ALSEP Heat Flow Experiment. H.N.C. in Electrical Engineering, Hatfield College of Technology, England, 1964. Responsible for the development, fabrication, testing, and calibration of the heat-flow instrument for the Apollo Lunar Surface Experiments Package. Also assists in the engineering evaluation of lunar operational data. Previously worked on missile inertial systems as section leader in the Precision Products group at British Aircraft Corporation. Other areas of design and development responsibility have included microwave instrumentation, multistage rocket systems, and commercial computers. Member: Institution of Electronic and Radio Engineers.

William K. Stephenson
NASA Manned Spacecraft Center
Houston, Texas

Manager, Test and Check-Out, Science and Application Directorate. B.S.M.E., University of Texas, 1959. Currently responsible for test and check-out for the Earth Resources Experiment Package (EREP) and the Orbital Workshop Experiments to be flown in the Skylab program. Previously responsible for operation of and data management for the Apollo lunar experiments (ALSEP), with particular emphasis on telemetry design and science data reporting. Also handled the operation, data management, and testing of experiments flown on the Gemini program.

Warren M. Tosh
Aerospace Systems Division
Ann Arbor, Michigan

Engineering Manager, Apollo Lunar Surface Experiments Package (ALSEP) program. Engineering studies at Oklahoma State University and Capital Radio Engineering Institute. Previously served as ALSEP Experiments Manager and ALSEP Data Subsystem Group Supervisor. Was Project Engineer for Shipboard Communications and Radar Systems planning, installation, and test. Formerly Associate Project Supervisor for design, development, and test of antijam communications equipment. Also Project Supervisor for Ultrahigh-Frequency Satellite Communications System.

KEY TO ABBREVIATIONS AND ACRONYMS

AGC	automatic gain control
ALCS	ALSEP computer system
ALSEP	Apollo Lunar Surface Experiments Package
ASDS	active seismic detection system
ASE	Active Seismic Experiment
ASI	Apollo standard initiator
BTU	British thermal unit
CCATS	command, control, and telemetry system
CCGE	Cold-Cathode Ion Gage Experiment
CG	center of gravity
CMD	command
CPLEE	Charged-Particle Lunar Environment Experiment
CRES	corrosion-resistant eutectic steel
CSE	Central Station electronics
CST	Central Standard Time
CVW	command verification word
DD	Dust Detector
DRT	dome-removal tool
DSS	data subsystem
DTREM	dust, thermal, and radiation engineering measurements
EASEP	Early Apollo Scientific Experiments Package
EDC	end detonating cartridge
EHT	experiment handling tool
EMF	electromotive force
EMI	electromagnetic interference
EMU	extravehicular mobility unit
EPS	electric power subsystem
EVA	extravehicular activity
FCA	fuel cask assembly
FET	field-effect transistor
FF	flip-flop
FTT	fuel-transfer tool
GLA	grenade launch assembly
GSFC	Goddard Space Flight Center
HFE	Heat Flow Experiment
HNS	hexanitrostilbene
HSD	high-speed data
LEAM	Lunar Ejecta and Meteorites
LM	Lunar Module
LMS	Lunar Mass Spectrometer
LPX, LPY	long-period horizontal seismometers
LPZ	long-period vertical seismometer
LRRR	Laser-Ranging Retroreflector
LRV	Lunar Roving Vehicle
LSM	Lunar Surface Magnetometer
LSPE	Lunar Seismic Profiling Experiment
LTA	launch-tube assembly
LURE	Lunar Ranging Experiment
MCC	Mission Control Center
MIT	Massachusetts Institute of Technology
MOCR	Mission Operations Control Room
MODEM	modulator/demodulator
MPA	mortar package assembly
MSC	Manned Spacecraft Center
MSFN	Manned Space Flight Network
NASA	National Aeronautics and Space Administration
NASCOM	NASA Communications
NBS	National Bureau of Standards
OPS	oxygen purge system
PBT	polynomial buffer terminal
PCM	pulse code modulation
PDM	power dissipation module
PDU	power distribution unit
PHA	pulse-height analysis
PLSS	portable life-support system
PSE	Passive Seismic Experiment
RTCC	Real-Time Computer Complex
RTE	real-time event
RTG	radioisotope thermoelectric generator
SBASI	single-bridgewire Apollo standard initiator
SEQ	scientific-equipment
SIDE	Suprathermal Ion Detector Experiment
SLA	spacecraft/Lunar Module adapter
SOR	Science Operations Room
SPZ	short-period seismometer
SSR	Staff Support Room
SWS	Solar Wind Spectrometer
TDRT	tie-down release tool
TM	telemetry
TOF	time-of-flight
TRAJ	trajectory
TTY	teletype-quality circuit
UHT	universal handling tool
USB	unified S band
WBD	wide-band data

Philosophy of the BENDIX TECHNICAL JOURNAL

External to the Corporation, the Journal will convey to its readers in expanded papers the scope and nature of original work in a specialized area. The Journal is meant to complement rather than be competitive with other scientific and technical society journals.

Internal to the Corporation, the Journal will inform its readers of achievements, developments, capabilities, and personalities within the Bendix organization. It will also provide research and design information. Finally, it will serve as an important incentive to potential authors within the various divisions of the Corporation.

Each issue of the Journal will cover a single specialized topic, preselected within a technology, discipline, or business area framework.

Each issue will be guided by an editorial panel whose members are technical experts from the various divisions and subsidiaries active in fields related to the issue topic.

Each issue will attempt to span the whole spectrum of technical activities within the Bendix organization, from research and development through engineering, design, manufacture, and technical services.

The Bendix Corporation
Executive Offices
Bendix Center
Southfield, Michigan 48076

LITHO IN U.S.A.